The haematological factors and their disruption by organophosphorus compounds

Nada Omar Binzager

A thesis submitted in partial fulfilment of the requirements of Nottingham Trent University for the degree of

Doctor of Philosophy

August 2019

Copyright Statement

Declaration

I, Nada O. Binzager, hereby declare that the work presented in this thesis was conducted by myself. Exceptions to this have been clearly stated in the text.

Abstract

Haematological parameters are typically monitored to detect changes in haemostasis due to illness or exposure to toxins. Of interest to the present study was the possibility that exposure to organophosphorous (OP) compounds might disrupt enzymes involved in the coagulation cascade includes (e.g. the plasma transglutaminase (TG) factor XIIIa and thrombin) and the proliferation and viability of white cells. Toxin-induced disruption of such enzyme activities or white cell number could interfere with the haemostatic balance. There have been limited studies on OP effects on coagulation enzymes and blood cells. The purpose of this study was to investigate the effects of the OPs phenyl saligenin phosphate (PSP), diazinon (DZ), chlorpyrifos (CPF), parathion (PTH), diazoxon (DZO), chlorpyrifos oxon (CPO), paraoxon (POX) on plasma and purified cholinesterases (AChE & BChE), FXIIIa and thrombin activities in plasma and pure enzyme preparations, and the growth and viability THP-1 leukemic monocyte cells.

The effects of OPs on enzyme activities were monitored using colorimetric activity assays of purified enzymes or whole plasma protein extracts, after samples had been pre-incubated with OPs. All OPs showed the expected patterns of toxicity against their recognised ChE targets. Most OPs demonstrated the ability to inhibit one or other of the transamidase activities in a concentration-dependent manner, being more effective against the pure enzyme. Thrombin inhibition was observed with some OPs but was more striking in whole plasma. All OPs reduced the levels of D-dimer detectable by ELISA. Covalent binding assays involving SDS-PAGE analysis of plasma proteins, rFXIIIa and purified thrombin incubated with rhodamine-labelled PSP, demonstrated covalent binding of PSP to both enzymes which could be competed out by non-labelled OPs. MS analysis revealed novel covalent adducts formed between pure FXIIIa and either unlabeled PSP or the 3 oxon OPs.

THP-1 cells proliferation and viability were decreased by most OPs in a concentration and time-dependent manner, although CPO promoted proliferation at an early time point prior a decline. In conclusion, the results obtained provide evidence that FXIIIa transamidase activities are inhibited by OPs and that FXIIIa could be a novel target of OP toxicity. Moreover, data suggest that OPs can disrupt the regulation of THP-1 proliferation. Future work is recommended to identify adduct forming sites on novel OP-binding proteins in plasma and THP-1 cells and to further examine the effects on THP-1 cells at a proteomic and genomic level.

Conference (Poster)

Poster presentation at Life Sciences 2019: Posttranslational Modification and Cell Signalling, March 2019. Organised by the Biochemical Society, British Pharmacological Society, and the Physiological Society. Poster title*:* **The effect of parathion toxicity on plasma transglutaminase (FXIIIa) activity.**

Nada Binzager, Philip Bonner and Alan Hargreaves. "**The effects of organophosphorous compounds on human plasma FXIIIa activity**". School of Science and Technology 11th Annual Research Conference (STAR conference), Nottingham Trent University (May 2016). Poster and oral presentation.

Acknowledgements

All my thanks go to my Lord Allah almighty, who has always been there for me. To guide, secure and give me all patience to continue, without my believe in Allah I would be lost. My deepest gratitude and love go to my parents who always were there to support me, providing me unfailing support, continuous encouragements and prayers all my way. Without their love and wonderful spirit, I wouldn't be able to make it to this stage.

Also, my heartfelt thanks to my brothers Waleed, Fouad, Mohammad and their families. Special deepest thanks to my youngest brother, Abdulaziz, who left everything behind him to accompany and support me during my study time abroad for almost nine years of scholarship. Also, I appreciate all support and encouragement from my cousins and all other family members.

I would also like to acknowledge my sponsor of scholarship provided by Ministry of health and Ministry of Higher Education of Saudi Arabia for all their support, care, help and facilities were provided to complete my studies.

I would like to impress my sincere thanks and appreciation to my supervisor Dr. Alan Hargreaves for all guidance, help, support, continuous encouragement. Moreover, I am so grateful for his exceptional supervision and help particularly during the thesis evaluation. He taught me how to be a scientist. Also, I would like to thank my second supervisor Dr. Philp Bonner for his professional help during lab work.

I would also like to acknowledge Nottingham Trent University, for all support they provided to me as international student.

My special thanks to my lovely friends Rana Zaidan, Alanood Algarni, Intissar Abushagur, Iqraa Kataria, Nagina Siddique, Hayat Binhowail, Aysha Karama, Reham Balahmar, Najlaa AlMazrouei, Nora Balahmar, Hayat Alzahrani, Shatha Felemban, Amna Alshamsi, Mariam Bajaber, Noor Bashmakh who have always been sharing with me my difficult moments and encouraging me to stand up and continue, thank you for being part of my life along this way, thank you for sharing my happiness and sadness moments and being my second family in Nottingham. To all my friends in KSA, Canada and here in the UK thank you for your contact and support. All my respect and thanks to the people who stood by me during this project and provided me all help and support.

List of Figures

List of Tables

List of Abbreviations

ACh	**Acetylcholine**
AChE	Acetylcholinesterase
AChE	Acetylcholinesterase
AChE	Acetylcholinesterase
APC	Activating protein C
AP-FXIII	Activation peptide FXIII
APH	Acylpeptide hydrolase
APTT	Activated partial thromboplastin time
ATSDR	Agency for Toxic Substances & Disease Registry
BChE	Butyrylcholinesterase
BChE	Butyrylcholinesterase
cFXIIIa	Activated cellular FXIII
ChEs	Cholinesterases
CPF	Chlorpyrifos
CPO	Chlorpyrifos-oxon
CYPs	Cytochromes
DEP	Dialkylphosphate, diethylphosphate
DETP	Diethylthiophosphate
DZ	Diazinon
DZO	Diazoxon
ECM	Extracellular matrix
EPCR	Endothelial protein C receptor
Gln	Glutamine

GpIbα	Platelet glycoprotein receptor
IARC	International Agency for Research on Cancer
MAPK	Mitogen-activated protein kinase
MDC	Monodansylcadaverine
NTE	neuropathy target esterase
OPIDN	Organophosphate-induced delayed neuropathy
OPs	Organophosphorus compounds
OPs	Organophosphate
P	Phosphate atom
PAI-1 or 2	Plasminogen activator inhibitor type 1 or 2
PAR	Protease activated receptor
PAR1, 3, 4	Protease activated receptor 1, 3 and 4
PC	Protein C
PON1	Paraoxnase 1
POX	Paraoxon
PS	Protein S
PSP	Phenyl saligenin phosphate
PT	Prothrombin time
PTH	Parathion
SCOTP	Saligenin cyclic-o-tolyl phosphate
TAFI	Thrombin activatable fibrinolysis inhibitor
TCP	6-trichloro-2-pyridinol
TF	Tissue factor
TFPI	Tissue factor pathway inhibitor
TM	Thrombomodulin

TOCP	Triortho-cresyl phosphate
TOCP	Tri ortho cresyl phosphate
TOTP	Tri-ortho-tolyl phosphate
α2-AP	α2-antiplasmin
α_2-PI	α_2-plasmin inhibitor

Table of Content

Chapter 1: Introduction

1.1 Background

Blood has many of haematological factors including a variety of proteins and cells types, such as haemoglobin, red cells, white cells, platelets, and specific proteins involved in vital processes, such as haemostasis, which have been studied widely as diagnostic and monitoring tools for blood diseases (Blann & Ahmed, 2014; Etim *et al.*, 2014). Haemostasis is one of the crucial biological processes in blood, as it maintains blood in a fluid condition within the vascular system, having defence mechanisms against bleeding and thrombosis. It involves complex processes, such as vascular spasm to restrain the flow of blood to the wounded area, platelet plug formation, the coagulation cascade leading to fibrin deposition, (and therefore ensuring stability of the clot), clot retraction and tissue repair, and finally coagulation inhibitors and fibrinolytic systems to restore the blood flow (Pallister & Watson, 2011). As summarized in Fig 1.1, the complex coagulation cascade is driven by a complex of enzymatic pathways, which involves several proteins, cofactors, zymogen-to-enzyme conversion steps and allows two starting points involving the extrinsic and intrinsic reactions, which merge into a common pathway where coagulation is completed (Pallister & Watson, 2011; Lupu *et al.*, 2016).

Following injury, the zymogen coagulation proteins in the blood are sequentially activated into their enzymically active form (Lupu *et al.*, 2016). The extrinsic pathway is the main contributor that sparks the physiological activation of coagulation. It is triggered within a few seconds, when the tissue factor (TF) from the injured area is exposed to blood (Blood Laboratory n.d). TF acts as a cofactor for the activated form of factor VII (FVIIa), serine protease, and binds to it to form an enzymatic complex TF-FVIIa, which propagates the cleavage of factor X to the activated form FXa in the presence of Ca^{2+} (Lupu *et al.*, 2016).

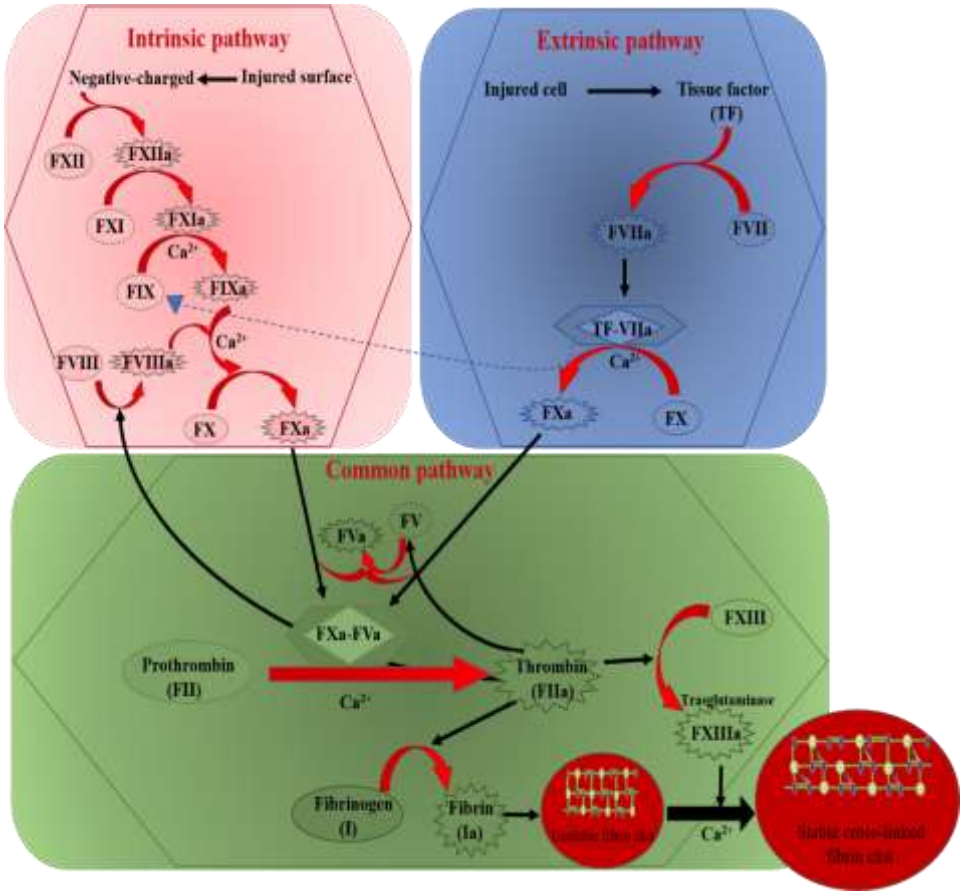

Figure 1- 1: The physiological response of the coagulation cascade to vascular injury.

Three vital pathways are involved in this process; the activation of extrinsic pathway by released tissue factor sparks the physiological activation of protein cascade, while the intrinsic pathway stimulated by negatively charged surfaces and begin a sequential coagulation factors activation. Both of these pathways converge on the common pathway, at a point where FXa accelerates the activation of the zymogen prothrombin to thrombin which is then able to regulate and activate many coagulation factors in a cascade which ends with cleavage fibrinogen to fibrin to form a clot mesh, which is cross-linked and stabilized by FXIIIa (a member of the transglutaminase family) to form a fibrin mesh. Modified from (Lupu *et al.*, 2016).

The intrinsic pathway, also known as the contact activation pathway, plays a secondary role in haemostasis under normal physiological conditions (Lupu *et al.*, 2016), which takes a few minutes to occur (Blood Laboratory n.d). This process can be initiated and form a clot upon contact with a negative charged glass surface that represents the negative charge of the body surface (Neuenschwander, 2006) Once the negative charged injured surface in the body makes contact with the blood or plasma, the coagulation factors are activated sequentially, starting from FXII to FXIIa. The later, in the presence of calcium ions then activates FXI to FXIa, which activates FIX to FIXa; moreover, as a part of amplification system, the TF-FVIIa-Ca^{2+} complex is also able to activate FIX (Licari & Kovacic, 2009). FVIII, which is activated in advance, by the trace amount of thrombin that had been activated through the extrinsic pathway, to FVIIIa in turn forms a complex with FIXa to activate FX to FXa (Lupu *et al.*, 2016). Both pathways lead to the activation of Factor X (FX) in the common pathway and the subsequent generation of thrombin. The common pathway is the final step in this cascade, which proceeds to the conversion of soluble fibrinogen into an insoluble fibrin network. Once the FXa is generated, either from extrinsic or intrinsic pathways, it will form a complex with calcium ions and activated nonenzymatic cofactor FV (FVa), which is also activated by thrombin, to proteolytically active prothrombin (FII) to generate enzymically active thrombin (FIIa) (Bereczky *et al.*, 2003). Thrombin is the protease that proteolytically processes fibrinogen to produce insoluble fibrine monomers, which form fibrin strands and polymerize into an unstable clot mesh. In the meantime, thrombin also proteolytically converts the transglutaminase pro-enzyme FXIII from its in-active form to the activated form FXIIIa, which plays the final role in the coagulation cascade by catalysing the cross-linking of the unstable fibrin mesh to form stabilized insoluble clot as shown in Fig 1.1 (Bereczky *et al.*, 2003).

Most of environmental pollutants are potentially toxic to the human body and are implicated in developing diseases, which induce chronic effect on neuronal, cardiac, and muscular tissues, and increase the risk of cancer, etc. (Gupta, 2006). Organophosphorus compounds (OPs) have pesticide and non-pesticide applications, as they are widely used in agriculture, household product and aircraft engine oil (Grube *et al.*, 2011; Hargreaves *et al.*, 2006). Exposure to OPs has been linked with serious health issues over the past few decades, affecting both neuronal and non-neuronal tissues, which has been proposed to involve disruption of a range of biological process (Eleršek & Filipič, 2011). OPs usually inhibit serine esterase such acetylcholinesterase as primary targets but there is increasing evidence that they may have other targets; they also disrupt Ca^{2+} homeostasis, thus affecting the activities of a range of Ca^{2+} depending protein such as calpain and transglutaminase 2 (Chambers & Oppenheimer, 2004; Hargreaves, 2012).

As thrombin (serine esterase) and FXIIIa (a form of transglutaminase) are enzymes involved in the blood clotting cascade, they represent potential blood-borne targets of OPs. Both enzymes have major role in coagulation, in addition to other roles in different processes. Coagulation disorders associated with disruption of these enzymes can lead to critical bleeding issues. An investigation of the ability of OPs to interfere with these enzymes' activities was therefore of interest to the present study.

1.2 Thrombin

Thrombin is considered to be a key player in the coagulation cascade where it has control for the boosting and attenuation of its own formation, and has Janus-faced characteristics for pro- and anti-coagulant activities (Huntington, 2008). Prothrombin, known as FII, is a zymogen that is converted to the serine protease thrombin (FIIa), which has at least four distinct binding sites for Na^{+}, substrates, cofactors, and inhibitors (Brummel *et al.*, 2002).

Thrombin a positive feedback, as it amplifies the coagulation factors FV, FVIII, XI, and FXIII, and also cleaves fibrinogen to form fibrin monomers, which polymerize to form the fibrin network (Brummel *et al.*, 2002). In addition, it has been found that platelets are activated through protease activated receptor (PAR)-1, 3, and 4 by thrombin (Huntington, 2012). Likewise, thrombin acts as a negative feedback regulator for coagulation factors by activating protein C (APC), and thrombin-activatable fibrinolysis inhibitor (TAFI) (Brummel *et al.*, 2002; Bode, 2005; & Huntington, 2012).

1.2.1 Structure:

The active form thrombin is a 37 kDa serine protease generated by proteolytic cleavage of prothrombin (Mutch *et al.*, 2001). It is a Na^+ -activated serine protease of the chymotrypsin family that has two six-stranded asymmetrical β-barrels, both of which house residues of the catalytic triad of the active site His57, Asp102 and Ser195 (Huntington, 2005). The traditional thrombin structure is viewed in the standard orientation represent the peptide bond of serine proteases includes essential scissile peptide bond of substrate binding residues, which was identified by mutagenesis and structural studies, that so-called P1-P1' and are numbered sequentially toward the N- to C-termini (Fig 1.2) (Huntington, 2005). The subsite hydrophobic interactions occur at P1 arginine side chain, which is buried into the deep S1 pocket to form a salt bridge with aspartic acid 189 at the base of the pocket, also P4 of substrate residue interacted with aryl binding pocket S4. Due to that the thrombin in haemostasis is highly substrate-specific (Huntington, 2008).

Thrombin has specifically a deep active site cleft referred to as a ‘canyon’, this is due to inserted loops above (60-loop) and below (γ-loop) the active site. The 60-loop has a hydrophobic manner that gives rigid form; on the other hand, the γ-loop is more hydrophilic which produces flexibility that can make the contact with substrate proteins. These loops can directly interact with the substrate peptide. Also, it can serve to restrict access of other

flexible and long substrates or mediate the surface of complementary proteins to the catalytic site of thrombin (Huntington, 2005; Huntington, 2008).

Moreover, thrombin has other sites relevant to its activity, including two anion exosite for interaction areas and Na^+ binding (Huntington, 2005). Exosite I, which is located "east" of the catalytic active site, mainly known as fibrin(ogen), thrombomodulin (TM) and protease activated receptor 1, 3 and 4 (PAR1, PAR4, and PAR4) interaction site. While exosite II, which is located "west" of the catalytic active site, is the more basic of the two sites, and was identified as heparin, platelet glycoprotein receptor GpIbα interaction site (Di Cera, 2003). Most of the natural thrombin substrates and cofactors utilize one or both exosites (Huntington, 2005). De Cera and his colleagues (1995) identified the Na^+ binding site position on thrombin. The Na^+ binding site plays an important role in regulating thrombin function and is located "southwest" of the catalytic active site. Interaction of Na^+ at that site can induce two distinct thrombin conformations that are so-called slow and fast forms, which enhances substrates or other cofactor proteins binding and catalysis (Dang *et al.*, 1995). Since thrombin is an allosteric enzyme, the equilibrium between fast state (Na^+ -bound) and slow state (Na^+ -free) become arbiter of procoagulant/anticoagulant activities of thrombin, respectively (Dang *et al.*, 1995). The specificity of fast form is higher for the procoagulant substrates fibrinogen, fibrin, PAR1 and PAR4, while the slow form is more specific for anticoagulant substrates, such as protein C (Di Cera, 2003).

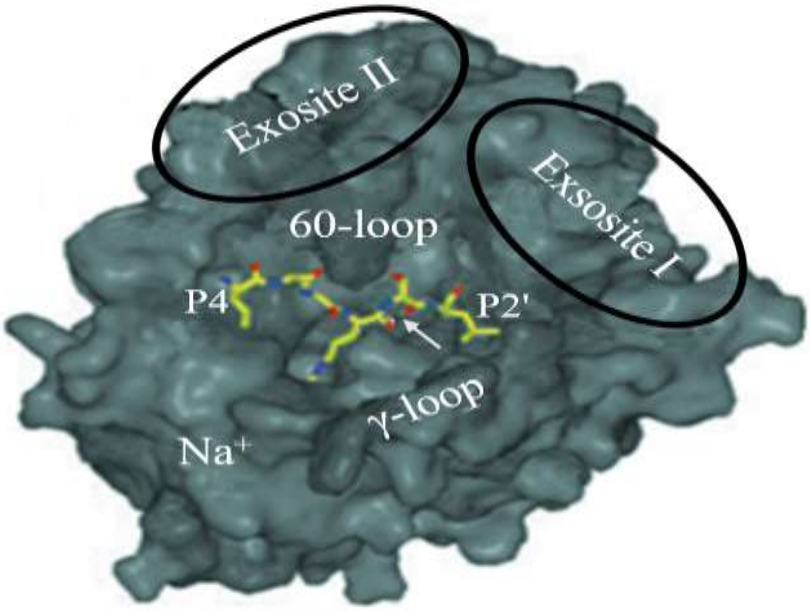

Figure 1- 2: The crystallographic structure of thrombin.

The standard orientation of thrombin reveals the active site is occupied the centre, where a peptide substrate will run from the left to the right, from its N- to C- terminal. The P4 to P2', substrate residues of antithrombin (yellow rods), including the reactive centre bond (P1-P1') indicated by white arrow. Thrombin active site is remarkably deep due to the presence of the 60-loop from above, and γ-loop from below the active site. A substrate and cofactor recognition areas are identified at two major anion binding exosites (Exosite I & II) as indicated by the ovals. The Na+ binding site which is active site adjacent, play critical role to make thrombin less activity. Modified from (Huntington, 2005).

1.3 Thrombin and coagulation cascade

As mentioned before, the central role of thrombin is in the regulation of the coagulation cascade, boosting the cleavage of fibrinogen to fibrin to form the clot mesh on platelet plug and activation of the prozymogen FXIII to FXIIIa that catalyses cross-linking of the mesh to form stable clot. The regulatory role of thrombin in coagulation starts when a small amount of thrombin is generated and performs in a positive feedback pathway (Fig 1.3) that

is able to amplify the system through more production of FVa, FVIIa, FVIIIa, and FXIa. This mechanism in healthy adults is sufficient for supplying thrombin production (Licari & Kovacic, 2009). Moreover, the activation of FXI by thrombin positive feedback in patients with FXII deficiency prevents serious haemorrhage (Brooks *et al.*, 1994). However, part of this amplification mechanism fails in cases of FXI deficiency, which results in multiple bleeding for the same injury (Gomez & Bolton-Maggs, 2008). Moreover, thrombin also amplifies platelet activation by cleavage of PAR1, resulting in stimulation of numerous of GPIIb/IIIa platelet receptors that flip in the membrane of the outer surface of platelet, and produce aggregates (Joo, 2012).

On the other hand, thrombin mediates some biological process that boost anticoagulation and fibrinolysis. This thrombin regulating mechanism is called the negative feedback pathway (Fig 1.3) (Huntington, 2008). TM introduced by endothelial cells inhibits fibrinogen binding at exosite 1 and binds itself instead, forming a thrombin-TM complex that has an anticoagulant effect. This reaction becomes greater in the absence of Na^+ (Dang *et al.*, 1995). Thrombin-TM inhibits further endothelial cell and platelet activation, and activates TAFI to TAFIa, which inhibits fibrinolysis (Huntington, 2008). Also, APC is generated at the time protein C (PC) is binding to endothelial protein C receptor (EPCR) and reacts with thrombin-TM, which is binding to endothelial membrane (Licari & Kovacic, 2009). Then, APC forms a complex with protein S (PS) to catalyse FVa and FVIIIa inactivation, which directly reduces the rate of thrombin generation. In addition, APC raises fibrinolysis by inhibiting plasminogen activator inhibitor-1 (PAI-1) that inhibits plasmin formation and as a consequence reduces the level of fibrinolysis (Licari & Kovacic, 2009).

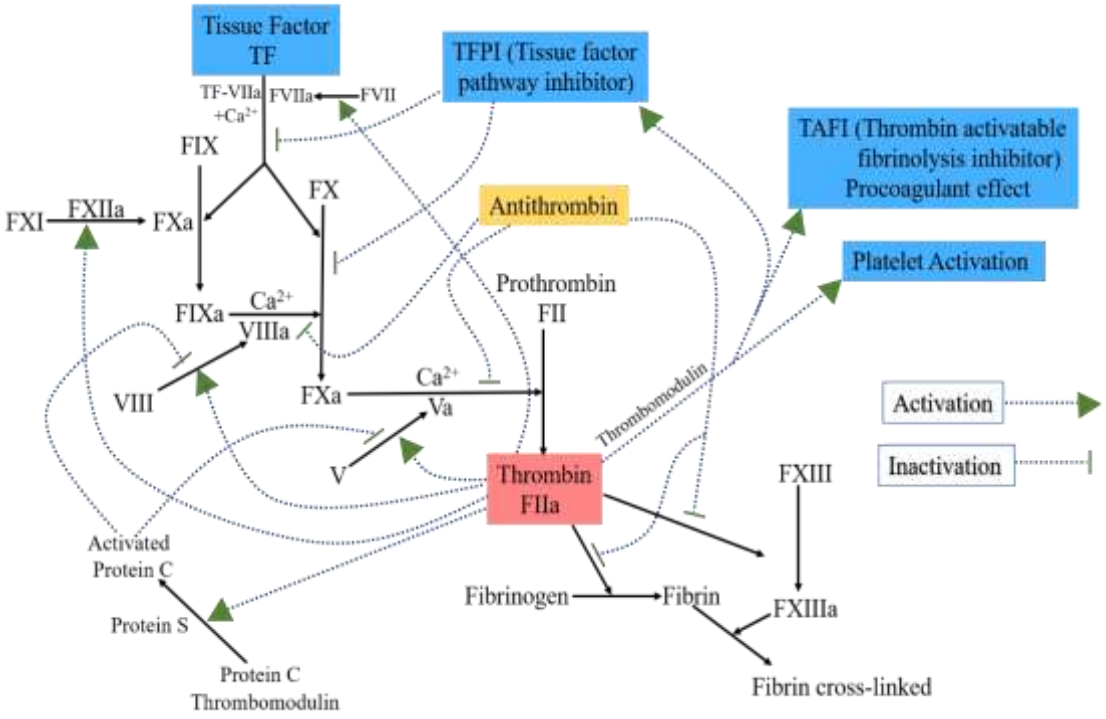

Figure 1- 3: Thrombin amplification mechanism.
Adabted from (Licari & Kovacic, 2009).

1.4 Thrombin dysfunction

Thrombin dysfunction results in thrombo-haemorrhagic disorder identified by immoderate thrombin generation that lead to its dissemination all over the systemic circulation (Stief, 2006). Over activation of endothelial and monocytes cells involved in some diseases due to excessive release of TF stimulates thrombin production throughout the coagulation cascade. Platelet depletion occurs under abnormal thrombin production leading to altered shape and aggregation of platelets (Gentry & Wood, 2005). In many cell types such as platelets, monocytes, fibroblasts, myocytes, etc., thrombin has cellular effects that are mediated through protease-activated receptors (PARs). After the receptor is activated by thrombin its activation is irreversible. Under normal conditions these PARs are biologically replaced; however, excessive thrombin production induces a systemic inflammatory response (Licari & Kovacic, 2009). Moreover, these PARs have the ability to stimulate cell growth and

differentiation, macrophage, endothelial, and smooth muscle cell proliferation, and angiogenesis, which are important to enhance healing of tissues, thus suggesting involvement of thrombin in tumour biology under abnormal thrombin conditions (Licari & Kovacic, 2009). Fibrinolysis is hindered because of high concentration of PAI-1, which inhibit plasmin generation, and elevate the level of TAFI, which increase clot resistance to plasmin. Due to the rambunctious inflammatory response, the anticoagulant mechanism including antithrombin, PC, and tissue factor pathway inhibitor (TFPI) is damaged as a result of reduction of TM and EPCR (Gentry & Wood, 2005).

1.5 Transglutaminase

Transglutaminases (TGs) are ubiquitous and widely distributed enzymes in most of mammals, they were first isolated from guinea pig liver and characterised in the late 1950s (Clarke *et al.*, 1959). Clarke *et al.* (1959) described these proteins as having the ability to catalyse calcium-dependent post-translational modification of other proteins. As shown in Table 1.1 currently there are nine genes identified as encoding TG isozymes, named TGs 1-7 and FXIII, which are catalytic forms, and the ninth one is erythrocyte membrane protein band 4.2, which is a structural and non-catalytic form (Grenard *et al.*, 2001). The circulating zymogen FXIII was the first characterized TG in blood plasma; it is converted to its activated form (FXIIIa) in a thrombin depended manner to promote fibrin clot stabilization (Griffin *et al.*, 2002). TGs 1-7 and FXIII shared the same amino acid sequence at the active site (Trp-Cys-His-Asp), whereas protein 4.2 has an alanine mutation of the active site cysteine and is therefore catalytically inactive (Korsgren *et al.*, 1990).

From the family members FXIII and TG1 have an additional pro-peptide sequence in the NH_2 terminal that may be cleaved to form the active enzyme (Iismaa *et al.*, 2009). The transamidation reaction of TG is basically initiated by Ca^{2+} binding to form the active form

of TG, which catalyses the post-translational modification of proteins, for example by formation of isopeptide bonds through an acyl transfer reaction between the ε-amino group of protein-bond lysine residues and γ-carboxamide groups of glutamine residues to form ε(γ-glutamyl) lysine bonds (Lorand & Graham, 2003). The mechanism of this reaction includes two main steps. First, the acyl donor glutamine substrate binds to the catalytic site of enzyme to form a thioester bond with the exposed cysteine of activated TG, and ammonia is released. Second, an amine donor binds to a thioester intermediate bond and reforming the enzyme catalytic active site. If the primary amine is the amine donor at selected peptide-bound glutamine residues, the amine incorporation reaction will be the resultant protein post-translational modification (Klöck & Khosla, 2012). On the other hand, if the implicated group is peptide-bond lysine, the reaction will result in the crosslinking of the two proteins. However, the reaction will result in deamidation if the group is water molecule, TG reactions described in Fig 1.4 (Griffin *et al.*, 2002; Iismaa *et al.*, 2009; Eckert, 2014). TGs modulate variety of activities such as membrane stabilization, signal transduction, and protein polymerization, which in turn regulate an enormous range of physiological functions (Eckert, 2014; Schröder & Kohler, 2013).

Table 1- 1: Members of the transglutaminase (TG) enzyme family.
TG classification and synonyms, molecular weight, tissue distribution, biological functions. Modified from (Odii & Coussons, 2014).

Identified TG forms	Synonyms	Molecular mass in kDa	Tissue expression	Prevalent function
FACTOR XIII	Fibrin stabilizing factor Plasma transglutaminase	83	Plasma, platelets, chondrocytes, astrocytes, monocytes, macrophages, heart, eye, dendritic cells	Stabilization blood clot, wound healing, bone growth, ECM stabilization
TG1	Keratinocyte transglutaminase, type 1 TG	90	Keratinocytes, membrane, squamous epithelia, and cytosol.	Keratinocytes epidermal differentiation and cell envelope formation
TG2	Tissue transglutaminase, type 2 TG, Gαh, cytosolic transglutaminase, liver TG	78	Ubiquitous in many different tissues, cytosol, membrane, nucleus and extracellular	ECM adhesion, matrix stabilisation, cell differentiation, cell survival, signaling, apoptosis
TG3	Epidermal transglutaminase, type 3 TG, TGE	77	Epidermis, hair follicle, cytosol, brain	Keratinocyte differentiation, GTPase activity, terminal differentiation of cell envelope formation
TG4	Prostatic transglutaminase, type 4 TG, TGP	77	Prostate gland, seminal plasma, prostatic fluids	Prostate isoform, reproduction and fertility, semen coagulation in rodents
TG5	Type 5 TG, TGX	81	Epithelial tissues	Keratinocyte differentiation and cornified cell envelope assembly
TG6	Type 6 TG, TGY	78	Skin epidermis	Development and motor function
TG7	Type 7 TG, TGZ	81	Ubiquitous	Not characterised
BAND 4.2	Erythrocyte membrane protein band 4.2	72	Erythrocyte membranes, bone marrow, spleen, foetal liver	Maintain erythrocyte membrane integrity and mechanical properties

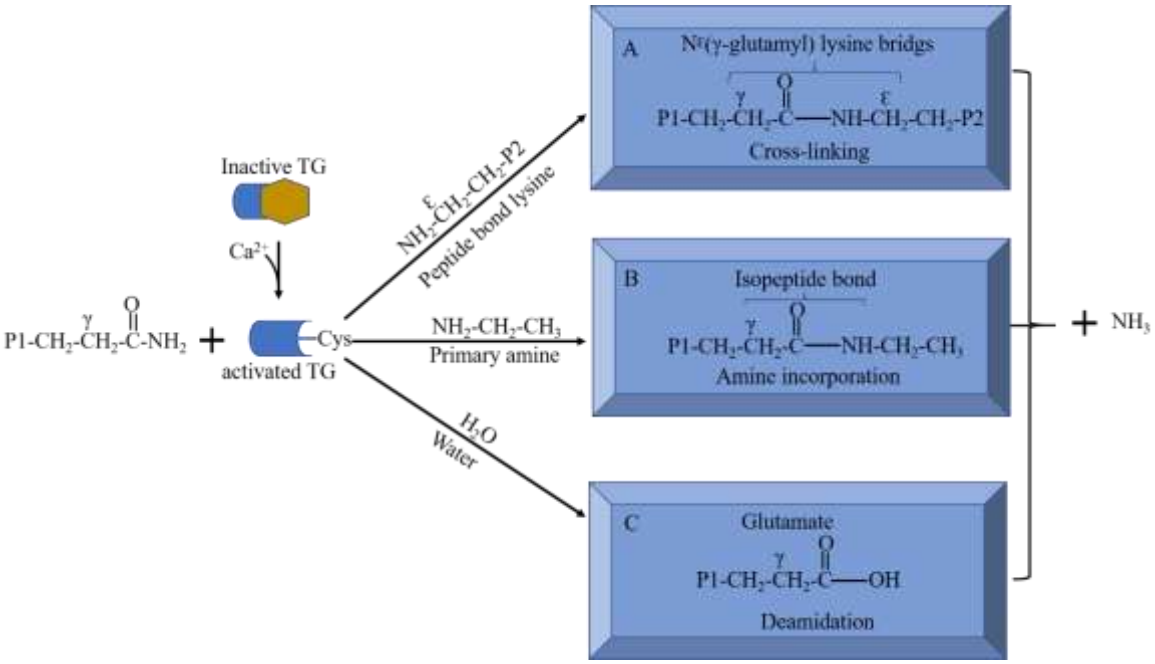

Figure 1- 4: Transglutaminase transamidation reaction.

Pathway A represent the protein crosslinking reaction between γ-carboxamide group of peptidyl glutamine residue (P1) and ε-amino group of peptidyl lysine residue (P2). Pathway B illustrates the amine incorporation reaction between a γ-carboxamide group of glutamine residue and a primary amine. Pathway C shows the deamidation reaction between γ-carboxamide group of glutamine residue and water molecule (Adapted from Algarni, 2018).

1.6 FXIII

The history of FXIII started more than 70 years ago, when it was known as fibrin stabilizing factor (Loewy *et al.*, 1961). In the early 1960s it was termed factor XIII by the International Committee on Blood Clooting Factor until 2007, when it was recommended by the International Society of Thrombosis and Haemostasis, Scientific and Standarization Committee that it should be abbreviated and termed FXIII (Muszbek *et al.*, 2007). In the beginning, FXIII was not a topic of high interest for research until the early 1980s, when it became a more attractive field of research (Muszbek *et al.*, 2011). It circulates in blood as heterotetramer A_2B_2, the A_2 subunit always forming a complexed with the B_2 subunit in

normal condition but only the B_2 subunit is present as free dimer in plasma (Muszbek *et al.*, 1999).

1.6.1 FXIII structure

The plasma transglutaminase (FXIII) complex consists of heterotetrameric ensemble (pFXIII-A_2B_2) (with a total molecular mass of approximately 326 kDa). The dimer catalytic A-subunits (FXIII-A_2) each have a molecular weight of ~83 kDa and are encoded by the F13A1 gene. The A subunits are encapsulated by dimer carrier B-subunits (FXIII-B_2) each of which has a molecular mass of ~80 kDa (Iismaa *et al.*, 2009; Muszbek *et al.*, 2011). FXIII-A contains five domains: The N-terminal activation peptide (AP-FXIII), a β-sandwich domain, a catalytic core including catalytic site Cys314, β-barrel 1, and β-barrel 2 (Fig 1.5) (Muszbek *et al.*, 2011; Schröder & Kohler, 2013; Shi & Wang, 2017). FXIII-B is present as free form FXIII-B_2 and complexed form as part of the ensemble FXIII-A_2B_2 in plasma, and serves as a carrier protein of FXIIIA that accelerates cross-linking fibrin monomers by boosting formation of the complex between proenzyme FXIII, fibrinogen, and its activator thrombin (Schröder & Kohler, 2013; Souri *et al.*, 2015). Also, a free form of FXIII-A_2 exists but only in intracellularly, denoted as either (cellular) cFXIII or cFXIII-A_2, mainly in platelets, megakaryocytes, monocytes, macrophages, chondrocytes, osteocytes and osteoblasts (Schröder & Kohler, 2013).

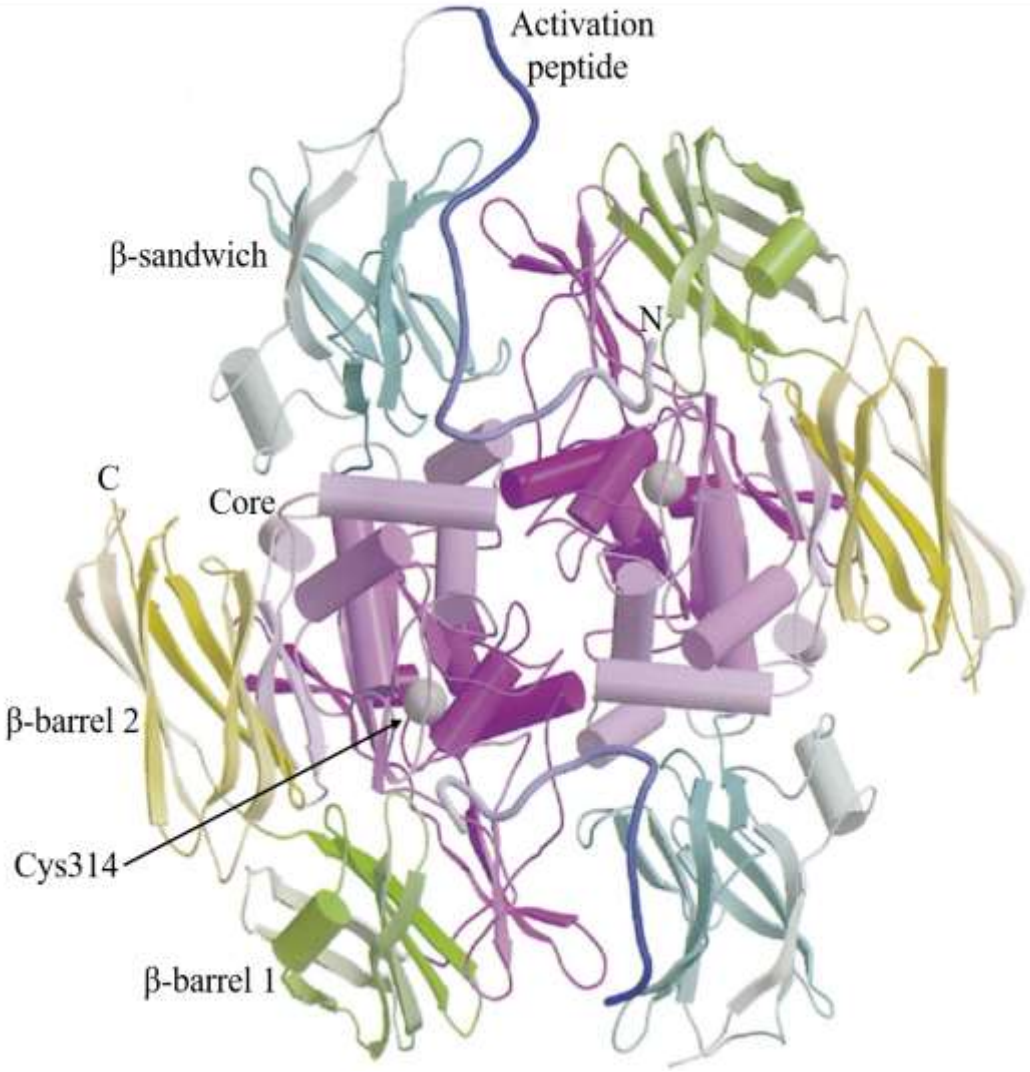

Figure 1- 5: FXIII-A_2 subunit structure.

The genral structure of the factor XIII A_2 dimer. Cylinders and arrows represent α-helices and β-strands, respectively, and the two active sites are marked by gray spheres. The N- (activation peptide) and C-terminal and structural domains of one A-subunit are labeled. Adapted from (Muszbek *et al.*, 1999).

1.6.2 FXIII activation

FXIII circulates in plasma as an inactive zymogen that is activated only at sites of vascular injury. The proteolytic FXIII activation is triggered when thrombin cleaves off AP-FXIII by hydrolyzing Arg37-Gly38 and weakens the interaction between A- and B- subunits (pXIII-A'_2B_2) (Muszbek *et al.*, 2011). Then, the B-subunits dissociate in a calcium-dependent manner via interactions with high affinity Ca^{2+} binding sites on A-subunits, a type of activation which requires much more than physiological Ca^{2+} concentration (Iismaa *et al.*,

2009; Muszbek *et al.*, 2011). Thence, (pXIII-A'$_2$B$_2$) becomes completely transformed to an active form pFXIIIa or pFXIII-A$^*_2$, which exposes the intermediate thioester bond at Cys314 in the catalytic sites of A-FXIII for the transglutaminase reaction to form a covalent bond between a peptide bond of γ-glutamine and ε -lysine residue, as shown inFig 1.5 (Schröder & Kohler, 2013). Both pFXIII activation steps are greatly enhanced by fibrinogen/fibrin (Schröder & Kohler, 2013; Shi & Wang, 2017). The non-proteolytic intracellular FXIII activation is a thrombin-independent way to generate activated cellular FXIII (cFXIIIa, or cFXIII-A$_2^o$) based on even low concentrations of Ca^{2+}. However, the studies showed that the elevation of intracellular Ca^{2+} level is induced by thrombin or Ca^{2+} ionophore, which initiates the intracellular activation of cFXIII without proteolysis (Muszbek *et al.*, 2011; Bagoly *et al.*, 2012). Interestingly, complete activation of dimer FXIII-A can occur if only one of AP-FXIII of A-subunit is released so, thus a dimer comprising a cleaved and an uncleaved A-subunit (FXIII-A*A^o) can have a full enzymatic activity (Muszbek *et al.*, 2011).

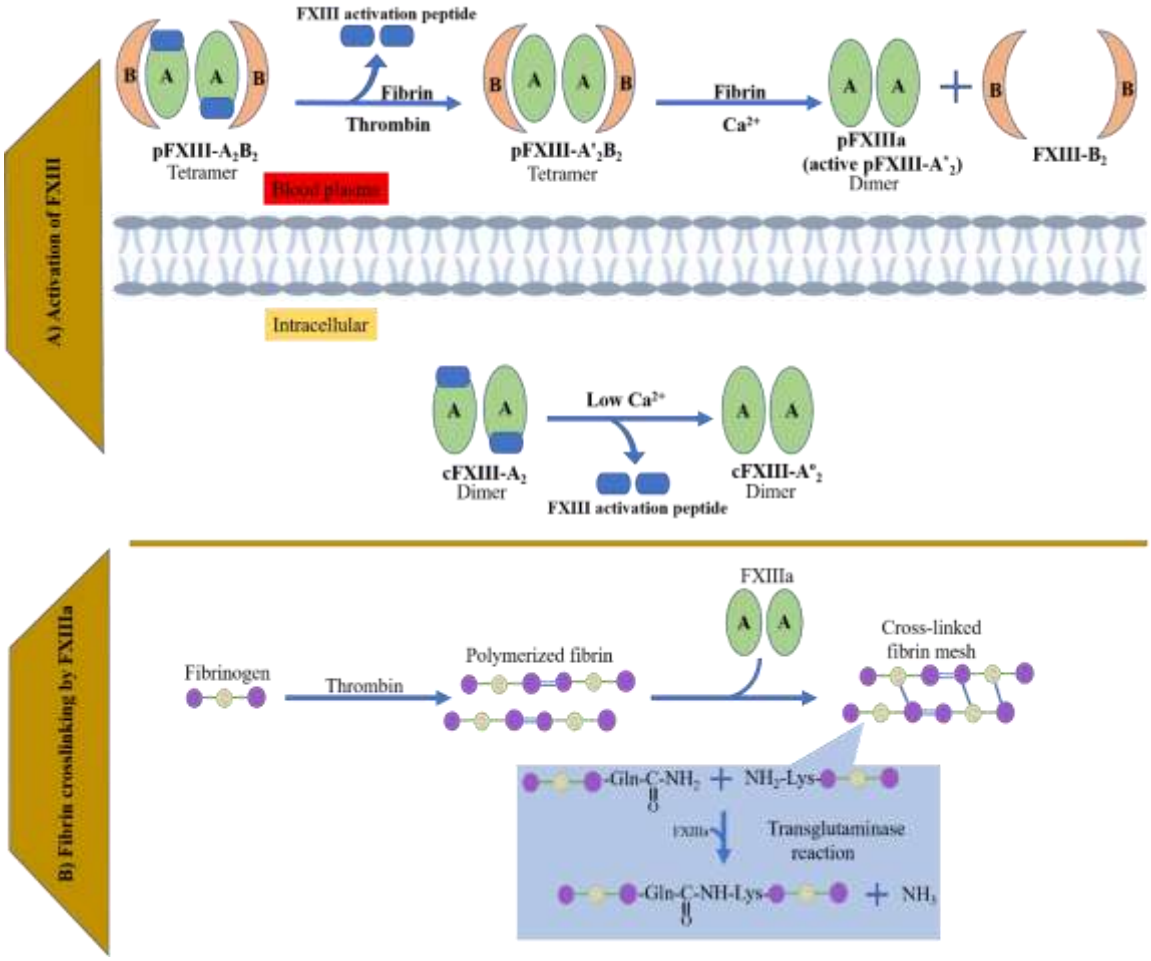

Figure 1- 6: Activation of plasma and cellular FXIII.

A) In blood plasma thrombin initiated the activation and cleave FXIII to pFXIII-A'$_2$B$_2$, in the presence Ca^{2+} the FXIII-B subunit disassociates and fibrin accelerates this process to produce the activated form (pFXIIIa or pFXIII-A$^*_2$) of FXIII. However, intracellular activation occurs at low Ca^{2+} concentration that converts FXIII to the activated form cFXIII-A$^o_2$. B) Transglutaminase reaction mediated by activated FXIII (FXIIIa) that cross-links glutamine (Gln) and Lysine (Lys) residues of fibrin monomers, which leads to an insoluble fibrin network.

1.6.3 FXIII functions

1.6.3.1 Haemostasis and thrombosis

The pivotal extracellular role of pFXIIIa in blood coagulation comes in the final stage of the blood clotting cascade, where it acts in stabilizing the fibrin mesh (Dahlbäck, 2000). In the coagulation process, pFXIIIa catalyses the covalent linkage of fibrin monomers at injury sites to form an insoluble clot. pFXIIIa cross-links both fibrin and fibrinogen, although the

reaction with fibrinogen is slower (Muszbek *et al.*, 2011, Mouapi *et al.*, 2016; Shi & Wang, 2017). pFXIIIa by transamidase activity cross-links fibrin γ- γ, γ- α, and α-α chains into fibrin clots (Richardson *et al.*, 2013; Hethershaw *et al.*, 2014). The γ-chains are immediately cross-linked into dimers, although α-chains are more slowly reactive to polymerize into multimers (Muszbek *et al.*, 2011). It was reported that pFXIIIa also cross-links α2-antiplasmin (α2-AP) to fibrin, which results in raising the rigidity and strength of the fibrin clot and protects it from circulation shear stress (Muszbek *et al.*, 2011; Hethershaw *et al.*, 2014). Furthermore, pFXIIIa has important protection roles in haemostasis process by influencing fibrinolysis by reacting with other proteins into fibrin(ogen) by crosslinking. For example, α_2-plasmin inhibitor (α_2-PI) the main fibrinolytic enzyme plasmin, which is cross-linked to α-chain of fibrin(ogen) to produce fibrin clot degradation (Muszbek *et al.*, 2011; Shi & Wang, 2017). Moreover, another fibrinolysis agent that are cross-linked to fibrin clot by pFXIIIa include plasminogen activator inhibitor type 2 (PAI-2) and thrombin activatable fibrinolysis inhibitor (TAFI) (Muszbek *et al.*, 2011; Shi & Wang, 2017).However, studies showed that upnormal excusive pFXIIIa level in plasma causing an elevation of extent of fibrin α-chain cross-linked that inhibit the clot degradation (Muszbek *et al.*, 1999).

1.6.3.2 In monocyte/macrophage function:

cFXIII-A_2 was discovered in monocyte and macrophage since 1980s (Henriksson *et al.*, 1985; Muszbek *et al.*, 1985), and its expression in suspended monocyte and attached macrophages has been under intensive research that turned out to be a marker reaction of these cell physiological and pathological sub studies (Quatresooz *et al.*, 2008). cFXIII activity in monocyte long-term culture showed three to four-fold increase on day 8 in culture (Conkling *et al.*, 1989). However, this fold increased in monocyte/macrophage differentiation on day 3 (Sárváry *et al.*, 2004). Interestingly, the cFXIII level was observed to increase more in monocytic leukemia cells compared to the normal peripheral blood

monocytes (Kappelmayer *et al.*, 2005). Many reports revealed the presence of cFXIII in monocytes, macrophages, dendritic cells, histiocytes, placenta, and uterus but only few studies focused on intracellular function of cFXIII in these cells (Bohn & Schwick, 1971; Polgar *et al.*, 1990; Koseki-Kuno *et al.*, 2003; Muszbek *et al.*, 2011). It has been found that monocytes in FXIII-deficient patients that are exempt of cFXIII, showed defective capacity of Fcγ receptors, complement, and receptor-mediated phagocytosis (Sárváry *et al.*, 2004). Another study revealed that the expression of cFXIII and quantity of phagocytosing monocytes/macrophages in cell culture were increased, but after the addition of monodansylcadaverine (MDC), a competitive inhibitor and transglutaminase substrate, a significant inhibition in receptor-mediated phagocytosis was found (Kávai *et al.*, 1992). Dendritic cells deficient cFXIII showed significant inhibition of basal migration and response of chemokine CCL19, cell component induce the migration (Jayo *et al.*, 2009). Also, of interest were the covalent cross-linked cellular angiotensin receptor 1 (AT_1) dimers that play a role in cell signaling events, such as enhancing $G\alpha_{q/11}$ stimulated signaling, and the adhesion of monocytes to endothelial cells. AbdAlla *et al.* (2004) reported that cFXIIIa correlated with AT_1 dimerization by covalent cross-linking, since no cross-linking of AT_1 was shown in monocytes of cFXIII-deficient patients. For example, it has been pointed that the AT_1 dimers cross-linked by cFXIIa in mice monocytes promote atherogenesis, but the latter was reduced when cFXIIIa was inhibited as AT_1 dimers were reduced (Eckert *et al.*, 2014). Heretofore, there are limited studies on cFXIII in monocyte cell lines, in this study the human monocyte derived from an acute monocytic leukemia cell lines THP-1 was used to study the effect of organophosphate compounds on FXIII production.

1.6.3.3 Other FXIII functions

FXIIIa is involved in biological process, such as wound healing. It was found that poor wound healing related to FXIII deficiency (Lauer *et al.*, 2002). Inbal *et al.* (2005) reported

that FXIII deficient mice showed significantly limited wound healing, which was alleviated only by FXIII medication. In addition, human concentrated FXIII supplement accelerated wound healing and minimized blood loss in surgical cancer patients (Korte *et al.*, 2009). It has been found that FXIII colocalizes with and binds to extracellular matrix (ECM) assembly sites (Barry & Mosher, 1990). Moreover, the studies revealed that mediation of wound healing is correlated with ECM integrity through direct cell binding and reorganization (Corbett & Schwarzbauer, 1998; Helm *et al.*, 2007). Fibroblasts produce ECM proteins, which form a scaffold for reparative scars and facilitate wound healing. The ECM-bound FXIII increases fibroblast proliferation (Weigel et al., 1989; Sindrilaru & Scharffetter-Kochanek, 2013; Tracy *et al.*, 2016). Also, immobilized FXIIIa adheres to fibroblasts in an integrin-dependent manner, which stimulates activatory signal transduction and formats the cellular change (Ueki *et al.*, 1996; Takahashi *et al.*, 2000, Somanath *et al.*, 2009). Due to the existence of many of FXIII substrates in ECM, such as fibronectin, collagen, thrombospondin, and vWF in addition to plasma proteins like fibrinogen, FXIIIa-mediated protein crosslinking can adjust ECM structure, thereby providing a more appropriate surface for fibroblast migration (Richardson *et al.*, 2013).

FXIII is required in embryo implantation through normal pregnancy and women who have FXIII deficiency experience frequent miscarriages (Ariens *et al.*, 2002). Since FXIII is required for the formation of the cytotrophoblastic shell that enable placental attachment to the uterus (Muszbek *et al.*, 2011). Although, FXIII presence in uterus and placenta suggests the involvement of cFXIII macrophages in normal pregnancy, its function in these cells remains ambiguous. However, it is believed that its function may be associated to the crosslinking of the extracellular proteins in these tissues (Muszbek *et al.*, 2011). Medically speaking, a regular FXIII concentrate supplementation is the optimum and safest method to prevent abortion and end up with successful full-term delivery in FXIII deficient women

(Naderi *et al.*, 2012). Further work is needed to fully understand the mechanism of action of FXIII in pregnancy.

Moreover, it has been suggested that activated plasma or cellular FXIII are involved in some other fundamental biological processes, such as reduction of permeability of vascular supply (Hirahara *et al.*, 1993). A deficiency in pFXIIIa initiates cardiac rupture following induction of ligation myocardial infraction (Souri *et al.*, 2008). High activity of FXIIIa has also been associated with coronary artery disease, thromboembolic disease, venous thrombotic disorders, cerebrovascular disease (Corral et al., 2000; Ariens et al., 2002), and bone and cartilage ECM formation, stabilization and assembly (Johnson *et al.*, 2001).

1.6.3.4 FXIII and TG2

Tissue TG (TG2) is a multifunctional enzyme that exist in both intracellular and extracellular forms (Nurminskaya & Belkin, 2012). TG2 is the most abundant and extensively distributed member of the TG family and it is involved in the modulation of various biological function (Eckert *et al.*, 2014). FXIIIa and TG2 both belong to the same group of enzymes that share some roles through their ability to mediate covalent protein cross-linking activity to modulate biological functions throughout the body (Eckert *et al.*, 2014).

Both of them are released into the vascular ECM, where they covalently modify some proteins of ECM, resulting in the enhancement of ECM stability (Aeschlimann & Thomazy, 2000; Lorand & Graham, 2003). For instance, cross-linking of ECM proteins increases fibronectin and collagen fibril rigidity causing an increase in ECM stiffness (Nelea *et al.*, 2008; Spurlin *et al.*, 2009), which enhances fibroblast and osteoblast adhesion (Chau et al., 2005; Forsprecher *et al.*, 2009). In addition, several studies reported the pivotal role of FXIIIa and TG2 in ECM to boost integrin-mediated signalling in transmembrane adhesion. It has also been reported that extracellular FXIIIa and TG2 are involved in regulation of

growth factor receptor signalling (Takahashi *et al.*, 2000; Kulkarni & Jackson, 2004; Zemskov *et al.*, 2006). Moreover, it has been found that cFXIIIa and TG2 have important roles supporting the cytoplasmic biological processes involved in cell signalling (Lorand & Graham, 2003; Walther *et al.*, 2011). It has been reported that cFXIIIa and TG2 have been identified in cartilaginous and osseous tissues. For example, the cross-linking activity of cFXIIIa and TG2, accompanied by deposition of fibronectin and collagen type 1 into the ECM, is associated with differentiation of osteoblasts (Nurminskaya & Kaartinen, 2006; Cui & Kaartinen, 2015).

1.6.3.5 FXIII deficiency

The average concentration of FXIII in plasma is 21.6 mg/l (0.07µM) (Yorfuji *et al.*, 1988), and recent work using one-step ELISA specific assay for tetrameric complex estimated to be 66-134% of $FXIIIA_2B_2$ (Katona *et al.*, 2000). The normal range of pFXIII activity is between (53.2% - 221.3%), and it has been noted that low levels of pFXIII < 5% are sufficient to allay bleeding (Anwar & Miloszewski, 1999). Congenital FXIII deficiency is due to genetic disorders in the encoding of either in FXIII-A subunit (known as type 2) or FXIII-B subunit (known as type 1) (Hsieh & Nugent, 2008). As a result of such mutations bleeding disorders are the most typical clinical manifestation. Defects in the FXIII-B gene were reported in < 5% of patients; however, the majority of FXIII deficiency reflect type 2 FXIII-A gene defects, which result in FXIII-A subunits being absent from extracellular and intracellular sites (Hsieh & Nugent, 2008). Severe FXIII deficiency is a rare condition that could happen to one in 3-5 million people in an inherited autosomal recessive pattern (Board *et al.*, 1993). Regular coagulation screening tests such as prothrombin time (PT), activated partial thromboplastin time (APTT) and thrombin time, are normal in cases of FXIII deficiency; nonetheless, FXIII deficiency can be detected using the clot solubility test with 5M urea or 1% monochloroacetic acid; in case the patient does not have FXIII deficiency

the clot will not dissolve in the solution, then this can be pursued by another sophisticated quantitative analysis (Karimi *et al.*, 2009).

Umbilical bleeding is the most distinctive and frequent symptom occurring in 80% of cases within a few days after birth (Anwar & Miloszewski, 1999). The intracranial haemorrhage incidence in congenital FXIII deficiency has much higher frequency and patients can face death or disability (Hsieh & Nugent, 2008). In patients with FXIII deficiency, clots can form normally but start to breakdown 24 to 48 hours later due to weak fibrin stabilization, leading to successive occurrence of bleeding such as postoperative, intramuscular, and post dental extraction mucosal bleeding (Hsieh & Nugent, 2008). Other common manifestations of severe FXIII deficiency are frequent spontaneous miscarriage and wound healing delay (Inbal & Dardik, 2006), in addition to its failure in its function in haemostasis, in wound healing, tissue repair and angiogenesis (Inbal & Dardik, 2006).

Acquired FXIII deficiency is the most common. Some cases of acquired FXIII deficiency have been associated with leukaemias, severe liver disease, systemic lupus erythematosus and disseminated intravascular coagulation (Tosetto *et al.*, 1993; Hsieh & Nugent, 2008). Furthermore, liver disease may result in limited production of FXIII-B, causing a decrease in the pFXIII half-life (Karimi *et al.*, 2009). However, acquired FXIII deficiency is mainly caused by some kind of inhibitor. These inhibitors could be autoantibodies directed against pFXIII and interfering with its function (Tosetto *et al.*, 1993). Inhibitors can be produced in association with medication such as penicillin, isoniazid and phenytoin (Tosetto *et al.*, 1993; Hsieh & Nugent, 2008). A further potential source is exposure to environmental pollutants such as organophosphorous compounds, which is the central area of interest to the current project.

1.7 Organophosphate compounds: uses and toxicity

Organophosphate (OPs) are chemical compounds that were synthesized by Lassaigne in the early 1800s, but in the early 1940s Schrader's group developed them into insecticides and synthesized around 2000 compounds, encompassing the pesticide parathion, paraoxon and chemical warfare agents such as sarin and tabun (Antonijevic & Stojiljkovic, 2007). OPs are used widely in agriculture and industry but there is concern that their widespread use may impact on animal and human health (Chambers & Oppenheimer, 2004). OPs are used as insecticides, due to their ability to inhibit insect acetylcholinesterase (AChE) activity, causing hyperactive cholinergic action and accumulation of acetylcholine (Pope, 1999). Also, they are used in industry (e.g. as flame retardants and oil additives) (Chambers & Oppenheimer, 2004). Additionally, to a limited extent, OP compounds are developed to be used as pharmaceutical drugs, for example trichlorfon in the treatment of schistosomiasis (Costa, 2006).

Accidental or deliberate release of OPs are responsible for causing environmental pollution and food contamination, affecting animal and human health, and it has been reported that almost 50% of acute pesticide related illnesses are due to OP toxicity (Calvert *et al.*, 2004). It has been estimated that ≥ 3 million people worldwide are exposed to OPs per year with around 300,000 deaths (Robb & Baker, 2019).

Nowadays, there are diverse practices in the use of OP pesticides in various fields due to their wide-ranging chemical and physical properties. For example, in developing countries they are used against plant pathogens, insects and microbial agents (Lotti, 2010). Some OPs are also applied as anti-wear additives in jet engine lubricants, due to their fire-resistant properties (Solbu *et al.*, 2007; Denola *et al.*, 2011). However, over time, several publications

have reported passengers suffering from chronic symptoms such as cognitive problems and even paralysis (Winder & Balouet, 2000; Harper, 2005; Liyasova *et al.*, 2011).

Potential adverse effects of overuse of OPs pose a significant risk to public health. Due to environmental pollution, it is not only agricultural workers that are in danger of exposure to these insecticides but also the general population are at risk (Mearns et al., 1994; Stephens et al., 1995). Moreover, long term exposure to low concentrations of OP compounds in food sources and the environment may not only cause chronic damage to the nervous system but also other body organs associated with chronic disease, for example: cancer, respiratory problems, cardiovascular, the immune system, etc. (Mostafalou & Abdollahi, 2013).

It was of interest to the current study to investigate the effects of phenyl saligenin phosphate (PSP), the organophosphorothioate insecticides diazinon, chlorpyrifos and parathion and their acutely toxic metabolites diazoxon, chlorpyrifos oxon and paraoxon on haematological parameters such as the activities of serum esterases and FXIIIa found in human plasma and the growth, viability and proliferation of monocyte cells.

1.7.1 Organophosphate compounds structure

All OP pesticides share the same fundamental structure involve an ester of a phosphoric acid derivate; it comprises a pentavalent central phosphate atom (P), which has a double bond with either sulphur (P=S) or oxygen (P=O). R1 and R2 are usually alkoxy side groups, while the X is the "leaving group" that is replaced by the oxygen atom of serine group in the active site of AChE (Fig 1.6) (Eleršek & Filipič, 2011). Many types of OPs have been used in animal and human studies (Lockridge, 2013; Chen & Cashman, 2013). As a part of the current study seven OPs were used, three of which are phosphorothioate compounds (P=S: parathion (PTH), diazinon (DZ) and chlorpyrifos (CPF)), three are their acutely toxic metabolite forms (oxons, P=O: paraoxon (POX), diazoxon (DZO) and chlorpyrifos-oxon

(CPO), and phenyl saligenin phosphate (PSP, the active congener metabolite form of triortho-cresyl phosphate; TOCP) (Fig 1.7).

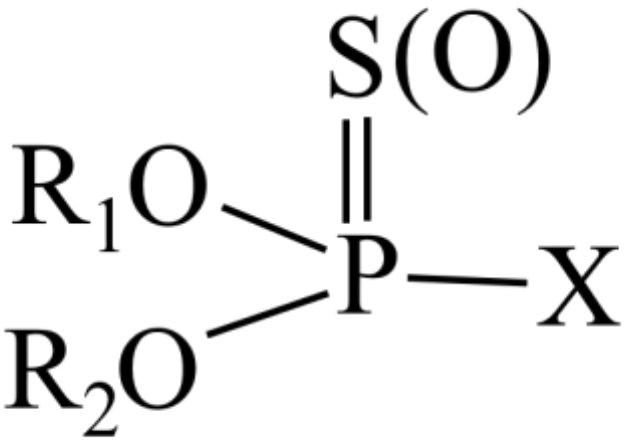

Figure 1- 7: General chemical structure of organophosphorous compound.

Double bond of phosphorus group attached to either sulphur or oxygen atoms. R1 and R2 are mainly alkoxy groups and X is ‘‘the leaving group’’, as it is reacting covalently during the phosphorylation of the AChE active site. Adapted from (Costa, 2006).

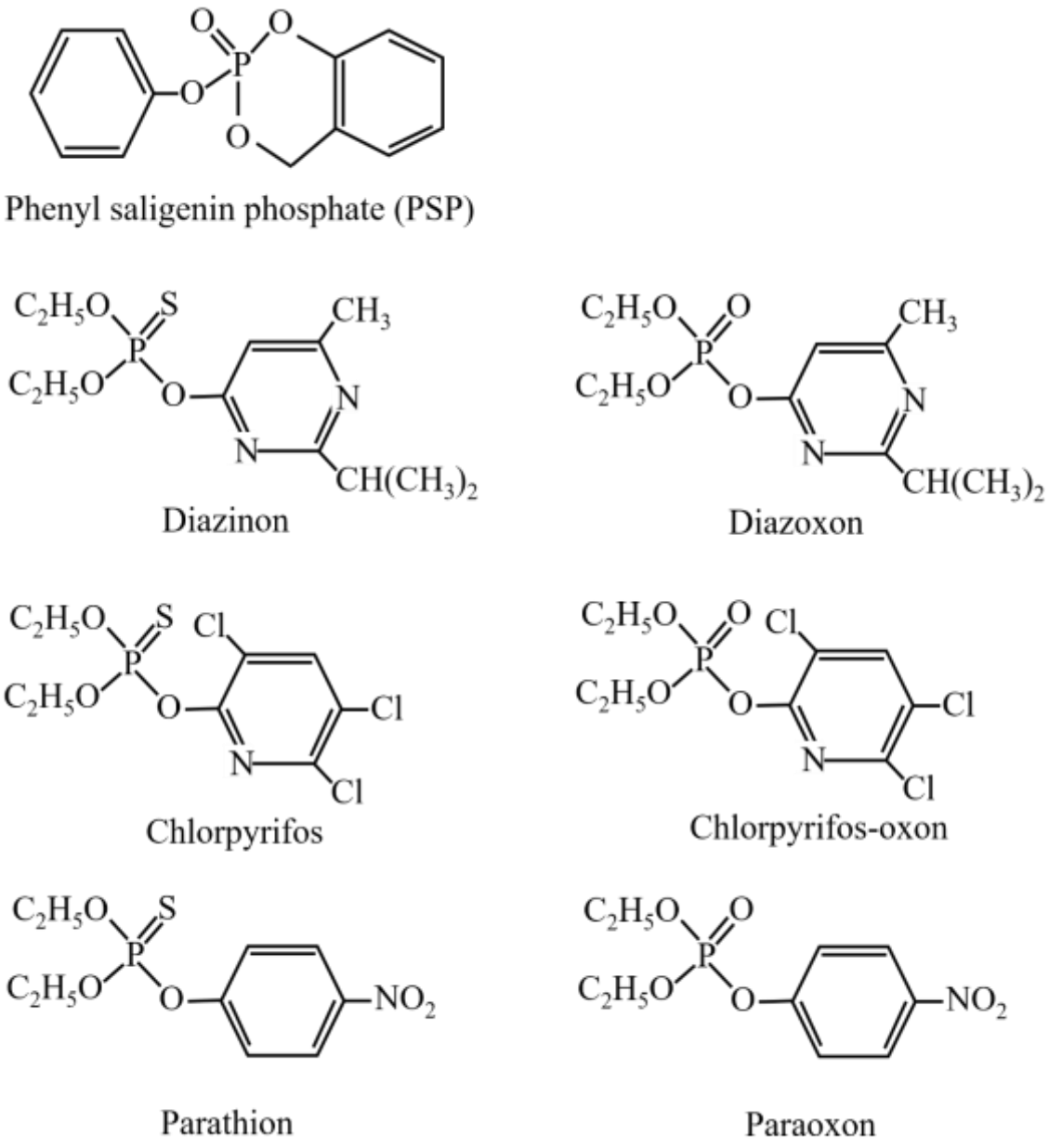

Figure 1- 8: Chemical structure of organophosphorus compounds.

The parent compound with sulfur atom and metabolized form with oxygen atom.

1.7.2 Organophosphate compounds mechanism

OP exposure may occur through ingestion, inhalation or contact with the skin (Karki et al., 2004). The most significant effect of acute toxicity of organophosphate is due to the inhibition of cholinesterases (ChEs). The primary target of OPs in the central nerve system the enzyme AChE, which belongs to the serine hydrolase family and is mainly found at neuromuscular junctions, where it is responsible for hydrolysis of the neurotransmitter acetylcholine (ACh) to produce acetate and choline (Ray & Richards, 2001). The result of AChE inhibition is the accumulation of ACh in the synaptic cleft, thereby overstimulating nicotinic and muscarinic receptors to cause neurotoxic effects, such as neuromuscular paralysis (for example continuous muscle contraction), throughout the entire body (Gupta, 2006).

Inhibition of AChE by OPs involves forming a covalent bond with a serine residue in the active site; as a consequence of this reaction, a transient intermediate complex is generated, which is partially hydrolysed through the loss of the leaving group, resulting in the formation of irreversibly organophosphorylated and inhibited AChE enzyme (Eaton et al., 2008), as shown in (Fig 1.8).

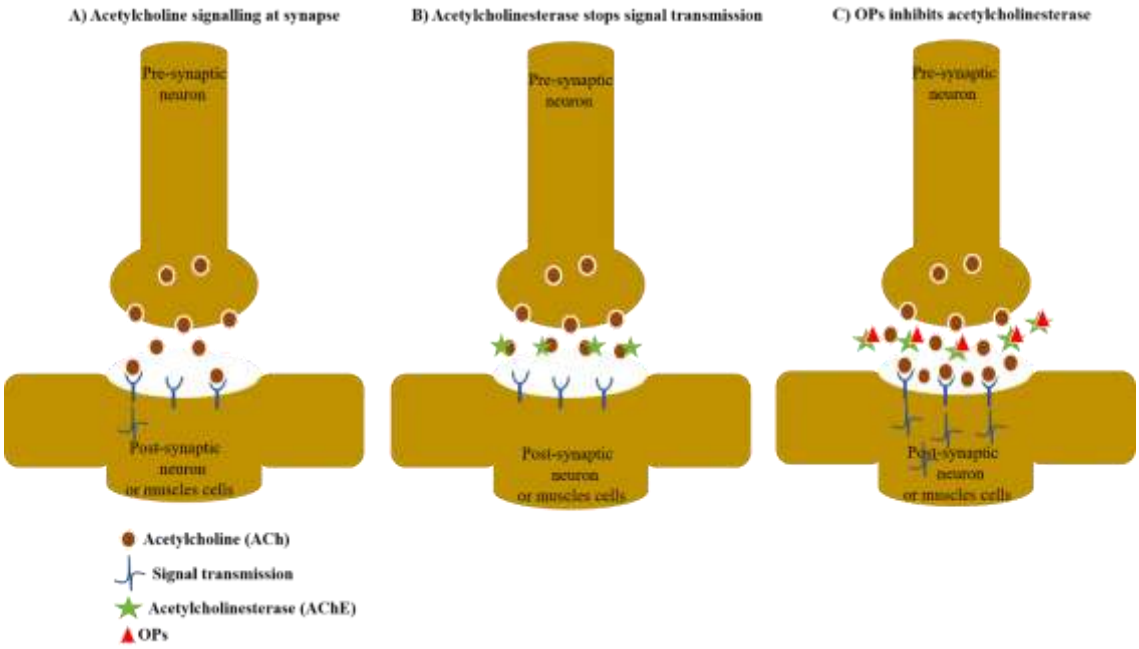

Figure 1- 9: The common organophosphorus compound mechanism.
(A) Pre-synaptic neuron releasing neurotransmitter acetylcholine and bind to receptors on the post-synaptic neuron or muscle cells. (B) AChE terminate ACh function by hydrolysis at cholinergic synapses. (C) Organophosphate compounds bind to AChE and inhibit enzyme action, causing free ACh accumulation at the synapse. Modified from (Felmban, 2016)

Abou-Donia and Lapadula (1990) reported that irreversible inhibition of AChE by different OPs usually happens within a few hours by automatic hydrolysis of the AChE-OP complex in what is termed an 'ageing' mechanism, where a non-enzymatic hydrolysis or dealkylation process results in loss of one or two of the alkoxy labile groups (R1, R2). The different OPs can be hydrolysed either via A-esterases such as paraoxonase 1 (PON1) or B-esterases such as AChE, butyrylcholinesterase (BChE), and neuropathy target esterase (NTE) (Costa *et al.*, 2003). For example, the catalytic hydrolysis of A-esterases is a well-known reaction that leads to detoxication, which involves breakdown OP compounds to their major metabolite components without affecting esterase activity (Costa *et al.*, 2003). On the contrary, the B-esterases exhibit a non-catalytic hydrolysis of OPs that causes significant inhibition of these serine esterase activity but cannot catalytically hydrolyse the OPs (Costa, 2006).

The severity of poisoning symptoms depends on the extent of the OP-AChE binding, where breaking the bond between phosphorous and serine esterase enzyme complex may take few hours to days and may be reversible or irreversible based on the chemical nature of the alkoxy side groups (R) (Chambers, 2004) (Costa, 2006). The reversible reaction of organophosphorylated serine esterase complex is a spontaneous reactivation, which can be accelerated by oximes; however, the irreversible reaction can undergo non-enzymatic hydrolysis process, that so-called aging, which ends up with deactivation of phosphorylated esterase through the loss of one of two alkoxy side groups (R) leaving an increased negative charge in the active site (Costa, 2006), as shown in Figure 1.9.

PON1 and cytochromes (CYPs) are synthesized in liver and circulate in the plasma. They have a protective role against the acute toxic effects of OPs via hydrolysis of both parent or metabolite (oxon) compounds (Coombes et al., 2014). Some CYPs bioactivate the parent compounds of OP to their oxons with different substrate specificities, and some CYPs catalyze reduction reaction that cause detoxification of OPs. Moreover, some CYPs have difference also in detoxification process such as CYP2B6 which metabolise CPF to oxon form and metabolise PTH primarily to p-nitropheol. In addition, PON1 is named from its ability to hydrolyse the oxon of PTH; however, it has found that the mice with deleted PON1 gene are oversensitive to the toxicity of CPO and DZO compared to wild mice (Li et al., 2000).

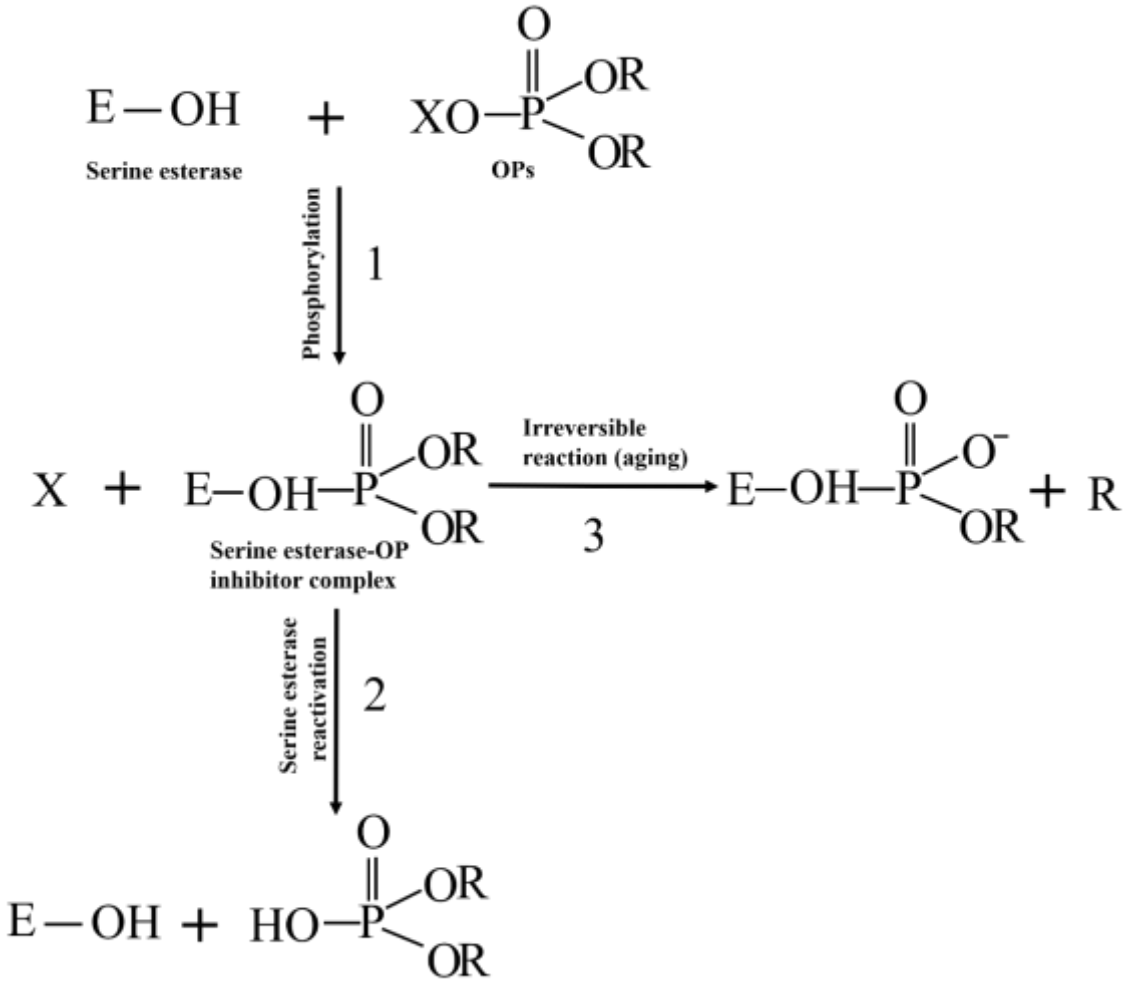

Figure 1- 10: The biochemical interactions between organophosphorus compounds and serine esterase.
Modified from (Costa, 2006).

1.7.3 Characteristics of the OPs used in this study

1.7.3.1 Phenyl saligenin phosphate

PSP (2-hydroxyphenyl) methyl (2-methylphenyl) hydrogen phosphate) (Fig 1.7) is a structural analogue of saligenin cyclic-o-tolyl phosphate (SCOTP), the active metabolite form of tri *ortho* cresyl phosphate (TOCP) (Harp *et al.*,1997; Fowler *et al.*, 2001). TOCP or PSP are not pesticides but are mainly used as anti-wear additives in aircraft engine oil (Abou-Donia & Lapadula, 1990). It has been found that the inhalation of aircraft cabin aerosols can result in memory loss and cognitive dysfunction (De Nola & Mazurek, 2008;

Michaelis, 2011). Comprehensive studies revealed that some OPs, involving PSP and TOCP, interact by organophosphorylation and inhibition of NTE which leads to organophosphate-induced delayed neuropathy (OPIDN) *in vivo* (Abou-Donia & Lapadula, 1990). Studies showed that both PSP and TOCP act similarly to produce neurodegenerative poisoning (Hargreaves, 2012).

Nevertheless, up to date, knowledge is still limited on human exposure to aerosolized jet engine lubricants; this therefore introduces a wide area for research which needs to be undertaken (Baker et al., 2013). PSP has been found to interfere with other cellular targets such as NTE, mitogen-activated protein kinase (MAPK) signaling, cytoskeletal proteins and tissue transglutaminase enzyme activity (Hargreaves *et al.*, 2006; Harris *et al.*, 2009; Pomeroy-Black & Ehrich, 2012). Therefore, it is useful to discuss other targets associated with PSP toxicity, in order to more fully understand the potential molecular basis of PSP toxicity.

1.7.3.1.1 Molecular target of PSP

PSP is known to be a classical NTE enzyme inhibitor (Baker *et al.*, 2013). Moreover, NTE is present in large concentrations in neuronal cells, although NTE activity has been demonstrated at lower levels in non-neuronal tissue and cells such as placenta, testicles, kidney, and lymphocytes (Sigolaeva *et al.*, 2001; Moser *et al.*, 2004; Gallazzini *et al.*, 2006). Organophosphorylation of NTE by OPs is certainly necessary for the development of OPIDN (Costa, 2006). Complete inhibition NTE by PSP leads to prevention of the outgrowth of axon-like processes in differentiating N2a cells (Flaskos *et al.*, 1994). Moreover, NTE inhibition by OP leads to calpain-mediated proteolytic degradation and modification of axonal morphology, which is thought to be an early event of OPIDN (Ehrich & Jortner, 2010).

In addition, studies have reported the effect of PSP toxicity on MAPK and phosphoinositide-3-kinase/protein kinase B (PI-3K/PKB) signaling, which function differently in the neuronal response to OP exposure, as they are normally regulate the vital cell process (Hargreaves *et al.*, 2006; Pomeroy-Black & Ehrich, 2012). Previous studies have shown that phosphorylation of PKB and MEK1/2 protein kinases in human SH-SY5Y neuroblastoma cells was increased by low concentrations (e.g. 0.01-1.0 µM) of PSP (Carlson *et al.*, 2000; Pomeroy-Black & Ehrich, 2012). Furthermore, exposure of differentiating mouse N2a neuroblastoma cells to PSP (2.5 µM; 4 h) led to activation of the extracellular-signal-regulated kinases 1/2 (ERK1/2), which was associated with the inhibition of NTE and neurite outgrowth (Hargreaves *et al.*, 2006). Thus, exposure to OPIDN-inducing OPs disrupts cell signaling pathways important in neuronal survival and differentiation.

1.7.3.2 Diazinon

Diazinon (DZ) (O, O-diethyl-O-(2-isopropyl-4-methyl-6-pyrimidinyl phosphorothionate) and its oxygenated, diazoxon (DZO) analogue (Fig 1.7), are components of one of the most widely used pesticides. Although DZ was banned from certain uses in the USA, it is still commonly used in agriculture in the USA and abroad (Grube *et al.*, 2011). According to the Agency for Toxic Substances & Disease Registry (ATSDR), even though the amount of DZ exposure is most likely small, via ingestion of food from sprayed crops, those people who live close to crops sprayed with such pesticides are at risk for higher exposure to these pesticides and subsequent adverse health effects (ATSDR, 2008). DZ has been restricted due to its greater ability to be trapped in water compared to other pesticides, which makes it move easily to other areas through fog and rain droplets (Larkin & Tjeerdema, 2000). In water, the parent compound DZ can be metabolised to its oxon form (Wu *et al.*, 2007). Studies also found that photolysis based on temperature, pH, and water purity has an important role in DZ degradation in either water or air (Larkin and Tjeerdema, 2000). DZ

has a history of use to control pests on cattle and is a large source of occupational exposure for those who conduct the "sheep-dipping", moreover, some farm workers use this hazardous technique that was found seriously affecting farm workers health, and studies reported that 146 sheep dip-exposed sheep farmers had impaired neuropsychological performance (Stephens *et al.*, 1995; Hatjian *et al.*, 2000).

In vivo, DZ metabolism is mediated by several cytochrome P450 isoforms and B-esterases, which are responsible for its detoxification in liver, blood and intestines. For that reason, resistance to toxicity relies on the balance between bioactivation and detoxification after the exposure to DZ (Poet *et al.*, 2003). DZO is hydrolysed by PON1 to dialkylphosphate, diethylphosphate (DEP) and diethylthiophosphate (DETP), which are excreted in urine (Hatjian *et al.*, 2000). AChE inhibition is the primary mechanism by which DZ and its metabolite form DZO induce neurotoxicity, but other non-cholinesterase targets have been identified. For example, both DZ and DZO have been reported to inhibit neurite outgrowth of axonal processes in the N2a mouse neuroblastoma cell line (Flaskos *et al.*, 2007; Sidiropoulou *et al.*, 2009). It has also been reported that DZ can cause mutagenicity producing chromosome abnormalities and impaired sister chromatid exchange (Cox, 2000). Other studies have shown that DZ toxicity induces renal dysfunction; for example, DZ exposure decreases the activity of glutathione-S transferase and quinine reductase, which leads to elevated levels of blood urea nitrogen and serum creatinine (Shah & Iqbal, 2010).

1.7.3.3 Chlorpyrifos

The chemical structures of chlorpyrifos (CPF) (O, O-diethyl O-3,5,6-trichloropyridin-2-yl phosphorothioate, chlorpyrifos-ethyl) and its oxidation form chlorpyrifos oxon (CPO) are shown in Fig 1.7. Globally, CPF is the OP most extensively used as an active pesticide in the agricultural and non-agricultural sectors, the latter including professional gardens and

homes (Fenske et al.,2002; Eaton *et al.*, 2008). This pesticide is lipophilic (i.e. poorly soluble in water) but it does dissolve in most organic solvents (Ki *et al.*, 2013). There is a wide range of CPF uses to control pests and insects within residential environments and it also is applied to several major crops such as corn, vegetables, and fruits, etc. (Eaton *et al.*, 2008; Salyha, 2010). The usage of CPF is massively increasing, and it is labelled as an EPA (Enviromental Protection Agency, in USA) class II toxicant, as it prompts the same acute toxic effects as the common acetylcholinesterase (AChE) inhibiting pesticides, only there are discordant data in the literature on the mutagenic and carcinogenic potential of CPF (Dreiher *et al.*, 2005; Cui *et al.*, 2006).

CPF enters the body through inhalation, ingestion, dermal contact, and occupational exposure to CPF is very common, with toxic effects suffered by agricultural workers, sheep dippers, pesticide sprayers, farmers and their families; furthermore, a prospective group study showed that CPF manufacturing workers were at risk of CPF toxicity (Albers *et al.*, 2004; Muñoz-Quezada *et al.*, 2012). As for the previously-mentioned OPs, the *in vivo* biotransformation of CPF via oxidation reaction is mainly by CYP450 isoforms such as CYP2B6 and CYP3A4, to form the active metabolite DETP and 3,5,6-trichloro-2-pyridinol (TCP) (Croom et al., 2010). Moreover, PON1 is significantly more efficient at hydrolyzing CPO (Richter et al., 2009). However, exposure to small amounts of more than 0.001–0.01 µg/kg/day of these toxic pesticides is considered a health risk for farm workers (Eaton *et al.*, 2008).

The main target of CPF is the inhibition of AChE, although CPO is a more powerful inhibitor of AChE *in vivo* than CPF (Eaton *et al.*, 2008). Other studies reported that CPF shows neurotoxic effects at concentrations not causing inhibition of AChE (Garcia *et al.*, 2002; Çetinkaya & Baydan, 2010; Zamfir *et al.*, 2011). Nonspecific central nervous symptoms such as reduced motor activity, impairment in the learning skills, memory, and behavior

change, cognitive slowing, depression, and other symptoms are associated with neurodegenerative effects after long term exposure to low doses of CPF (Terry Jr *et al.*, 2012; Yan *et al.*, 2012). Moreover, studies have shown that there is a relationship between long-term low dose CPF exposure, increased weight and induction of thigmotaxic behaviour (Peris-Sampedro *et al.*, 2015; López-Granero *et al.*, 2016)

1.7.3.4 Parathion

Parathion (PTH) (*O*, *O*, diethyl *O*-*p*-nitrophenyl phosphorothioate), and its oxidation form paraoxon (POX) (Fig 1.7) insecticides are used widely in agriculture and public health. Despite the fact that PTH use has been restricted within the USA and EU since the 1980s, it is still used worldwide due to its effectiveness, potency, and low cost (Mutch *et al.*, 1999; Guyton *et al.*, 2015). The metabolism of PTH is the same across species (Guyton *et al.*, 2015). The desulphuration of the pentavalent phosphate group to oxygen analogue (oxon) causes the activation of PTH to POX, which is the more toxic form (Costa, 2006). These compounds are metabolised via a number of activation and detoxification processes that mainly occur in the liver but can also occur in extrahepatic tissues. Parathion is oxidised by CYP450 to form POX, the detoxification of which involves the action of PON1 to produce DEP and *p*-nitrophenol (Costa, 2006).

International Agency for Research on Cancer (IARC), in France 2015, reported that PTH could possibly be carcinogenic to humans (Guyton *et al.*, 2015). For example, in mice parathion induced increases in bronchioloalveolar adenoma and carcinoma in males and lymphoma in females; however, in rats, PTH exposure induced either or combined adrenal cortical adenoma or carcinoma (National Toxicology Program, 1979). A variety of carcinogenic symptoms were observed in pancreatic, thyroid and mammary glands after PTH exposure (Cabello *et al.*, 2001). It has been reported in occupational health studies that

PTH was detected in several tissues and associated with cancers, yet the evidence in humans remains sparse (Guyton *et al.*, 2015).

1.7.4 OPs and serine esterase inhibition

1.7.4.1 Cholinesterase

Cholinesterases (ChEs) are members of the serine esterase family, which belong to hydrolase enzymes that act on different carboxylic esters. They are generally divided in two groups: ‘‘true’’ acetylcholinesterase (AChE) ~70 kDa ‘‘pseudo’’ butyrylcholinesterase (BChE) ~85 kDa, both of them form tetrameric serine esterase glycoproteins complexes (Davis *et al.*, 1997; Marsillach *et al.*, 2013). They can be distinguished basically on kinetic substrate preference, tissues localization, and sensitivity to selective inhibitors; however, they show several points of similarity, including mechanism of action (Davis *et al.*, 1997). AChE is a well-known important enzyme for neuronal signalling, that catalyses the hydrolysis of ACh, a common neurotransmitter in the central and peripheral nervous systems, to choline and acetic acid, to terminate the signal transmission. It is generally found in nerve ending, erythrocytes, spleen, lung, and in the all parts of the brain (Patocka *et al*., 2004; Čolović *et al.*, 2013). The catalytic mechanism of BChE is similar to that of AChE, but it has distinctive characteristics in terms of substrate specificity and inhibitor sensitivity. It is presence in plasma, liver, numerous, pancreas, smooth muscles, intestines, heart, and white matter of brain (Patocka *et al*., 2004; Čolović *et al.*, 2013). Although AChE plays the main role in terminating the ACh transmission action between synapses, BChE may be a substitute for AChE deficiency (Masson & Lockridge, 2010).

ChE are involved in degradation of many drugs and toxins esters, also they are covalently inhibited by OPs. AChE inhibition resulting in accumulation of ACh in the synapses produces an over stimulation of the nicotinic and muscarinic receptors (Pope, 1999). The

oxidized phosphate group of OPs blocks the action of ChEs by organophosphorylating the hydroxyl group of serine in the active site. Furthermore, the loss of one of the OP's alkoxy groups, as explained in fig. 1.6, completely deactivates the esterase, causing irreversible inhibition of 'aged' ChE (Costa, 2006). Inhibition of AChE and BChE activity is nowadays the standard method utilized for the biological monitoring of OP exposure (Marsillach *et al.*, 2013). However, growing evidence suggests that ChEs are not the only targets of OPs, since other enzymes and proteins targets of OPs have been identified (Ray & Richards, 2001; Casida & Quistad, 2005).

1.7.4.2 Neuropathy target esterase

Another crucial serine esterase target for some OPs is neuropathy target esterase (NTE). This enzyme is present in the endoplasmic reticulum and is important for lipid metabolism (van Tienhoven *et al.*, 2002). Furthermore, NTE enzyme displays elevated catalytic activity in neuronal cells, plus non-neuronal cells such as kidney, lymphocytes, and testicles. NTE plays a crucial role in nervous system development and signal transduction (Moser *et al.*, 2000). Therefore, any disruption of neuronal NTE leads to defective endoplasmic reticulum, nerve cell body vacuolation, and unusual reticular aggregates resulting in defects of cellular function (Akassoglou *et al.*, 2004). The inhibition and aging of this enzyme, which has the same mechanism as described for ChEs, is correlated with a disorder called organophosphate induced delayed neuropathy (OPIDN)., which is characterized by shaking of hands and feet, weak muscles, ataxia and loss of sensory function (Abou-Donia & Lapadula, 1990). The symptoms appear after a delay of 10 to 20 days following OP exposure (Abou-Donia & Lapadula, 1990, Goel & Aggarwal, 2007).

1.7.4.3 Acylpeptide hydrolase

Acylpeptide hydrolase (APH) is a serine esterase that hydrolyses acyl peptides; it is present in red blood cells where it modulates detoxification through cleaving N-acetylated peptides (Perrier *et al.,* 2005). It is also present in different tissues including brain and liver (Marsillach *et al.*, 2013). APH activity showed more sensitivity to some but not all OPs than did AChE and BChE, an effect that was observed long after *in vivo* OP exposure due to the long red blood cell half-life; thus, APH inhibition may be detected over a longer period of time compared to ChEs (Quistad *et al.*, 2005; Marsillach *et al.*, 2013). Cardona et al. (2013) revealed that acute CPF exposure can inhibit APH activity up to 31 days until complete activity recovery. *In vivo* exposure to some metabolites of OPs showed the ability to inhibit APH even at lower concentration compared to those required for ChE inhibition (Richards *et al.,* 2000). Based on these observations, APH activity inhibition could be used as a long term biomarker for monitoring OP toxicity.

1.7.5 Other OPs adduct

OP adducts were detected on the tyrosine-411 residue of albumin protein. Albumin is the most abundant blood protein, representing 56 % and 47 % of human and rat plasma protein, respectively (Tarhoni *et al.*, 2008). With a molecular weight of approximately 67 kDa, it is synthesized in and secreted by the liver. Albumin has aryl acylamidase and esterase-like activities but does not have a serine catalytic binding site (Marsillach *et al.*, 2013). The common functions of albumin are maintaining pH and osmotic pressure, but it also has the ability to bind to and transport intracellular biological component such as bilirubin and fatty acids, and also several extracellular compounds and xenobiotics (Tarhoni *et al.*, 2008). The half-life of albumin in plasma is around 20 days in humans and 3 days in rats (Tarhoni *et al.*, 2008). Some *in vivo* and *in vitro* research has already demonstrated the covalent binding of OPs, such as sarin, soman, CPO and PTH to albumin (Black *et al.*, 1999; Li *et al.*, 2007a).

Albumin-OP adduct formation was proposed as suitable biomarker for OP exposure (Li *et al.*, 2010). The administration of low concentrations of OPs did not inhibit AChE activity in mice but OP labelling of albumin was detected mostly on tyrosine-411 (Schopfer *et al.*, 2005). Thus, a protective role of albumin-OP binding was argued, effectively decreasing the amount of OP available for serine hydrolase inhibition (Peeples *et al.*, 2004). It has been revealed that the tyrosine-OP bond is more stable and is, unlike OP adducts to serine active sites on ChEs, resistant to ageing thereby allowing for more time of exposure detection and easily OP-tyrosine identification (Lockridge & Schopfer, 2010). However, as the rate of OP binding with albumin is much slower than for BChE, BChE inhibition is a more sensitive biomarker (Li *et al.*, 2007c).

Other studies detected OP binding at tyrosine residues of bovine tubulin and transferrin from human and mouse (Grigoryan *et al.*, 2008). Moreover, Jiang *et al.* (2010) reported that CPF and CPO adducts were detected on mouse brain tubulin tyrosine residues. In addition, OP adducts were detected on lysine residues on variety of proteins such as human albumin, keratins, bovine tubulins, and mouse transferrin (Grigoryan *et al.*, 2009). The residues of tyrosine and lysine OP-adducts in different proteins without serine active sites suggest that many other proteins could possibly be adducted to OPs.

1.7.6 OP effects on Ca^{2+}-dependent enzymes

PSP, which is associated with OPIDN induction in animal models (El-Fawal *et al.*, 1990; El-Fawal & McCain, 2008), inhibits the neurite outgrowth and induces elevated phosphorylation of the neurofilament heavy chain that is a substrate for TG2 (Hargreaves *et al.*, 2006; Martin *et al.*, 2011). Moreover, it has been suggested that PSP has the capability to increase Ca^{2+}-dependent phosphorylation of proteins and possibly the activity of other enzymes activated by Ca^{2+} (Flaskos *et al.*, 2006). *In vitro* (24 h) exposure of mitotic cultured cells to PSP correlated with the disruption of TG2 activity in cell lysates. However,

inhibition of TG2 activity was observed in lysates from mouse N2a neuroblastoma cells, but in contrast TG2 activity increased in lysates from the human HepG2 hepatoma cell line (Harris *et al.*, 2009). Altered protein level in both cells was suggested to be the main reason for the differences in TG2 activity changes observed (Harris *et al.*, 2009). In addition, Muñoz *et al.* (2010) reported in his study that the TG2 activity in lysates of rat C6 glioma cells exposed top CPF for 24 h showed a significant increase in TG2 activity. These data are consistent with the notion that OP exposure may directly or indirectly disrupt the cellular activity of Ca^{2+} dependent enzymes such as TG2 via interactions with non-cholinesterase targets.

1.7.7 OPs effect on heamatological parameters

Studies have shown that serine esterase and serine protease are sensitive to some OP compounds (Chambers & Oppenheimer, 2004). Blood coagulation-associated protease interactions with OPs are still under investigation, with a few studies showing that thrombin activity is inhibited *in vitro* by some active form of OPs (Quistad & Casida, 2000; Golderman *et al.*, 2016). Petroianu (1997) reported POX-induced prolongation in partial thromoplatin time (PTT) but no change in the prothrombin time (PT) in human blood. They speculated that POX inhibited serine proteases in the coagulation cascade, which caused hypocoagulability, plus alteration in platelet function, which play important roles in coagulation intrinsic pathway activation. This hypothesis was further studied in mini pigs that were injected with paraoxon and produced similar findings (Petroianu *et al.*, 1999). Moreover, it has been reported that DZ and CPF exposure can significantly disrupt a number of haematological parameters, such as CBC (complete blood count) values and biochemical measurements in blood plasma (Ambali *et al.*, 2007; Banaee *et al.*, 2008; Andreadis *et al.*, 2014).

FXIIIa is present in platelets and in monocytes/macrophages, and differentiation of monocytes into dendritic cells results in elevated intracellular level of cFXIII. This suggests that cFXIII may be involved in impaired receptor-mediated phagocytosis in monocytes (Muszbek *et al.*, 2011). One study revealed that 8 days following acute nerve agent poisoning (soman), there was a decrease in the number of hematopoietic stem cell circulating in blood and, blood cell count revealed reductions in lymphocytes and monocytes (Colllomet *et al.*, 2005). Acute myocardial infarction, heart failure, infarct expansion, and cardiac rupture were all observed in FXIII-deficient mice, presumably due to in appropriate recovery of the myocardial tissue (Karimi *et al.*, 2009). In this respect, a case was reported of a 40-year old man was admitted to an Emergency Department with a primary diagnosis of OP insecticide poisoning; after a few days, his condition deteriorated and myocardial infarction was diagnosed (Kumar *et al.*, 2014). Some recent studies at NTU have shown that OP exposure disrupts the cellular activity of TG2 in neural and hepatic cells (Howden, 2006; Harris *et al.*, 2009; Muñoz, *et al.*, 2010). Based on these previous studies it is possible that other types of TGs may be targets of OP toxicity.

1.8 Aims of the thesis

1- To confirm the biological effect of OPs on acetyl and butyryl cholinesterase activity in human plasma and purified enzymes.

2- To study the effect of OPs on pure and plasma FXIIIa and to determine whether OPs interact directly with FXIIIa.

3- To study the effect of OPs on pure and plasma thrombin and whether OPs interact directly with thrombin.

4- To study the effect of OPs on the viability and proliferation of THP-1 monocytic cell line.

Chapter 2: Materials and Methods

2.1 Materials

All laboratory reagents used were high grade and most of them purchased from Sigma-Aldrich Co Ltd (Pool, UK) unless otherwise specified.

Table 2- 1: List of some reagents and material

Reagents	Code	Supplier
Alamar Blue®	BUF012B	Bio-Rad (Watford, UK)
Acetylcholinesterase from *Electrophorus electricus* (electric eel)	C3389	Sigma Aldrich (Haverhill, UK)
Acetylthiocholine iodide	A5751	
Albumin bovine fraction V (BSA)	A1302	Melford (Chelsworth, UK)
AccuGel 29:1 acrylamide (40% (w/v) 29:1 acrylamide/bisacrylamide)	A2-0068	Geneflow (Lichfield, UK)
Ammonium persulphate (APS) (Ultra Pure)	A2-0200	
Bicinchoninic acid (BCA)	23223	Sigma Aldrich (Haverhill, UK)
Butyrylcholinesterase from equine serum	C4290	
β-Mercaptoethanol	M3148	
Casein sodium salt from bovine milk	C8654	
Copper (II) phthalocyanine	C2284	
5-5′-Dithiobis 2-nitrobenzoic acid (DTNB)	D8130	
DL-Dithioothreitol	D0632	

Dimethyl sulfoxide (DMSO)	CHE1854	Fisher scientific, (Loughborough, UK)
Extravidin® Peroxidase	E2886	Sigma Aldrich (Haverhill, UK)
F96 Maxisorp Nunc-immuno plate	148865	Scientific Laboratory Supplies, (SLS, Nottingham UK)
FXIII-substrate peptide F11KA	B010	Zedira gmbh (Darmstadt, Germany)
Human D-Dimer ELISA kit	ab196269	Abcam (Cambridge, UK)
Hydrogen peroxide (H_2O_2) 30% (w/v)	H1009	Fisher scientific, (Loughborough, UK)
Iodacetamide	I1149	Sigma Aldrich (Haverhill, UK)
Methanol analytical reagent grade	M400/17	Fisher scientific, (Loughborough, UK)
N-(5-Aminopentyl)biotinamide trifluoroacetate salt	A5348	Sigma Aldrich (Haverhill, UK)
N,N,N',N'-tetramethylethylenediamine (TEMED)	EC503	
Phosphatase inhibitor cocktail	B15001-B	Bimake.com (Ely, UK)
Protease inhibitors cocktail Set III, EDTA free	539134	Calbiochem (Watford, UK)
ProteoPrep® Immunoaffinity Albumin and IgG Depletion kit	PROTIA	Sigma Aldrich (Haverhill, UK)

Pure human rFXIIIa activated	T070	Zedira gmbh (Darmstadt, Germany)
4X ProtoGel Resolving Buffer (1.5M Tris-HCl, 0.4% SDS, pH 8.8)	B9-0010	Geneflow (Lichfield, UK)
ProtoGel Stacking Buffer (0.5M Tris HCl 0.4% SDS, pH 6.8)	B9-0014	
Sar-Pro-Arg-p-nitroanilide dihydrochloride Thrombin substrate	S9009	Sigma Aldrich (Haverhill, UK)
S-Butyrylthiocholine iodide	20820	
Sodium phosphate monobasic (anhydrous)	S-8282	
Sodium phosphate dibasic (anhydrous)	S2002	Melford (Chelsworth, UK)
SuperSignal™ West Pico Plus Chemiluminescent Substrate	34577	Fisher scientific, (Loughborough, UK)
3,3′,5,5′-Tetramethylbenzidine (TMB)	T2885	Sigma Aldrich (Haverhill, UK)
Thrombin from human plasma	T1063	
Tris(hydroxymethyl)aminomethane	B2005	Melford (Chelsworth, UK)
Whole human plasma	P9523-5ML	Sigma Aldrich (Haverhill, UK)

2.1.1 Western Blot reagent

Amersham Protran 0.2 μm pore size nitrocellulose membrane from General Electric.

Table 2- 2: Antibodies.

Antibodies	Working dilution (western blotting)	Code	Supplier
Factor XIIIA (A-4) mouse monoclonal	1:500	9271122	Santa Cruz Biotechnology (Wembley, UK)
Anti-mouse IgG-HRP	1:500	A4416	Sigma-Aldrich (Haverhill,UK)

2.1.2 Cell culture reagents

RPMI-1640 medium containing 4500 mg/l glucose, 2 mM L-glutamine, 1 mM sodium pyruvate, 10mM HEPES, 1500 mg/l sodium bicarbonate was purchased from American Type Culture Collection (ATCC® 30-2001™). Penicillin (10,000 U/ml)/streptomycin (10,000 µg/ml); foetal bovine serum (FBS), phosphate buffered saline (PBS) were all obtained from Life Technologies (Invitrogen, UK). AlamarBlue™ Cell Viability Reagent from BioRad product number (BUF012B). Trypan blue solution 0.4% (w/v) was obtained from BioRad.

2.1.3 Cell culture plastic ware

Sterile cell culture plastic was supplied by Scientific Laboratory Supplies (Nottingham, UK). Disposable Haemocytometer C-Chip slides, were supplied by Labtech International Ltd, UK. Cryotube vials (Nunc brand products), were purchased from Merck Ltd. Leicester, UK.

2.1.4 Cell line

THP-1 is derived from peripheral blood of a 1-year-old male human with acute monocytic leukemia (Scannell *et al.*, 1993). It was purchased from American Type Culture Collection (ATCC® TIB-202™).

2.1.5 Organophosphorus compounds

Dansyl phenyl saligenin phosphate (PSP), rhodamine-labelled and unlabeled PSP were synthesized by Tom Pearson (Supervised by Dr. Chris Garner, School of Science of Technology, Nottingham Trent University). Chlorpyrifos, chlorpyrifos oxon, diazinon, and diazoxon were purchased from Greyhound Chromatography and Allied Chemicals (Birkenhead, Merseyside, UK). Parathion was obtained from Flukar. Paraoxon. Stock concentrations of 100 mM OPs were diluted in DMSO (dimethyl sulphoxide), which was present in all treatments including the control at a final concentration of 0.5 % (v/v).

2.2 Methods

2.2.1 Enzymes activity assays

2.2.1.1 Protein estimation

Protein concentrations in each sample batch were measured by the bicinchoninic acid (BCA) (Smith et al., 1985). Protein assay kit obtained from Sigma-Aldrich and using bovine serum albumin (BSA) as the protein standard. Briefly, Bovine serum albumin (BSA) was prepared in a range of 0-2 mg/ml either in (0.1M Tris-HCl pH 8.5, 5 mM $CaCl_2$ (0.1M Tris-HCl, pH 8.5), or SDS buffer) to produce a linear standard. 20 µl of Standard or protein sample were added to 96-well flat-bottomed plate in triplicate. A volume of 200 µl of working BSA 1% (w/v) (reagent A) and copper II sulphate pentahydrate 4% (w/v) (reagent B) were mixed together in a 50:1 ratio was added to each well then, the plate incubated at 37°C for 30 min. The plate reader was used to read the absorbance at 570 nm

and calibration graph was plotted to measure the protein content of the samples against the BSA standard curve.

2.2.1.2 Sample preparation

2.2.1.2.1 For FXIII activity in human plasma and purified protein

Human plasma was reconstituted in 5 ml distilled water, aliquoted and stored at -20°C for future work. The optimum concentration for each enzyme assay was determined by testing a range of dilutions of reconstituted plasma in 0.1M Tris-HCl pH 8.5. A similar approach was adopted for reconstituted pure recombinant FXIIIa (rFXIIIa). It was found that a plasma protein concentration about 1.5 mg/ml (1/16 dilution) was optimal for amine incorporation assays and about 0.8 mg/ml (1/32 dilution) for peptide crosslinking assays. Also, it was found that optimum concentration for pure rFXIIIa 0.02 ng/ µl was the in amine incorporation and 0.005 ng/µl peptide crosslinking assays. These concentrations gave low back ground signal with optimum linear activity.

2.2.1.2.2 For thrombin activity in human plasma and purified protein

It has been found after testing a range of dilutions of reconstituted human plasma and purified thrombin from human plasma in 0.1M Tris-HCl pH 8.5 that optimum concentration of reconstituted human plasma was 0.2 mg/ ml (1/128 dilution), and for purified thrombin from human plasma was 0.05 U/ml.

2.2.1.2.3 Albumin and IgG depletion from plasma samples

According to manufacturer of ProteoPrep® Immunoaffinity Albumin and IgG Depletion kit from Sigma Aldrich, the procedure of depletion was performed at room temperature 20 °C. First, to remove the storage solution, the bottom tip of spin column was broken, and the red cap was loosened then the spen column was centrifuged in 2 ml collection tube at 8,000 rpm (5,000 ' g) for 10 seconds. After this, 400 µl of equilibration buffer was added to the medium

of the spin column then centrifuged in the manner as the previous step. This step was repeated twice and on the final centrifuge the time was 30 seconds. The buffer in the collection tube was discarded and the spin column was placed into fresh collection tube. In the third step, to deplete th albumin and IgG from plasma, 100 µl of reconstituted plasma was added into spin column and incubate for 10 min at room temperature to ensure the sapmle was immediately adsorded into the medium, otherwise rediluted with equilibration buffer. Next, the spin column was centrifuged at 10,000 rpm (8,000 ' g) for 60 seconds. The eluate in the collection tube was reapply to the same spin column and then reincubated and centrifuged as the previous step. In the fourth step, 125 µl equilibration buffer was added to the spin column then centrifuged for 60 seconds to wash the remaining unbound proteins into same collection tube from third step. Finally, the albumin/IgG depleted plasma in the collection tube was aliquoted and storaged at -80 °C.

2.2.1.3 Preparation of OPs

Master stocks of 1:1 serial dilutions of OPS in DMSO starting from 10 mM were stored at -20ºC. Final concentrations in each activity assay were 50,25, 12, 6, 3, 1.5, 0.8, 0.4, 0.2, 0.1 µM of (PSP, diazinon, diazoxon, chlorpyrifos, chlorpyrifos oxon, parathion, parathoxon) obtained from Greyhound Chromatography (Birkenhead, UK) or Sigma-Aldrich (with the exception of PSP, where was synthesized in-house). They were incubated with samples for 30 min on ice before starting the reaction.

2.2.1.4 Transglutaminase activity assays

2.2.1.4.1 Biotin cadaverine-incorporation assay for TG plasma and purified FXIIIa activity

The biotin-cadaverine incorporation assay of Slaughter *et al.* (1992), which was modified by the method of Lilley *et al.* (1998), was used to measure TG-mediated amine crosslinking

activity. The 96-well plates were coated at 4 ºC overnight with 250 µl of N, N'-dimethylcasein (10 mg/ml) in 0.1 M Tris-HCl, pH 8.5. After the unbound N, N'-dimethylcasein was discarded, the wells were blocked with bovine serum albumin (3% (w/v) in (0.1M Tris-HCl, pH 8.5) for 60 min and washed three times with distilled water. A typical assay comprised 50µl of 0.1 M Tris-HCl pH 8.5 containing either human plasma protein (~1.5mg/ml) or rFXIII (0.02 ng/ µl) samples, and the substrate buffer 150 µl containing the substrate 42.4 µM N-(5-aminopentyl) biotinamide with either 6.67 mM $CaCl_2$ or 2 mM EDTA (0.1M Tris-HCl, pH 8.5) and 1:2000 β-mercaptoethanol, in a total volume of 200 µl per well of 96-well plate. Sample were incubated for 2 h at 37°C, after which the content was discarded, and the plate was washed three times with distilled water. Then, 200 µl of ExtrAvidin peroxidase diluted 1:5000 in bovine serum albumin (1% in 0.1 M Tris-HCL, pH 8.5) were added per well, followed by 60 min incubation at 37°C. The plate was subsequently washed three times with distilled water and prior to color development by adding 200 µl developing solution containing 0.1 M sodium acetate pH 6 and 0.03 % (v/v) hydrogen peroxide and tetramethylbenzidine (TMB 5 mg/ml). The reaction was stopped after 15 min incubation at 25°C by adding 50 µl of 5 M sulphuric acid per well. Then a plate reader was used to measure the enzyme activity at 450nm.

2.2.1.4.2 Peptide crosslinking assay for TG plasma and purified FXIIIa activity

The assay was performed according to the method described by Trigwell *et al.*, (2004) with modifications. Briefly, 96 well microtitre plates were coated overnight at 4ºC with casein (1 mg/ml) in 0.1 M Tris-HCl, pH 8.5 (250 µl per well). The plate was washed three times with distilled water and blocked with 250 µl of 3 % (w/v) BSA in 0.1 M Tris-HCl, pH 8.5 and incubated for one hour at room temperature. The wells were washed as before; then either 150 µl 6.67 mM $CaCl_2$ or 13.3 mM EDTA buffer containing 2.5 µM peptide F11KA

(DQMMLPWPAVAL) and (Hitomi *et al.*, 2009) and 1:2000 β-mercaptoethanol was added to the triplicate 50 µl of the sample (0.8 mg/ml human plasma or 0.005 ng/µl purified human FXIIIa) in each well and allowed the reaction to proceed for 1 h at 37ºC. The reaction development and termination were performed as described in the previous assay.

2.2.2 D-Dimer ELISA

According to manufacturer with minor modification ab-196269 - D-dimer *in vitro* SimpleStep Enzyme-Linked Immunosorbent Assay kit (Abcam) was used to determine and quantify D-dimer protein in human plasma. The assay standards were prepared in 6.67 mM $CaCl_2$ in (0.1M Tris-HCl, pH 8.5). A 75 µl of human plasma protein (~1.5mg/ml) sample was diluted in (0.1M Tris-HCl, pH 8.5) and incubated with organophosphorus compounds final concentration either (25 or 50) µM for 30 min at 4 ºC, then clot formation was made by adding 225 µl of 6.67 mM $CaCl_2$ in (0.1M Tris-HCl, pH 8.5) to plasma sample and incubated further for 3 hours at 37ºC before centrifugation at 10,000 rpm for 30 min, shake the tube gently to disconnect the clot from tube wall. A 50 µl of all standards and samples were added to appropriate well in each microplate strips then 50 µl of the antibody cocktail was added to each well, seal the strips and incubate on shaker for 1 h at room temperature. 1X of the kit's washing buffer was used three times and leave it to dry for few minutes on paper towels. A 100 µl of kit's TMB substrate was added to each well and incubate for 10 minutes in the dark then 100 µl of stop solution was added then shake and read endpoint at 450 nm. Subsequent reaction forms a yellow colour product, which change is proportional to the D-dimer present in the sample.

2.2.3 Acetylcholinesterase activity

A modified method of Ellman *et al.* (1961) was used to measure the acetylcholinesterase activity in human plasma (~1.5 mg/ml) and pure acetylcholinesterase of electric eel (0.4 µg/ml) diluted in 0.1M phosphate buffer pH 7.4 (0.1M of sodium phosphate dibasic pH 9

was added to 0.1M of sodium phosphate monobasic pH 4). A volume of 100 µl of sample was added to the 96-well plate in four replicates, followed by a mixture of 100 µl of substrate solution containing 2.5 mM acetylthiocholine iodide and 100 µl of 1.25 mM of 5,5-dithiobis (2-nitro-benzoic acid) (DNTB) in 0.1M phosphate buffer pH 7.4 to start the reaction. The absorbance change was the recorded every 30 seconds for 10 min at 405 nm using a CLARIOstar microplate reader.

2.2.4 Butyrylcholinesterase activity

Butyrylcholinesterase activity was determined by the modified method of Ellman *et al.* (1961) in human plasma (~1.5 mg/ml) and pure equine butyrylcholinesterase (0.4 µg/ml) diluted in 0.1M phosphate buffer pH 7.4. A volume of 100 µl of sample was added to the 96-well plate in four replicates, followed by a mixture of 100 µl of substrate solution containing 2.5 mM butyrylthiocholine iodide and 100 µl of 1.25 mM of 5,5-dithiobis (2-nitro-benzoic acid) (DNTB) in 0.1M phosphate buffer pH 7.4 to start the reaction. The absorbance change was the recorded every 30 seconds for 10 min at 405 nm using a CLARIOstar microplate reader.

2.2.5 Thrombin activity

Master stock of lyophilized human plasma thrombin was prepared in 250 U/ml in 100 mM Tris pH 8.5 then stored in aliquots at -20 ˚C. 100 µl of Thrombin (0.05 U/ml) in 100 mM Tris pH 8.5 was applied to a 96-well microtiter plate in four replicates, followed by 100 µl of thrombin substrate Sar-Pro-Arg-p-nitroanilide (0.5 mM) in 100 mM Tris pH 8.5, which was prepared from stock solution (30 mM) in DMSO, to start the reaction. The absorbance change was the recorded every 10 minutes for 90 minutes at 405 nm using CLARIOstar microplate reader.

Human plasma protein (~0.2 mg/ml) in 100 mM Tris pH 8.5, it was optimized to equalize the same amount of pure thrombin activity. 100 µl of plasma protein dilution was applied to

a 96-well microtiter plate in four replicates, followed by 100 µl of thrombin substrate Sar-Pro-Arg-p-nitroanilide (1.7 mM) in 100 mM Tris pH 8.5, to start the reaction. The absorbance change was the recorded every 30 minutes for 4 hours at 405 nm using CLARIOstar microplate reader.

2.2.6 Mass spectrometry for purified FXIIIa treated with OPs

Initial Steps:

Sample preparation:

rFXIIIa (5 µg) was diluted in 5µl of 0.1 M Tris-HCl, pH 8.5, thereafter adding 0.1µl of 80 mM PSP, DZO, CPO or POX and control samples received the same volume of DMSO. Samples were incubated for 30 min at 4 ºC. Then 30 µl of 6.67 mM $CaCl_2$ in 0.1M Tris-HCl, pH 8.5 were added, followed by further incubation for 1 h at 37 ºC. This resulted in final concentrations of 200 µM OP and 0.25 % (v/v) DMSO. Then 15 µl of 8 M urea and 1.5 µl of 0.2 % (w/v) Protease MAX ™ (Sigma) were added to the protein solution, which was then mixed by vortexing and 58.5 µl of 50 mM TEAB (Sigma) were added and the mixture incubated on ice for 15 min. The solution was centrifuged at 14,000 x *g* for 15 min at 4ºC. The samples were then transferred into a fresh labelled tubes for the reduction and alkylation steps.

Reduction and Alkylation:

In this step, 1.0 µl of 0.5 M dithiothreitol (Sigma) was added to samples and incubated at 56°C for 20 minutes in a water bath. Following this, 2.7 µl of 0.55 M iodoacetamide (Sigma) were added and the sample mixed well and incubated at room temperature in the dark for 15 min.

Trypsinisation:

This step was carried out using freshly made trypsin by adding 20 µl of 1 mM HCl (Sigma) to re-suspend all trypsin completely. Protein (5µg) together with 100 µl of 50 mM TEAB (Sigma) solution was mixed with 2 µg of trypsin, vortex-mixed and incubated at 37°C overnight with gentle shaking.

Final step:

After trypsinisation, the samples were concentrated using a SpeedVac concentrator for 30-40 minutes. Finally, 20 µl of 5 % acetonitrile (Sigma) /0.1 % formic acid solution (Sigma) was added to the samples, which were then transferred into a new tube.

Each sample was analysed by the John van Geest Cancer Research Centre team on a Sciex TripleTOF 6600 mass spectrometer coupled in line with an Exigent expert nano LC 425 system running in micro flow (5 µL/min) in data dependent (IDA) mode. In brief, 4 µl of each sample were injected and trapped onto a YMC Triart-C18 pre-column (0.3 x 5 mm 300 µm ID) at a flow rate of 10 µL/min for 2 min. The sample was then eluted off the pre-column and onto a YMC Triart-C18 analytical column (15 cm, 3 µm, 300 µm ID) that was in line with the electrospray ionisation source of the 6600 MS. The following linear gradients were used: solvent B (2 % acetonitrile + 0.1 % formic acid) and solvent A (0.1 % formic acid), increasing from 2 % to 40 % over an 87 min time course. Electrospray ionisation was performed by applying +5500 V via a 50 µm electrode using the Duospray source (Sciex). IDA acquisition mode was used with a top 30 ion fragmentation followed by 15 sec exclusion using rolling collision energy. Data was analysed using PEAKS Studio X (Bioinformatic solutions Inc, Canada).

2.2.7 Sodium dodecyl sulphate-polyacrylamide gel electrophoresis (SDS-PAGE) and Western blot

To examine the expression of the proteins of interest, SDS- PAGE and Western blotting were utilized.

2.2.7.1 Preparation of buffers

2.2.7.1.1 10 % (w/v) Ammonium persulphate (APS)

It was prepared by dissolving 0.2 mg of APS into 20 µl of distilled water.

2.2.7.1.2 4X Laemmli Buffer

A total volume of 10.2 ml of 40% (v/v) glycerol, 8% (w/v) SDS, 20 (v/v) β-mercaptoethanol, 0.01% (w/v) bromophenol blue and 0.1 M Tris HCL, at pH 6.8.

2.2.7.1.3 Running buffer

Total volume of 1L containing 25.6 mM Tris-base, 192 mM glycine and SDS 0.1 % (w/v) at pH 8.3.

2.2.7.1.4 Transfer Buffer

Total volume of 1L containing 48 mM Tris-base 39 mM glycine, 0.037% (w/v) SDS and 20% methanol.

2.2.7.1.5 Blocking buffer

1X of Tris-buffered saline (TBS) containing 3% BSA.

2.2.7.1.6 Washing buffer (TBS/Tween 20)

Total volume of 1L of 1X of TBS containing 5 ml of (10%) Tween 20; final concentration (0.05%) of Tween 20 in 1L of 1X of TBS.

2.2.7.1.7 RIPA cell lysis buffer

RIPA solution ingredients for 50 ml is:

- 1.87 ml of 4M NaCl
- 0.5 ml of 0.5M EDTA
- 2.5 ml of 1MTris HCL pH8

- 0.5 ml IGPAL
- 0.5 % (w/v) Sodium deoxycholate
- 0.5 ml 10% (w/v) SDS
- 42 ml distilled water

2.2.7.2 SDS-PAGE

Based on the molecular weight of the investigated proteins, acrylamide resolving gel was prepared in all the experiments (Table 2.3). The resolving gel which separates the proteins by size, the gels were prepared according to manufacturer's instructions (Geneflow Ltd, Staffordshire, UK). A Bio-Rad mini-PROTEAN III™ electrophoresis chamber was used. Spacers, combs and two clean glass plates of 1.5 mm thickness were used. The 8, 10, or 12% (w/v) acrylamide resolving gel mixture was prepared according to protein size. The acrylamide resolving gel mixture was prepared according to the number of gels that were going to be used, as indicated in Table 2.3 Acrylamide polymerisation was then initiated by the addition of the volumes indicated of 10% (w/v) APS and TEMED, after which the mixture was swirled gently. Then 8 ml of resolving gel mixture were transferred into each cast to allow sufficient space for a stacking gel to be added later. Distilled water was carefully overlaid on the top layer of the freshly poured gel mixture to create a smooth interface and prevent any gel shrinkage. The gel mix was allowed to polymerise at room temperature for approximately 30 to 40 min. Once the resolving gel had polymerised, water was removed, the required amount of 4% (w/v) polyacrylamide stacking gel was prepared and polymerised by the adding of 10% APS and TEMED as indicated in Table 2.3. The stacking gel is used in order to allows proteins entry and accumulation at its interface with the resolving gel. Immediately after the stacking gel was poured, a plastic comb 1.5mm (Bio-Rad) was placed to form the sample wells. The gel mixture was then allowed to polymerise for 30 min at room temperature. Following polymerisation, the gels were placed in the

electrophoretic tank to which electrophoresis running buffer was added. The protein samples were performed according to the method described by Laemmli *et al.*, (1970). Briefly, the samples were denatured in 4X Laemmli sample buffer and were heated at 95°C for 5 minutes. The 8, 10, 12 % (w/v) polyacrylamide resolving gel as shown in Table 2.3 for THP-1 cell laysate, (plasma, pure FXIIIa), and pure Thrombin samples; respectively. The samples were loaded along with 5 µl Precision Plus Protein™ all blue standards (GeneFlow) in the left-hand first lane then the rest of samples. To organise the samples in the stacking gel, electrophoresis was run initially at 50 volts for 10 min, then the voltage was increased to 200 volts until the dye front reached the bottom of the gel in 45 min, then gel was removed carefully.

Table 2- 3: Polyacrylamide gel preparation ingredients.
Resolving (8,10,12 % w/v) and stacking (4% w/v), shown are the volumes required of each reagent for a total volume of 20ml.

Component	**Acrylamide resolving gel**			**Acrylamide Stacking gel**
	8%	**10%**	**12%**	**4%**
AccuGel 29:1 40% (w/v)	4 ml	5 ml	6 ml	1.5ml
4X ProtoGel Resolving Buffer	6 ml	5 ml	5 ml	-
ProtoGel Stacking Buffer	-	-	-	2.5ml
Distilled Water	10 ml	9.78 ml	8.78	5.9ml
TEMED		20 µl		5 µl
10% APS		200 µl		25 µl

2.2.7.3 Western blotting

On completion of the separation of proteins by SDS-PAGE, the gel was removed from the plate and the stacking gel was cut off. The remaining resolving gel, which contained the separated proteins, was electrophoretically transferred onto nitrocellulose membrane filters by wet blotting (Towbin et al., 1979). Briefly, before starting the procedure all filter papers, sponges and nitrocellulose membrane were soaked in transfer buffer for 5 min then transfer sandwich was set up on the side of the transfer cassette facing the anode (+) as following steps; sponge – 2 filter paper - nitrocellulose membrane – gel – 2 filter paper – sponge; then bubbles were gently removed. This assembled sandwich was then securely fixed in the transfer cassette and placed into transfer tank that contained transfer buffer. Proteins were transferred at 30 volts was applied overnight at room temperature. After electrotransfer of the proteins, the nitrocellulose membrane was stained by Ponceau red stain (Sigma-Aldrich Co Ltd, Gillingham, UK) to confirm protein transfer from the gel. The membranes were washed with Tris-buffered saline (TBS) then blocked for 1 h at room temperature with 3% (w/v) skimmed milk powder in TBS containing 0.05% (v/v) Tween-20 with mild agitation. Blocking is essential to prevent non-specific binding of the antibodies to the membrane in subsequent steps. Blots were then incubated overnight with gentle agitation at 4°C in blocking buffer containing the primary antibodies (1:500) Factor XIIIa mouse monoclonal (Table 2.2). After incubation, the primary antibodies were removed, and blots washed six times for 10 min in TBS/Tween 20. After washing, blots were probed with the appropriate (1:500) horseradish peroxidase (HRP)-conjugated secondary antibodies for 4 h at room temperature in blocking buffer (Table 2.2). Following six time washing as previous step to remove the unbounded secondary antibody, then developed using the SuperSignal™ West Pico Chemiluminescent substrate (Fisher scientific, UK). Images of the blots were captured by the iBright FL1000 system and the bands were quantified by densitometry using

Advanced Image Data Analysis software (AIDA) (Fuji; version 3.52). All band densities were measured and corrected for background, then normalised to band densities for internal control. Data are expressed as a percentage of the average value of the peak area compared to its corresponding control ± SEM. To confirm uniform protein loading in the gel primary antibodies specific to GAPDH were used

2.2.8 Binding assays

2.2.8.1 Binding of labelled PSP to plasma TG

Pure rFXIIIa (0.2 µg), whole plasma (15 µg), and depleted plasma (15 µg), which was depleted by using ProteoPrep® Immunoaffinity Albumin and IgG Depletion kit was used from (Sigma-Aldrich), pure thrombin (0.5 µg) were prepared in 0.1M Tris-HCL pH 8.5. They were then incubated with or without 25 µM rhodamine-labelled PSP for 30 min at 4 °C. Then 4X Laemmli electrophoresis sample buffer was added and the samples were heated at 95 °C for 5 min, followed by separation by SDS-PAGE. 10% and 12%, polyacrylamide gel was used to (FXIIIa and depleted samples) and thrombin; respectively.

The gel was fixed in 10% (v/v) methanol and 5% (v/v) acetic acid overnight. It was then washed in distilled water before imaging. Digital images of the gel were captured by using LAS4000 imaging system using green light and the bands were quantified by densitometry using (Advanced Image Data Analysis software (AIDA) version 3.52). Protein band were revealed by staining with Coomassie Briliant Blue.

2.2.8.2 Binding Competition assay of PSP

Pure rFXIIIa (0.2 µg) or depleted plasma (15 µg) were incubated at 4 ºC with rhodamine-labelled PSP (25µM; 30 min), unlabeled PSP (100 µM; 15 min) followed by labelled PSP (25 µM; 15 min) or with DMSO solvent alone (0.25 % v/v; 30min). They were then incubated for a further 1 h at 37 ºC. The same experiment was repeated with rFXIIIa (0.2 µg)

and pure thrombin (0.5 µg) with one of each unlabelled PSP, DIZ, DZO, CPF, CPO, PTH, POX (200 µM; 15 min) followed by labelled PSP (25 µM; 15 min) with DMSO solvent alone (0.25 % v/v; 30min). They were then incubated for a further 1 h at 37 ºC.

Then the reaction was stopped by the addition of 1:3 volume of 4X Laemmli electrophoresis sample buffer and the samples were heated at 95°C for 5 minutes, followed by separation by SDS-PAGE as previously described.

2.2.9 Two-Dimensional Electrophorsis (2-DE)

2D gel electrophoresis could separate proteins in a mixture according to their charge isoelectric point or (pI), first dimension going across small gel strip named isoelectric focusing gel (IEF) and the second dimension based on their molecular weight on SDS-PAGE. This reproducible technique enables protein identification when combined with mass spectrometry. and assessment of protein expression levels.

Depleted plasma samples each have (100 µg) in 200 µl were incubated with rhodamine-labelled PSP (25µM; 30 min) or with DMSO solvent alone (0.25 % v/v; 30min). The 200 µl of each sample was then precipitated 1 ml of acetone and kept overnight in -20 °C. After that, the precipitated depleted plasma samples were then centrifuged at 20,000 rpm at 4°C for 15 min and the supernatant removed. The pellets were partially covered to prevent any contamination and left to dry for 1 h in the fume cupboard. Then was added to each sample 120 µl of rehydration buffer (Biolite®ampholytes (pH 3-10), 8 M urea, 50 mM DTT, 0.0002% (w/v) bromophenol blue, 4% (w/v) CHAPS, 0.2% (v/v) Biolite®ampholytes (pH 3-10) in deionised water). In the first-dimension (isoelectric focusing), 120 µl of the sample was applied on to an IEF focusing tray making sure that the spreading of the protein sample was even and makes contact with the cathode and anode of the wires. Then a 7 cm 3-10 pH ReadyStripTM IPG strips (pH 3−10; Bio-Rad, UK) was applied in the IEF tray in contact

with the protein sample without any air bubbles and sample protein was absorbed into the IPG gel to allow a passive rehydration for 1 h at room temperature. After that, mineral oil (Bio-Rad laboratories, Hertfordshire, UK) was added on top of the IPG strip to avoid buffer evaporation. The protein sample then went through active rehydration at 50 V for 16 hours. Once the rehydration was completed, IEF system electrode wicks (Bio-Rad laboratories, Hertfordshire, UK) were added in-between the top of the electrodes in the focusing tray and the IPG strip to ensure an effective focusing and to get rid of excess salt. A linear voltage slope up to 250 V was then applied for 20 min. A second linear voltage slope increasing to 4000 V was applied for 2 h. A rapid voltage slope to 4000 V for 10,000 Volt-hours was then applied. Finally, a rapid voltage slope down to 500V was applied to the gel for 25 h. After that, IPG strips were equilibrated by placing the IPG strips in 2500 µl of equilibration buffer 1 (1.5 M Tris/HCl pH 8.8, 6 M urea, 50 % (v/v) glycerol, 2 % (w/v) DTT, 2 % (w/v) SDS, in deionised water) for 10 min at room temperature with gentle agitation. Equilibration buffer 1 was then removed and 2500 µl of equilibration buffer 2 added (2 % (w/v) SDS, 50 % (v/v) glycerol, 6 M urea, 2.5 % (w/v) iodoacetamide, 1.5 M Tris/HCl pH 8.8, in deionised water) for 10 min at room temperature with gentle agitation. After equilibration, proteins were resolved in IPG strips and applied for the second dimension gel, were proteins are separated according to their molecular size. IPG strips were placed on the top of 10 % (w/v) SDS acrylamide gel (including a stacking gel) as described in section (2.2.7.2). Then a 0.5 cm strip of filter paper was immersed in a mixture of 10 % (v/v) protein ladder (Precision Plus ProteinTM dual standards, Bio-Rad laboratories, UK, Hertfordshire) and 90 % (v/v) 4x Laemmli buffer (40 % (v/v) glycerol, 8 % w/v SDS, 0.01 % (w/v) bromophenol blue, 250 mM TRIS-HCl pH 6.8, 10 % (v/v) β-mercaptoethanol, in deionised water) and placed at the IPG strips side for comparison of molecular weight. Gel molten ReadyPrepTM (Bio-Rad laboratories, UK, Hertfordshire) were then added over the IPG strip. A 1X electrophoresis

buffer was added in to electrophoresis container (Bio-Rad laboratories, UK, Hertfordshire) and 200 V was applied for 45 min to allow protein separation. After electrophoresis, the gels were washed for 5 min in deionised water for three times. The gels were captured by using LAS4000 imaging system using green light and then stained by ProtoBlueTMsafe colloidal coomassie G-250 stain (Bio-Rad laboratories, IK, Hertfordshire), and the gel left for staining overnight at room temperature. After staining, the gel was then washed for 1 h in deionised water to remove any additional background staining. Stained gels were imaged by Syngene G-box with Genesnap software.

2.2.10 Cell culture

2.2.10.1 Growing the cells

Human cells (THP-1) vile was thaw in 2 min in 37°C then immediately moved slowly in1 ml medium worm RPMI-1640 growth medium then mixed gently and moved to 10 ml growth medium and centrifugation at 300 x g at room temperature for 5 min to wash off DMSO of cryoprecipitation. Then the excess medium was thrown and 1 ml of growth medium was added again to resuspend the cell pellet gently then moved them to T25 culture flask contain 5 ml growth medium, then cells were incubated at 37°C in a humidified atmosphere of 95% air /5% CO2. Daily check on the cells, it took five days for the cell recovering and first 5 ml of fresh growth medium was added, then three days later another 10 ml growth medium was added, until the growing of cell become regular and the viability higher than 75% then from now on will move the cells to T75 and subculture and maintain.

Suspended cells (THP-1) maintained in T75 culture flask in RPMI-1640 growth medium each 50 µl of medium supplemented with 2 mM L-glutamine, 10% (v/v) FBS, penicillin (100 U/ml) and streptomycin (100 µg/ml) and 50 µl of β-mercaptoethanol (0.05 mM) which prepared in stock in filter sterilised PBS (170 µl concentrated β-mercaptoethanol to

50 µl sterilised PBS, then refiltered again in a new 50 µl tube and keep it in fridge). Cells were incubated at 37°C in a humidified atmosphere of 95% air /5% CO2.

2.2.10.2 Maintenance and subculture of cells

The suspension cells were passaged every three to five days when the cells density reaches 8 x 10^5 to 1 x 10^6 viable cells/ml not exceed the 1 x 10^6 cells/ml. The cell cultures were either passaged to maintain the cell line or used for the experiment which was established with subsequent resuspension 2 x 10^5 cells/ml as the supplier recommended. The cells were sub-cultured (1:3 split ratio). Experiments were performed on passage numbers 4-25 because later passages would be more susceptible to the effect of genetic drift.

2.2.10.3 Counting and testing the viability of cells for experimental analysis

Cells were split or resuspended for experimental analysis when they reached 1 x 10^6 cells/ml density in the maintenance flasks. Automated cell counting has become the robust alternative process to manual haemocytometer cell counting as it can provide a total cell count in a fraction of the time. TC20 automated cell counter (BioRad, Hemel Hempstead, UK) used as Automated cell counting device. The device utilised prepared TC20 Trypan blue dye (0.4% Trypan blue (w/v) in 0.81% (w/v) sodium chloride and 0.06% (w/v) potassium phosphate dibasic solution). Trypan blue dye is based on the blue acid dye chromophores which react and are taken up by the internal region of non-viable cells through a damaged membrane, whereas viable cells do not take up this dye (Wang, 2006). A volume of 10 µl of cell suspension was added to 10 µl of Trypan blue solution and left for 2 min to allow for cells to be exposed to the stain. A volume of 10 µl of this mixture was then loaded into a chamber of the counting slide. The slide was inserted into the slide slot of the TC20 cell counter and cell counting was automatically initiated as soon as the cell counter detected the presence of

the slide and Trypan blue dye. Viable cell counts per ml were used to determine the volume necessary to seed the cells at a required cell density in growth medium. Density of 2 x 10^5 cells/ml of THP-1 cells was resuspended with loading volume 20 ml/flask. Flasks were then incubated at 37°C in a humidified atmosphere of 95% air/5% CO2 for 4 days to allow for cell recovery.

2.2.10.4 Cell viability assessment

AlamarBlue (AB) is an easy assay designed to measure quantitatively the proliferation of different kind of human and animal cell line. This assay does not need to wash or fix and extract the cell as required in other commonly used assays. As in this project the THP-1 monocyte were used as suspension cells in the growth medium, it has been found that this assay is work properly with suspension cell THP-1 (Hatziieremia *et al.*, 2006). It is recommended that the plating density and incubation time be determined for the cell line. Harvest cells which are in log phase growth stage and determine cell count. Add 10 µl alamarBlue in to 100 µl of the cells medium volume in the well. Return plates to incubator. For any given cell density selected, the incubation time can be determined as the time taken for the control cells to turn the indicator from the oxidized (blue) form to the fully reduced (pink)form. Remove the plate and measure absorbance for cell density 2 x 10^5 cells/ml after 24 h and for 8 x 10^5 cells/ml after 4 h. Measurement of absorbance at a wavelength of 570nm and 600nm. Calculating the reduction percentage of alamarBlue by using the following formula:

$$\text{Reduction Percentage} = \frac{(E_{oxi}600 \times A_{570}) - (E_{oxi}570 \times A_{600})}{(E_{red}570 \times C_{600}) - (E_{red}600 \times C_{570})} \times 100$$

Where E is the molar extinction coefficient, which has units of L mol^{-1} cm^{-1} (Libretexts, 2020), A is absorbance of test wells, C absorbance of negative control well (medium, alamarBlue reagent, no cells).

$E_{oxi}570$ = 80586, $E_{oxi}600$ =117216, $E_{red}570$= 155677, and $E_{red}600$=14652

2.2.10.5 Preparation of cell lysates

Briefly, THP-1 cells were grown in T75 tissue culture flasks as described in section (2.2.10.1). Following treatments, suspension cells in growth medium were collected and centrifugated at 300 x g at room temperature for 5 min. The supernatant was discarded and cells pellet was then washed by suspending in chill PBS followed by centrifugation at 300 x g at room temperature for 5 min to pellet cells. The supernatant was discarded and the cell pellet resuspended in 600 µl of ice cold RIPA lysis buffer. The cells were incubated with lysis buffer for 20 min on ice with vortex ever 5 min and then clarified by centrifugation at 4°C for 10 min at 14000 x g. The supernatant was collected and transferred to a new Eppendorf tube for protein estimation and further analysis.

2.2.10.6 Exposure of cells to organophosphate compounds

PSP, DZO, CPO and POX were prepared as 1, 10, and 100 mM concentration stock solutions in DMSO. 2µl of each concentration (0.1, 1 and 10 µM final concentrations) were added to 20 ml growth medium/flask with density of 2 x 10^5 cells/ml of THP-1 cells. Controls cells were treated with 2 µl DMSO final concentration 0.01% (v/v). All flasks kept incubated at 37°C in a humidified atmosphere of 95% air/5% CO_2 for four days. Cells imaging inverted microscop with NIS-Elements F 4.00.00 were used first and last day of treatment and test cells viability of each flask. Ending the experiment by collecting the washing the pellets and lysis them as described in (2.2.10.5) then prepared according to the required assay.

2.3 Statistical analysis

Graph Pad Prism (version 7) (Graph Pad software, California, USA) was used to represent all data graphs. All analysis methods were confirmed for normality of distribution using Shapiro-Wilk normality test with 95 % confidence interval. Then, the significance of the differences between the average of the values for each treatment were compared to the corresponding control or other treatment group either by performing one-way ANOVA followed by "Tukey's Multiple Comparison Test'', and the Dunnett comparison test", or by two-way ANOVA for group comparison, respectively. Both methods took into account multiple comparison, with 95 % confidence interval. Results represent mean ± SEM and p-value less than 0.05 were considered statistically significant.

Chapter 3: Characterisation of the inhibition of cholinesterase by organophosphorus compound

3.1 Introduction

Cholinesterase is a family of serine hydrolase enzymes whose primary role is to catalyse the hydrolysis of the neurotransmitter acetylcholine and other choline esters to allow a cholinergic neuron to return to resting state (Čolović *et al.*, 2013). Cholinesterase activity has been deployed as an environmental pollution biosensor (Jońca *et al.*, 2015). Some cholinesterases act as an endogenous bioscavenger for anticholinesterase agent as the first line of defence against toxic compounds reaching the bloodstream (Jońca *et al.*, 2015). Organophosphate compounds used in different applications, especially as pesticides, are known to be potential inhibitors of cholinesterase activities, which have been used for a long time as clinical biomarkers for determination of exposure to nerve agents and pesticides contamination (Tham *et al.*, 2017). The most common way to detect exposure to OPs is measuring the activity of AChE or BChE activity in human blood (Jońca *et al.*, 2015).

Determination of blood or plasma cholinesterases activity is now a standard laboratory assays. Investigation of the activity of plasma BChE was used for monitoring of OP exposure and predicting the severity of poisoning (Abdullat *et al.*, 2006; Eddleston *et al.*, 2008). It was revealed that AChE and BChE are sensitive markers in moderately poisoned patients (Dhotre *et al.*, 2014). Work by Jońca *et al.* (2015) indicated that some clinical factors can influence kinetic parameters of BChE activity in blood. In the current study, the effects of OPs of interest on the activities of purified electric eel AChE and equine BChE were monitored and compared with the corresponding activities in human plasma to differentiate OP compounds with respect to their potency against each enzyme in isolation and in a more biological environment. Electric eel AChE and equine BChE are the most widely used for bioassay applications because of the high inhibition sensitivity that OP compounds pesticides have on them (Miao *et al.*, 2010;

Čolović *et al.*, 2011). Indeed, OPs may induce different levels of inhibition *in vivo* or *in vitro* AChE and BChE activities (Skrinjaric-Spoljar *et al.*, 1973; Eyer, 2003; Casida and Quistad, 2005; Üner *et al.*, 2006).

A different study used different condition to study the effect and to validate the previous efficacy of OPs on blood and plasma cholinesterases. For example, an *in vitro* investigation of the efficacy of CPO on BChE, the results revealed that mutant active site of BChE showed lower inhibtion with CPO comparing to the wild-type of BChE (Amitai *et al.*, 1998). Another *in vitro* study investigated the effects of single and simultaneous exposure to DZ, CPF and their oxon analogues DZO and CPO on electric eel AChE, which confirmed that the parent compounds were weaker inhibitors than their oxon analogues but all forms behaved in a concentration-dependent manner with different potencies (Čolović *et al.*, 2011). Liyasova *et al.*, (2011) found that half of the blood samples taken from jet airplane passengers revealed that the active site serine of BChE reacted with the active metabolite of tri-o-cresyl phosphate which is cresyl saligenin phosphate (CBDP) - the analogue form of PSP - and produce a stable phosphorylated adduct.

There are a variety of methods to study the cholinesterase activity but the most simple, accurate, and low cost is the Ellman method (Miao *et al.*, 2010). Enzymological characteristic of cholinesterases are defined by the specificity of their substrate; moreover, the different structure of the esterified substrate controls the kinetic parameters of enzymatic hydrolysis (Rozengart and Basova, 2009). The Ellman method is based on determining the amount of thiocholine released, which is quantified by its reaction with DTNB, producing yellow 5-thio-2-nitrobenzoate anion (Ellman *et al.*, 1961). The assay uses the synthetic thiol esters acetylthiocholine and butyrylthiocholine, which bear a close resemblance to acetylcholine and

butyrylcholine, respectively (Basova *et al.*, 2018). However, one study displayed high rates of hydrolysis when AChE was incubated with acetylthiocholine but showed far less activity in the presence of butyrylthiocholine (Tham *et al.*, 2017).

Before investigating their impact on the haematological parameters such as FXIIIa and thrombin activity, it was important to confirm the biological activity of the OPs of interest against known major targets. The main aim of the work presented in this chapter was, therefore, to confirm the behaviour of OPs towards pure cholinesterases and their corresponding activities in human plasma. This was achieved by using by the Ellman method (Ellman *et al.*, 1961) using acetylthiocholine and butyrylthiocholine as substrate for AChE and BChE, respectively.

3.2 Results

3.2.1 Effect of OPs on plasma and purified acetylcholinesterase activity

In order to establish the relationship between the toxicity of OPs and the level of AChE activity, enzyme activity was measured by a modified Ellman assay which was performed using either human plasma (~1.5 mg protein/ml) or pure electric eel AChE (0.4 µg/ml) in the presence and absence of several OPs over a range of concentrations incubated on 4ºC for 30min, as indicated in (section 2.2.3). The results in Fig 3.1 and Fig 3. 2 revealed that plasma AChE may be more sensitive to parent organophosphorothiote OPs than was pure AChE of electric eel.

Interestingly, the effect of PSP on plasma AChE activity started to cause a noticeable reduction from 0.8 µM and significant inhibition at 6 µM and above (Fig 3.1 A) compared to no effect on pure AChE (Fig 3.2 A). PTH (Fig 3.1 D) was the most toxic parent compound to plasma AChE, as a significant reduction was observed starting from 1.5 µM concentration until the activity was undetectable at 25 µM and above. One the other hand, CPF inhibited pure AChE by 40% at the highest exposure concentration (50 µM). DZO, CPO and POX inhibited both plasma and pure AChE activities much more potently than the parent compounds (Fig 3.1 & 3.2 E, F, G). In cases where more than 50 % inhibition was observed, the IC_{50} values were determined as summarised in Table 3.1 (IC_{50} plots are shown in appendix 8.1 & 8.2). Generally, the oxon compounds were more potent than their parent compound in assays of AChE in both plasma and purified enzyme samples.

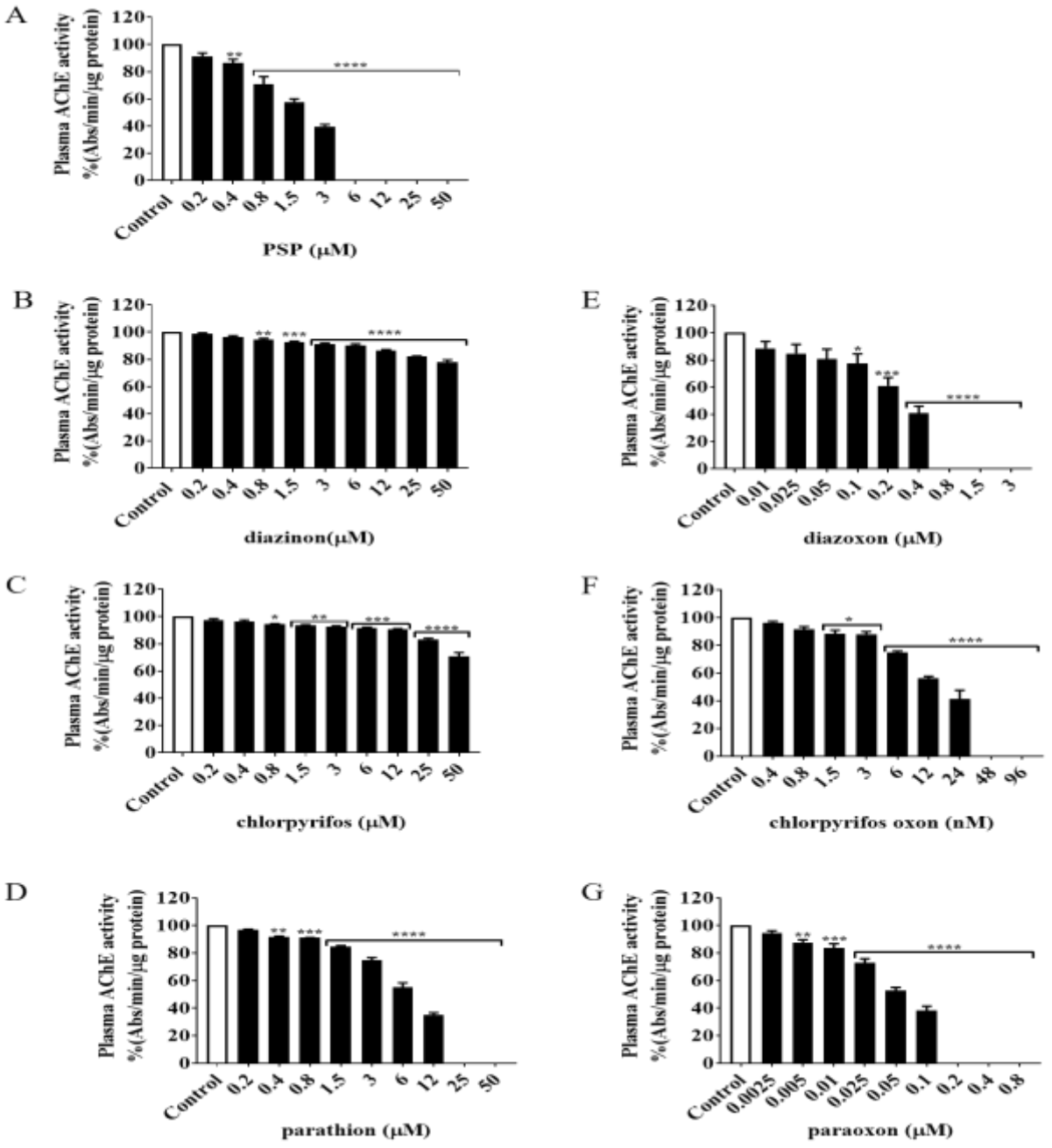

Figure 3- 1: Effect of OPs on plasma acetylcholinesterase activity.

Diluted human plasma samples (~1.5 mg/ml) were incubated 30 min on ice with a range of OP concentrations, as indicated prior to being subjected to the Ellman assay as described in materials and methods. A) PSP, B) diazinon, C) chlorpyrifos, D) parathion, E) diazoxon, F) chlorpyrifos oxon and G) paraoxon. Data points represent the mean ± SEM of acetylcholinesterase specific activity from three independent experiments. *p<0.05, **p<0.01, ***p<0.001, ****p<0.0001 versus non OP-treated control (=100%).

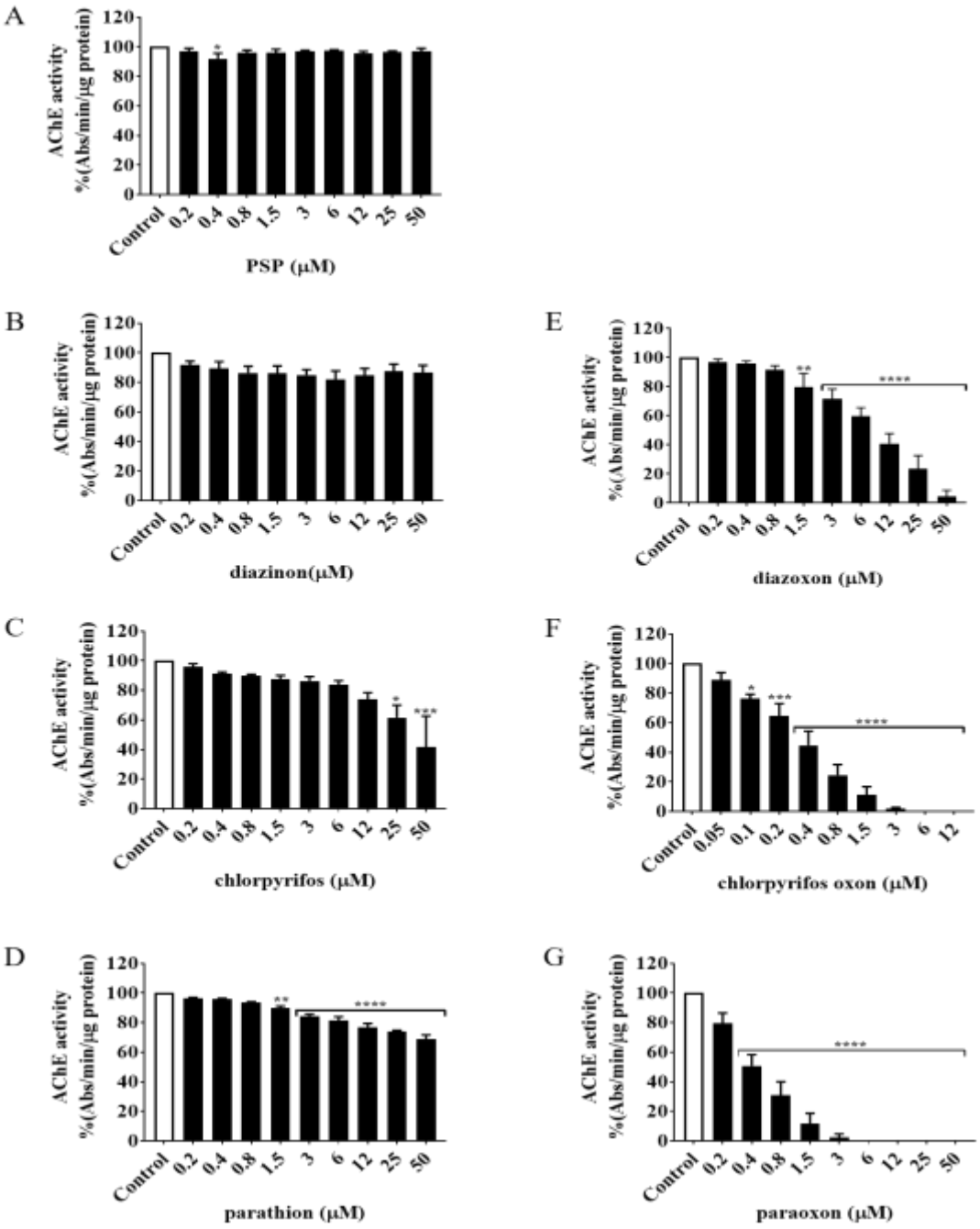

Figure 3- 2: Effect of OP on pure acetylcholinesterase activity.

Pure electric eel acetylcholinesterase (0.4 µg/ml) samples were incubated 30 min on ice with a range of OPs as indicated prior to being subjected to the Ellman assay as described in materials and methods. A) PSP, B) diazinon, C) chlorpyrifos, D) parathion, E) diazoxon, F) chlorpyrifos oxon, G) paraoxon. Data points represent the mean ± SEM of acetylcholinesterase specific activity from three independent experiments. *p<0.05, **p<0.01, ***p<0.001, ****p<0.0001 versus non OP-treated control (=100%).

3.2.2 Effect of OPs on plasma and purified butyrylcholinesterase activity

The main abundant choliesterase in plasma is BChE (Masson & Lockridge, 2010), for which reason it was also necessary to examine the relationship between the toxicity of OPs and the level of plasma BChE. The assays were performed using either human plasma (~1.5 mg protein/ml) or pure equine BChE (0.4 µg/ml) in the presence and absence of a wide range of concentrations of the same OPs incubated on 4ºC for 30min, as indicated in section 2.2.4. From the results in Fig 3.3 and Fig 3.4 it can be seen that PSP has a significant effect by decreasing the activity on both plasma and pure BChE, but the toxicity effect was higher on plasma BChE where it was initiated from 0.2 µM and induced statistically significant inhibition at 12 µM and above (Fig 3.3 A). As for AChE, there was much stronger inhibition in both plasma and pure BChE activities by the oxon forms compared to parent compounds (Fig 3.3 & 3.4 E, F, G). Plasma BChE was more sensitive to DZO and POX (Fig 3.3 E & G) than was pure BChE. However, CPO treatment of pure BChE (Fig 3.4 F) with significant inhibition from 6 nM. Nevertheless, it was noticeable the significant inhibition in pure BChE activity from 12 µM of parent compound of CPF (Fig 3.4 C). For most OPs the IC_{50} values for BChE were determined and are shown in Table 3.1 (IC_{50} plots are shown in appendix 8.2 & 8.3). In general, both pure and human plasma BChE activities were more sensitive than AChE to both parent organophosphorothiote and oxon OPs.

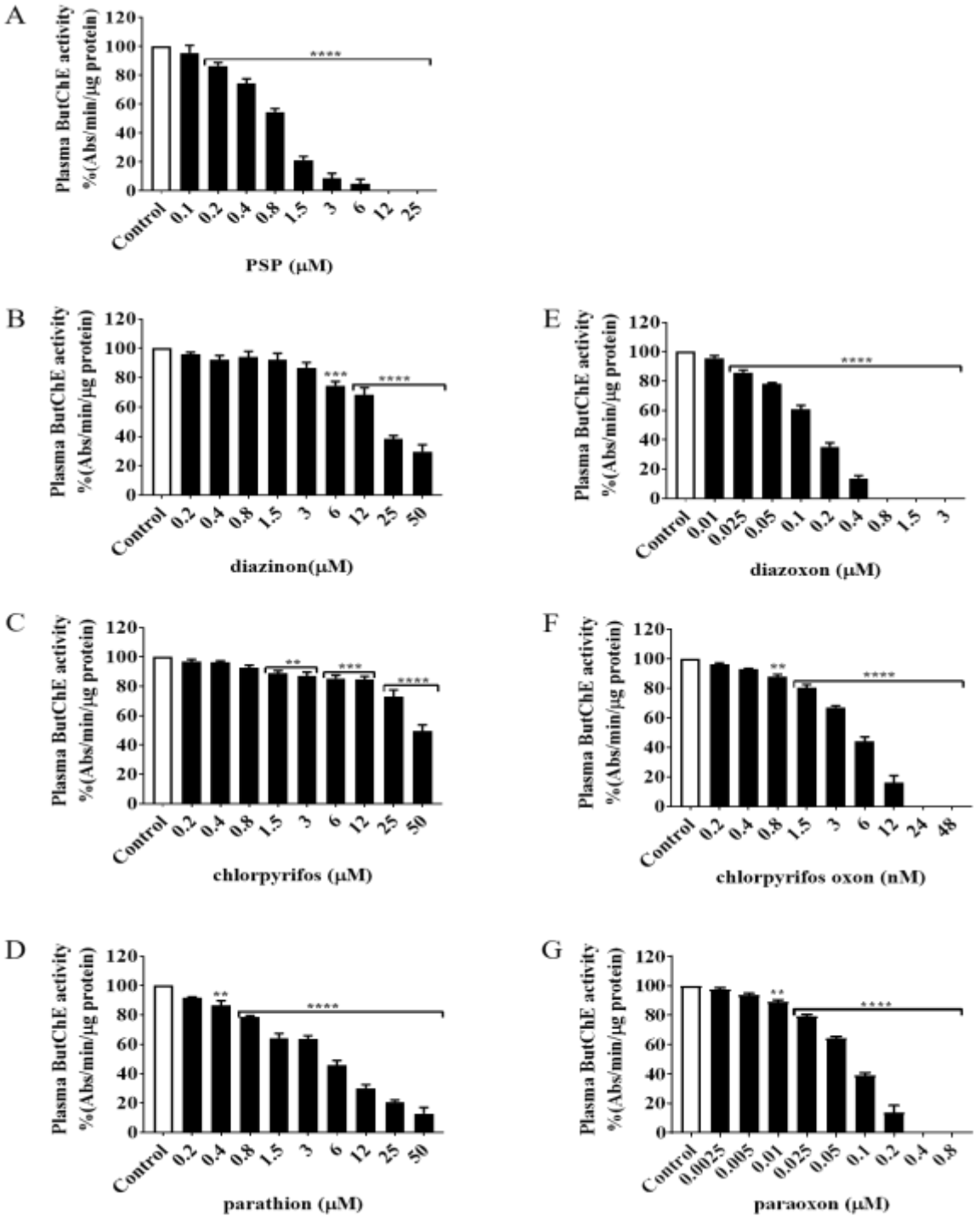

Figure 3- 3: Effect of OPs on plasma butyrylcholinesterase activity.

Diluted human plasma samples (~1.5 mg/ml) were incubated 30 min on ice with a range of OPs concentrations as indicated in graphs prior to being subjected to the Ellman assay as described in materials and methods. A) PSP, B) chlorpyrifos, C) chlorpyrifos oxon, D) diazinon, F) diazoxon, and G) diazinon. Data points represent the mean ± SEM of butyrylcholinesterase specific activity from three independent experiments. *p<0.05, **p<0.01, ***p<0.001, ****p<0.0001 versus non OP-treated control (=100%).

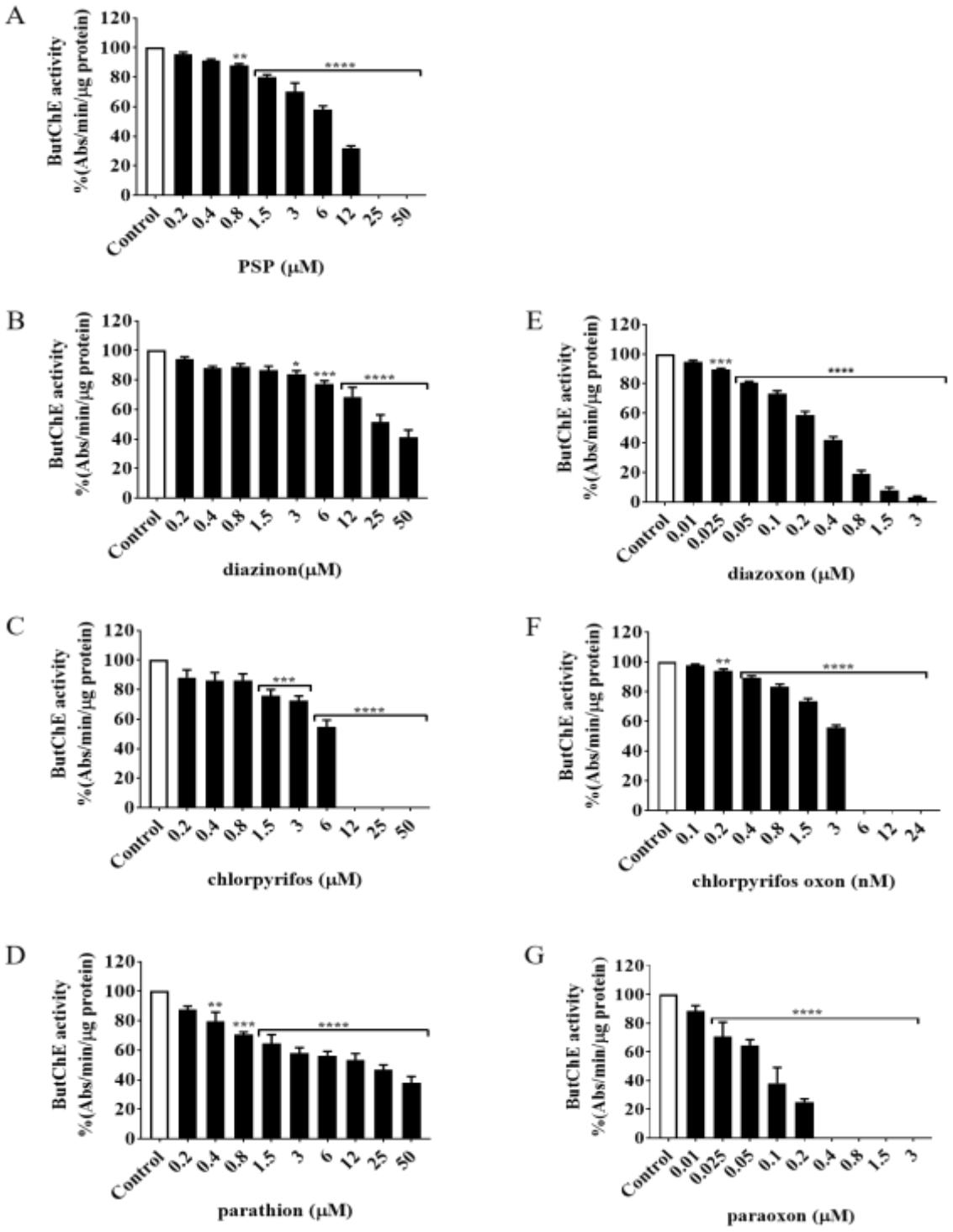

Figure 3- 4: Effect of OP on pure butyrylcholinesterase activity.

Pure equine butyrylcholinesterase (0.4 µg/ml) samples were incubated 30 min on ice with a range of OPs as indicated prior to being subjected to the Ellman assay as described in materials and methods. A) PSP, B) diazinon, C) chlorpyrifos, D) parathion, E) diazoxon, F) chlorpyrifos oxon, G) paraoxon. Data points represent the mean ± SEM of butyrylcholinesterase specific activity from three independent experiments. *p<0.05, **p<0.01, ***p<0.001, ****p<0.0001 versus non OP-treated control (=100%).

Table 3- 1: Summary of IC_{50} values for OP compounds against plasma and pure AChE and ButChE enzyme activities.

NR = significant inhibition observed but IC_{50} value was not reached.

Organophosphorus compound	IC_{50}			
	Plasma AChE (µM)	Pure AChE (µM)	Plasma BChE (µM)	Pure BChE (µM)
PSP	1.7 (±0.03)	NR	0.79 (±0.01)	6.1 (±0.03)
Diazinon	NR	NR	20 (±0.04)	34 (±0.09)
Diazoxon	0.2 (±0.02)	7.8 (±0.03)	0.12 (±0.02)	0.25 (±0.02)
Chlorpyrifos	NR	NR	71 (±0.09)	4.8 (±0.05)
Chlorpyrifos oxon	0.003 (±0.04)	0.33(±0.03)	0.05 (±0.02)	0.03 (±0.03)
Parathion	6.6 (±0.03)	NR	4.7 (±0.03)	9.7 (±0.09)
Paraoxon	0.05 (±0.03)	0.44 (±0.04)	0.07 (±0.02)	0.07 (±0.03)

3.2.1 Substrate specificity of cholinesterases

As a result of the unexpectedly strong inhibition of acetylthiocholine hydrolysis by plasma cholinesterases following PSP exposure, it was important to assess the specificity of cholinesterase for the two substrates (acetylthiocholine iodide and S-butyrylthiocholine iodide) used in this study to determine whether the some of the observed effects of OPs were due to AChE inhibition or the ability of BChE to hydrolyse its preferred substrate. For this, the Ellman assay was used on both pure enzymes' (electric eel AChE and equine BChE) in the presence and absence of a range of concentrations both substrates. The effect of substrate concentration is shown in Fig. 3.5. For the tested substrate concentrations, (Fig 3.5 A) pure AChE activity showed no interaction with the substrate butyrylthiocholine iodide. However, the pure BChE activity showed an apparent Michaelian behavior, with both its preferred substrate and with acetylthiocholine iodide (Fig 3.5 B). It was clear that both enzymes hydrolysed their own intended substrate (Fig 3.5 C & D) AChE had a Km for its preferred substrate of 0.05 mM (Fig 3.5 C) but was unable to hydrolyse butyrylthiocholine (Fig 3.5 A). When the apparent Km values of BChE for the two different substrates were calculated by the Michaelis-Menten method, the results were found to be very similar, with only 0.06 mM difference (Fig 3.5 B & D). Thus, the substrate specificity experiments show that BChE can effectively hydrolyse acetylthiocholine iodide as well as butyrylthiocholine, but AChE cannot hydrolyse butyrylthiocholine iodide.

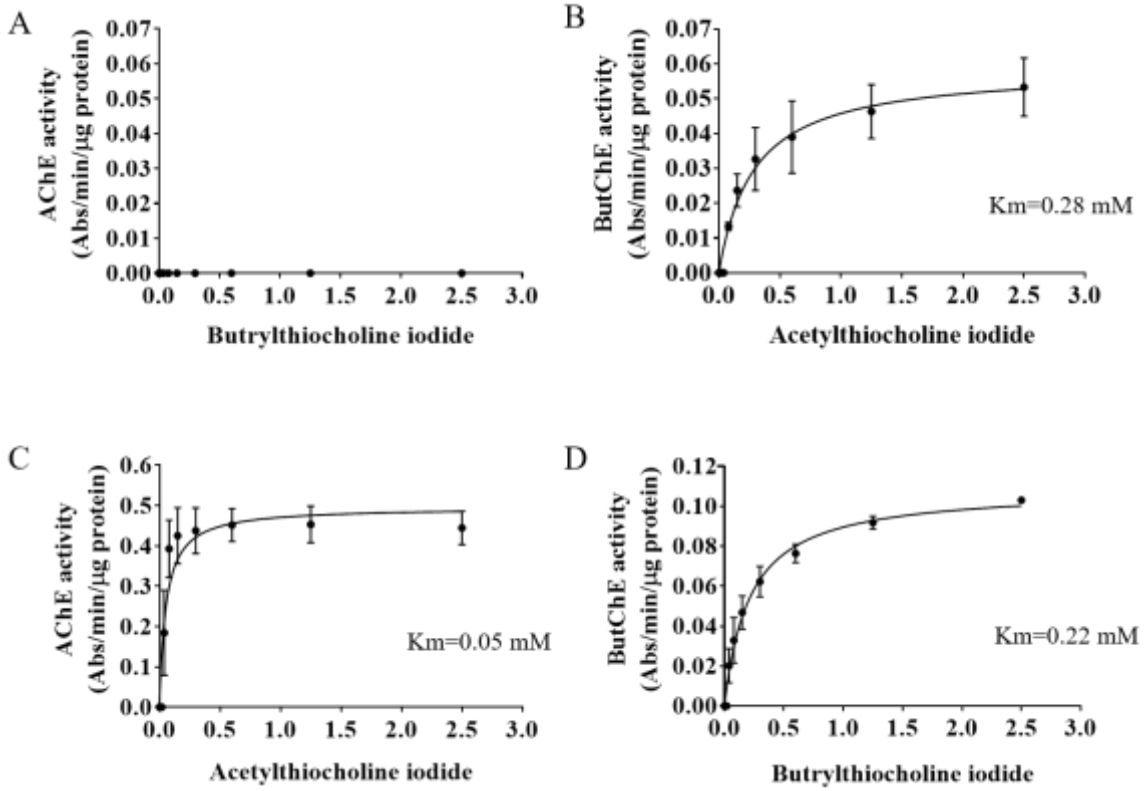

Figure 3- 5: Substrate specificity of cholinesterases.

Pure electric eel AChE (A, C) and equine BChE (B, D) (0.4 µg/ml) were incubated in the presence of a range of substrate concentrations S-butyrylthiocholine iodide (A, D), and acetylthiocholine iodide (B, C), prior to being subjected to the Ellman assay, as described in materials and methods. Data represent enzyme activity as mean absorbance change per min ± SEM for three independent experiments.

3.3 Discussion

Cholinesterases have been widely studied, and they are accepted as biomarkers for the OP toxicity, since it has been proven that they are one of their major targets (Nigg & Knaak, 2000). In plasma, it has been suggested that the dominant type is BChE, whereas AChE is mainly in erythrocyte membranes. A previous study showed that human 12th-week fetal serum might contain 40% AChE (Hahn *et al.*, 1993), whereas others confirmed that adult plasma has less than 1% of AChE activity (Brimijoin & Hammond, 1988; Thompson, 1999; Nigg & Knaak, 2000). The work presented in this chapter aimed to validate the effect of the some of the most widely used OPs and compare that variation of toxicity effect between AChE and BChE. In the current work, the activity of cholinesterases was determened by the Ellman assay (Ellman *et al*., 1961) using the preferred substrate for each enzyme (acetylthiocholine iodide and butyrylthiocholine iodide) and the chromogenic reagent DTNB to detect the thiocholine product released. The results confirm that the parent OPs and their oxon metabolites exhibit the expected relative toxicity effects on pure cholinesterases, in that the latter are more potent, thus showing that all compounds tested were biologically active. However, the substrate specificity observed for the pure cholinesterases indicates that BChE can hydrolyse the AChE substrate acetylthiocholine iodide but not the opposite. Therefore, given that AChE is less abundant than BChE in plasma, it is likely that some of the unexpected effects on acetylthiocholine hydrolysis may have been due to inhibition of BChE.

AChE activity was tested with a wide range of organophosphorus compound and a variety of samples (Thompson, 1999). In the current study it was clear that the bioactivated oxon metabolite form of OPs was more toxic towards AChE activity in both samples (human plasma and electric eel AChE) in a concentration dependent manner but with different

inhibitory potencies. The rank order of the most toxic on plasma samples follows as: CPO, POX, DZO and PSP (Fig 3.1 E, F, G, A). It was also noticeable in the current work that the inhibition was concentration-dependent with CPO being effective of in the low nM range (Fig 3.1 E, F, G). Then the of POX and DZO levels were in the low µM concentration ranges, which corresponded to those findings of previous studies that pointed to the grater rate of inhibitory action following oxidative bioactivation of insecticide compounds either *in vitro* or *in vivo* despite their different conditions and methods (Casida & Quistad, 2005; Kaushik *et al.*, 2007). Another study found that inhibitory potencies of DZO and CPO were 100 times more than DZ and CPF on cell culture of erythrocyte AChE activity after three days exposure (Čolović *et al.*, 2010; Čolović *et al.*, 2011). Moreover, other previous research had shown the very low AChE IC_{50} (0.1-0.3 µM) of PSP in a human neuroblastoma cell line (Ehrich *et al.*, 1997), very similar to the complete inhibition of human plasma ChE in this current study using acetylthiocholine as the substrate (IC_{50} 1.7 µM ±0.03 PSP: Table 3.1).

Some studies found very high AChE concentrations in the eel *Electrophorus electricus* and considered the most abundant source of this enzyme and used as purified source of AChE (Assis, Bezerra & Carvalho Jr, 2011). In the current study, the effect of OPs on purified AChE activity (Fig 3.2) showed different potencies compared to those in plasma (Fig 3.1). PSP and DZ toxicity showed no significant effect; in addition, the bioactivated compounds in plasma were more potent than purified enzyme. Since the OPs are substrate analogues of acetylcholine which are thought to interact with the serine hydroxyl moiety of the AChE active site leading to organophosphorylation (Čolović *et al.*, 2011). The lack of the biological effect environment of plasma could be one reason for PSP and DZ inhibition effect and reduced the significant effect of PTH on purified protein (Fig 3.2 A, B, C, D), and that could lead to missing the reacting with the active site. This speculation is in agreement with a study showing that *in vitro* influence of DZ on human lymphocyte, fibroblast and erythrocyte

AChE had a dose-dependent higher induced enzyme activities inhibition than their human commercial purified protein which was almost negligible compared to biological environment samples (Čolović *et al.*, 2011). However, the CPF toxin effect on purified AChE with no biological protein environment as in plasma sample reduced < 50% of AChE activity at 50 µM comparing to the same concentration on plasma AChE. Čolović *et al.* (2011) reported an almost complete inhibition of the electric eel purified AChE in the presence of 20 µM CPF concentration, moreover, the studies showed that albumin is the most abundant plasma protein binds with organophosphate compound, and MALDI-TOF mass spectrometer showed tyrosine adduct CPF-albumin (Li *et al.*, 2013). Another explanation for the different effects on plasma and electric eel acetylcholinesterase activity could be that BChE was affected, which necessitated a study of the effect of the same OPs on pure (equine) and human plasma BChE.

BChE, which is also known as plasma cholinesterase, is a serine hydrolase present in most mammalian tissues with highest levels in liver and plasma (Nigg & Knaak, 2000). It is thought that BChE is not the primary toxicity target of OPs, but it has been found that many OPs compounds have a more pronounced toxic effect on BChE than AChE (Lockridge & Masson, 2000; Wogram *et al.*, 2001; Casida & Quistad 2005). This is in agreement with data obtained in the present study, showing that all OPs were more potent inhibitors of butyrylthiocholine hydrolysis in both pure enzyme and human plasma samples.

The substrates specificity was assessed in purified AChE and BChE Fig 3.5 to determine which of the two cholinesterases (AChE or BChE) is most affected in plasma samples treated with OPs. It is known that acetyl(thio)choline is the preferable substrate for AChE and butyryl(thio)choline for BChE (Basova *et al.*, 2018).

In the current study the reaction of each enzyme with the other's intended substrate was tested, the purified BChE being able to hydrolyse both acetylthiocholine and butyrylthiocholine iodide (with Km values of 0.28 µM and 0.22 µM, respectively), whereas the purified AChE did not hydrolyse the butyrylthiocholine iodide (Fig 3.5). Therefore, the data obtained in the current study suggest that BChE (but not AChE) can effectively hydrolyse both substrates indicating that it may account for most of the cholinesterase activity in all plasma samples. In agreement with these findings, a study by Liu *et al.*, 2007 illustrated that fish (Carassius auratus) brain AChE had found that brain AChE had a much higher affinity and hydrolysing efficiency to acetylthiocholine iodide than to butyrylthiocholine iodide (Liu *et al.*, 2007; Tham *et al.*, 2017). Furthermore, another study which measured ChE activity in blood collected from healthy male and female volunteers compared to purified human ChE, revealed that the neurotransmitter acetylcholine was an outstanding substrate for BChE (Masson & Lockridge, 2010). Indeed, BChE was found to hydrolyse acetylthiocholine at a rate just two-fold lower than butylrylthiocholine (Wetherell & French, 1986). A study focused on substrate selectivity of human BChE and its mutants estimated a Km of 33 µM for acetylthiocholine iodide substrate which was hydrolysed by the wild-type BChE comparing to 17 µM for butyrylthiocholine iodiede (Hou *et al.*, 2013). The BChE active site structurally showed a broader substrate specificity than AChE (Pohanks, 2011).

Thus, the selective measurement of BChE in the presence of AChE in plasma can be achieved because butyrylthiocholine is hydrolsed by BChE more specifically. However, measurement of AChE in the presence of BChE is difficult due to the ability of BChE to also hydrolyse acetylthiocholine iodide, and the lack of a specific inhibitor that inhibits BChE without inhibiting AChE activity (Naik *et al.*, 2013).

The current study suggest that the cholinesterase inhibition in plasma AChE assays was likely to be a reflection of BChE activity, for example in the case of PSP, which had no effect on the purified AChE yet plasma ChE activity was significantly inhibited using acetylthiocholine as the substrate Aldrige (1954) proposed that tri-*o*-cresyl phosphate (TOCP), when modified to a more toxic product CBDP *in vivo* exhibited increased inhibition of BChE but not AChE, an effect was also observed *in vitro* using rat-liver slices to produce the same toxic effect. It was subsequently shown that CBDP formed organophosphorylated adducts on active site serines (Ser-203 for human AChE and Ser-198 for human BChE); *in vivo* the inhibition effect by low dose exposure to CBDP on AChE is not as much as it is on BChE, for which reason BChE inhibition serves as a useful biomarker for exposure to T*O*CP (Liyasova *et al.*, 2011). Moreover, by looking to the rest of the results of the OPs effect Fig 3.1 on plasma AChE and plasma ButChE Fig 3.3 there was a closer scenario of results manner.

The results in the current work both plasma samples different substrate highlighted that BChE reacted with parent OP compounds and showed various effect. It is well known that oxidized form of organophosphorus compounds is the more toxic than their parent forms on cholinesterase enzyme activities (Brimijoin and Hammond, 1988; Čolović *et al.*, 2010; Čolović *et al.*, 2011). Most of the studies focus their research on the oxon form and their binding to the active site, but it has found that some phosphorothioate compounds cause some activity inhibition even before they are oxidized. For example, Tacal & Lockridge (2010) found that diazinon formed adducts with highly purified human BChE, and in the activity assay 52% ‘slow’ inhibition was observed in BChE 3.6 mg/ml over 15 h exposure to 50 µM DZ, suggesting that this could occur via a thiono-thiolo rearrangement.

A previous study by Amitai *et al.*, (1998) incubated POX with purified human BChE (1.3 U/ml) with a higher butyrylthiocholine Km (0.5 mM) compared to the current study (Fig

3.5); their inhibition kinetics data showed about 50% inhibition at 0.055 µM POX after 40 min, which is proportionately almost the same as its effect on to plasma and purified BChE in the current study (Figs 3.3 and 3.4). In the same study of Amitai *et al.* (1998) they also incubated the same sample with CPO, and they mentioned that results showed direct inhibition in BChE activity depended on CPO concentration, they confirmed that BChE served as a biomarker for CPO toxicity due to rapid interaction between them. In the agreement the current study revealed that CPO inhibits BChE at lower than or about 24 nM concentration either whole plasma of purified protein (Figs 3.3 and 3.4).

There are no major studies on the effect of DZ and DZO on BChE activity. The current research showed that DZ comparing to purified BChE had inhibited ≥ 30 % of plasma BChE activity showed almost ≤ 40 % activity inhibition at high concentration 50 µM, but the oxon form of DZO showed complete inhibition of plasma BChE activity at 0.8 µM, conversely, purified BChE showed ≥10% activity at 3 µM (Figs 3.3 and 3.4). Although different samples and methods comparing to current study some studies showed significant inhibition by DZ, a previous study injected i.p. 100 mg/kg body wt into male rat 340-370 g with dissolved DZ in olive oil illustrated about 65% significant inhibition of BChE activity after 3 hours injection (Tomokuni & Hasegawa, 1985). Another study used a different method but the same type of rat male and female divided into four groups into (two groups/sex) weighing (90-100 g). They were feed for 7 days with 25 ppm and 2 ppm of DZ mixed with their diet it showed significant inhibition for both male and female with higher concentration by 50 % and 42 % however the lower concentration showed 5 % and 29 %, respectively, which indicated that rats female are more sensitive to DZ toxicity (Davies & Holub, 1980).

The samples of plasma treated with parent OPs (Figs 3.1 and 3.3) showed significant inhibition of BChE activity with both substrates, though it was more pronounced for butyrylthiocholine, This could be explained by these parent organophosphorothiotes

being metabolised in plasma by molecules such as cytochrome P450 in plasma exosomes to produce the more potent oxon form (Fabrizi *et al.*, 1999; Foxeberg *et al.*, 2011; Kumar, 2015). Also, BChE is known to have a larger active site pocket than AChE (about 500 $Å^3$ compare to 300 $Å^3$), respectively, which makes BChE less substrate-specific than AChE, as it can hold bulkier substrates or inhibitors (Masson & Lockridge, 2010).

In conclusion, the results presented in this chapter indicate that the OPs used in the current study exhibit the expected manner of toxicity against pure cholinesterases, which serves as a useful positive control for their acute biological effects. The apparent inhibition of plasma AChE by PSP but no effect on pure AChE can be explained by the ability of BChE, of which PSP is a potent inhibitor to hydrolyse acetylthiocholine. The effect of parent organophosphorothioate compound on plasma cholinesterases may be due to their ability to bind to larger active site on BChE.

Chapter 4: Effects of organophosphorous compounds on pure and plasma FXIIIa

4.1 Introduction

One of the important biological processes in blood is haemostasis, which maintains and protects the balance between thrombosis and bleeding. The end result of clot formation is a network of fibrin stabilized by being cross-linked through the action of FXIII, which is a transglutaminase zymogen that is activated by thrombin-mediated cleavage to produce FXIIIa (Martins *et al.*, 2014). Transglutaminases (TGs) are a group of enzymes that catalyse crosslinking between the side chains of protein-bound lysine and glutamine, and incorporation of polyamine into protein-bond glutamine, during which processes a molecule of ammonia is released (Lin and Ting, 2006). Although FXIIIa is important at the end of the coagulation cascade, FXIIIa deficiency causes disparate diseases such as bleeding disorders, etc. (Muszbek *et al.*, 2011; Board *et al.*, 1993).

Since OPs have the potential to produce various kinds of toxicity, such as acute intoxication via their primary target, which involves the inhibition of acetylcholinesterase in the nervous system and at neuromuscular junctions; also, low level exposure produces long lasting chronic toxicity in non-target tissues and organs in the body (Ray & Richards, 2001; Eleršek & Filipic, 2011). Limited studies have suggested that environmental toxins such as OPs may disrupt the activity of coagulation enzymes (Petroianu *et al.*, 1999). Moreover, it has been reported that exposure to diazinon, chlorpyrifos and other OPs may disrupt a number of haematological parameters, such as CBC (complete blood count) values and biochemical measurements in blood plasma (Rahman & Siddiqui, 2006; Ambali *et al.*, 2007; Banaee *et al.*, 2008; Andreadis *et al.*, 2014).

There is serious blood loss after some cardiac surgery; a study by Ternström *et al.* (2010) found noticeable dissociation in plasma coagulation factors activity postoperatively, but observations showed FXIII activity in preoperative and postoperative stages correlated

inversely to postoperative blood loss after coronary artery bypass graft. Also, their results pointed to correlation between preoperative and postoperative FXIII concentration to postoperative bleeding. Larsen *et al.* (2012) found rebleeding and clot instability following aneurysmal subarachnoid haemorrhage (SAH). Reduced FXIIIa activity produced a reduction of clot stability which caused 50-90% of the rebleeding occurring within 6 hours of the primary bleeding. The association between FXIIIa activity or concentration and coronary disease has been recognized (Muszbek *et al.*, 2008) but causality has not yet been proven (Reinhart, 2003; Ternström *et al.*, 2010).

Acute myocardial infarction, heart failure, infarct expansion, and cardiac rupture were observed in FXIII deficient mice, perhaps due to inappropriate recovery of the myocardial tissue (Karimi *et al.*, 2009). In this respect, a case was reported of a 40-year old man who was admitted to a hospital emergency department with primary diagnosis of OP insecticide poisoning; after a few days, his condition deteriorated and myocardial infarction was diagnosed (Kumar *et al.*, 2014).

Some recent studies at NTU have shown that OP exposure disrupts the cellular activity of tissue TG in neural and hepatic cells (Howden, 2006; Harris *et al.*, 2009; Muñoz *et al.*, 2010). Based on these previous studies it is possible that other types of TGs, including coagulation FXIIIa, could be targets of OP toxicity.

The aim of the work presented in this chapter was to study the effects of a range of concentrations of the OPs PSP, DZ, DZO, CPF, CPO, PTH and POX on transamidase activities of plasma and purified FXIIIa. It was also of interest to study covalent binding and competitive binding using SDS-PAGE and image analysis of FXIIIa incubated with a fluorescent rhodamine-PSP (Rh-PSP) probe. The effect of OPs on plasma clotting was

further investigated using a D-Dimer ELISA kit. A further aim was to identify potential FXIIIa binding of all OPs used by mass spectrometry.

4.2 Results

4.2.1 Effects of organophosphorus compounds on plasma TG-mediated amine incorporation and peptide crosslinking activity

Initial experiments in this study investigated whether the OPs were able to affect the TG-mediated amine incorporation and peptide cross-linking activity in plasma. Plasma samples were pre-incubated 30 min on ice with a range of OP concentrations and subjected to incubation with biotin-cadaverine (for amine incorporation) or biotin-labelled F11KA (for peptide crosslinking), as indicated in (section 2.2.1.4.1 & 2.2.1.4.2). The results for amine incorporation showed slight (10-20 %) but statistically significant inhibition of TG activity by PSP, DZ, CPF and DZO (Fig 4.1 A, B, C, E) . A fluctuating pattern of inhibtion was exhibited with PTH treatment, whereas approximately 20-30% steady decline in activity was observed in the presence of CPO and POX (Fig 4.1 D, F,G).

On the other hand, in the plasma TG-mediated peptide crosslinking assay slight but significant inhibition of enzyme activity was observed following exposure to PSP, PTH, DZO, and CPO (Fig 4.2 A, D, F), but DZ, CPF, and POX had no significant effect (Fig 4.2 B, C, G). An IC_{50} value was not reached for any OP although statistically significant inhibition was observed for six out of seven compounds (Table 4.1). Overall, these data indicate that certain OP compounds can affect plasma TG activity as determined by biotin-cadaverine incorporation and protein cross-linking activity and that CPO has the greatest effect on peptide cross-linking, inhibiting by up to 35% of control values.

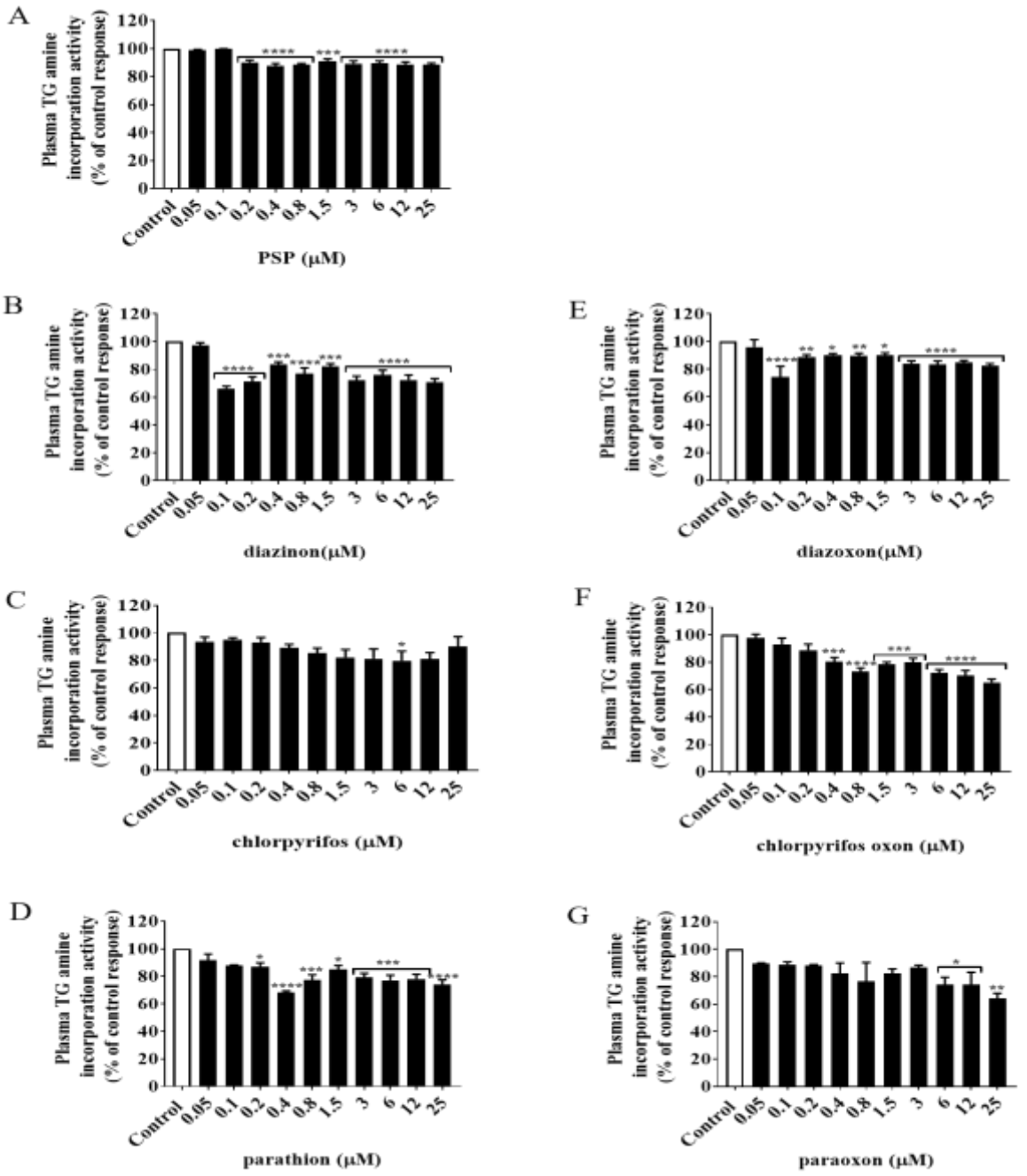

Figure 4- 1: The effect of OPs on plasma TG-mediated amine incorporation activity.

Diluted human plasma samples (~1.5 mg/ml) were pre-incubated for 30 min on ice with the indicated concentrations of each OP in the biotin-cadaverine incorporation assay, as described in Materials and Methods. Plots shown are for: A) PSP, B) diazinon, C) chlorpyrifos, D) parathion, E) diazoxon, F) chlorpyrifos oxon and G) paraoxon. Data points represent the mean ± SEM of normalized plasma TG activity from seven independent experiments. *p<0.05, **p<0.01, ***p<0.001, ****p<0.0001 versus non OP-treated control (=100%).

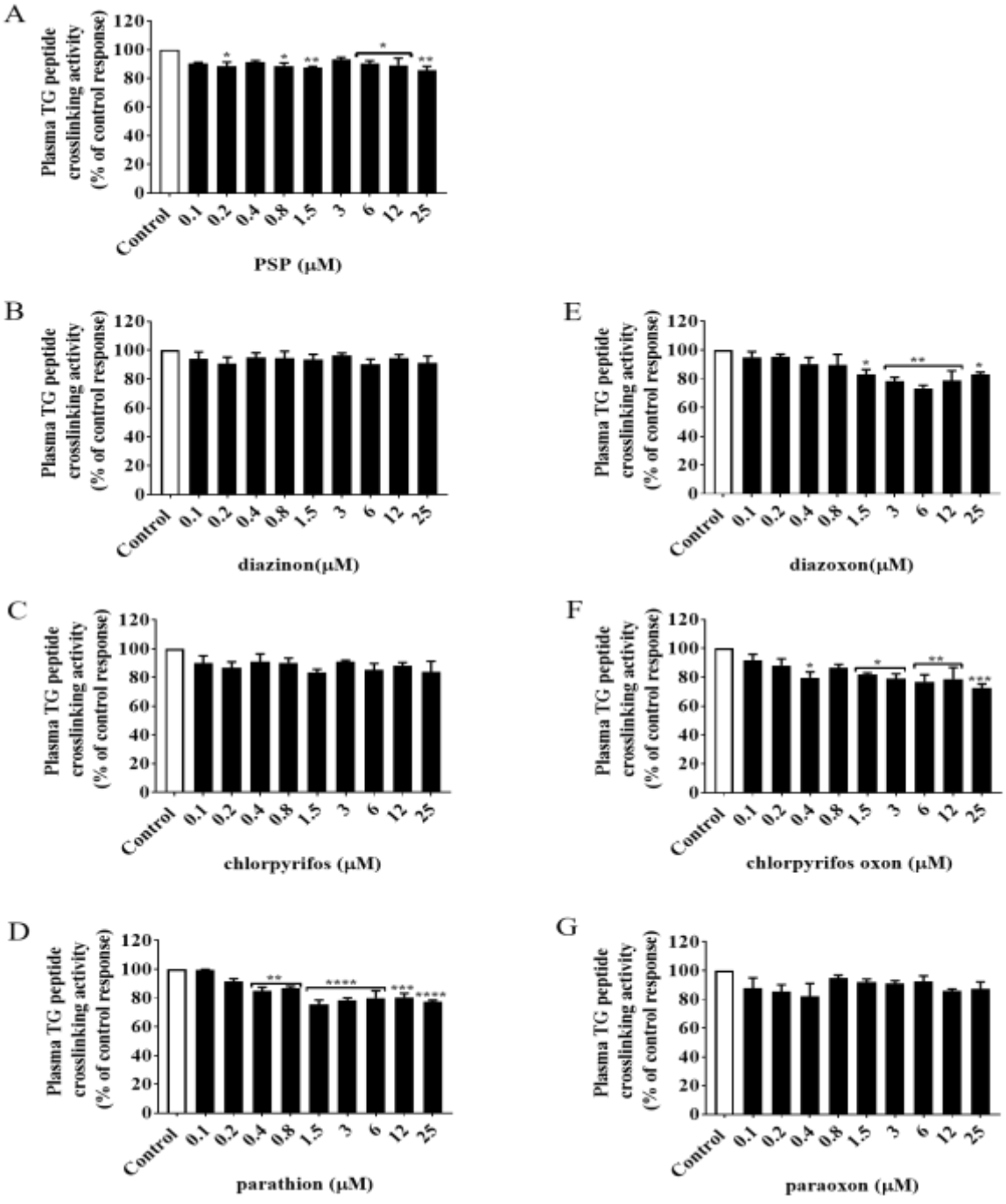

Figure 4- 2: The effect of OPs on plasma TG-mediated peptide crosslinking activity.

Diluted human plasma samples (~0.8 mg/ml) were pre-incubated for 30 min on ice with the indicated concentrations of each OP in the biotin-labelled peptide F11KA crosslinking assay, as described in Materials and Methods. Plots shown are for: A) PSP, B) diazinon, C) chlorpyrifos, D) parathion, E) diazoxon, F) chlorpyrifos oxon and G) paraoxon. Data points represent the mean ± SEM of normalized plasma TG activity from three independent experiments. *p<0.05, **p<0.01, ***p< 0.001, ****p< 0.0001 versus non OP-treated control (=100%).

4.2.2 Effects of organophosphorus compounds on pure FXIIIa-mediated amine incorporation and peptide crosslinking activity

To characterize the OP effect specifically on purified rFXIIIa- mediated amine incorporation and peptide cross-linking activity, rFXIII samples were pre-incubated 30 min on ice with a range of OP concentrations and subjected to incubation with biotin-cadaverine (for amine incorporation) or biotin-labelled F11KA (for peptide crosslinking), as described in (section 2.2.1.4.1 & 2.2.1.4.2). The results revealed a variable significant effect from all OPs on rFXIIIa-mediated amine incorporation activity (Fig 4.3). Concentrations of 12 and 25 µM showed inhibition effects on FXIIIa activity by 20 % in the case of PSP and CPF (Fig 4.3 A, C), and 60 % or more for DZ, DZO and PTH (Fig 4.3 B, E, D), whereas CPO and POX exhibited significant but not huge inhibition of activity (Fig 4.3 F, G).

Significant activity reduction in rFXIIIa-mediated peptide crosslinking activity was observed, as shown in Fig 4.4. There was between 60 % to 70 % inhibition effect by DZ, CPO and POX (Fig 4.4 B, F, G). Furthermore, the highest inhibition of approximately 80 % or more was induced by CPF and PTH (Fig 4.4 C, D), whereas the lowest inhibition effect of between 20 % and 40 % was caused by DZO and PSP, respectively (Fig 4.4 E, A). When there was more than 50 % inhibition of rFXIIIa-mediated peptide crosslinking activity, the IC_{50} values were determined as summarized in Table 4.1 (IC_{50} plots are shown in appendix 8.5 & 8.6). Generally, most of parent and oxon compounds were significantly potent on rFXIIIa biotin-cadaverine incorporation, but a distinct effect of OPs was obvious on rFXIIIa peptide cross-linking activity.

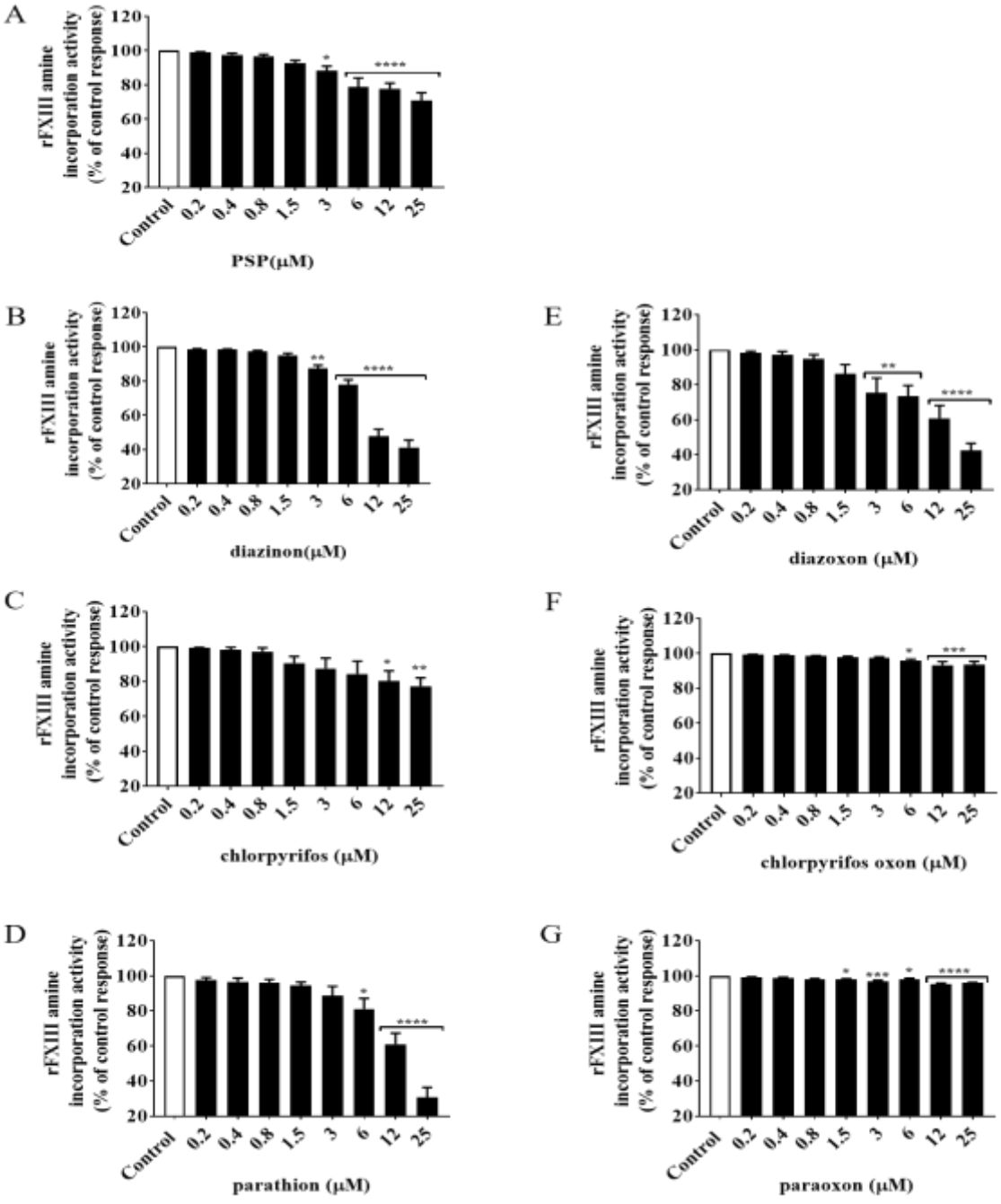

Figure 4- 3: The effect of OPs on pure rFXIII-mediated amine incorporation activity.

Human rFXIII (~0.02 ng/µl) was pre-incubated for 30 min on ice with the indicated concentrations of each OP in the biotin-cadaverine incorporation assay, as described in Materials and Methods. Plots shown are for: A) PSP, B) diazinon, C) chlorpyrifos, D) parathion, E) diazoxon, F) chlorpyrifos oxon and G) paraoxon. Data points represent the mean ± SEM of normalized pure rFXIII activity from three independent experiments. *p<0.05, **p<0.01, ***p<0.001, ****p< 0.0001 versus non OP-treated control (=100%).

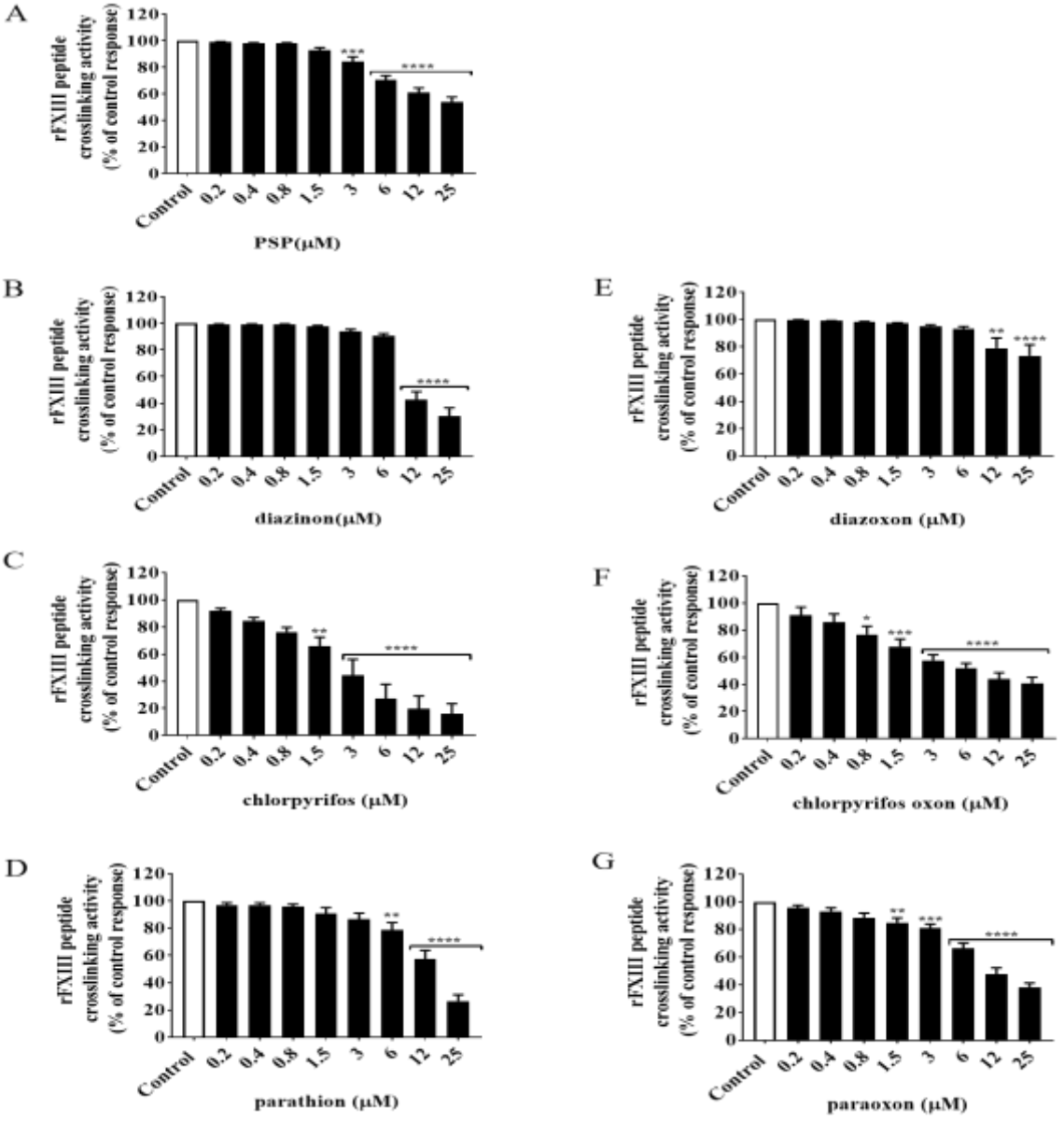

Figure 4- 4: The effect of OPs on pure rFXIII-mediated peptide crosslinking activity.

Human rFXIII (~0.005 ng/µl) was pre-incubated for 30 min on ice with the indicated concentrations of each OP in the biotin-labelled peptide F11KA crosslinking assay, as described in Materials and Methods. Plots shown are for: A) PSP, B) diazinon, C) chlorpyrifos, D) parathion, E) diazoxon, F) chlorpyrifos oxon and G) paraoxon. Data points represent the mean ± SEM of normalized pure rFXIII activity from three independent experiments. *p<0.05, **p<0.01, ***p<0.001, ****p<0.0001 versus non OP-treated control (=100%).

Table 4- 1: Summary of IC_{50} values for OP compounds against plasma TG and rFXIII-mediated amine incorporation and peptide crosslinking activity.

NR = significant inhibition observed but IC_{50} value was not reached. NE = no significant effect.

Organophosphorus compound	IC_{50} (µM)			
	Plasma TG-mediated amine incorporation	Plasma TG-mediated peptide crosslinking	rFXIII-mediated amine incorporation	rFXIII-mediated peptide crosslinking
PSP	NR	NR	45 (±0.04)	21 (±0.03)
Diazinon	NR	NE	17 (±0.03)	16 (±0.05)
Diazoxon	NR	NR	17 (±0.05)	62 (±0.06)
Chlorpyrifos	NE	NE	60 (±0.08)	2.7 (±0.06)
Chlorpyrifos oxon	NR	NR	NR	6.5 (±0.06)
Parathion	NR	NR	18 (±0.06)	15 (±0.04)
Paraoxon	NR	NE	NR	13 (±0.03)

4.2.3 SDS-PAGE and 2D-PAGE analysis for rhodamine-PSP binding to plasma TG

In order to determine whether PSP could bind covalently to plasma TG samples, a pure rFXIIIa (5µg), depleted plasma as described in (section 2.2.1.2.3) and whole plasma samples both (15 µg), all were incubated with rhodamine labelled-PSP, as described in (section 2.2.8.1). The samples were subjected to SDS-PAGE and visualized under green light, followed by staining with InstantBlue ™ to confirm the presence of protein in each sample. As shown in Fig 4.5 A, a polypeptide band of approximately 83 kDa in each sample was labeled with Rh-PSP. A number of other bands were also labeled in whole and depleted plasma. The gels were stained with InstantBlue ™, Coomassie blue-based staining solution for protein gels, to confirm the presence of proteins in samples (Fig 4.5 B). The quantification of purified FXIIIa, depleted plasma and whole plasma bands clearly revealed that differences in fluorescence intensity when Rh-PSP was present compared to extracts incubated with 0.25 % (v/v) DMSO (control) (Fig 4.5 C).

In addition, the identification of binding was also tested by 2D-PAGE. Depleted plasma (100 µg) was incubated with 0.25 % (v/v) DMSO (control) and 25µM of Rh-PSP, as described in (section 2.2.9). Visualization of 2D gels under green incident light source (520 nm) revealed that the 2D gel separation of depleted plasma incubated with Rh-PSP showed several fluorescent protein spots (Fig 4.6 B) compared to 2D-PAGE analysis of the control sample of depleted plasma without labeled PSP, which did not show any fluorescent spots (Fig 4.6 A). After visualization, the gels were stained with InstantBlue ™ stain to confirm the presence of proteins in samples (Fig 4.6 C, D).

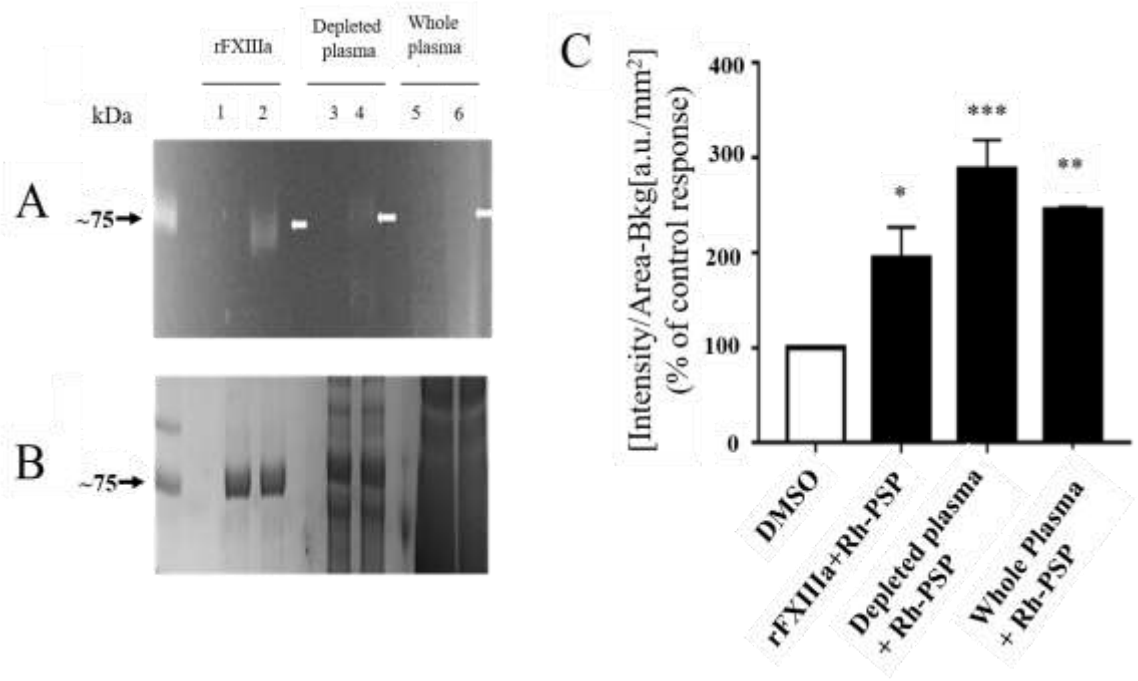

Figure 4- 5: Visualization of proteins labelled with rhodamine-PSP (SDS-PAGE).

Pure rFXIIIa (2.5µg), depleted and whole plasma samples (15 µg) and were incubated in the absence (lane 1, lane3, lane 5) and presence (lane 2, lane 4, lane 6) of 25 µM Rh-PSP, as indicated in Materials and Methods. Panel A) Gels were visualized under green incident light source (520nm) using a LAS4000 imaging system. Panel B) Gels were stained with InstantBlue ™ to confirm the presence of protein bands. Panel C) Densitometric analysis for Rh-PSP binding, DMSO represents the control incubated in the absence of Rh-PSP. Data represent the mean of fluorescence intensity ±SEM from three independent experiments. *p<0.05, **p<0.01, ***p<0.001 versus non OP-treated control (=100%).

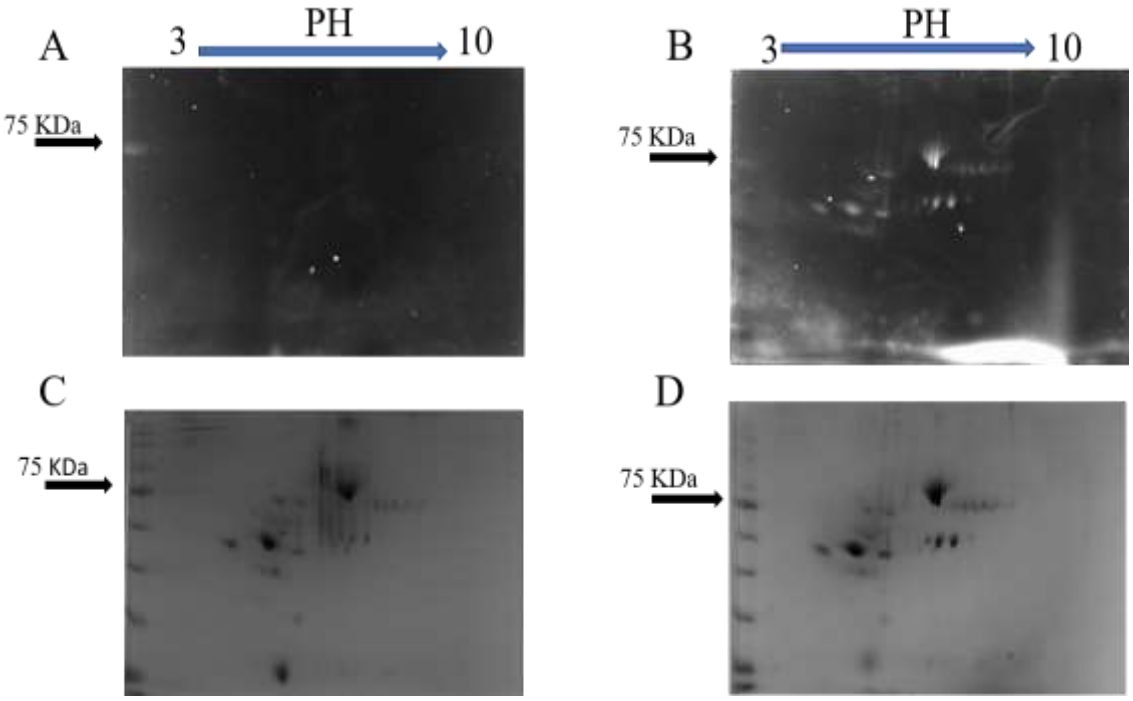

Figure 4- 6: Visualization of proteins labelled with rhodamine-PSP (2D-PAGE).

Depleted plasma (100µg) was untreated or treated with Rh-PSP (one hour at 37ºC, 25µM) and samples processed and analysed by 2D-PAGE using pH 3-10 gradient strips. Gels were visualized under green incident light source (520 nm) using a LAS4000 imaging system. Panel A) control sample containing100 µg of depleted plasma incubated with 0.25% (v/v) DMSO; Panel B) 100µg of depleted plasma incubated with 25µM of Rh-PSP, (C and D) control and labeled PSP treated sample Gels, respectively, were stained with InstantBlue ™ to confirm the presence of protein bands.

4.2.4 SDS-PAGE analysis for rhodamine-PSP competition binding to plasma TG and rFXIII

In order to determine whether Rh-labelled PSP was binding in the same manner as unlabeled PSP a competition assay was carried out. For this, pure FXIIIa and depleted plasma were incubated in the presence and absence of labelled and unlabeled PSP, or both forms of PSP, also testing the competition with labelled PSP and unlabeled PSP and other OP on purified rFXIIIa, prior to analysis by SDS-PAGE and fluorescence imaging, as indicated in (section 2.2.8.2). The results shown in Fig 4.7 A indicate that the intensities of fluorescent bands decreased in purified rFXIII and depleted plasma samples that contain both labeled and unlabeled PSP compared to those incubated with labeled PSP only. Densitometric analysis confirmed that the signal intensity for an 83 kDa band was significantly reduced in the presence of competition by unlabeled PSP for both pure rFXIIIa and depleted plasma (Fig 4.7 C).

Further competition assays were then performed with the other OPs.The results of such competition binding assays, which are shown in lanes 3, 4, 5 (Fig 4.8 A, Fig 4.9 A) and 6 (Fig 4.9 A) showed variable fluorescence intensity changes compared to the controls in lane 1 0.25% (v/v) (DMSO) and lane 2 (Rh-PSP) (Fig 4.8 A, Fig 4.9 A). The difference between control untreated protein lane 1 and the treated protein with labeled Rh-PSP (lane 2), as before, showed significant strong intensity of binding (Fig 4.8 A, Fig 4.9 A). The quantification of band fluorescence intensity for competition binding compared to control (labeled protein with Rh-PSP) showed that the most significant intensity difference by 2 fold decreased was by the unlabeled CPO comparing to quantification value of the control (labeled protein with Rh-PSP) on that gel (Fig 4.9 C), also DZO was the most competitive compound compared to the control (labeled protein with Rh-PSP) on the other gel (Fig 4.8 C), whilst the quantification of DZ and POX bands showed slight but not significant

intensity decreases compared to their control (labeled protein with Rh-PSP) on each gel (Fig 4.8 C) and (Fig 4.9 C) respectively. The gels were stained with InstantBlue ™ stain to confirm the presence of proteins in samples (Fig 4.7 B, 4.8 B, 4.9 B). Overall, the results showed fluorescent label Rh-PSP binding in all samples variability in the amount of competition by other OPs.

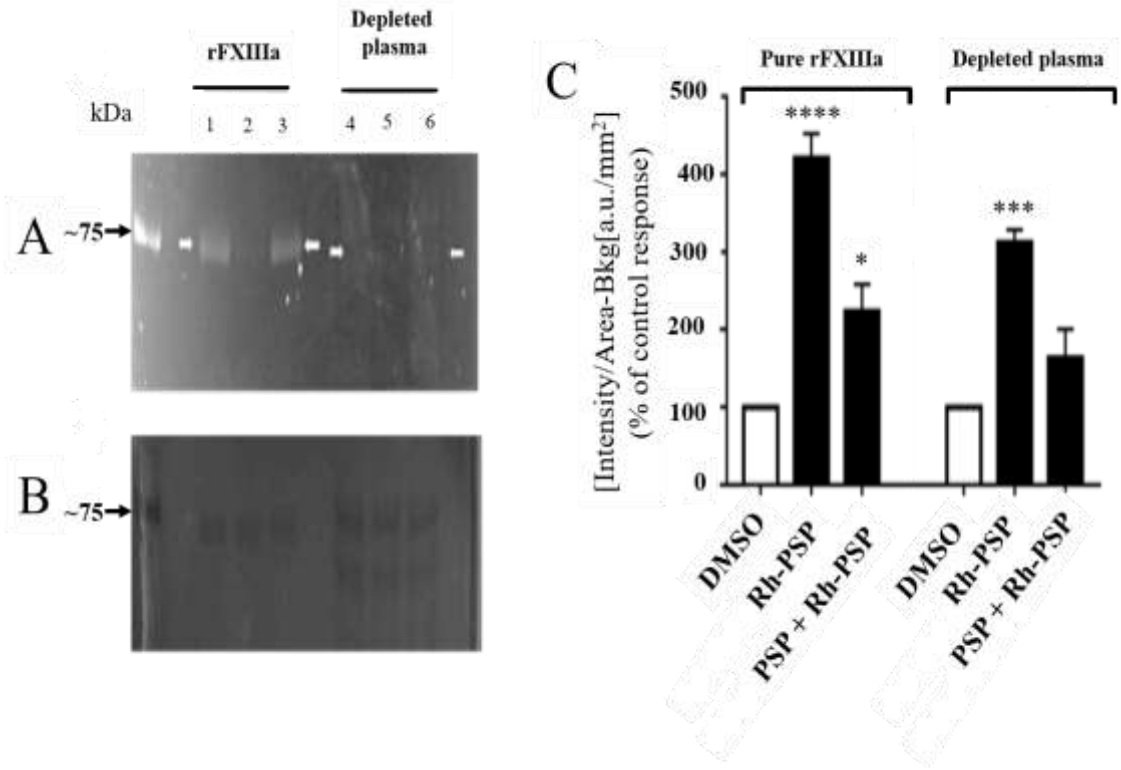

Figure 4- 7: Visualization of proteins labeled with competition binding of rhodamine-PSP and PSP.

Pure rFXIIIa (2.5µg) and depleted plasma samples (15µg) were incubatedfor 30 min on ice then for one hour at 37ºC with 0.25% (v/v) DMSO (Lane2, lane5), 25µM Rh-PSP (lane 1, lane 4) and both 25µM Rh-PSP + 100µM PSP (lane3, lane 6). Panel A) Gels were visualized under green incident light (520nm) using a LAS4000 imaging system. Panel B) Gels were stained with InstantBlue ™ to confirm the presence of protein bands. Panel C) Densitometric analysis for rhodamine-PSP binding. Data represent the mean of fluorescence intensity ±SEM from three independent experiments. *p<0.05, ***p<0.001, ****p<0.0001 versus non OP-treated control (=100%).

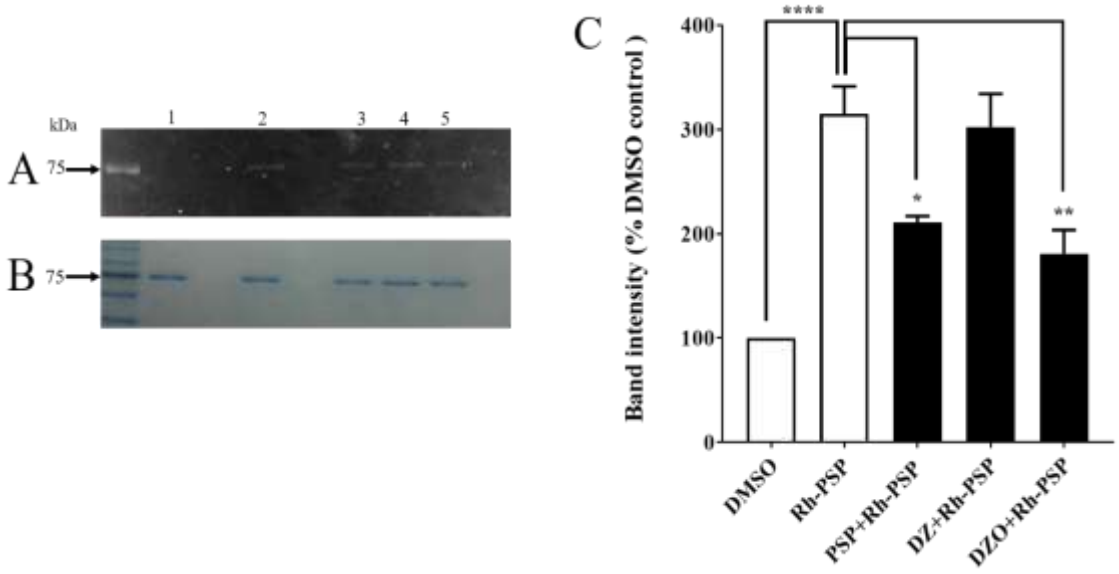

Figure 4- 8: Visualization of proteins labeled with competition binding of rhodamine-PSP and unlabeled PSP, DZ, and DZO.

Pure rFXIIIa (2µg) was incubated for 30 min on ice then for one hour at 37ºC with 0.25% (v/v) DMSO (Lane1), 25µM of Rh-PSP (lane 2) and both 25µM of Rh-PSP + 200µM of PSP, DZ, DZO (lane3, lane 4, lane 5); respectively. Panel A) Gels were visualized under green incident light (520nm) using a LAS4000 imaging system. Panel B) Gels were stained with InstantBlue ™ to confirm the presence of protein bands. Panel C) Densitometric analysis for rhodamine-PSP binding. Data represent the mean of fluorescence intensity ±SEM from three independent experiments. *p<0.05, **p<0.01, ****p<0.0001 relative to the DMSO control (=100%).

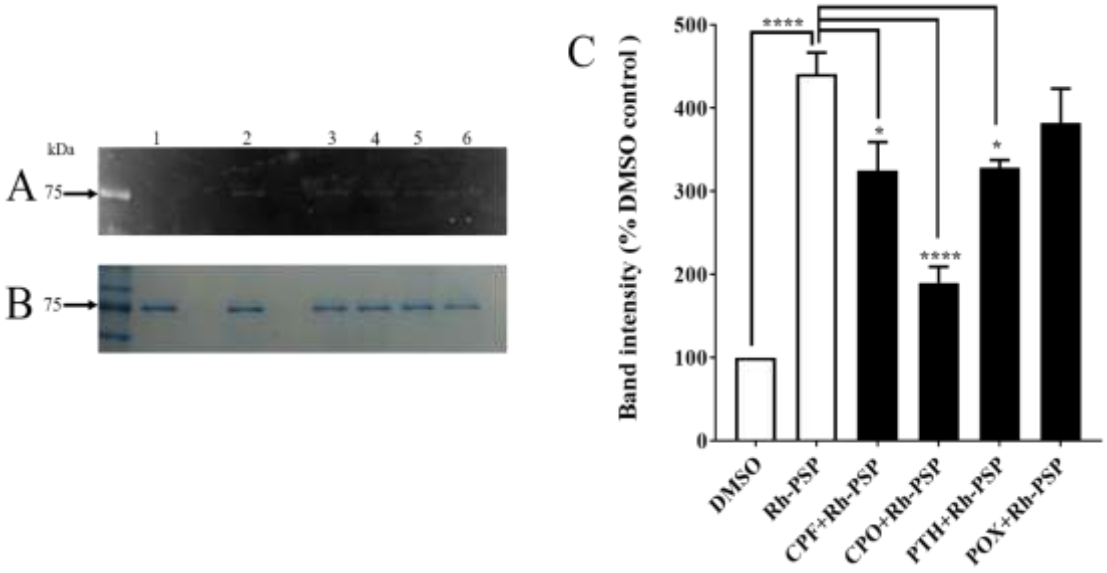

Figure 4- 9: Visualization of proteins labeled with competition binding of rhodamine-PSP and unlabeled CPF, CPO, PTH, POX.

Pure rFXIIIa (2µg) was incubated for 30 min on ice then for one hour at 37ºC with 0.25% (v/v) DMSO (Lane1), 25µM of rhodamine-PSP (lane 2) and both 25µM of rhodamine-PSP + 200 µM of CPF, CPO, PTH, POX (lane3, lane 4, lane 5, lane 6); respectively. Panel A) Gels were visualized under green incident light (520nm) using a LAS4000 imaging system. Panel B) Gels were stained with InstantBlue ™ to confirm the presence of protein bands. Panel C) Densitometric analysis for Rh-PSP binding. Data represent the mean of fluorescence intensity ±SEM from three independent experiments. *p<0.05, ****p<0.0001 relative to the DMSO control (=100%).

4.2.5 Effects organophosphorus compounds on clot product formation

In order to study the OPs effect on clot stabilization, a human plasma turbidimetric assay was applied to measure the amount of clot formed. The results showed that method was not sensitive enough to detect changes occurring under OP treatment. For this reason, an alternative method was developed for studying the impact of OPs on clot stabilization by measuring the fibrinolysis product D-dimer. Plasma (~1.5 mg protein /ml) samples were pre-incubated 30 min on ice with either 25 or 50 µM concentrations of OPs, after which samples were incubated for three hours at 37ºC to form the clot before measuring D-dimer formation by sandwich ELISA, as indicated in (section 2.2.2). The observation from this experiment revealed a significant reduction by 20-40 % in D-dimer formation at both concentrations sequentially (Fig 4.10 A, B). It was clear that DZ caused the strongest inhibition at both concenterations.

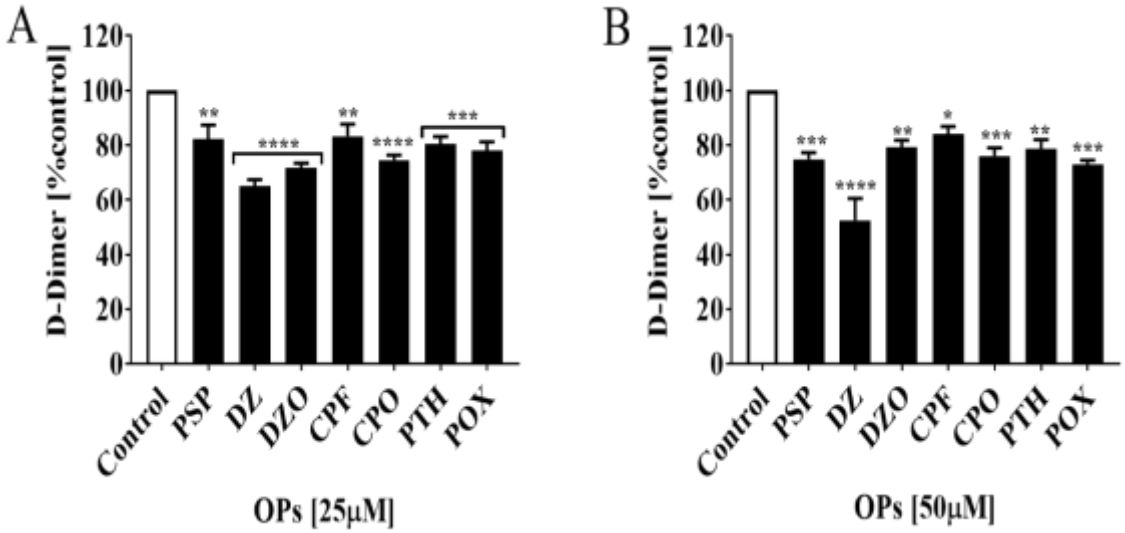

Figure 4- 10: D-Dimer levels in human plasma treated with organophosphorus compounds.

Diluted human plasma samples (~1.5 mg/ml) were pre-incubated for 30 min on ice with either a 25 µM or 50 µM concentration of the OPsPSP, DZ, CPF, CPO, PTH and POX. To start the clot, 5 mM $CaCl_2$ was added and incubated for three hours at 37ºC, after which D-dimer was quantified using the D-Dimer Human Simplestep ELISA®Kitassay. Data points represent the mean ± SEM of normalized plasma TG activity from four independent experiments. ** p<0.01, *** p<0.001, **** p<0.0001 versus non OP-treated control (=100%).

4.2.6 Identification of protein organophosphate adduct by mass spectrometry

To identify novel OP adducts on plasma TG protein, analysis was done by the team of John van Geest Cancer Research Centre using the Sciex TripleTOF 6600 mass spectrometry was carried out for 5 µg of rFXIIIa pre-incubated for 30 min at 4ºC with PSP, DZO, CPO and POX at final concentrations of 200 µM and a control sample incubated with 0.25% DMSO, before a further incubation for 1 h at 37 ºC with 6.67 mM $CaCl_2$ as indicated in (section 2.2.6). As the analyses have produced a very large data set, this work focuses only on the mass shifts corresponding to the covalent binding of PSP, O-diethylphosphorylation, O-ethylphosphorylation and phosphorylation (STY) (Fig 4.11 A, B, C, D, E). Comparing to control sample the results showed after extract the matching with control sample that the sample of rFXIII incubated with PSP showed some binding of PSP at serines 341 and 711. On the other hand, the oxon OPs showed a variety of O-diethylphosphorylation, O-ethylphosphorylation and phosphorylation (STY), but the CPO showed the highest number of O-diethylphosphorylation on tyrosine (Y) and lysine (K) residues, respectively. Fig 10.12 summarizes all positions of OP adduct binding.

A


1 MSETSRTAFG GRRAVPPNNS NAAEDDLPTV ELQGVVPRGV NLQEFLNVTS VHLFKERWDT NKVDHHTDKY ENNKLIVRRG
81 QSFYVQIDFS RPYDPRRDLF RVEYVIGRYP QENKGTYIPV PIVSELQSGK WGAKIVMRED RSVRLSIQSS PKCIVGKFRM
161 YVAVWTPYGV LRTSRNPETD TYILFNPWCE DDAVYLDNEK EREEYVLNDI GVIFYGEVND IKTRSWSYGQ FEDGILDTCL
241 YVMDRAQMDL SGRGNPIKVS RVGSAMVNAK DDEGVLVGSW DNIYAYGVPP SAWTGSVDIL LEYRSSENPV RYGQCWVFAG
321 VFNTFLRCLG IPARIVTNYF SAHDNDANLQ MDIFLEEDGN VNSKLTKDSV WNYHCWNEAW MTRPDLPVGF GGWQAVDSTP
401 QENSDGMYRC GPASVQAIKH GHVCFQFDAP FVFAEVNSDL IYITAKKDGT HVVENVDATH IGKLIVTKQI GGDGMMDITD
481 TYKFQEGQEE ERLALETALM YGAKKPLNTE GVMKSRSNVD MDFEVENAVL GKDFKLSITF RNNSHNRYTI TAYLSANITF
561 YTGVPKAEFK KETFDVTLEP LSFKKEAVLI QAGEYMGQLL EQASLHFFVT ARINETRDVL AKQKSTVLTI PEIIIKVRGT
641 QVVGSDMTVT VQFTNPLKET LRNVWVHLDG PGVTRPMKKM FREIRPNSTV QWEEVCRPWV SGHRKLIASM SSDSLRHVYG
721 ELDVQIQRRP SM

B


1 MSETSRTAFG GRRAVPPNNS NAAEDDLPTV ELQGVVPRGV NLQEFLNVTS VHLFKERWDT NKVDHHTDKY ENNKLIVRRG
81 QSFYVQIDFS RPYDPRRDLF RVEYVIGRYP QENKGTYIPV PIVSELQSGK WGAKIVMRED RSVRLSIQSS PKCIVGKFRM
161 YVAVWTPYGV LRTSRNPETD TYILFNPWCE DDAVYLDNEK EREEYVLNDI GVIFYGEVND IKTRSWSYGQ FEDGILDTCL
241 YVMDRAQMDL SGRGNPIKVS RVGSAMVNAK DDEGVLVGSW DNIYAYGVPP SAWTGSVDIL LEYRSSENPV RYGQCWVFAG
321 VFNTFLRCLG IPARIVTNYF SAHDNDANLQ MDIFLEEDGN VNSKLTKDSV WNYHCWNEAW MTRPDLPVGF GGWQAVDSTP
401 QENSDGMYRC GPASVQAIKH GHVCFQFDAP FVFAEVNSDL IYITAKKDGT HVVENVDATH IGKLIVTKQI GGDGMMDITD
481 TYKFQEGQEE ERLALETALM YGAKKPLNTE GVMKSRSNVD MDFEVENAVL GKDFKLSITF RNNSHNRYTI TAYLSANITF
561 YTGVPKAEFK KETFDVTLEP LSFKKEAVLI QAGEYMGQLL EQASLHFFVT ARINETRDVL AKQKSTVLTI PEIIIKVRGT
641 QVVGSDMTVT VQFTNPLKET LRNVWVHLDG PGVTRPMKKM FREIRPNSTV QWEEVCRPWV SGHRKLIASM SSDSLRHVYG
721 ELDVQIQRRP SM

C


1 MSETSRTAFG GRRAVPPNNS NAAEDDLPTV ELQGVVPRGV NLQEFLNVTS VHLFKERWDT NKVDHHTDKY ENNKLIVRRG
81 QSFYVQIDFS RPYDPRRDLF RVEYVIGRYP QENKGTYIPV PIVSELQSGK WGAKIVMRED RSVRLSIQSS PKCIVGKFRM
161 YVAVWTPYGV LRTSRNPETD TYILFNPWCE DDAVYLDNEK EREEYVLNDI GVIFYGEVND IKTRSWSYGQ FEDGILDTCL
241 YVMDRAQMDL SGRGNPIKVS RVGSAMVNAK DDEGVLVGSW DNIYAYGVPP SAWTGSVDIL LEYRSSENPV RYGQCWVFAG
321 VFNTFLRCLG IPARIVTNYF SAHDNDANLQ MDIFLEEDGN VNSKLTKDSV WNYHCWNEAW MTRPDLPVGF GGWQAVDSTP
401 QENSDGMYRC GPASVQAIKH GHVCFQFDAP FVFAEVNSDL IYITAKKDGT HVVENVDATH IGKLIVTKQI GGDGMMDITD
481 TYKFQEGQEE ERLALETALM YGAKKPLNTE GVMKSRSNVD MDFEVENAVL GKDFKLSITF RNNSHNRYTI TAYLSANITF
561 YTGVPKAEFK KETFDVTLEP LSFKKEAVLI QAGEYMGQLL EQASLHFFVT ARINETRDVL AKQKSTVLTI PEIIIKVRGT
641 QVVGSDMTVT VQFTNPLKET LRNVWVHLDG PGVTRPMKKM FREIRPNSTV QWEEVCRPWV SGHRKLIASM SSDSLRHVYG
721 ELDVQIQRRP SM

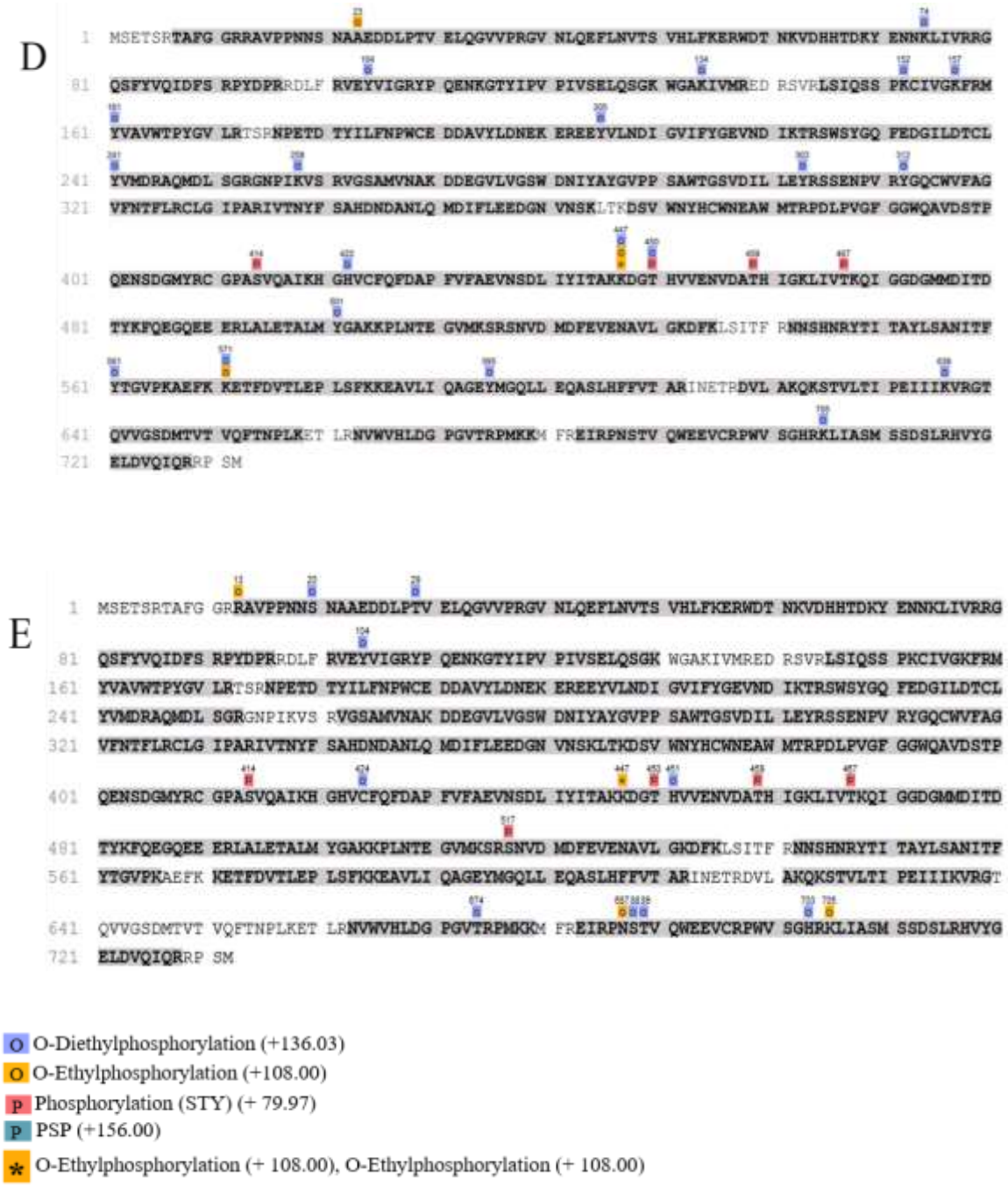

Figure 4- 11: Mapping of proposed OP adducts on rFXIIIa following mass spectrometry.

Sample (5 µg) of purified rFXIIIa was treated with (A) solvent vehicle 0.25 % (v/v) DMSO as a control, and 200 µM of (B) PSP, (C) DZO, (D) CPO and (POX) with emphasis on band shifts for the binding of PSP, O-ethylphosphoryltion and O-diethylphosphorylation. The cut off value AScore ≥ 20.

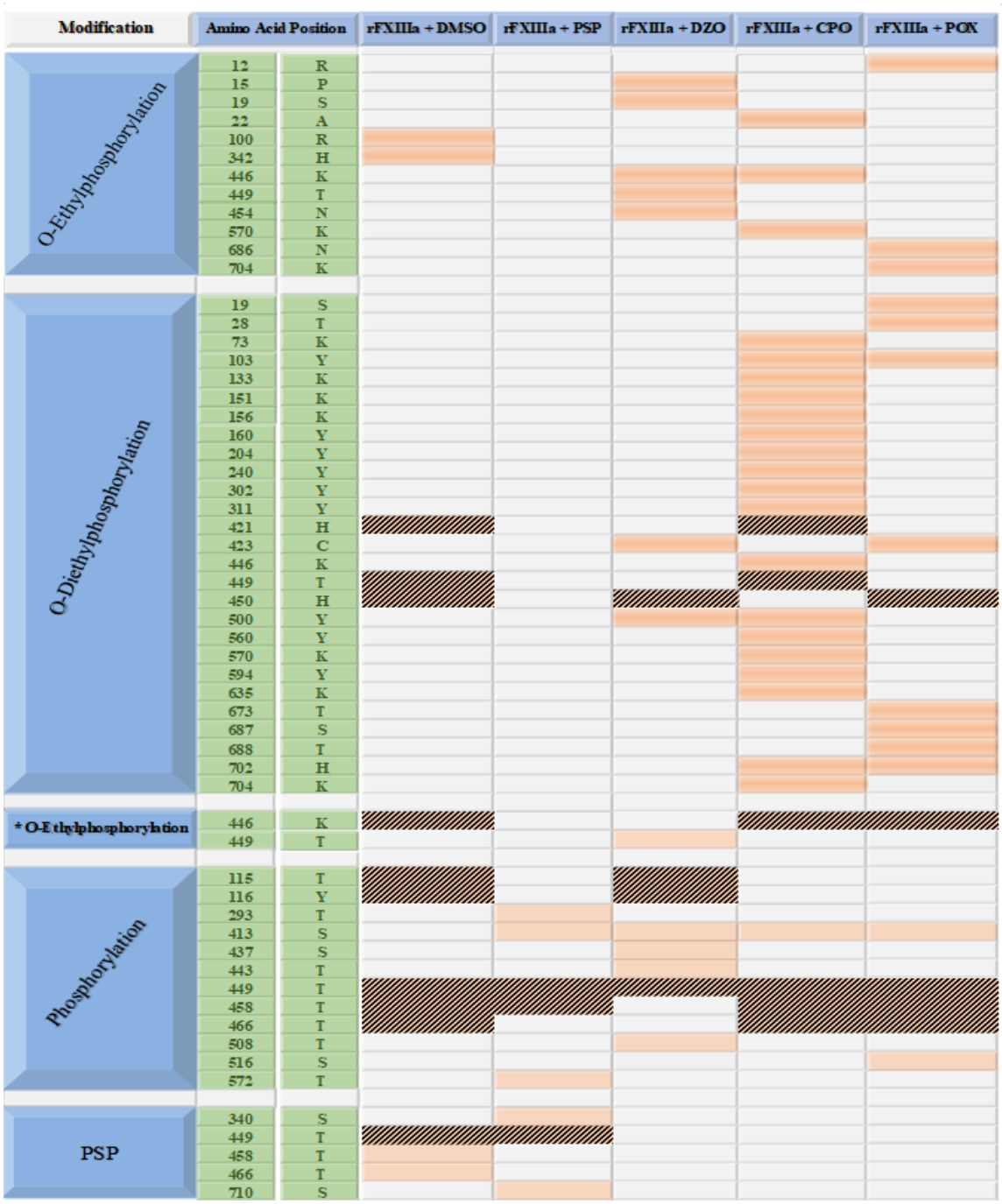

Figure 4- 12: Summary of rFXIIIa protein modification after incubation with OP compounds.

This table is a summary of the modifications mapped in Fig 12. The orange colour represents the individual modification on amino acids, and the diagonal stripes represent similarity compared to the control (rFXIIIa with 0.25 % (v/v) DMSO).

4.3 Discussion

FXIIIa is a transglutaminase that has multiple biological actions in the body. It is involved in last step of haemostasis, its function there being considered very essential to stabilize the fibrin mesh by cross-linking lysine-glutamyl side chains to form an unbreakable clot (Martins *et al.*, 2014). Any abnormalities on FXIIIa may cause serious bleeding (Muszbek *et al.*, 2011). In the present study, the ability of OPs to interfere with FXIIIa activity and the probability of their binding to FXIIIa were studied. Overall, the results presented in this chapter showed that some of the OPs can inhibit transamidase activity of plasma and pure FXIIIa measured by amine incorporation and peptide cross-linking assays, but the inhibition was greater with purified FXIIIa. This corresponded to results of inhibition of plasma clot formation that were measured by D-Dimer ELISA. Analysis by 1D and 2D SDS-PAGE and mass spectrophotometry showed that OPs were also capable of covalent binding with rFXIIIa.

In assays involving pre-exposure to OPs, transamidase assays (Fig 4.1 & 4.2) showed slight but significant inhibition of plasma TG-mediated amine incorporation and peptide crosslinking activities, although an IC_{50} value was not reached. CPF showed no significant effect on both activities, whereas there were no significant changes induced by DZ or POX in plasma peptide crosslinking activity. However, data for other OPs suggested that plasma TG-mediated amine incorporation activity was more sensitive to OP toxicity, where CPO was the most effective inhibitor of plasma TG activity. In contrast, rFXIIIa-mediated amine incorporation and peptide crosslinking activities both showed higher sensitivity to OP toxicity than plasma TG (Fig 4.3 & 4.4) and IC_{50} values were determined. Moreover, the rFXIIIa-mediated peptide crosslinking activity showed more sensitivity to OP toxicity than did the amine incorporation assay. Surprisingly, parent compounds in both activities of

rFXIIIa had more potency than the metabolite form. For example, CPO showed the statistically significant effect at 0.8 µM (Fig 4.4 F) on rFXIIIa-mediated peptide crosslinking activity but 50 % of activity was lost by ≤ 6µM of CPO concentration (IC_{50} 6.5 µM); however, CPF (Fig 4.4 C) was the most potent among the others where more than 50 % of activity was inhibited by ≤ 3µM of CPF concentration (IC_{50} 2.7 µM). Also, it was noticeable the significant effect of parent compounds DZ and PTH compared to their oxon metabolite forms in amine incorporation activity with rFXIIIa and plasma TG, respectively. In addition, PSP showed significant effect on both rFXIIIa and plasma TG -mediated peptide crosslinking and amine incorporation activities, respectively.

Some studies suggest that PSP may alter cell signaling and that the latter is responsible for the increased activity noticed in the cytosolic TG (Howden, 2003; Hargreaves *et al.*, 2006). However, studies on cultured N2a neuroblastoma and HepG2 hepatoma cell lines, PSP (3µM) exposure resulted in altered tissue transglutaminase-mediated amine incorporation activity, where it was decreased in N2a and increased in HepG2 cells (Harris *et al.*, 2009). Moreover, Muñoz, *et al.* (2010) showed that tissue transglutaminase-mediated amine incorporation activity in rat C6 glioma cells increased after 24h exposure to 10µM chlorpyrifos. In the latter study, increased activity of guinea pig liver TG2 *in vitro* following treatment with OP suggested the possibility of a direct interaction between OPs and TG. Although, it has been pointed that parent OPs compound are weak inhibitors of their acute toxicity target AChE and their bioactivated form the oxons are considered the primary acute toxicants in nerve tissue (Poet *et al.*, 2003), in the current study some of the parent compounds showed more inhibitory potential against TG activity than their oxon form.

The inhibition effect of DZ, CPF, PTH could be due to the reaction either with forms of parent, oxon, or may be with one of their common metabolite products, without oxidation the diethylthiophosphate (DETP), or after oxidation the diethylphosphate (DEP),

respectively, since the presence of pesticide parent and their metabolites product were indicated (including DETP and DEP) in human biological fluids using liquid chromatography-mass spectrophotometry (Manini *et al.*, 2004). On the other hand, the effect of inhibition could be due to a specific reaction based on a structural effect of DZ, CPF, PTH or with their final metabolite products, 2-isopropyl-4-methyl-6-hydroxpyrimidine (IMHP), 3,5,6-TCP, *p*-nitrophenol, respectively (Brzak *et al.*, 1998; Poet *et al.*, 2003). In addition, the end products of OP metabolites may adversely affect human health (Melching-Kollmuß *et al.*, 2010; Rathod & Garg, 2017). It has been suggested that the toxic effect of phenol compounds that may be released from these pesticides and their derivatives and the side effects of chronic exposure may cause pathological changes due to their accumulation in the skin, esophagus, blood plasma, lungs, liver, kidneys and also the urogenital tract (Michałowicz & Duda, 2007). The strength of toxic impact of these phenol compound stems from the position and the type of the substituent which include a range of components including chlorine atoms, nitrate, methyl or ethyl groups in the case of pesticide OPs (Michałowicz & Duda, 2007). It has been reported that metabolite forms of DZ, CPF, PTH the IMHP, 3,5,6-TCP, *p*-nitrophenol, respectively, are classified as Carmer class III compounds that have structural features that do not permit a strong assumption of safety and could even have significant toxicity (Melching-Kollmuß *et al.*, 2010).

The significant effect of the parent compound CPF on pure FXIII- mediated amine incorporation (Fig 4.3 C) and peptide crosslinking (Fig 4.4 C) *in vitro* might be due to binding of the released tri chlorophenols attached to thio organophosphorous compound with higher potency than those attached to the oxidized organophosphorous. In this respect, previous study has done by Boyd *et al.* (2001) demonstrated mono-, di-, and tri-chlorophenols that used in agriculture objective to study their effect on different kinds of bacteria and the results manifested that the toxicity of chlorophenols to the bacteria was

dependent upon the position of the chlorine atoms on the benzene ring and the degree of chlorination. Moreover, it has been indicated that the metabolite form of DZ either the active DZO or IMHP, have much higher Michelis constant Km value than CPF metabolite products either the CPO or 3,5,6-TCP, suggesting that the toxicity effect of DZ will be much lower than that of CPF, due mostly to the quantity of bioactivation of the parent pesticide (Poet *et al.*, 2003). However, in the current work that was opposite to DZ effect on plasma (Fig 4.1 B) and pure FXIIIa (Fig 4.3 B) -mediated amine incorporation activity, which could be direct effect of parent thiophosphate toward enzyme activity especially on pure FXIII at higher concentration where 50% of the activity was lost. These findings suggest that DZ might be more effective in the biological environment, as in plasma, as it has less effect on pure FXIIIa-mediated amine incorporation activity. Also, it could be speculated that PTH, which also inhibited FXIIIa activity by more than 50% in both amine incorporation (Fig 4.3 D) and peptide crosslinking assays (Fig 4.4 D) compared to lower effects on both activities in plasma TG (Fig 4.1 & 4.2 D). Thus, the current finding and previous studies suggest that OPs can interact with and/or disrupt TG activity.

The low effect of OPs on plasma samples compared to their stronger potent effect on pure FXIIIa could be due the lack of a biological environment, which has many of proteins and chemical compounds that may interact with OPs and decrease their effect on FXIII. For example, several studies showed that OPs bind and interact with other plasma proteins such as ChEs, albumin and transferrin (Li *et al.*, 2008; Marsillach *et al.*, 2013).

Albumin is the most abundant plasma protein, representing more than 50% of the total protein in human blood plasma (Li *et al.*, 2007). It is known that albumin can form stable adducts with OPs (Li *et al.*, 2007; Tarhoni *et al.*, 2008; Chen *et al.*, 2013). Depletion of major proteins in plasma is one potential technique to improve the detection of low abundant proteins that could be disease biomarkers (Echan *et al.*, 2005). For that reason, the possibility

that the presence of albumin protein in plasma could decrease the amount of OP available to interact with plasma TG should be considered.

The possibility that the inhibitory effects of PSP on FXIIIa activity involved covalent binding of PSP to plasma TG was confirmed by the detection on SDS-PAGE of rhodamine-PSP binding to pure FXIIIa, and a similar molecular weight band in depleted plasma. This is the first time that covalent binding of OP to FXIIIa has been demonstrated. It was interesting to note that there were other labelled bands in depleted plasma and a smear of bands throughout the entire gel for whole plasma proteins (Fig 4.5), suggesting that other serum proteins were capable of binding covalently to PSP. The other PSP binding proteins presumably correspond to those previously identified as OP binding, namely albumin and ChEs, etc. (Marsillach *et al.*, 2013). However, it will be of interest to determine whether, in addition to FXIIIa, other novel PSP-binding serum proteins can be detected in depleted plasma samples. The depleted plasma protein extract incubated with labelled PSP was separated by 2D-PAGE and the result compared to control showed several labeled PSP binding spots that suggest other low abundant proteins in depleted plasma can interact with PSP; however, due to constraints of time, protein spots could not be identified by further analysis (Fig 4.6). The data obtained from follow-up competition experiments using pure FXIIIa and depleted plasma (Fig 4.7) in which samples were pre-incubated with unlabeled PSP prior to addition of labelled PSP confirmed that the Rh-PSP was binding to the same site as non-labelled PSP. The competition assay was applied again on pure FXIIIa with the other (non-labelled) OPs and labelled PSP showing significant competition in binding site in specific cases. For example, DZ and POX demonstrated slightly weaker fluorescense comparing to the intensity of only labelled PSP binding, suggesting that binding may not be near the PSP binding site. However, the other OPs showed higher competition with non-

labelled OP on the binding site and the variation in competition which could be a sign of more than one binding site or that they might not all bind at to the same positions.

Clot stabilization under OP treatment was studied by turbidimetric clot method, which detects the scattering of light by the forming clot but it was hard to detect any significant changes using this approach, suggesting no detectable effect on clot size. However, the D-dimer assay was then adopted as a more sensitive method to show changes in the plasma clotting cascade, being used as diagnostic and management tool for the monitoring of thrombotic and bleeding disorders (Bates, 2012).

In the current study the clot was created after plasma samples were treated with or without two concentrations (25 and 50 μM) of OPs, after which and D-dimer levels were measured to determine whether the fibrin mesh exhibited the same level of covalently crosslinked D-dimers within fibrin monomers (Fig 4.10). Seemingly, all OPs had significant effects on clot formation, which eventually affects D-dimer formation as a consequence. This is in broad agreement with the significant inhibition effect of OPs on TG-mediated transamidase activities, although the relative contribution of disrupted amine incorporation and protein crosslinking remain to be determined. It was noticeable that DZ had the most potent effect at both concentrations in the D-dimer assay, reaching about 50% decrease of D-dimer level in the sample with 50 μM of DZ, whereas DZ had a more significant on TG-mediated amine incorporation activity. This could reflect the possibility that DZ may interfere with either mechanism or activity of TG in the clotting cascade at least in part through an amine incorporation mediated pathway. Previous studies have reported that are high levels of natural polyamines in the human body, which may serve as substrates for transglutaminase in cells and body fluid (Folk *et al.*, 1980).

The indication from much of the literature is that OP compounds bind to proteins that have an active site serine, such as serine hydrolases; however, other studies demonstrated that there are other sites that could be possible targets for OP adduct fromationm, such as tyrosine residues in tubulin, albumin, and transferrin (Li *et al.*, 2008; Marsillach *et al.*, 2013). Mass spectrometry analysis is a very sensitive technique to determine the location of covalent binding site(s) on proteins such as purified protein FXIII, which has an active site cysteine314. Only the metabolite OP compounds were analysed by MS in the current study and it was obvious from the results (Fig 4.11) that there may be several modifications and different adducts in different binding sites, by comparing mass shifts to the control sample (Fig 4.11 A). The MS results was numbered the amino acids with extra methionine in the beginning and ending of the protein sequence. However, the numbering was corrected according to the literature, which highlighted that serine is in the next to the last position, which favors the elimination of initiator methionine, and then in the mature molecule NH_2 terminal serine residue acetylated and amino acid numbering starting with the Ser amino acid (Muszbek *et al.*, 2011). The Ser-413, which is present in the catalytic core domain, was the common phosphorylated site by PSP, DZO, CPO, and POX (Fig 4.11 B, C, D, & E), which could be the competing site of binding with PSP. The PSP adducts showed fewer binding sites than the oxon metabolite OPs and they were mainly on two threonine and two serine amino acids, but it was interesting to note that Thr293-phosphorylated is only a few amino acids away from active site Cys314 and Ser340-PSP is nearby Asp343. Studies reported that a strong salt bridge between Arg11 in AP-FXIII domain and Asp343 in core domain to make Cys314 inaccessible for substrate and other chemical molecules (Muszbek *et al.*, 2011). On the other hand, the most modification change at wide range of 50:50 tyrosine and lysine diethylphosphorylated was observed for CPO. The diethylphosphorylated adduct was disrtributed between the β-sandwich and catalytic core

domains, the closest to catalytic active site were Tyr302 and 311. Moreover, CPO formed an ethylphosphorylated adduct on Ala22 in AP-FXIII and Lys570 in β-barrel 1 domains. Some studies refer to the fact that a major adduct of CPO on albumin is tyrosine-diethylphosphorylated and becomes irreversibly modified *in vivo* in humans poisoned by CPF (Li *et al.*, 2013). Also ***in vitro*** experiments showed that CPO can covalently modify tyrosine on some proteins including keratins, tubulin, and transferrin (Schopfer *et al.*, 2010). In addition, some modifications were detected on rFXIII incubated with DZO and POX, including ethylphosphorylated and diethylphosphorylated close from Arg11 in AP-FXIII domains which could affect the stability of the salt bridge between Arg11and Asp343 and as a result affect the catalytic site position Cys314. Interestingly, DZO, CPO, and POX treatments induced ethylphosphorylated-adducts on different amino acid spread all over the main four domains, all metabolite OP adducts formed and their positions on the rFXIII are demonstrated in Fig 4.12. Due to constraints of time, adducts formed with the parent compound have not yet been studied but should be considered in further work.

Chapter 5: Effects of organophosphorous compounds on thrombin

5.1 Introduction

The key factor of coagulation, which is one of the important dynamic biological processes in blood, is the proteolytic enzyme thrombin. Thrombin is a serine protease that plays an essential role in the whole process, cleaving over 12 substrates and interacting with at least 6 cofactors involved in clot formation (Huntington, 2005). It amplifies the coagulation factors and activates platelet aggregation, moreover controlling the activity of coagulation inhibitors (Huntington, 2012). However, any thrombin dysfunction may lead to haemorrhagic disorders (Stief, 2006).

OPs have been identified as serine protease and esterase inhibitors due to organophosphorylation of the active site serine (Chambers & Oppenheimer, 2004). The main OP serine esterase targets are the cholinesterases AChE and BChE, the inhibition of which is nowadays the standard method utilized for the biological monitoring of OP exposure (Marsillach *et al.*, 2013). Moreover, many studies refer to other proteins as OP sensitive serine hydrolases, such as digestive proteases (chymotrypsin, trypsin and elastase), NTE, and some blood clotting factors, such as thrombin, plasmin, kallikrein, etc. (Quistad & Casida, 2000; Reiner, 2001; Quistad & Casida, 2005). Unfortunately, studies of OP effects on blood coagulation serine protease factors are limited. Henson *et al.* (1976) confirmed that high concentration of the OP diisopropylphosphonofluoridate (DFP) inhibited serine esterases (proteases) including thrombin, which stimulates platelet granule secretion. In addition, when the clotting factors thrombin, plasmin, and kallikrein were examined in the presence of some of OPs, the results showed that thrombin was the most sensitive to inhibition by the most potent inhibitors in the order: tributylphosphorotrithioate (tribufos) also known as DEF, phenyl saliginen cyclic phosphate (PSCP or PSP), and DFP (Quistad & Casida, 2000). Furthermore, a significant inhibitory and prolongation effect of POX has been

observed in the thrombin activity coagulation test suggesting that it interferes with thrombin activity (Golderman *et al.*, 2016).

The work in this chapter was planned to study the effects of a range of concentrations of the OPs PSP, DZ, DZO, CPF, CPO, PTH, POX on the activities of purified and plasma thrombin. It was also of interest to study covalent binding and competitive binding using SDS-PAGE and image analysis of thrombin incubated with a fluorescent rhodamine-PSP (Rh-PSP) probe.

5.2 Results

5.2.1 Effects of organophosphorus compounds on purified thrombin activity

Thrombin assays were performed to investigate whether the OPs were able to affect the activity of purified human thrombin. Purified thrombin samples were pre-incubated 30 min on ice with a range of OP concentrations prior to the addition of 0.5 mM thrombin substrate Sar-Pro-Arg-p-nitroanilide, as indicated in (section 2.2.5). The results showed slight (10 %) but statistically significant inhibition of purified thrombin activity by PSP (Fig 5.1 A), and the most significant inhibition effect was from CPF on purified thrombin (Fig 5.1 C) with an IC_{50} value of 22 µM, but only concentrations of 25 and 50 µM showed inhibition effects >50 %, and >80 %, respectively. In contrast, the other OPs showed no significant effect under the conditions tested.

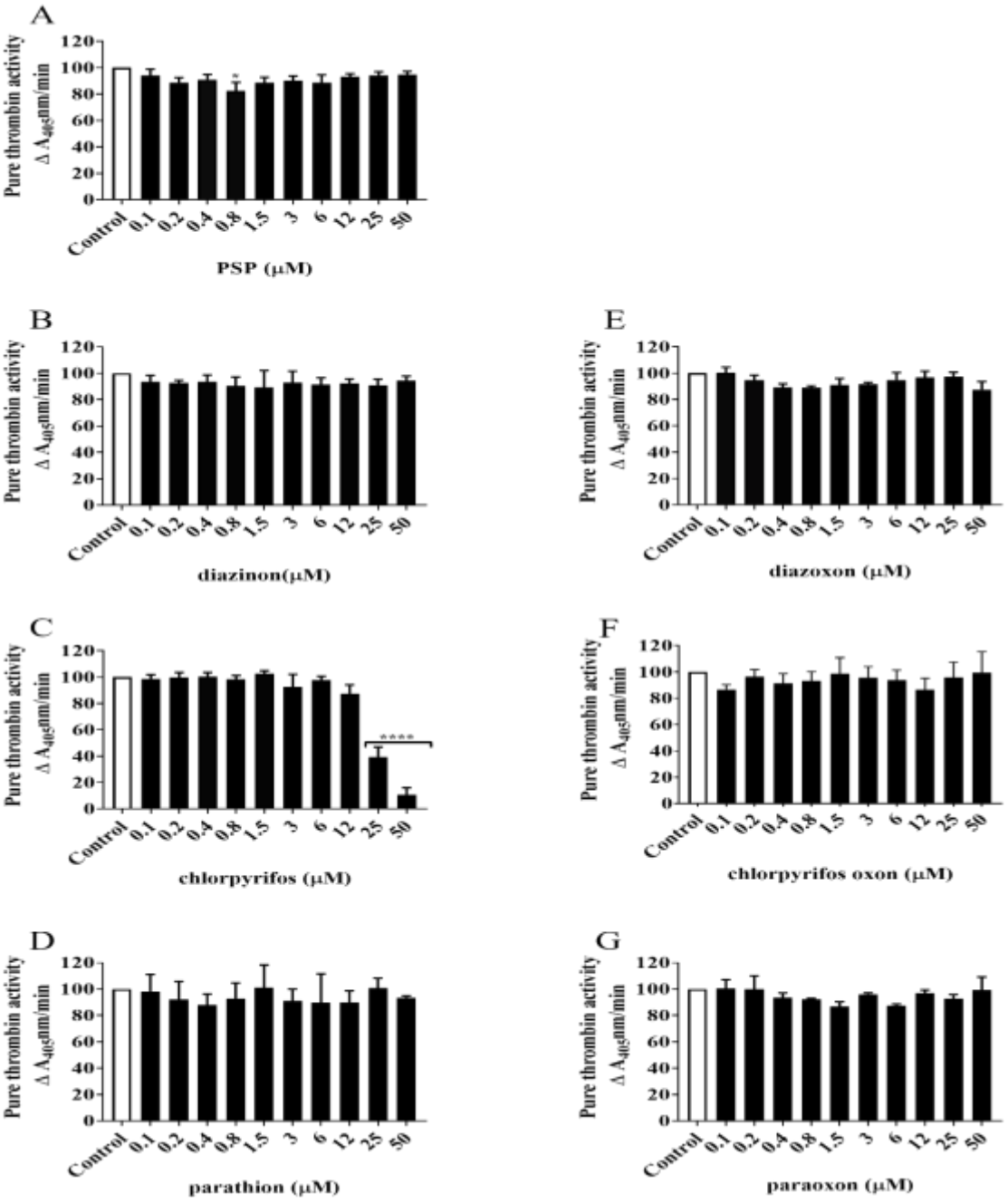

Figure 5- 1: Effects of OPs on pure thrombin activity.

Diluted human pure thrombin samples (~0.05 U/ml) were incubated 30 min on ice with a range of concentrations of OPs, as indicated in the graphs. Plots shown are for: A) PSP, B) diazinon, C) chlorpyrifos, D) parathion, E) diazoxon, and F) chlorpyrifos oxon, G) paraoxon. The reaction was initiated by adding 0.5 mM Sar-Pro-Arg-p-nitroanilde. Data points represent the mean percentage ± SEM of pure thrombin specific activity from three independent experiments. *p<0.05, ****p< 0.0001 versus non OP-treated control (=100%).

5.2.2 Effects of organophosphorus compounds on human plasma thrombin activity

In order to study OP effects on human plasma thrombin activity, the assay was first of all optimised. As the optimisation of plasma thrombin concentration with a range of OPs concentrations consumed a lot of subtrate reagent, plasma samples were pre-incubated 30 min on ice with either 25 or 50 µM concentrations of OPs, followed by the addition of 1.6 mM thrombin substrate Sar-Pro-Arg-p-nitroanilide to initiate the reaction, as indicated in section 2.2.1.2.2. The outcome of experiments studying the effects of 25 µM OPs on plasma thrombin activity showed that there was approximately 40% inhibition of plasma thrombin activity by CPF only (Fig 5.2 A). However, 50 µM CPF, CPO, and POX showed significant inhibition of thrombin activity. Overall, CPF showed a greater inhibitory effect than the other OPs against plasma thrombin activity at both concentrations.

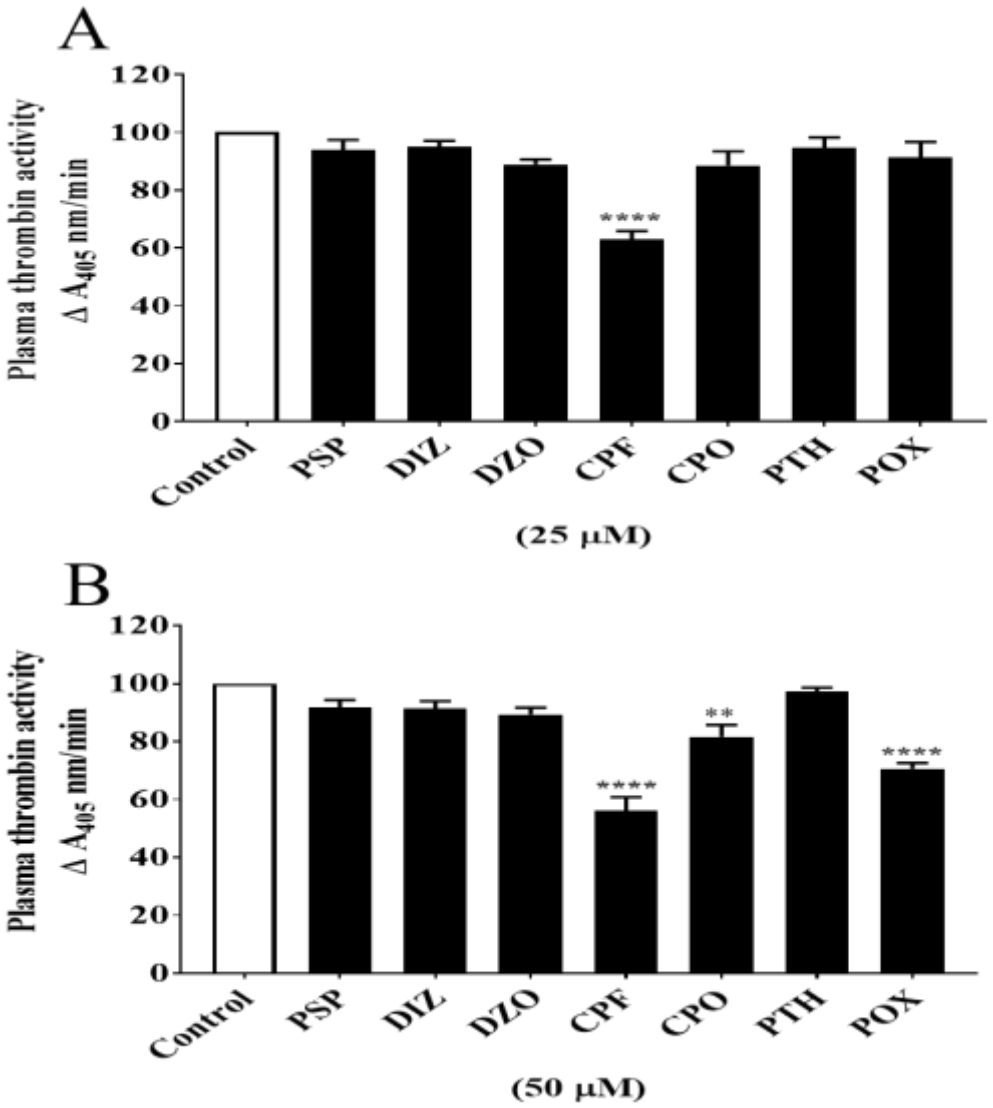

Figure 5- 2: Effect of OPs on plasma thrombin activity.

Diluted human plasma samples (~0.2 mg/ml) were pre-incubated for 30 min on ice with either (A) 25 µM or (B) 50 µM concentrations of the OPs PSP, DZ, CPF, CPO, PTH and POX. The raection was initiated by adding 1.6 mM Sar-Pro-Arg-p-nitroanilde. Data points represent the mean ± SEM of pure thrombin specific activity from three independent experiments. **p<0.01, ****p< 0.0001 versus non OP-treated control (=100%).

5.2.3 SDS-PAGE analysis for rhodamine-PSP competition binding to human purified thrombin.

In order to determine whether Rh-labelled PSP was binding in the same manner as unlabeled PSP and other OPs on purified thrombin, a competition assay was carried out. For this, human purified thrombin samples were incubated in the presence and absence of labelled PSP, also testing the competition with labelled PSP and unlabeled PSP and other OP, prior to analysis by SDS-PAGE and fluorescence imaging as indicated in section 2.2.8.2. The results shown in Figures 5.3A and 5.4 A infer that the intensities of fluorescent bands after Rh-PSP binding are decreased in purified thrombin when competed out with unlabeled OPs. The difference in the intensity between untreated protein (lane 1) and the protein incubated with labeled Rh-PSP (lane 2) indicated strong intensity of PSP binding to thrombin in lane 2 (Fig 5.3 A, Fig 5.3 A).The competition binding on purified thrombin between unlabeled and labelled OPs in lanes 3, 4 and 5 (Figs 5.3 A and 5.4 A) showed visibly lower intensity of fluorescence compared to controls in lane 1 0.25% (v/v) (DMSO) and lane 2 (Rh-PSP) (Fig 5.3 A, Fig 5.4 A).

Moreover, the densitometric analysis confirmed that the signal intensity for the 35 kDa thrombin band was significantly reduced in the presence of competition by unlabeled OPs for purified thrombin in lanes 3, 4, 5 (Figs 5.3 and 5.4 C) and 6 (Fig 5.4 C). The quantification of band intensities of competing binding compared to control (labeled protein with Rh-PSP) showed that intensity was reduced 4-fold with unlabeled PSP, DZ, and DZO (Fig 5.3 C), and about 2-fold in the case of unlabeled CPF, CPO, PTH and POX (Fig 5.4 C). The gels were stained with InstantBlue ^{TM} stain to confirm the presence of protein in samples (Fig 5.3 B, 5.4 B). Overall, the results showed competition in all samples incubated with both labelled PSP and unlabeled OPs.

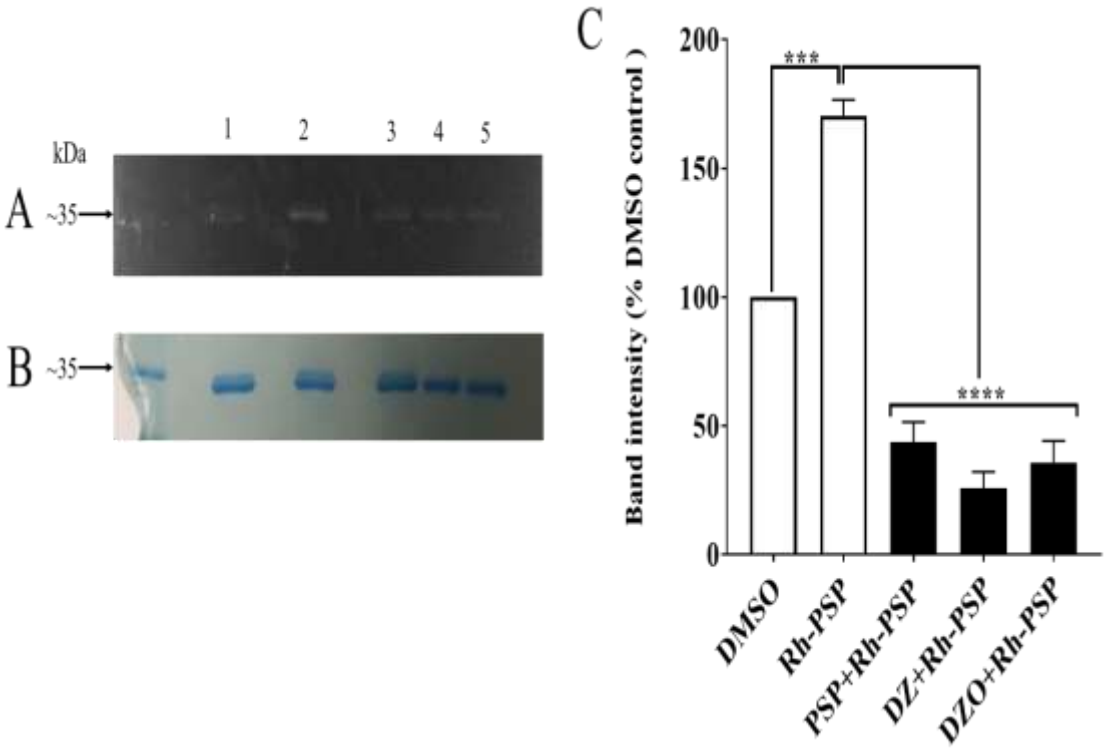

Figure 5- 3: Visualization of thrombin labeled with competition binding of rhodamine-PSP and unlabeled PSP, DZ, DZO.

Pure thrombin (2µg) was incubated for 30 min on ice with 0.25% (v/v) DMSO (Lane1), 25µM of Rh-PSP (lane 2) and both 25µM of Rh-PSP + 200µM of PSP, DZ, DZO (lane3, lane 4, lane 5); respectively. Panel A) Gels were visualized under green incident light (520nm) using a LAS4000 imaging system. Panel B) Gels were stained with InstantBlue ™ to confirm the presence of protein bands. Panel C) Densitometric analysis for Rh-PSP binding. Data represent the mean of fluorescence intensity ±SEM from three independent experiments. ***p<0.001, ****p<0.0001 relative to the DMSO control (=100%).

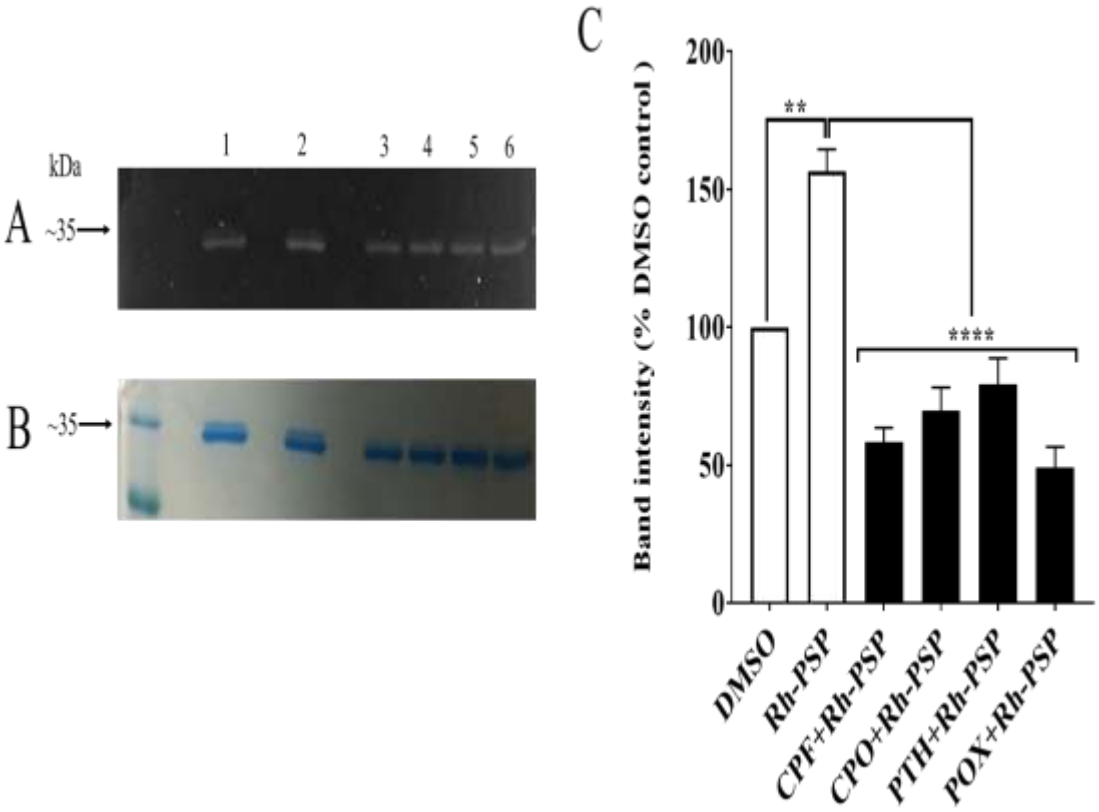

Figure 5- 4: Visualization of thrombin labeled with competition binding of rhodamine-PSP and unlabeled CPF, CPO, PTH, POX.

Pure thrombin (2µg) was incubated for 30 min on ice with 0.25% (v/v) DMSO (Lane1), 25 µM of Rh-PSP (lane 2) and both 25 µM of Rh-PSP + 200 µM of CPF, CPO, PTH, POX (lane3, lane 4, lane 5, lane 6); respectively. Panel A) Gels were visualized under green incident light (520nm) using a LAS4000 imaging system. Panel B) Gels were stained with InstantBlue ™ to confirm the presence of protein bands. Panel C) Densitometric analysis for Rh-PSP binding. Data represent the mean of fluorescence intensity ±SEM from three independent experiments. ** $p<0.01$, **** $p<0.0001$ relative to the DMSO control (=100%).

5.3 Discussion

Thrombin is a coagulation factor that is generated in the last part of coagulation (common pathway) but its role in haemostasis in not limited (Huntington, 2005). Abnormalities in thrombin generation could lead to unstable clot formation, resulting in a serious bleed (Lupu *et al.*, 2016). In the current work, the effect of OPs on thrombin activity and the chance of their binding to purified thrombin were studied. Overall, the results presented in this chapter showed that a few of the OPs can inhibit plasma thrombin activity in high concentration, but only CPF caused inhibition of activity in both purified and plasma thrombin. The possibility of covalent binding of PSP to thrombin protein was confirmed by the detection on SDS-PAGE of rhodamine-PSP binding to purified thrombin. Moreover, the data obtained from competition experiments, in which samples were pre-incubated with unlabeled OPs prior to addition of labelled PSP, indicated that the rhodamine-PSP was binding to the same site as non-labelled OPs.

The optimization experiments of thrombin activity demonstrated a protein and substrate concentration-dependent increase in both purified and plasma. Unfortunately, these optimizations consumed more substrate than expected, causing a shortage in substrate reagent.

In the current work human purified thrombin activity was slightly affected by PSP, but it was most sensitive to CPF at 25 and 50 µM concentrations in agreement with the effect of CPF on plasma thrombin (Fig 5.1 C & 5.2 A, B). The higher potency of the CPF effect on purified thrombin might be due the lack of a biological environment comparable to that in plasma samples. This could be due to a potential interaction with either the leaving group (diethylthiophosphate) or with phosphate atom replacing the leaving group position. For example, it has found that adducts were formed on highly purified human BChE incubated

with DZ, and 3.6 mg/ml BChE over 15 h exposure to 50 µM DZ effect reduced activity by 52% suggesting 'slow' inhibition, which could occur through a thiono-thiolo rearrangement (Tacal & Lockridge, 2010). Also, the CPF significant effect on inhibition plasma thrombin activity was 2 and 6-fold different from 25 and 50 µM purified thrombin, respectively, suggesting that the biological environment had interfered with CPF potency on plasma thrombin activity. A developed analytical method to measurement directs the oxon and TCP formation from CPF compound has found that the bioactivation of CPF by CYPs to the oxon metabolites form CPO leads to a more potent effect in the biological environment (Poet *et al.*, 2003). Moreover, this could extend to deactivation of CPO by both CYPs and PON1 to TCP (Poet *et al.*, 2003; Kumar, 2015). This agrees with current findings for CPO inhibition of plasma thrombin (Fig 5.2 B). In addition, in the current work the potency effect of POX on plasma thrombin (Fig 5.2 B) revealed that POX could have a major effect on plasma thrombin at higher concentrations.

CPO and POX inhibition effects were previously studied *in vitro* on 0.2 U purified thrombin from bovine plasma pre-incubated 15min at 25ºC before adding 100 µM CBZ-Gly-Pro-Arg-4-nitroanilide substrate and the absorbance change (404 nm) was monitored for 10 min. The results revealed that thrombin was not very sensitive to CPO and POX toxicity, with the IC_{50} for both being more than 100 µM (Quistad & Casida, 2000). Moreover, under the same study conditions, the PSP effect on purified thrombin was studied, and the results indicated that PSP was a more potent than CPO and POX, with an IC_{50} of 26 µM (Quistad & Casida, 2000). However, in the current study PSP showed only a slight effect on purified thrombin and no effect at all on plasma thrombin activity. The variation of results between the previous study and the present study could be due to either the enzyme source and substrate differences, as in the current study purified human thrombin was used, and

Sar-Pro-Arg-p-nitroanilide substrate, which has a higher K_{cat} and lower Km than CBZ-Gly-Pro-Arg-4-nitroanilide (Hortin *et al.*, 2001).

On the other hand, another study by Golderman *et al.* (2016) investigated the effect of POX toxicity on 0.05 U/ml thrombin purified from bovine plasma pre-incubated 10 min on ice before adding 14 µM Boc-Asp-(OBzl)-Pro-Arg-AMC fluorescent substrate and the absorbance change recorded at (440-460 nm) for 60 min. Their results indicated that 500 µM POX completely inhibited purified thrombin activity, whereas, 50 µM POX showed 70 % inhibition of purified thrombin activity. That is in good agreement with the current study, suggesting that POX inhibited thrombin activity in a concentration-dependent manner. Also, because of the potentially higher sensitivity of the fluorescent substrate it may have been possible to detect a greater effect of POX on thrombin activity. Gargiulo *et al.* (1981) pointed that employing a fluorescent instead of a chromogenic substrate will allow the measurement of smaller quantities of protease enzymes in body fluids.

Furthermore, the present study monitored the absorbance change of purified and plasma thrombin activity (405 nm) for 90 and 240 min, respectively, which might have enhanced the ability to detect the inhibitory effect of POX on human plasma thrombin. In the previous study of Quistad & Casida (2000) they monitored the absorbance change for 10 min only, and they could not detect any POX effect lower than 100 µM. However, Golderman *et al.* (2016) conducted their study on the same species (bovine thrombin) as Quistad & Casida (2000) but they apply longer absorbance change for 60 min, and were able to detect significant inhibition of thrombin activity by POX. Increasing the pre-incubation time or decreasing the amount of thrombin used can improve fluorometric assay sensitivity (Gargiulo *et al.* 1981). Thus, longer incubation time with OP and/or lower enzyme

concentration could enhance the stoichiometric reaction with thrombin enzyme in chromogenic assay.

Previous studies investigated the POX effect on coagulation system due to its ability to inhibit thrombin activity, prothrombin time (PT) the extrinsic and common pathways, activated partial thromboplastin time (aPTT) the intrinsic and common pathways, and thrombin time (TT), the final part of coagulation where fibrinogen converts to fibrin (Golderman *et al.*, 2016). Reconstituted human plasma incubated with 500 µM POX for 10 min, revealed no effect on the coagulation system (Golderman *et al.*, 2016). Nevertheless, 9 µg/ml POX showed a significant *in vitro* effect on human blood coagulation assessed by thrombelastography (TEG), indicating that clot formation time was prolonged about 12-fold compared to non OP-treated samples (Petroianu *et al.*, 1997). In an *in vivo* study done on mini pigs injected with 54mg/kg POX, blood samples were collected after 150 min exhibited hypocoagulability by PTT prolongation (Petroianu *et al.*, 1999).

In Rh-PSP-thrombin binding assays, Rh-PSP bind to thrombin band was obvious with high intensity of fluorescence after SDS-PAGE, which confirms the covalent binding of PSP to thrombin protein. The PSP binding site is presumably the active site serine, corresponding to that previously identified in other serine esterases, such as BChE (Marsillach *et al.*, 2011; Marsillach *et al.*, 2013).

Competition binding between Rh-PSP and other OPs on thrombin bands showed significant competition in binding site that reduced the fluorescence intensity to background levels with all unlabeled OPs, which suggests that competition may occur on a single site of the protein sequence. Unfortunately, due of constraints of time and materials, it was not possible to do mass spectrometry to determine the binding site(s). Previous studies have confirmed the

adduct of OPs presence on the active site serine of serine hydrolases, for example ChE is diethyl phosphorylated by oxon OPs (Thompson *et al.*, 2010).

Also, all OPs used in present study showed covalent binding to thrombin on gel analysis and at the same time most of them did not affect thrombin activity under the conditions tested, which could be explained by the possibility that the OPs bind to thrombin without inhibiting the activity. In this respect, one study showed that, when the DFP was incubated with egg-white lysozyme, Taka-amylase A, and papain, tyrosine residues were covalently labeled but the OP-modified enzymes possessed the full activity (Lockridge & Schopfer, 2010)

In summary, the data presented in this chapter indicate that CPF has a notable toxic effect against purified thrombin activity, whereas, CPF, CPO and POX affect the plasma thrombin activity. OP effects on thrombin activity may rely on incubation time and occur in a concentration dependent manner. Furthermore, studies of OP binding to thrombin protein indicate the possibility of OP adduct formation. However, further investigation is needed to confirm the specific location of the binding (site)s by mass spectrometry.

Chapter 6: Effects of organophosphorous Compounds on THP-1 cells

6.1 Introduction

cFXIII-A_2 expression has been found in in white blood cells (e.g. monocytes and macrophages), platelets, dendritic cells, histiocytes, placenta, and uterus, but there are limited studies on cFXIII intracellular function in these cells (Polgar *et al.*, 1990; Koseki-Kuno *et al.*, 2003; Muszbek *et al.*, 2011, Dashty *et al.*, 2012). Such work has revealed that the role of FXIII is not confined to haemostasis only, but it also performs as an intracellular transglutaminase (Törőcsik *et al.*, 2005; Muszbek *et al.*, 2011). Monocytes are involved in the immune system, where they have the ability to destroy unusual invaders; moreover, they have a role in improving healing and repairing tissues (Sporn *et al.*, 1990). As any defect in cFXIII-A_2 could affect the physiological and pathological settings of haematological parameters (monocytes and macrophage), it became a biomarker for different subsets of these cells (Quatresooz *et al.*, 2008). Some OPs have toxic effects on haematological constituents such as RBC, WB, PLT and alter their function (Petroianu, 1997; Svoboda *et al.*, 2001; Celik & Suzek, 2008).

Some studies indicated that POX had the ability to cause hypocoagulability and platelet dysfunction through disruption of the coagulation cascade (Petroianu, 1997; Petroianu *et al.*, 1999). Moreover, soman (an acute OP nerve agent) caused decline in haematopoietic stem cell levels in blood circulation, resulting in a reduction in lymphocytes and monocytes (Colllomet *et al.*, 2005). Significant decline was observed in WB count which caused lymphopenia and granulocytosis after acute exposure to DZ (Svoboda *et al.*, 2001). In addition, a previous study revealed that CPF induced a significant decrease in WB cell counts, but CPF in presence of vitamin C lead to significant elevation of WB cells, suggesting a protective role of antioxidants against OP toxicity (Ambali *et al.*, 2007). Also, another study revealed that methyl PTH stimulated the immune system by increasing the WB cell counts

as a protection role (Celik & Suzek, 2008). Other studies have described the same toxic effect of CPF causing a significant increase on WB cell count, suggesting immune system activation after CPF exposure (Okechukwu et al., 2007; Modesto & Martinez, 2010; Ural, 2013).

There are a limited number of monocyte leukaemia cell lines, such as the U-937 histiocytic lymphoma cell line, the acute myelomonocytic leukaemia cell line 230, and the human monocytic leukaemia cell line THP-1, which retains its monocytic properties; the latter has been established to be a useful tool for studying the role of monocytes in the human immune response (Tsuchiya *et al.*, 1980). The THP-1 cell line has become widely used to study the regulation and function of monocytes and macrophages in the blood system (Qin, 2012).

The aim of the work presented in this chapter was to study the effects of OPs on the proliferation and viability of THP-1 cells. Therefore, optimization of THP-1 cell growth and confirmation of the presence of cFXIII-A_2 was necessary. Proliferation and viability of THP-1 cells were studied in the absence and presence of OPs using Trypan Blue and alamarBlue assays. Immunoblotting was performed using anti-human FXIII antibody to probe Western blots of THP-1 cell lysates.

6.2 Results

6.2.1 THP-1 cell in culture

To determine the cell growth characteristics of THP-1 monocyte-like cell line, a standard growth curve was generated, as described in section 2.2.10.1. Fig 6.1 shows images of THP-1 cells in culture for up to 13 days. The THP-1 cells exhibited a round shape, grew in suspension and formed loose clumps. Cells showed rapid division and proliferation during the first few days of seeding. By days 7-9, cell numbers seemed to stabilize as the flask becomes crowded. In days 11-13, the colour of the culture medium changed (yellowish) due to pH drop and some cells shrank in size.

Fig 6.2 A, B, C shows cells total count, live cell count, and % viability of the THP-1 cells during culturing for 13 days. The THP-1 cell density after 24 hours (day one) of seeding culturing was similar to the starting density ~ 2 x 10^5 cells. However, in the two following days, the cell density was shown to gradually increase (Fig 6.2 A & B). At day 8-9, a significant increase in cell density to approximately 2 x10^6 cells/ml was observed and this was shown to be steady for 2 more days followed by a decline. On the other handr, cell viability started to fall by day 9 (Fig 6.2 C). In conclusion, the optimum growth phase for sub culturing and further experimental testing on THP-1 was up to day 7.

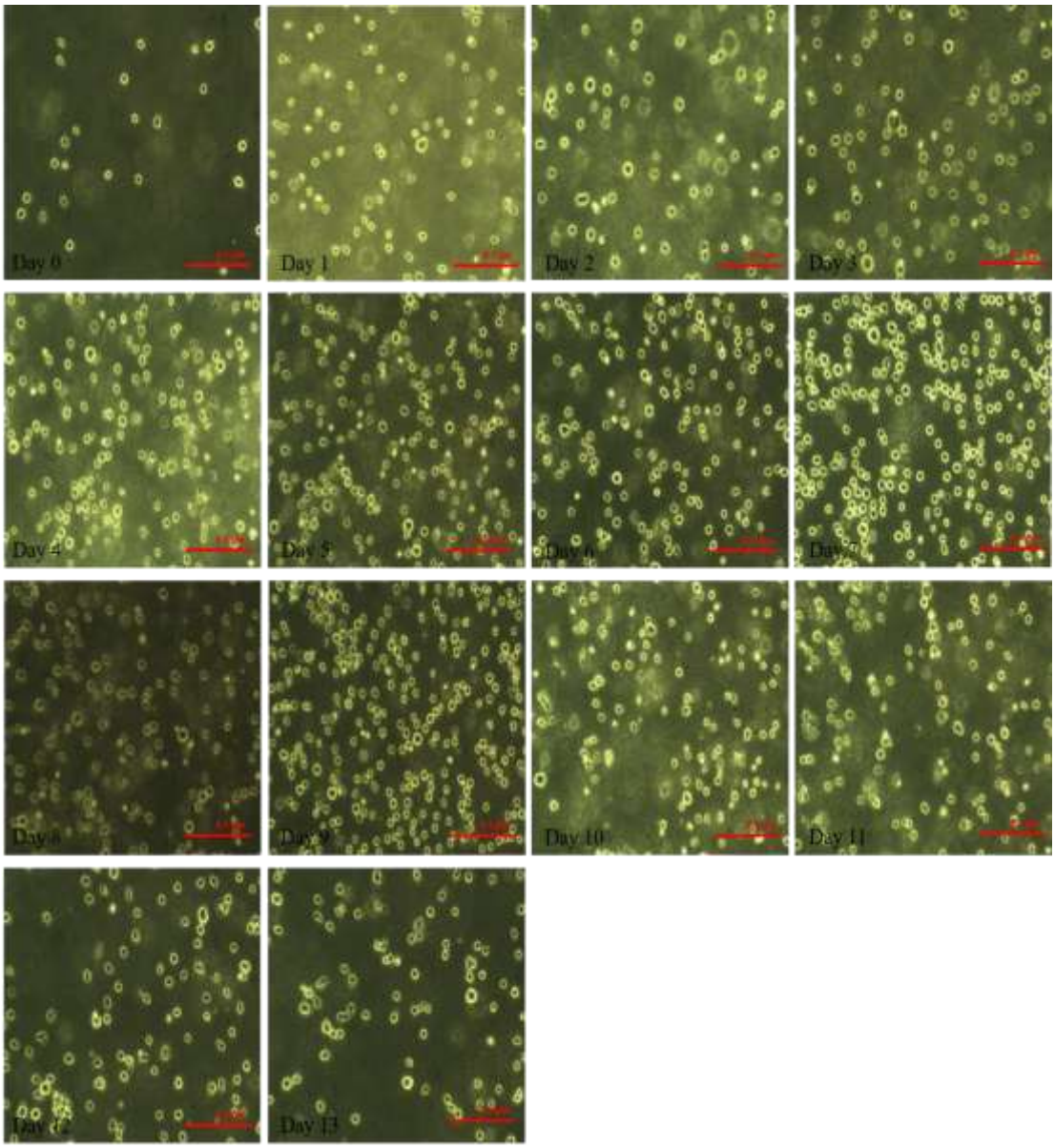

Figure 6- 1: Images of THP-1 cells during 13 days culturing.

THP-1 cells were plated at a density of 200,000 cells/ml per T75 flask cultured in growth medium and incubated for up to 13 days, as described in Materials and Methods. Cells were monitored using an inverted light microscope at (10x) magnification. Scale bar 0.1 µm.

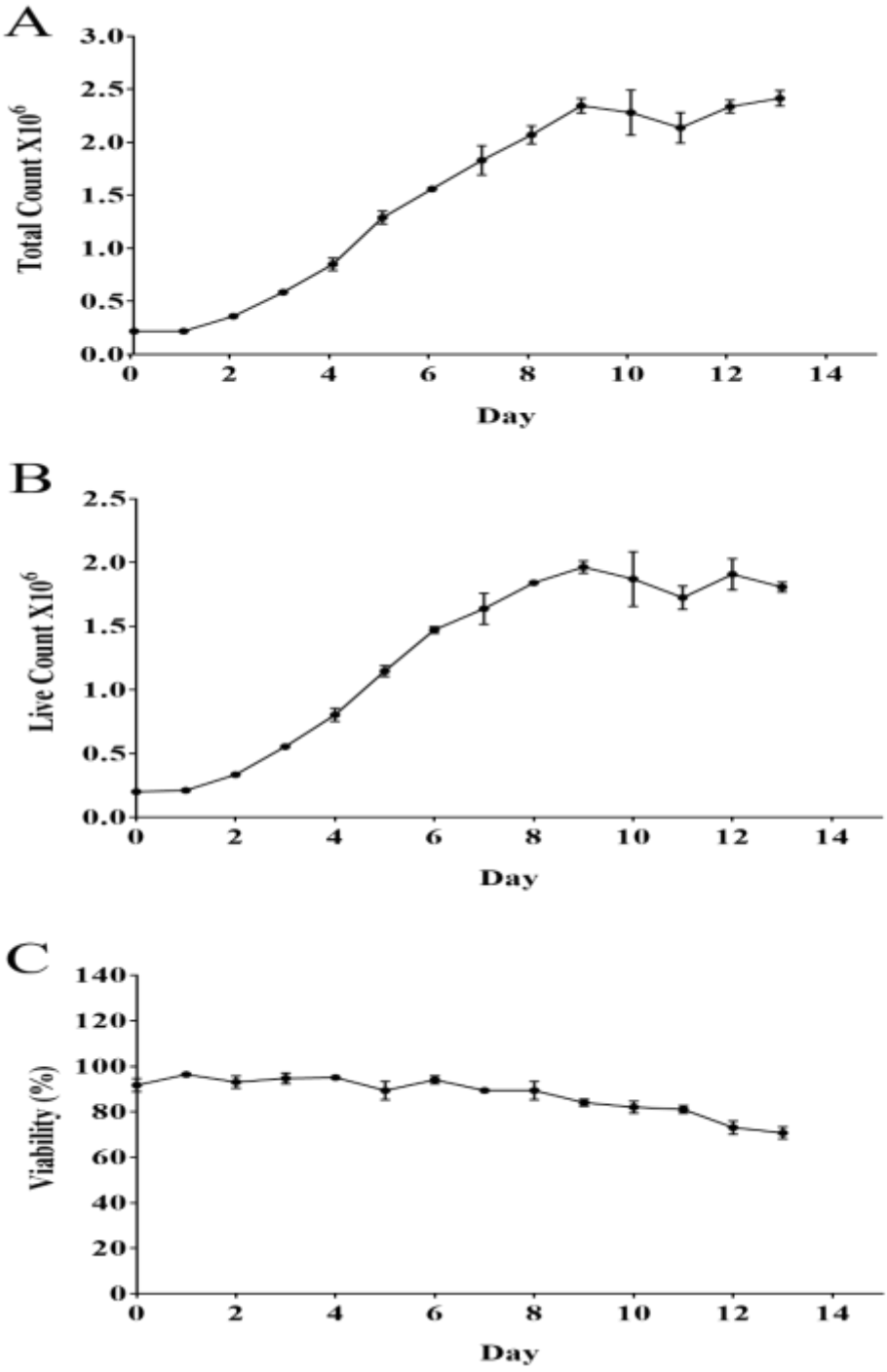

Figure 6- 2: Growth curve of THP-1 cells.

Cells were plated at a density of 200,000 cells/ml in growth medium and incubated for up to 13 days. Shown are the total cell count (A), live cell count (B), and % viability (C) measured by Trypan blue exclusion assay. Data are expressed as mean ± SEM for 3 independent experiments.

6.2.2 Effects of DMSO on THP-1 cells proliferation and viability

As OPs were dissolved in DMSO, in order to study the OP effect on THP-1 cells it was first of all necessary to optimize the DMSO concentration to be sure that any effect on the cells was due to the OPs alone. A cell density of 2 x 10^5 cells/ml was plated in growth medium and incubated with a range of DMSO concentrations for up to 7 days, as described in section 2.2.10.1. The results shown in Fig 6.3 A indicated that proliferation of THP-1 was affected by DMSO concentrations of 0.25% and above, while there was no cytotoxic effect on viability (Fig 6.3 B). In general, it was optimum to keep DMSO concentration below 0.05%.

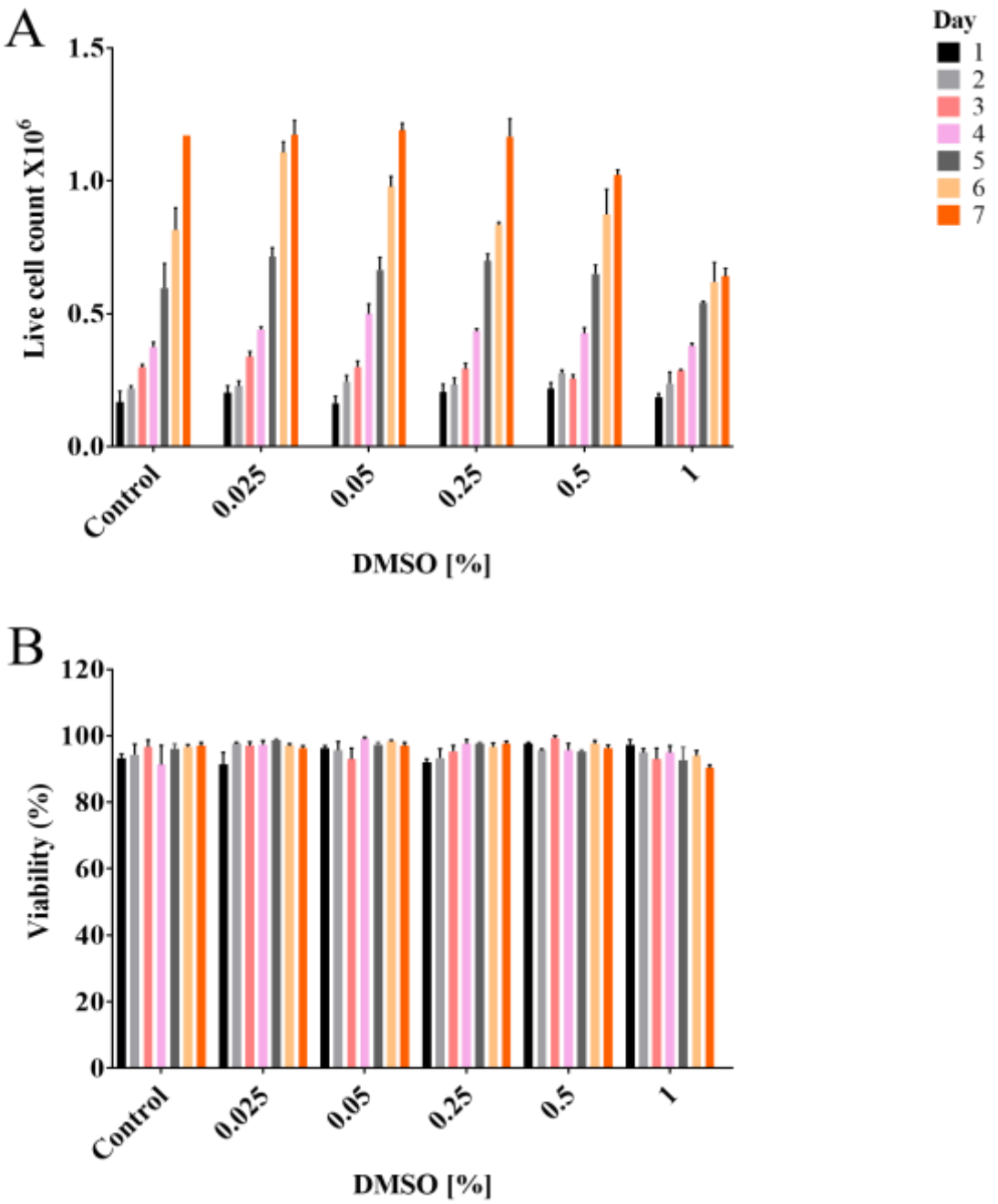

Figure 6- 3: Effect of DMSO on THP-1 proliferation and viability.

Cells were plated at a density of 200,000 cells/ml in growth medium and incubated for up to 7 days with the concentrations of DMSO indicated or untreated as control. The cell proliferation (A) and % viability (B) were measured by Trypan Blue exclusion assay. Data are expressed as mean ± SEM for 3 independent experiments.

6.2.3 AlamarBlue assay optimization for THP-1 cell viability

In order to have another viability assay, the alamarBlue assay was deemed suitable for THP-1 suspension cells. More than one cell density was plated and incubated for up to 48 h with alamarBlue, as described in section 2.2.10.4. The results in Fig 6.4 showed that the standard curve was linear between 0-8 hours for lower cell density, while at the higher cell density the linearity of the curve was lost in a shorter time than for lower cell density. However, there was no longer a linearity relationship above 8 h under any conditions. Eventually, the optimum was established to be measuring absorbance for cell density 0.2 x 10^6 cells/ml after 8 h and for 0.8 x 10^6 cells/ml after 4 h.

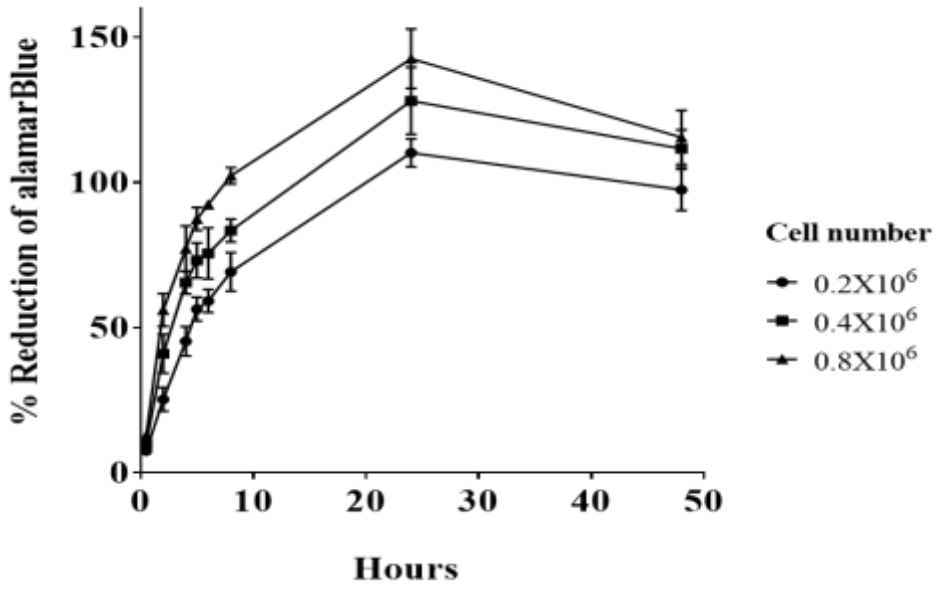

Figure 6- 4: Optimization of alamarBlue incubation time with THP-1 cells.

Cells were plated at the cell densities indicated and incubated for up to 48 h with alamarBlue. Data are expressed as mean ± SEM for 3 independent experiments.

6.2.4 Detection of cFXIII-A_2 in THP-1 cell lysates

This was necessary to elucidate the expression of the cFXIII-A_2 in monocyte cells, as its presence was confirmed previously (Muszbek *et al.*, 1988; Conkling *et al.*, 1989). Western blot analysis was performed as described in (section 2.2.7.3) to confirm cFXIII-A2 expression in THP-1 cells. The electrophoretic migration of reactive bands was compared with purified rFXIII at the 83 kDa position, and with depleted and whole plasma samples run in parallel. FXIIIa was detected in the position of an 83 kDa for all samples (Fig 6.5). In addition, the observations showed a strong uncleaved intensity band (180 kDa) of FXIII with degradation products representing FXIII-A_2 from THP-1 lysate and whole plasma sample FXIII-A_2. However, the uncleaved FXIII band did not appear on blots of depleted plasma but the degradation band of cFXIII-A_2 was detected.

In order to confirm that FBS was clear of cFXIII-A_2, a Western blot analysis was performed as described in (section 2.2.7.3) with 30, 50, 100 µg of FBS protein probed with anti-human FXIII. The blot showed only a ca. 50 kDa bans with variable intensity in FBS samples, whereas the THP-1 lysate showed cFXIII-A_2 at 83 kDa. In conclusion, the cFXIII-A_2 presence in THP-1 cells was confirmed and it is not likely to be due to cross-reactivity with protein components in FBS.

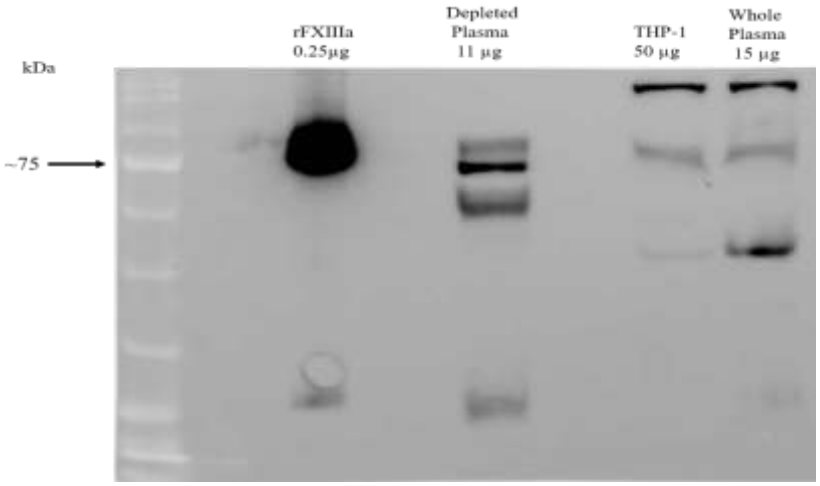

Figure 6- 5: Detection of FXIII in THP-1 cell lysates.

Pure rFXIIIa (0.25µg), depleted plasma sample (11 µg), cell lysate of THP-1 proteins (50 µg) and whole plasma protein (15 µg) were separated by SDS-PAGE and Western blotting. Blots were probed with anti-human FXIII antibody (1:1000), followed by incubation with secondary antibody HRP-conjugated anti-mouse IgG. Immunoreactive bands were visualized using a Syngene imager after incubation with ECL reagent.

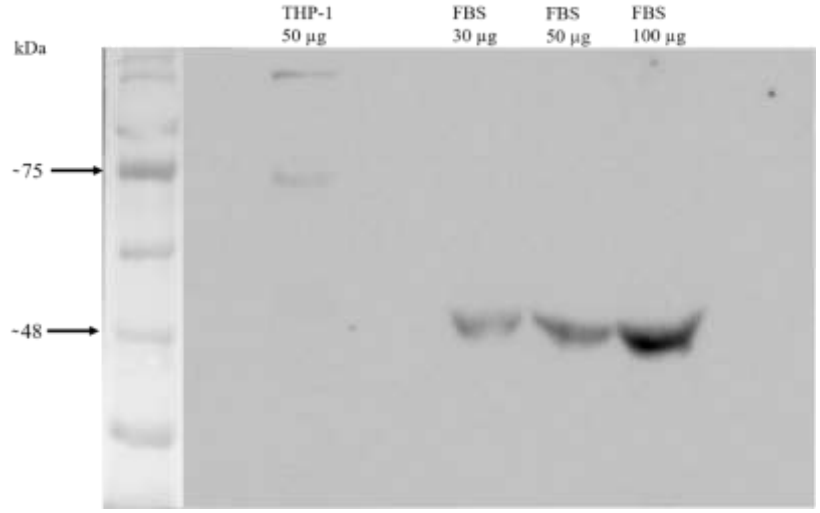

Figure 6- 6: Testing for FXIIIa presence in fetal bovine serum.

THP-1 (50 µg), FBS (30 µg), FBS (50 µg), FBS (100 µg). Blot was probed with anti-human FXIII antibody (1:1000), followed by incubation with secondary antibody anti mouse IgG HRP conjugated. Immunoreactive bands were visualized using Syngene transillumniator after incubation with BCL reagent.

6.2.5 Effect of OPs on the proliferation and viability of THP-1 cells

In order to study the effect of OPs on THP-1 cell proliferation and viability, as described in (section 2.2.10.1), 2 x 10^5 cells/ml were plated in growth medium and treated with PSP, DZ, DZO, CPF, CPO, PTH, and POX at three final concentration of each (1, 10, and 100 µM) and incubated for up to 6 days. The results are shown in Fig 6.7. PSP showed no significant effect on proliferation and caused only a slight but significant decrease in viability and alamarBlue reduction at selected low concentrations (Fig 6.7 A). The lowest concentration of OP (1 µM) induced significant decreases in proliferation in the case of DZ, PTH and POX on day 6 of incubation (Fig 6.7 B, F, G), whereas 10 µM PTH treatment resulted in a significant decline by day 4 (Fig 6.7 F) and 10 µM CPF, CPO and PTH had a similar effect by day 6 (Fig 6.7 D, E, G). The most significant effect of OPs came from the 100 µM concentration, which was observed for PTH on day 2, for DZO, CPF, CPO, PTH and POX on day 4 and with DZ, DZO, CPF, PTH and POX) on day 6 (Fig 6.7 B, C, D, E, F, G). In addition, THP-1 cell metabolic activity showed significant decline within a few hours of incubation from day 0 to day 6 by with PTH, DZ, CPF, DZO and POX, as monitored by the alamarBlue assay (Fig 6.7 F, B, D, C, G). On the other hand, some OPs showed significant viability decrease from day 2 to 6 (e.g. PTH, CPF) by Trypan blue exclusion (Fig 6.7 F, C). In conclusion, most OPs except (CPO day 4) caused significant reductions in THP-1 cell proliferation in a concentration- and time-dependent manner, at high concentrations showing significant decreases in both proliferation and viability except for PSP, which only showed slight effects.

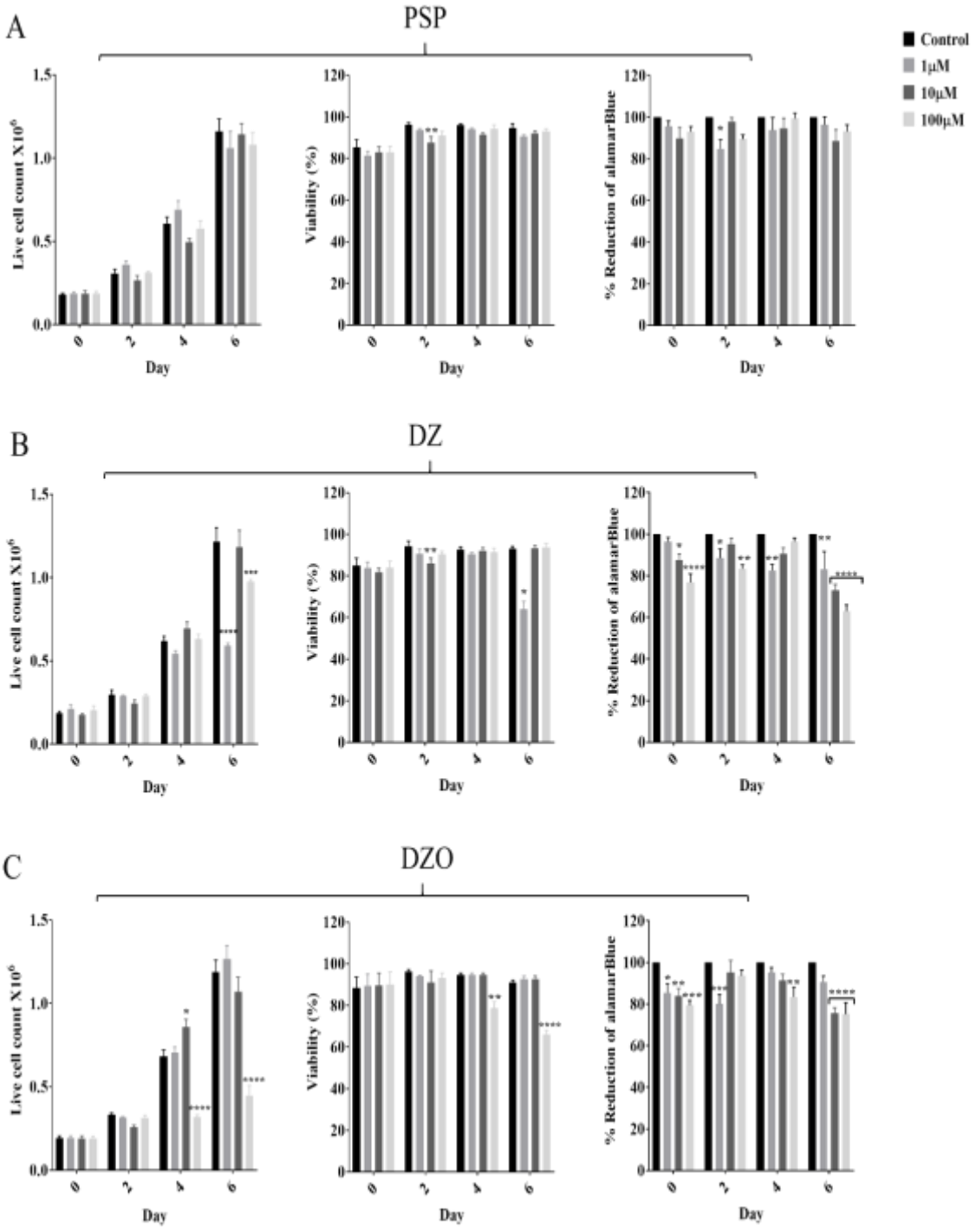
A
PSP
Control
1µM
10µM
100µM
Live cell count X10⁶
Viability (%)
% Reduction of alamarBlue
Day
B
DZ
C
DZO

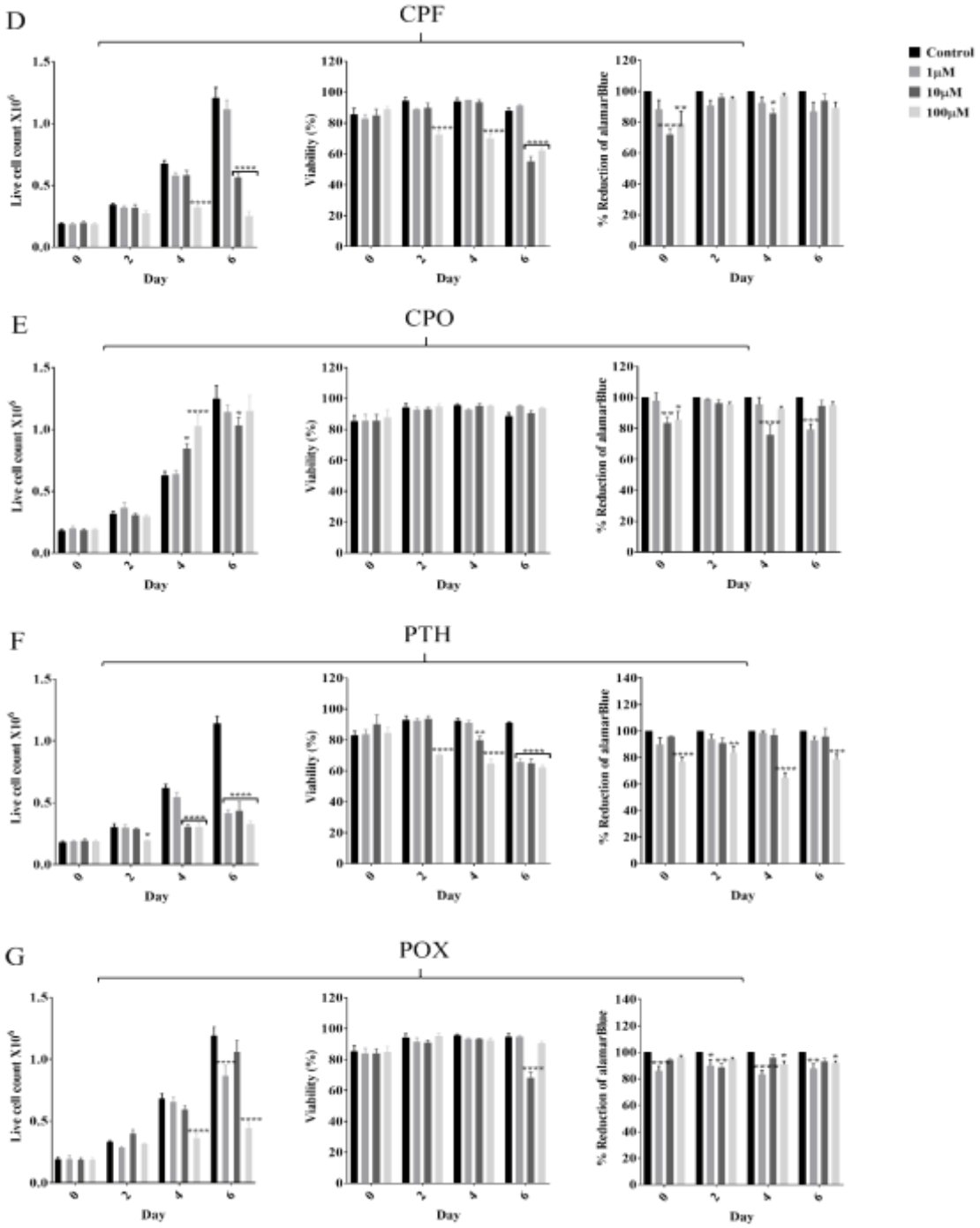

Figure 6- 7: The effect of OPs on THP-1 cell growth and viability.

Cells were plated at a density of 200,000 cells/ml in T25 cell culture flasks and incubated for up to 6 days in the absence and presence of PSP (A), DZ (B), DZO (C), CPF (D), CPO (E), PTH (F), and POX (G) at three final concentration of each (1, 10, and 100 µM). Control sample was treated with 0.01 % (v/v) DMSO. The live cell count, and % viability of cells were measured by Trypan blue exclusion assay whereas metabolic effects of each toxin were indicated by alamarBlue assay. Data points of three independent experiments represent the mean ± SEM *p<0.05, **p<0.01, ***p< 0.001, ****p< 0.0001 versus non OP-treated control.

6.2.6 Effect of lower concentration of OPs on the proliferation and viability of THP-1 cells

In order to study the effect of selected OPs at lower concentrations on THP-1 cell proliferation and viability, as described in (section 2.2.10.1), 2 x 10^5 cells/ml were plated in growth medium and treated with PSP, DZO, CPF, PTH at three final concentration of each (0.1, 1, and 10 µM) and incubated for up to 4 days. The results shown in Fig 6.8 showed that exposure to 10 µM PSP had an elevating effect on THP-1 cell proliferation on day 4, the other concentration also increased the proliferation on day 4 but without statistical significance. Also, PSP caused a significant decrease in metabolic activityat 1 µM on day 2 and with 0.1, 1 and 10 µM on day 4 (Fig 6.8 A), as determinedby the alamarBlue assay. On exposure to DZO THP-1 cells exhibited 20 % decrease inalamarBlue reduction at 1 and 10 µM on day 2 andwith 0.1, 1 and 10 µM on day 4 (Fig 6.8 B). Moreover, 0.1, 1 and 10 µM CPF treatment induced a 50% decline in THP-1 cell proliferation compared to the control non OP-treated cells, while the viability measurements in both Trypan Blue exclusion and alamarBlue assays showed significant decreases with 10 µM CPF on day 4 (Fig 6.8 C). In addition, 10 µM PTH treatment also showed a significant decrease on day 4 in cell proliferation and viability on both Trypan blue exclusion and alamarBlue assays (Fig 6.8 D). Microscope images for OP effects on THP-1 cells were recorded on day 0 and day 4 (See appendix 8.8 & 8.9) In conclusion, CPF was the most toxic compound among the selected OPs by (0.1, 1, 10) µM causing significant inhibition of THP-1 proliferation and reduced viability. Also, 10 µM of PSP, CPF, and PTH showed a cytotoxic effect on THP-1 cell proliferation and metabolic activity.

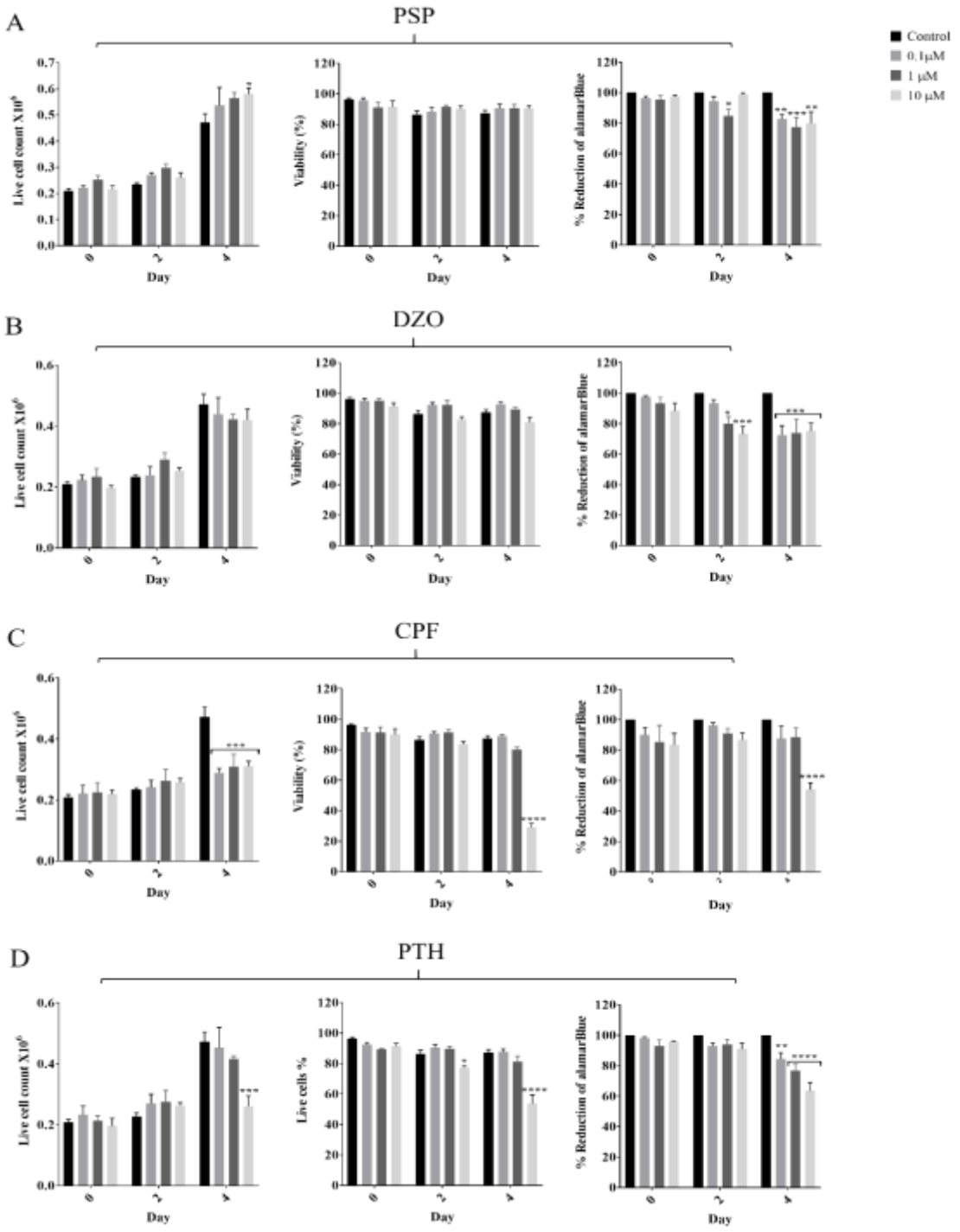

Figure 6- 8: The effect of lower concentration of selected OPs on growth and viability of THP-1 cells.

Cells density were plated at a density of 200,000 cells/ml in T75 cell culture flask. Cells were incubated for up to 4 days and treated with PSP (A), DZO (B), CPF (C), and PTH (D) with three final concentration of each 0.1, 1, and 10 µM. Control sample was treated with 0.01 % (v/v) DMSO. The live count, and % viability of cells were measured by trypan blue exclusion assay beside to the cell viability indicated by alamarBlue assay of each toxin. Data points of three independent experiments represent the mean ± SEM *p<0.05, **p<0.01, ***p< 0.001, ****p< 0.0001 versus non OP-treated control.

6.2.7 Effect of OPs on cFXIII-A_2 of THP-1 lysate

In order to study the OPs effect on cFXIII-A_2 production of THP-1 monocyte cells, 2 x 10^5 cells/ml were plated in growth medium and treated with PSP, DZO, CPF, PTH at three final concentration of each 0.1, 1, and 10 µM and incubated for up to 4 days, as described in section 2.2.10.1. Then Western blot analysis was performed for untreated and OP-treated THP-1 cell lysates, as described in (section 2.2.7.3). Unfortunately, no bands were detected at the 83 kDa position for THP-1cell lysate proteins either for control untreated samples or for those treated with OPs (Fig 6.9 A, B). However, purified rFXIIIa was used as positive control to confirm anti-human FXIII antibody probing, also β-actin expression (42 kDa bands) were detected on probed blots of THP-1 lysates to confirm equal protein loading (Fig 6.9 A, B).

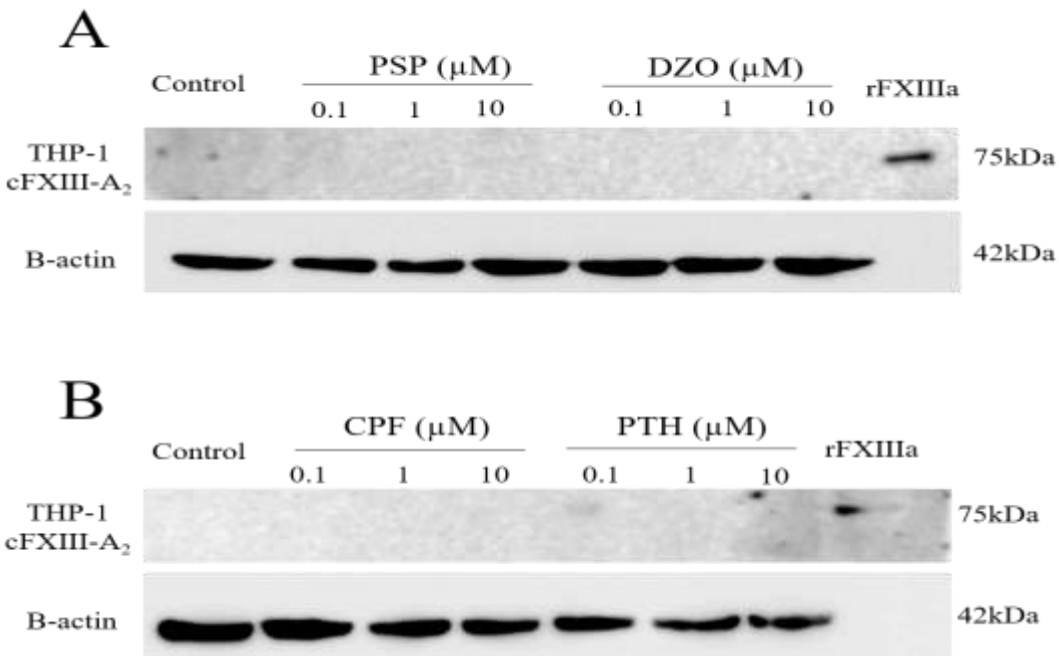

Figure 6- 9: The effect of OPs on FXIIIa of THP-1 cells.

Cells were plated at a density of 200,000 cells/ml in T75 cell culture flasks andincubated for up to 4 days in the absenc and presence of PSP or DZO(A) and CPF and PTH (B), at final concentration of 0.1, 1, and 10 µM. The control sample was treated with 0.01 % (v/v) DMSO. Cell lysates of THP-1 (50 µg) and pure rFXIIIa (0.05µg) were blotted and probed with anti-human FXIII antibody (1:1000), followed by incubation with secondary antibody HRP-conjugated anti-mouse IgG. Immunoreactive bands were visualized using a Syngene imager after incubation with ECL reagent. Lysates were also analysed for β-actin expression to confirm equal protein loading.

6.2.8 Discussion

Cellular FXIIIa exists as a dimeric catalytic subunit (cFXIII-A_2) in a variety of cell types. Monocytes/macrophages express cFXIII-A_2 antigen and activity (Muszbek *et al.*, 1988; Conkling *et al.*, 1989). Cellular FXIII-A_2 was not detected in monocytes of patienst with cFXIII-A_2 deficiency (Muszbek *et al.*, 1988). It has been reported that OPs can significantly disrupt some haematological parameters such as CBC including monocytes (Ambali *et al.*, 2007; Banaee *et al.*, 2008; Andreadis *et al.*, 2014). In the present study, the OP effects on monocyte cell growth and viability was studied using the THP-1 monocytic leukaemia cell line. Some optimization tests were required before exposing the THP-1 cells to selected OPs. The selected OPs: PSP, DZO, CPF, PTH were incubated with THP-1 for up to 4 days and there was some effect on live cell count and viability which were monitored by Trypan blue exclusion and alamarBlue assays. Also, the microscopic observation of some OP-treated cells indicated some morphological changes.

It was essential to optimise the cell line's growth and characteristics before performing any experiment that require the utilization of the cell line for *in vitro* investigation, as any unusual change of cell growth can have a significant effect on the experimental results (Wang, 2006). According to the literature and to the manufacturer's instruction, 2 x 10^5 THP-1 cells/ml density was selected as the plating density, as monitored and defined in previous work (Tsuchiya *et al.*, 1980; Banka *et al.*, 1991; Liu *et al.*, 2009; Aldo *et al.*, 2016). In the current study, according to the cell growth standard curve (Fig. 6.2 B) the optimal period for sub-culturing and further experimental treatments of THP-1 cells was shown to be before day 7 of cell growth. An ideal standard growth curve for various cultured cell lines has 4 different phases including lag, log or growth phase, stationary and decline phases (Wang, 2006). Day 7 was shown to be at the end of the growth phase of THP-1 cells, in which cells exhibited rapid division and proliferation (Fig. 6.1). For that reason, the earlier exponential growth

phase (2-5 days) might better as cells are dividing rapidly and not yet near the stationary phase. It was recommended in this phase for cell line to be assessed and maintained for different cellular functions before they enter the stationary phase (Freshney, 2006) in days 8-10 (Fig. 6.2 B). Budde *et al.* (1998) indicated that the setup of the sub-culturing and additional experimental treatments of cells is needed to be in the exponential phase to ensure cellular viability and enzymatic function, phenotypic and genetic stability. Accordingly, the day 7 of cells growth was adopted for sub-culturing and any subsequent experiments.

Organic solvents such as DMSO are usually used as a vehicle to dissolve hydrophobic compounds in biological experiments (Jain & Pento, 1991). Previous *in vitro* studies reported possible toxic effects of some organic solvents including DMSO, in which proliferation of cells was inhibited in a time- and dose-dependent manner (Qin *et al.*, 2011; Jamalzadeh *et al.*, 2016). It was therefore important in the present study to optimize the DMSO concentration, to a level that showed no effect on cell proliferation; this was found to be the case for concentrations below 0.05 % (v/v) (Fig 6.3).

The alamarBlue assay has been used for many years in studies of cytotoxicity and in viability assays, and it used for wide range of cell types including suspension cells (Rampersad, 2012). It is common to use tetrazolium salts such as MTT for anchorage dependent cells; however, reduced MTT is not soluble and the formazan crystals must be solubilized by DMSO after the medium has been removed, which is not that straightforward for suspension cells. The alamarBlue assay is a more suitable, reproducible and sensitive method for suspension cells, using oxidized resazurin as an active and non-toxic ingredient; it is reduced by NADPH and changes from blue to a fluorescent pink state. It is typically used on adherent THP-1 cells incubated with alamarBlue to measure their metabolic activity (Schmitt *et al.*, 2010; Manna *et al.*, 2014). Therefore, in the present study, the alamarBlue assay was optimized for

suspension culture (Fig 6.4) and assessed alongside Trypan blue exclusion as a method for measuring THP-1 cell viability and/or metabolic activity.

In the present study, characterization of uncleaved cFXIII-A_2 in THP-1 cell line was determined by probing Western blots of cell lysates with anti-human FXIII monoclonal antibody using. Detection of a reactive band at 83 kDa in probed blots of THP-1 cell lysates, which was weaker in intensity compared to depleted plasma and purified FXIII (Fig 6.5), confirmed the characteristic expression of a cellular form of FXIII by this cell line. cFXIII-A_2 level was observed to be higher in monocytic leukaemia cells compared to the normal blood monocytes (Kappelmayer *et al.*, 2005). Moreover, the uncleaved complete form of $FXIIIA_2B_2$ at position higher than ~180 kDa plus a lower molecular weight potential degradation product were detected on probed blots of THP-1 cell lysates and whole plasma (Fig 6.5). However, this higher sized uncleaved $FXIIIA_2B_2$, band was not detected on blots of depleted plasma, suggesting that it was absorbed by the depletion column. A study by Simon *et al.* (2012) identified uncleaved cFXIII-A_2 at ~83 kDa in leukemic promyelocytes in *de novo* AML M3 patients; moreover, cleaved and degradation products of cFXIII-A_2 were identified in lower kDa size ranges with lower expression amount compared to the cFXIIIa band at ~83 kDa. Different studies on normal human purified monocytes and macrophages identified cFXIIIa without degradation at 80 kDa in monocytes and at ~85 kDa in macrophage cells. The observation that, in the present study, FBS used in the growth medium was clear of an immunoreactive band at ~83 kDa, ruled out potential contamination by serum FXIIIa (Fig 6.6).

The main observed effect of OPs on THP-1 cells was decreasing cell proliferation in a concentration- and time-dependent manner (Fig 6.7). Some parent compounds and their metabolite form, such as DZ, DZO, PTH and POX showed stronger effects, decreasing by more than 50 % of live cell count by day 6 of incubation compared to control samples,

suggesting that might both the parent compound and the oxon metabolite behaved in a similar manner with respect to this parameter, unlike their very different potencies against their acute toxicity targets. The rank order of the most OP toxic on THP-1 cell proliferation was as follows: PTH>POX>CPF>DZO>DZ> CPO> PSP (Fig 6.7 F, G, D, C, B, E). On the other hand, the rank order of the most toxic OP towards THP-1 cell viability was as follows: PTH>DZ> DZO>CPF>CPO>POX>PSP (Fig 6.7 G, B, C, E, G, A). Therefore, a smaller group of OPs (PSP, DZO, CPF, and PTH) were subsequently selected to study their effect at lower concentrations (0.1, 1 and 10 µM) and for up to only 4 days incubation (Fig 6.8). Similar to the previous experiment the data obtained showed that the effect was concentration- and time-dependent. All of selected OPs induced decreases in THP-1 live cell counts. This is in agreement with a previous study on diazinon (2-32 mg/l) exposed fingerling European catfish, which showed acute toxicity on their hematological parameters, including powerful decreases in leukocyte, erythrocyte, hemoglobin, hematocrit, MCV, MCH, and MCHC values comparing to non OP-treated groups (Köprücü *et al.*, 2006). However, on the selected OPs group only the PSP on day 4 the live cell count was increased by increasing concentration of PSP, which could a defence mechanism behaviour; however, the metabolic activity of this group in order by lower to higher concentration was decreased (Fig 6.8 A). A study showed that ~ 38 µM of methyl parathion in water was drunk by albino rats for month and using a haematological analyser the results showed significant increases in WB cells, indicating immune system activation due to methyl parathion intoxication (Celik & Suzek, 2008). In another study, two groups of *Cyprinus carpio carpio* fish were exposed to 0.04 and 0.08 mg/l CPF dissolved their environment water for 14 days, resulting in a significant elevation in WB cell count, in a concentration-dependent manner compared to non OP-treated controls, suggesting that the immune system was responding to CPF toxicity (Ural, 2013). Although, the immunotoxicity mechanisms of OPs are not absolutely

clarified, several studies suggest that OPs can target molecules related to the immune system (Díaz-Resendiz *et al.*, 2015). The observed effects of OPs on THP-1 proliferation suggests that there might be an effect on the key prosses of regulation of proliferation either during mitosis or the interphase stage, which might affect DNA replication or cell growth.

On the other hand, the immunoblotting experiment to study the selected OPs effect on cFXIII-A_2 showed no bands of cFXIII-A_2 even in untreated OP control lysates, however rFXIII band indicated as a marker of anti-human FXIII antibody and to identify its position at ~83 kDa. It could be an issue in performing the lysate buffer or during preparing the samples. Due the constraint of time there was no chance to investigate the problem. This part of work needs to be completed in future work.

In conclusion, the results of this chapter indicated that OPs have a potency effect against the proliferation or viability of THP-1 cells, which could affect cFXIII-A_2 production. Thus, further studies are required to elucidate cFXIII-A_2 expression level under OPs treatment.

Chapter 7: General discussion and future work

7.1 Summary of findings

This study aimed to determine the effect of parent and activated metabolite OPs on pure and plasma cholinesterase, FXIIIa and thrombin activity by enzyme colorimetric assays. It was also of interest to establish whether OPs could form covalent adducts with FXIII and thrombin protein. Moreover, it was intended to assess the OPs toxicity on the proliferation and viability of THP-1 monocyte-like cells. Overall, OPs significantly affected all of these haematological parameters.

7.1.1 OPs effect on cholinesterase

AChE and BChE activity are widely used used as a biomarker to detect and monitor OP exposure since they are the primary targets of many OPs (Nigg & Knaak, 2000; Jońca *et al.*, 2015). Before investigating the OP effects on haematological parameters (such as FXIIIa, thrombin activity and proliferation and viability of monocytic THP-1 cell line) it was necessary to validate the effectiveness of OPs of interest against their primary target. Therefore, the first part of this thesis aimed to confirm the biological activity of the OPs toward pure cholinesterases and their corresponding activities in human plasma, The Ellman method (Ellman *et al.*, 1961) was utilized with acetylthiocholine and butyrylthiocholine as substrates for AChE and BChE, respectively, to determine cholinesterases activity.

Blood plasma samples mainly include BChE and the majority of AChE is found in erythrocytes, although fetal serum ChE was found to contain 40% AChE (Hahn *et al.*, 1993), whereas other studies confirmed that adult plasma has less than 1% of AChE activity (Brimijoin & Hammond, 1988; Thompson, 1999; Nigg & Knaak, 2000). On the other hand, in many different kinds of samples OP toxicity is typically indicated by testing the level of AChE activity (Thompson, 1999). In the current study, substrate specificities were assessed in purified AChE and BChE to determine which of the two ChEs (AChE or BChE) was most

affected in plasma samples treated with OPs. It is known that acetyl(thio)choline is the preferable substrate for AChE and butyryl(thio)choline for BChE (Basova *et al.*, 2018). In the current study the reaction of each enzyme with the other's intended substrate was tested, the purified BChE being able to hydrolyse both acetylthiocholine and butyrylthiocholine iodide (with Km values of 0.28 and 0.22 µM, respectively), whereas the purified AChE could only hydrolyse the acetylthiocholine iodide. Indeed, BChE was found to hydrolyse acetylthiocholine at a rate just two-fold lower than butylrylthiocholine (Wetherell & French, 1986). One study focussing on substrate selectivity of human BChE and its mutants estimated a Km of 33 µM for acetylthiocholine iodide substrate which was hydrolysed by the wild-type BChE compared to 17 µM for butyrylthiocholine iodide (Hou *et al.*, 2013). In another study, the BChE active site structurally showed a broader substrate specificity than AChE (Pohanks, 2011). Therefore, the data obtained in the current study, in agreement with previous work, suggest that BChE (but not AChE) can effectively hydrolyse both substrates indicating that it may account for most of the ChE activity in plasma samples. In further agreement with these findings, a study which measured ChE activity in blood collected from healthy male and female volunteers compared to purified human ChE, revealed that the neurotransmitter acetylcholine was an outstanding substrate for BChE (Masson & Lockridge, 2010).

The results in the present study with both pure enzymes and plasma samples highlighted the possibility that BChE activity was significantly disrupted by OP pesticide parent compounds, though it was more pronounced when butyrylthiocholine was used as the substrate. The ranking of parent OPs in order of toxicity on plasma BChE samples was PTH > DZ > CPF. However, in the case of purified BChE it was CPF > PTH > DZ. This difference could be due to the biological environment effect on parent OPs, suggesting they may be biotransformed in plasma by molecules such as cytochrome P450 in plasma exosomes to

produce the more potent oxon form (Fabrizi *et al.*, 1999; Foxeberg *et al.*, 2011; Kumar, 2015). Differences could also arise due to differential hydrolysis of specific oxons by plasma paraoxonases. BChE is known to have a larger active site pocket than AChE (about 500 $Å^3$ compare to 300 $Å^3$, respectively,) which makes BChE less substrate-specific than AChE, as it can hold bulkier substrates or inhibitors (Masson & Lockridge, 2010). The finding in present study that phosphorothioate compounds could inhibit purified BChE activity, agreed with the study of Tacal & Lockridge (2010), which also found that DZ formed adducts with highly purified human BChE.

It is well known that the oxon form of organophosphorus compounds are more toxic than their parent forms in terms of inhibitory effects on cholinesterase enzyme activities (Brimijoin and Hammond, 1988; Čolović *et al.*, 2010; Čolović *et al.*, 2011). It was interesting to note that both ChE activities in plasma samples were inhibited by PSP, which had no effect on the purified AChE yet plasma ChE activity was significantly inhibited using acetylthiocholine as the substrate. One study proposed that tri-*o*-cresyl phosphate (TOCP), when modified to a more toxic product CBDP *in vivo* exhibited increased inhibition of BChE but not AChE, an effect was also observed *in vitro* using rat-liver slices to produce the same toxic effect (Aldrige, 1954). It was subsequently shown that CBDP formed organophosphorylated adducts on active site serines (Ser-203 for human AChE and Ser-198 for human BChE). *In vivo* the inhibition effect by low dose exposure to CBDP on AChE is not as much as it is on BChE, for which reason BChE inhibition is the best biomarker for exposure to T*O*CP (Liyasova *et al.*, 2011).

In the present study it was confirmed that the oxon metabolite forms of OPs were more toxic than the parent compounds in a concentration dependent manner but with different inhibitory potencies towards both BChE and AChE. The rank order of toxicity for metabolite (oxon) OPs on plasma BChE activity for both substrates was CPO > POX >DZO. The same toxicity

order was found on purified BChE. Thus, CPO was the most potent OP against BChE activity showing inhibition lower than or about 24 nM with either whole plasma or purified protein. A previous study, using purified human BChE (1.3 U/ml) with a higher butyrylthiocholine Km (0.5 mM) after 40 min incubation, showed a direct inhibition of BChE activity dependent on CPO concentration, confirming that BChE inhibition served as a biomarker for CPO toxicity due to the rapid interaction of the enzyme with this OP (Amitai *et al.*, 1998). Moreover, in the same study, POX caused about 50% inhibition at 0.055 µM (Amitai *et al.*, 1998), which is very similar to its effect on plasma and purified BChE in the current study. There are limited studies of DZ and DZO effects on BChE; in the current study DZ exposure resulted in almost 60 % inhibition of ChE using butyryl thiocholine as the substrate for both plasma and purified BChE, and by more than 20 % using acetyl thiocholine as the substrate in plasma samples, the latter of which could be explained by the ability of BChE to hydrolyse acetylthiocholine less than butylrylthiocholine (Wetherell & French, 1986).

In the current study, PSP and DZ showed no significant effects on pure AChE activity. The lack of the biological effect such the one which is presence in plasma environment could be one reason for the lack of inhibition effect for these OPs on pure AChE; moreove; could be the same reason for the lower inhibition induced by PTH on purified enzymes compared to activities in whole plasma. This is in agreement with a study showing that, *in vitro,* DZ had a much stronger dose-dependent inhibition effect on human lymphocyte, fibroblast and erythrocyte AChE than it had on human purified protein, which was almost negligible compared to the cellular samples (Čolović *et al.*, 2010). However, the CPF toxic effect on purified AChE with no biological protein environment as in plasma sample reduced < 50% of AChE activity at 50 µM comparing to the same concentration on plasma AChE. A study

reported that 20 µM CPF effect an almost complete inhibition of the electric eel purified AChE (Čolović *et al.*, 2011).

In the present study, although the expected pattern of greater toxicity for the oxon metabolite form of pesticide OPs was consistently observed for both enzymes, all OPs were more potent against purified BChE than AChE.

7.1.1 OP effect on FXIII

FXIIIa is the transglutaminase coagulation factor that has an important role at the end of the blood clotting cascade, where it stabilizes the fibrin mesh by cross-linking lysine-glutamyl side chains to form an unbreakable clot (Martins *et al.*, 2014). The second aim of the current study was to identify the effect of OPs on FXIIIa and examine the possibility of their binding to FXIIIa. Transamidase activity assays and D-dimer ELISA were used to investigate the OP effect on FXIIIa activity and clot formation, respectively, whereas covalent binding was studied by SDS-PAGE and confirmed by mass spectrophotometry.

In the present study the effect of OPs on plasma TG showed slight but significant inhibition of plasma TG-mediated amine incorporation and peptide crosslinking activities. Moreover, the data for most OPs suggested that plasma TG-mediated amine incorporation activity was more sensitive to OP toxicity, with CPO being the most effective inhibitor of plasma TG activity. CPF showed no significant effect on either activity, whereas DZ and POX had no significant effect on peptide crosslinking activity in plasma. However, the data of OPs effect on purified rFXIIIa showed higher sensitivity to OP toxicity in both transamidase activity assays than was observed in plasma. In this case, the assay for rFXIIIa-mediated peptide crosslinking activity showed more sensitivity to OP toxicity than did the amine incorporation assay. Moreover, the parent OPs in both activities of rFXIIIa had more potency than the metabolite form of pesticide OPs. For example, the CPF exhibited an IC_{50} of 2.7µM whereas

the IC_{50} value for CPO was 6.5 µM on rFXIIIa-mediated peptide crosslinking activity. In addition, DZ and PTH showed the highest potency in rFXIIIa-mediated amine incorporation assays, giving IC_{50} values of 17 and 18 µM, respectively. The inhibition effect of DZ, CPF, PTH could be due to structural interactions according to each chemical structure and their metabolites product with and without oxidation. It has been suggested that the toxic effect of released phenol groups may be associated with these effects, the strength of toxic impact of these phenol compounds being based on the position and the type of substituent atoms (Michałowicz & Duda, 2007). Also, it has been reported that metabolite forms of DZ, CPF, PTH such as IMHP, 3, 5, 6-TCP and *p*-nitrophenol, respectively, are classified as Class III compounds that have structural features that may represent a safety hazard and pose a significant risk of toxicity (Melching-Kollmuß *et al.*, 2010). Moreover, PSP also showed a slight but significant effect on both rFXIIIa and plasma TG -mediated peptide crosslinking and amine incorporation activities, respectively. Therefore, the current study data showing significant effects of OPs on plasma TG, suggest that TG may represent a direct or indirect toxicity target of OPs.

For example, studies, previous studies suggest that PSP may alter cell signaling, including activities of kinases that regulate TG activity in cells and tissues TG (Howden, 2006). In studies on cultured N2a neuroblastoma and HepG2 hepatoma cell lines, PSP (3µM) exposure resulted in altered tissue transglutaminase-mediated amine incorporation activity, where it was decreased in N2a and increased in HepG2 cells (Harris *et al.*, 2009). Moreover, Muñoz, *et al.* (2010) showed that tissue transglutaminase-mediated amine incorporation activity in rat C6 glioma cells increased after 24h exposure to 10 µM CPF. In the latter study, increased activity of guinea pig liver TG2 *in vitro* following treatment with OP suggested the possibility of a direct interaction between OPs and TG. Although, it has been pointed that parent OP insecticide compounds are relatively weak inhibitors of their acute toxicity target

AChE and that their bioactivated forms (oxons) are considered to be the primary acute toxicants in nerve tissue (Poet *et al.*, 2003), in the current study some of the parent compounds showed more inhibitory potential against TG activity than their oxon form, suggesting a distinct structure activity relationship for the different enzyme activities.

In the present study the D-dimer levels were measured to determine whether the fibrin mesh exhibited the same level of covalently crosslinked D-dimers within fibrin monomers. The clot was created after plasma samples were treated with or without two concentrations (25 and 50 µM) of OPs. The data suggested that all OPs showed a significant inhibitory effect on clot formation by reducing D-dimer formation, a finding which agreed with the significant inhibition effect of OPs on TG-mediated transamidase activities. DZ had the most potent effect at both concentrations in the D-dimer assay, causing about 50% decrease in D-dimer level in the sample at 50 µM, whereas DZ had a more significant on TG-mediated amine incorporation activity. This could reflect the possibility that DZ may interfere with the clotting cascade at least in part through an amine incorporation-mediated pathway. Previous studies have reported that there are high levels of natural polyamines in the human body, which may serve as natural substrates for transglutaminase in cells and body fluid (Folk *et al.*, 1980).

To examine the possibility of covalent binding of PSP to plasma proteins including FXIII, it was necessary first to remove albumin from plasma to improve the detection of low abundant proteins, as studies indicated that these low abundant proteins could be disease biomarkers (Echan *et al.*, 2005). Binding was confirmed by the detection on 1 D SDS-PAGE of Rh-PSP binding to pure FXIIIa, and a similar molecular weight band in depleted plasma. This is the first time that covalent binding of OP to FXIIIa has been demonstrated. Also, the depleted plasma protein extract incubated with labelled PSP was separated by 2D-PAGE and, compared to control samples, showed several labeled PSP-binding spots suggesting that

other low abundance proteins in depleted plasma can interact with PSP. Some of the other PSP-binding proteins presumably correspond to those previously identified as OP binding, namely albumin and ChEs, etc (Marsillach *et al.*, 2013). Further analysis by mass spectrometry would help to identify the rest.

Competition experiments using pure FXIIIa incubated with both labelled PSP and other (non-labelled) OPs showed significant competition in binding site in specific cases. For example, DZ and POX demonstrated slightly weaker fluorescence compared to the intensity of labelled PSP binding alone, suggesting that binding may not be near the PSP binding site. However, the other OPs showed higher competition with non-labelled OP and the variation in competition could be a sign of more than one binding site or that they might not all bind to the same positions. In the current study only the metabolite OP compounds were analysed by MS to identify the location of covalent binding site(s) on purified protein FXIII, which has an active site cysteine314. The results showed that there may be several modification sites and different adducts at different binding sites, by comparing mass shift to the control sample. There was a common phosphorylated site in FXIIIa incubated with unlabelled PSP, DZO, CPO, and POX on Ser-413, which is located in the catalytic domain of FXIII, suggesting this could be a competing site of PSP binding and other OPs. PSP was also associated with Thr293-phosphorylated, which is only few amino acids away from the active site Cys314 and Ser340-PSP, which is near Asp343. Studies reported that a strong salt bridge between Arg11 in AP-FXIII domain and Asp343 in core domain to make Cys314 inaccessible for substrate and other chemical molecules (Muszbek *et al.*, 2011), indicating that other conformational changes in this region may affect catalytic activity However, the oxon metabolite OPs showed more adduct binding sites than were observed for PSP. CPO presented 50:50 tyrosine and lysine diethylphosphorylated residues distributed between the β-sandwich and catalytic core domains, the closest to the catalytic active site being Tyr302,

and 311, and formed an ethylphosphorylated adduct on Ala22 in AP-FXIII and Lys570 in *β*-barrel 1 domain. Previous studies identified that a major adduct of CPO on albumin is tyrosine-diethylphosphorylated and that this becomes irreversibly modified *in vivo* in humans poisoned by CPF (Li *et al.*, 2013). Also *in vitro* experiments showed that CPO can covalently modify tyrosine on other proteins including keratins, tubulin, and transferrin (Schopfer *et al.*, 2010). Moreover, DZO and POX exposure resulted in ethylphosphorylated and diethylphosphorylated adducts close to Arg11, which could affect the stability of the salt bridge between Arg11and Asp343 and as a result affect the catalytic site residue Cys314. A major finding in this part of work that DZO, CPO, and POX exposure induced mono ethylphosphorylated-adducts on different amino acid spread all over the main four domains of FXIIIa, as previous cases of 'aging' on non-esterase protein-OP adducts have not been reported.

7.1.2 OPs effect on thrombin

Thrombin is another coagulation factor that has an important role in the control of haemostasis (Huntington, 2005). The third aim of this study was to characterize the effect of OPs on thrombin activity and examine their binding to thrombin. Activity assays with Sar-Pro-Arg-p-nitroanilide substrate were used to investigate the OP effect on thrombin activity and covalent binding was studied by SDS-PAGE.

In the current study, purified and plasma thrombin activities were studied with and without OP exposure. Most of the OPs did not show any significant effect on purified thrombin even when the enzyme was diluted to 0.05 U/ml. However, CPF at 25 and 50 µM concentrations inhibited purified thrombin activity by about 60 % compared to the control, and a slight effect was observed for PSP. The strong CPF effect on purified thrombin could be enhanced due to the deficiency of a biological environment as in plasma as discussed earlier. As indicated in a previous study 50 µM DZ incubated with highly purified 3.6 mg/ml BChE

over 15h, caused 52 % reduction of BChE activity suggesting 'slow' inhibition, which may occur through a thiono-thiolo rearrangement (Tacal & Lockridge, 2010). Thus, the lack of effect could be due to the relatively short exposure time in the current study. In assays of plasma thrombin activity, showed 25 µM CPF and 50 µM CPF, CPO, and POX were the only OPs that had a significant inhibitory effect. The significant potency of CPF was again notable, inhibiting 40 % and 50 % of plasma thrombin activity at 25 and 50 µM, respectively. Previous studies have reported that the deactivation of CPO by cytochromes and PON1 produces TCP (Poet *et al.*, 2003; Kumar, 2015), suggesting that the biological environment of the plasma thrombin samples could bioactivate or degrade the CPF to its metabolite forms that are more toxic (with respect to ChE activity) or one of its breakdown metabolite products, such as TCP. This is consistent with current data showing CPO inhibition effect on plasma thrombin activity. In a previous study, which examined the effects of 500 µM and 50µM POX on 0.05 U/ml purified plasma bovine thrombin using the fluorescent substrate Boc-Asp (OBzl)-Pro-Arg-AMC, the results indicated complete inhibition of purified thrombin activity at 500 µM, where 50 µM POX showed 70 % inhibition of purified thrombin activity (Golderman *et al.*, 2016). However, another study using bovine thrombin (0.2 U) and the chromogenic substrate CBZ-Gly-Pro-Arg-4-nitroanilide substrate estimated an IC_{50} value for POX higher than 100 µM (Quistad & Casida, 2000). However, in the current study, 0.05 U/ml purified and 0.2 mg/ml plasma thrombin were pre-incubated with OPs on ice for 30 min before adding the chromogenic substrate Sar-Pro-Arg-p-nitroanilde. The decreased thrombin sample concentration may explain the enhanced effects observed in fluorometric assays (Gargiulo *et al.* 1981). Thus, using a fluorometric assay or prolonging the incubation time with reduced thrombin enzyme concentration might improve the stoichiometric reaction with thrombin enzyme in the chromogenic assay.

The binding assay in the current study showed a high intensity of fluorescent bands of thrombin after SDS-PAGE, confirming the covalent binding of Rh-PSP on thrombin protein. As thrombin is a serine esterase, it is likely that the PSP binding site is the active site serine, comparable to that already identified serine esterases, for instance BChE (Marsillach *et al.*, 2013). Moreover, competition assays between Rh-PSP and other OPs suggested that other OPs (including unlabeled PSP) could displace labelled PSP suggesting that competition might happen on a single site of thrombin protein. In addition, the presumed covalent binding of all OPs to thrombin protein on SDS-PAGE raises the possibility that some OPs can bind to thrombin without inhibiting its activity as shown in the purified thrombin activity assay. In agreement with this speculation, on study indicated that DFP incubated with egg white lysozyme, Taka-amylase A, and papain showed a modified tyrosine residue; however, the OP-modified enzymes have their fully activity (Lockridge & Schopfer, 2010). Alternatively, it may be that the level of covalent binding is insufficient to cause significant inhibition of thrombin under the conditions tested.

It is interesting to note from the data produced in the current study that, although cholinesterase, FXIIIa, thrombin activity and D-dimer evaluation, are associated with distinct proteins with different activity mechanisms, CPF was common inhibitor among all of the different assays, suggesting a multitude of CPF toxic effects in the biological environment (or on pure enzyme) possibly to top its greater ability to interact with these enzymes in different ways.

7.1.3 OPs effect on THP-1 cell line

Monocytes are a type of white blood cell (leukocyte) that, once the body is invaded, convert to macrophages as part of the immune response (Gordon & Taylor, 2005). The fourth aim of this study was to identify the effect of OPs on the proliferation and viability of THP-1

monocyte-like cells. Proliferation and viability were studied by Trypan Blue exclusion assay and the metabolic activity of the cells was monitored by the alamarBlue assay.

The data obtained in the current study showed that OPs could affect proliferation in a concentration and time-dependent manner. In the first set of experiment the 100 µM of DZ, DZO, PTH, POX had the strongest effects, where they decreased live cell count by 50 % on day 6 of toxin incubation compared to the non OP-treated control samples. This suggested that both phosphorothioate and oxon forms of insecticide OPs behaved in similar way with respect to monocyte cell growth in contrast to the different toxicities against their main acute toxicity targets in nerve tissue. Interestingly, 100 µM CPO on day 4 induced the elevation of live cell counts compared to control cells, before causing reduction on day 6, whereas, CPF inhibited the proliferation and viability at both time points. The effect observed on day 4 against the high concentration of CPO could be an immune reaction that had failed by day 6 because of the high concentration of toxin, as metabolic activity was significantly inhibited from day 0. This possibility is consistent with the findings of a study by Ural (2013), who exposed *Cyprinus carpio carpio* fish to 0.04 and 0.08 mg/l CPF for 14 days resulting in a significant increase of WB cell count suggestive of an immune response. Moreover, in the current study, PTH was the most toxic compound with respect to the reduction of cell proliferation and viability. A smaller group of OPs with lower concentration were selected and incubated with cells for up to 4 days only, giving further confirmation that OP effects on THP-1 cells are concentration and time-dependent. All selected OPs induced decline in THP-1 proliferation.

7.2 Future work

The present study evaluated the effect of OPs on plasma TG (FXIIIa) transamidase activities and the possible OP adducts on FXIIIa protein. The results showed significant inhibitory effects of several OPs on plasma TG or rFXIII-mediated amine and peptide incorporation activity, demonstrated the covalent binding of FXIIIa with labelled PSP, its displacement by unlabelled OPs, and the location of sites of adduct formation for PSP and the oxon forms of pesticide OPs. The data also showed the ability of specific OPs to inhibit and/or covalently bind to pure and plasma thrombin. Based on the current study's findings, I would make the following recommendations for future research: -

It would be of interest in future work to investigate the potential role of natural polyamine adduct formation (such as spermidine or spermine) in clotting and in OP toxicity, as these serve as a substrate for transglutaminases in body cells and fluid (Folk et al., 1980). It would also be of value to identify novel proteins forming OP adducts in depleted plasma from by SDS-PAGE, 2D-PAGE and MS analysis.

In addition, since the organophosphorothioates CPF, DZ and PTH also showed inhibition effects on rFXIII and thrombin, these compounds (like PSP and the oxons) could also form adducts on these proteins and this would be worthy of further study using MS analysis with rFXIIIa and thrombin incubated with parent OPs.

According to the current study, the effect of OPs on pure thrombin activity using chromogenic substrate appeared only after dilution to 0.5 U/ml, in agreement with Gargiulo *et al.* (1981) who used a fluorescent substrate. Further work with lower enzyme concentration, higher OP: thrombin ratio and longer incubation time, possibly using a more sensitive fluorescent substrate would be worthwhile. As the competition assays performed

in the current work suggested covalent binding to a common site for all OPs, confirmation of the binding site(s) location by MS would be of interest.

Since most OPs had an obvious effect on THP-1 cell proliferation, in some cases in the absence of cell death, these OPs could affect key processes that modulate cell proliferation. For example, as many studies have used antibodies to PCNA and Ki67 to study proliferation of THP-1cells (Sun *et al.*, 2016), a similar approach could be applied to study their expression in OP-treated THP-1 cells to confirm the effect of OPs on these and other intracellular proliferation regulatory molecules. A non-targeted proteomic approach (e.g. 2D-PAGE of cell lysates and MS of identification of protein showing expression changes on OP treatment) would help to determine the proteomic basis of OP effects. Quantitative RT-PCR would then establish which protein changes were affected by altered gene expression.

Moreover, given the observed effects of OPs on FXIIIa-mediated transamidase activity, it would be useful to study the effect of OPs on FXIII activity, production and secretion in THP-1 monocyte-like cells or in cells induced to differentiate into macrophages, in which FXIII expression is higher than in monocytes, (Conkling *et al.*, 1989; Sárváry *et al.*, 2004).

7.3 Concluding remarks

The present study addressed the question of whether OPs could disrupt the coagulation process through modulation of FXIIIa and thrombin activity, and by disturbing monocyte cell growth. Several OPs were shown to disrupt these haematological parameters. The findings demonstrated a potential ability of OPs to inhibit transamidase activities of both plasma TG and purified rFXIIIa. The ability of OPs to disrupt the coagulation cascade was further demonstrated when reduced levels of D-dimer were detected by ELISA. MS analysis revealed that PSP and the 3 oxon OPs formed a variety of covalent adducts with various amino acids in rFXIIIa. Plasma thrombin activity was inhibited by 25 and 50 µM concentrations of several OPs. Selected OPs induced increased proliferation at early exposure times, which could reflect an immune response. However, most of the OPs tested inhibited THP-1 monocyte-like cell proliferation and reduced metabolic activity at sub-lethal concentrations, suggesting that OPs can interfere with proliferation mechanisms of white cells. Therefore, more research about OPs on coagulation cascade factors would be useful to understand more fully how OPs can disrupt haemostasis. This knowledge would introduce a valuable insight into how proteins other than cholinesterases are affected by OPs and how such toxicity affects their function.

References

AbdAlla, S., Lother, H., Langer, A., el Faramawy, Y. and Quitterer, U., 2004. Factor XIIIA transglutaminase crosslinks AT1 receptor dimers of monocytes at the onset of atherosclerosis. *Cell,* 119 (3), 343-354.

Abdullat, I., Battah, A. and Hadidi, K., 2006. The use of serial measurement of plasma cholinesterase in the management of acute poisoning with organophosphates and carbamates. *Forensic Science International,* 162 (1-3), 126-130.

Abou-Donia, M.B., and Lapadula, D.M., 1990. Mechanisms of organophosphorus ester-induced delayed neurotoxicity: type I and type II. *Annual Review of Pharmacology and Toxicology,* 30 (1), 405-440.

Adam, S.S., Key, N.S. and Greenberg, C.S., 2009. D-dimer antigen: current concepts and future prospects. *Blood,* 113 (13), 2878-2887.

Aeschlimann, D., and Thomazy, V., 2000. Protein crosslinking in assembly and remodelling of extracellular matrices: the role of transglutaminases. *Connective Tissue Research,* 41 (1), 1-27.

Agency for Toxic Substances and Disease Registry (ATSDR), 2008. *Toxicological profile for Diazinon.* U.S. Department of Health and Human Services.

Akassoglou, K., Malester, B., Xu, J., Tessarollo, L., Rosenbluth, J. and Chao, M.V., 2004. Brain-specific deletion of neuropathy target esterase/swisscheese results in neurodegeneration. *Proceedings of the National Academy of Sciences of the United States of America,* 101 (14), 5075-5080.

Akimov, S.S., and Belkin, A.M., 2001. Cell surface tissue transglutaminase is involved in adhesion and migration of monocytic cells on fibronectin. *Blood,* 98 (5), 1567-1576.

Albers, J.W., Berent, S., Garabrant, D.H., Giordani, B., Schweitzer, S.J., Garrison, R.P. and Richardson, R.J., 2004. The effects of occupational exposure to chlorpyrifos on the neurologic examination of central nervous system function: a prospective cohort study. *Journal of Occupational and Environmental Medicine,* 46 (4), 367-378.

Aldo, P.B., Craveiro, V., Guller, S. and Mor, G., 2013. Effect of culture conditions on the phenotype of THP-1 monocyte cell line. *American Journal of Reproductive Immunology,* 70 (1), 80-86.

Aldridge, W.N., 1953. The differentiation of true and pseudo cholinesterase by organophosphorus compounds. *The Biochemical Journal,* 53 (1), 62-67.

Aldridge, W.N., 1954. Tricresyl phosphates and cholinesterase. *The Biochemical Journal,* 56 (2), 185-189.

Algarni, A.S., 2018. *Modulation of transglutaminase 2 by pituitary adenylyl cyclase activating polypeptide and nerve growth factor in neuroblastoma cells: A role in cell survival and neurite outgrowth.* PhD., Nottingham Trent University.

Alishahi, M., Mohammadi, A., Mesbah, M. and Razi Jalali, M., 2016. Haemato-immunological responses to diazinon chronic toxicity in Barbus sharpeyi. *Iranian Journal of Fisheries Sciences,* 15 (2), 870-885.

Al-Nasiry, S., Geusens, N., Hanssens, M., Luyten, C. and Pijnenborg, R., 2007. The use of Alamar Blue assay for quantitative analysis of viability, migration and invasion of choriocarcinoma cells. *Human Reproduction,* 22 (5), 1304-1309.

Alyamani, N., 2018. *Molecular-Genetics Studies of Organophosphate Induced Neurodegeneration in Differentiating Mammalian Cell lines and Neural Progenitor Stem Cells.* PhD, Nottingham Trent University.

Ambali, S., Akanbi, D., Igbokwe, N., Shittu, M., Kawu, M. and Ayo, J., 2007. Evaluation of subchronic chlorpyrifos poisoning on hematological and serum biochemical changes in mice and protective effect of vitamin C. *The Journal of Toxicological Sciences,* 32 (2), 111-120.

Amitai, G., Moorad, D., Adani, R. and Doctor, B., 1998. Inhibition of acetylcholinesterase and butyrylcholinesterase by chlorpyrifos-oxon. *Biochemical Pharmacology,* 56 (3), 293-299.

Andreadis, G., Albanis, T., Vagdatli, E., Vasara, E., Andreadou, E., Avramidis, N. and Patoucheas, D.P., 2014. Low dose exposure to organophosphate pesticides alters hematological parameters of farm workers from N. Greece. *Fresenius Environmental Bulletin,* 23 (9 A), 2322-2325.

Antonijevic, B., and Stojiljkovic, M.P., 2007. Unequal efficacy of pyridinium oximes in acute organophosphate poisoning. *Clinical Medicine & Research,* 5 (1), 71-82.

Anwar, R., and Miloszewski, K.J., 1999. Factor XIII deficiency. *British Journal of Haematology,* 107 (3), 468-484.

Ariens, R.A., Lai, T.S., Weisel, J.W., Greenberg, C.S. and Grant, P.J., 2002. Role of factor XIII in fibrin clot formation and effects of genetic polymorphisms. *Blood,* 100 (3), 743-754.

Asahina, T., Kobayashi, T., Takeuchi, K. and Kanayama, N., 2007. Congenital blood coagulation factor XIII deficiency and successful deliveries: a review of the literature. *Obstetrical & Gynecological Survey,* 62 (4), 255-260.

Assis, C.R.D., Bezerra, R.S. and Carvalho Jr, L.B., 2011. Fish cholinesterases as biomarkers of organophosphorus and carbamate pesticides. *In:* Fish cholinesterases as biomarkers of organophosphorus and carbamate pesticides. *Pesticides in the Modern World-Pests Control and Pesticides Exposure and Toxicity Assessment.* InTech, 2011, .

Bagoly, Z., Katona, É. and Muszbek, L., 2012. Factor XIII and inflammatory cells. *Thrombosis Research,* 129, S77-S81.

Baker, P.E., Cole, T.B., Cartwright, M., Suzuki, S.M., Thummel, K.E., Lin, Y.S., Co, A.L., Rettie, A.E., Kim, J.H. and Furlong, C.E., 2013. Identifying safer anti-wear triaryl phosphate additives for jet engine lubricants. *Chemico-Biological Interactions,* 203 (1), 257-264.

Banaee, M., Mirvagefei, A., Rafei, G. and Amiri, B.M., 2008. Effect of sub-lethal diazinon concentrations on blood plasma biochemistry.

Banka, C.L., Black, A.S., Dyer, C.A. and Curtiss, L.K., 1991. THP-1 cells form foam cells in response to coculture with lipoproteins but not platelets. *Journal of Lipid Research,* 32 (1), 35-43.

Basova, N., Kormilitsyn, B., Perchenok, A.Y., Rozengart, E., Saakov, V. and Suvorov, A., 2018. Substrate Specificity of Cholinesterases in Various Representatives of the Animal Kingdom. *Journal of Evolutionary Biochemistry and Physiology,* 54 (3), 157-174.

Bates, S.M., 2012. D-dimer assays in diagnosis and management of thrombotic and bleeding disorders. *In: Seminars in thrombosis and hemostasis,* Thieme Medical Publishers, pp. 673-682.

Bereczky, Z., Katona, É. and Muszbek, L., 2003. Fibrin stabilization (factor XIII), fibrin structure and thrombosis. *Pathophysiology of Haemostasis and Thrombosis,* 33 (5-6), 430-437.

Black, R.M., Harrison, J.M. and Read, R.W., 1999. The interaction of sarin and soman with plasma proteins: the identification of a novel phosphonylation site. *Archives of Toxicology,* 73 (2), 123-126.

Blann, A.D., and Ahmed, N., 2014. *Blood Science.* First edition ed. UK: John Wiley & Sons, Ltd.

Blood Laboratory n.d, *Hemostasis: PT and PTT tests,* The McGill Physiology Virtual Lab, Accessed 15 June 2019 , < https://www.medicine.mcgill.ca/physio/vlab/bloodlab/PT_PTT.htm>.

Board, P., Lososky, M. and Miloszewski, K., 1993. Factor XIII: inherited and acquired deficiency. *Blood Reviews,* 7 (4), 229-242.

Bohn, H., and Schwick, H.G., 1971. Isolation and characterization of a fibrin-stabilizing factor from human placenta. *Arzneimittel-Forschung,* 21 (10), 1432-1439.

Boyd, E.M., Killham, K. and Meharg, A.A., 2001. Toxicity of mono-, di-and tri-chlorophenols to lux marked terrestrial bacteria, Burkholderia species Rasc c2 and Pseudomonas fluorescens. *Chemosphere,* 43 (2), 157-166.

Brimijoin, S., and Hammond, P., 1988. Butyrylcholinesterase in human brain and acetylcholinesterase in human plasma: Trace enzymes measured by two-site immunoassay. *Journal of Neurochemistry,* 51 (4), 1227-1231.

Brooks, M., Dodds, W., Knowler, C. and Giger, U., 1994. Factor XI deficiency in Kerry blue terriers. *J.Am.Vet.Med.Assoc,* 205 (11), 1557-1561.

Brzak, K.A., Harms, D.W., Bartels, M.J. and Nolan, R.J., 1998. Determination of chlorpyrifos, chlorpyrifos oxon, and 3, 5, 6-trichloro-2-pyridinol in rat and human blood. *Journal of Analytical Toxicology,* 22 (3), 203-210.

Budde, I.P., Rohde, B.H., Bender, C.L. and Ullrich, M.S., 1998. Growth phase and temperature influence promoter activity, transcript abundance, and protein stability during biosynthesis of the Pseudomonas syringae phytotoxin coronatine. *Journal of Bacteriology,* 180 (6), 1360-1367.

Cabello, G., Valenzuela, M., Vilaxa, A., Duran, V., Rudolph, I., Hrepic, N. and Calaf, G., 2001. A rat mammary tumor model induced by the organophosphorous pesticides parathion and malathion, possibly through acetylcholinesterase inhibition. *Environmental Health Perspectives,* 109 (5), 471-479.

Calvert, G.M., Plate, D.K., Das, R., Rosales, R., Shafey, O., Thomsen, C., Male, D., Beckman, J., Arvizu, E. and Lackovic, M., 2004. Acute occupational pesticide-related illness in the US, 1998–1999: Surveillance findings from the SENSOR-pesticides program. *American Journal of Industrial Medicine,* 45 (1), 14-23.

Cardona, D., López-Granero, C., Cañadas, F., Llorens, J., Flores, P., Pancetti, F. and Sánchez-Santed, F., 2013. Dose-dependent regional brain acetylcholinesterase and acylpeptide hydrolase inhibition without cell death after chlorpyrifos administration. *The Journal of Toxicological Sciences,* 38 (2), 193-203.

Cashman, J.R., Berkman, C.E., Underiner, G., Kolly, C.A. and Hunter, A.D., 1998. Cocaine benzoyl thioester: Synthesis, kinetics of base hydrolysis, and application to the assay of cocaine esterases. *Chemical Research in Toxicology,* 11 (8), 895-901.

Casida, J.E., and Quistad, G.B., 2005. Serine hydrolase targets of organophosphorus toxicants. *Chemico-Biological Interactions,* 157, 277-283.

Celik, I., and Suzek, H., 2008. The hematological effects of methyl parathion in rats. *Journal of Hazardous Materials,* 153 (3), 1117-1121.

Çetinkaya, M., and Baydan, E., 2010. Investigation of in vitro effects of ethephon and chlorpyrifos, either alone or in combination, on rat intestinal muscle contraction. *Interdisciplinary Toxicology,* 3 (1), 35-39.

Chambers, J.E., and Oppenheimer, S.F., 2004. Organophosphates, serine esterase inhibition, and modeling of organophosphate toxicity. *Toxicological Sciences,* 77 (2), 185-187.

Chambers, J.E., and Oppenheimer, S.F., 2004. Organophosphates, serine esterase inhibition, and modeling of organophosphate toxicity. *Toxicological Sciences,* 77 (2), 185-187.

Chau, D.Y., Collighan, R.J., Verderio, E.A., Addy, V.L. and Griffin, M., 2005. The cellular response to transglutaminase-cross-linked collagen. *Biomaterials,* 26 (33), 6518-6529.

Chen, S., and Cashman, J.R., 2013. Organophosphate exposure: detection and remediation. *Advances in Molecular Toxicology.* Elsevier, 2013, pp. 207-233.

Chen, S., Zhang, J., Lumley, L. and Cashman, J.R., 2013. Immunodetection of serum albumin adducts as biomarkers for organophosphorus exposure. *The Journal of Pharmacology and Experimental Therapeutics,* 344 (2), 531-541.

Collombet, J., Mourcin, F., Grenier, N., Four, E., Masqueliez, C., Baubichon, D., Lallement, G. and Hérodin, F., 2005. Effect of soman poisoning on populations of bone marrow and peripheral blood cells in mice. *Neurotoxicology,* 26 (1), 89-98.

Čolović, M., Krstić, D., Petrović, S., Leskovac, A., Joksić, G., Savić, J., Franko, M., Trebše, P. and Vasić, V., 2010. Toxic effects of diazinon and its photodegradation products. *Toxicology Letters,* 193 (1), 9-18.

Čolović, M.B., Krstić, D.Z., Lazarević-Pašti, T.D., Bondžić, A.M. and Vasić, V.M., 2013. Acetylcholinesterase inhibitors: pharmacology and toxicology. *Current Neuropharmacology,* 11 (3), 315-335.

Čolović, M.B., Krstić, D.Z., Ušćumlić, G.S. and Vasić, V.M., 2011. Single and simultaneous exposure of acetylcholinesterase to diazinon, chlorpyrifos and their photodegradation products. *Pesticide Biochemistry and Physiology,* 100 (1), 16-22.

Conkling, P.R., Achyuthan, K.E., Greenberg, C.S., Newcomb, T.F. and Weinberg, J.B., 1989. Human mononuclear phagocyte transglutaminase activity cross-links fibrin. *Thrombosis Research,* 55 (1), 57-68.

Coombes, R.H., Meek, E.C., Dail, M.B., Chambers, H.W. and Chambers, J.E., 2014. Human paraoxonase 1 hydrolysis of nanomolar chlorpyrifos-oxon concentrations is unaffected by phenotype or Q192R genotype. *Toxicology Letters,* 230 (1), 57-61.

Corbett, S.A., and Schwarzbauer, J.E., 1998. Fibronectin–fibrin cross-linking: a regulator of cell behavior. *Trends in Cardiovascular Medicine,* 8 (8), 357-362.

Costa, L.G., Richter, R.J., Li, W., Cole, T., Guizzetti, M. and Furlong, C.E., 2003. Paraoxonase (PON 1) as a biomarker of susceptibility for organophosphate toxicity. *Biomarkers,* 8 (1), 1-12.

Cox, C., 2000. Diazinon: toxicology. *Journal of Pesticide Reform,* 20 (2), 15-21.

Croom, E.L., Wallace, A.D. and Hodgson, E., 2010. Human variation in CYP-specific chlorpyrifos metabolism. *Toxicology,* 276 (3), 184-191.

Cui, C., and Kaartinen, M.T., 2015. Transglutaminases in Bone Formation and Bone Matrix Stabilization. *Transglutaminases.* Springer, 2015, pp. 263-281.

Cui, Y., Guo, J., Xu, B. and Chen, Z., 2006. Potential of chlorpyrifos and cypermethrin forming DNA adducts. *Mutation Research/Genetic Toxicology and Environmental Mutagenesis,* 604 (1-2), 36-41.

Dahlbäck, B., 2000. Blood coagulation. *The Lancet,* 355 (9215), 1627-1632.

Dang, O.D., Vindigni, A. and Di Cera, E., 1995. An allosteric switch controls the procoagulant and anticoagulant activities of thrombin. *Proceedings of the National Academy of Sciences of the United States of America,* 92 (13), 5977-5981.

Dardik, R., Loscalzo, J. and Inbal, A., 2006. Factor XIII (FXIII) and angiogenesis. *Journal of Thrombosis and Haemostasis,* 4 (1), 19-25.

Dashty, M., Akbarkhanzadeh, V., Zeebregts, C.J., Spek, C.A., Sijbrands, E.J., Peppelenbosch, M.P. and Rezaee, F., 2012. Characterization of coagulation factor synthesis in nine human primary cell types. *Scientific Reports,* 2, 787.

Davies, D.B., and Holub, B.J., 1980. Comparative subacute toxicity of dietary diazinon in the male and female rat. *Toxicology and Applied Pharmacology,* 54 (3), 359-367.

Davis, L., Britten, J. and Morgan, M., 1997. Cholinesterase Its significance in anaesthetic practice. *Anaesthesia,* 52 (3), 244-260.

De Nola, G., Kibby, J. and Mazurek, W., 2008. Determination of ortho-cresyl phosphate isomers of tricresyl phosphate used in aircraft turbine engine oils by gas chromatography and mass spectrometry. *Journal of Chromatography A,* 1200 (2), 211-216.

Denola, G., Hanhela, P. and Mazurek, W., 2011. Determination of tricresyl phosphate air contamination in aircraft. *Annals of Occupational Hygiene,* 55 (7), 710-722.

Dhotre, S.N., Katkam, R.V., Joshi, N.G. and Deshpande, K.H., 2014. Study of acetyl cholinesterase, butyryl cholinestrase and β-glucuronidase in organophosphorus poisoning. *Indian Medical Gazette,* 148 (2), 51-57.

Di Cera, E., 2003. Thrombin interactions. *Chest,* 124 (3), 11S-17S.

Di Cera, E., Guinto, E.R., Vindigni, A., Dang, Q.D., Ayala, Y.M., Wuyi, M. and Tulinsky, A., 1995. The Na+ binding site of thrombin. *The Journal of Biological Chemistry,* 270 (38), 22089-22092.

Díaz-Resendiz, K.J.G., Toledo-Ibarra, G.A. and Girón-Pérez, M.I., 2015. Modulation of immune response by organophosphorus pesticides: fishes as a potential model in immunotoxicology. *Journal of Immunology Research,* 2015.

Dreiher, J., Novack, V., Barachana, M., Yerushalmi, R., Lugassy, G. and Shpilberg, O., 2005. Non-Hodgkin's lymphoma and residential proximity to toxic industrial waste in southern Israel. *Haematologica,* 90 (12), 1709-1710.

Eaton, D.L., Daroff, R.B., Autrup, H., Bridges, J., Buffler, P., Costa, L.G., Coyle, J., McKhann, G., Mobley, W.C. and Nadel, L., 2008. Review of the toxicology of chlorpyrifos with an emphasis on human exposure and neurodevelopment. *Critical Reviews in Toxicology,* 38 (sup2), 1-125.

Echan, L.A., Tang, H., Ali-Khan, N., Lee, K. and Speicher, D.W., 2005. Depletion of multiple high-abundance proteins improves protein profiling capacities of human serum and plasma. *Proteomics,* 5 (13), 3292-3303.

Eckert, R.L., Kaartinen, M.T., Nurminskaya, M., Belkin, A.M., Colak, G., Johnson, G.V. and Mehta, K., 2014. Transglutaminase regulation of cell function. *Physiological Reviews,* 94 (2), 383-417.

Eddleston, M., Eyer, P., Worek, F., Rezvi Sheriff, M. and Buckley, N.A., 2008. Predicting outcome using butyrylcholinesterase activity in organophosphorus pesticide self-poisoning. *QJM: An International Journal of Medicine,* 101 (6), 467-474.

Ehrich, M., and Jortner, B.S., 2010. Organophosphorus-induced delayed neuropathy. *Hayes' Handbook of Pesticide Toxicology.* Elsevier, 2010, pp. 1479-1504.

Ehrich, M., Correll, L. and Veronesi, B., 1997. Acetylcholinesterase and neuropathy target esterase inhibitions in neuroblastoma cells to distinguish organophosphorus compounds causing acute and delayed neurotoxicity. *Fundamental and Applied Toxicology,* 38 (1), 55-63.

Elersek, T., and Filipic, M., 2011. Organophosphorous pesticides-mechanisms of their toxicity. *Pesticides-the impacts of pesticides exposure.* IntechOpen, 2011.

El-Fawal, H.A., and McCain, W.C., 2008. Antibodies to neural proteins in organophosphorus-induced delayed neuropathy (OPIDN) and its amelioration. *Neurotoxicology and Teratology,* 30 (3), 161-166.

El-Fawal, H.A., Jortner, B.S. and Ehrich, M., 1990. Use of the biventer cervicis nerve-muscle preparation to detect early changes following exposure to organophosphates inducing delayed neuropathy. *Fundamental and Applied Toxicology,* 15 (1), 108-120.

Ellman, G.L., Courtney, K.D., Andres Jr, V. and Featherstone, R.M., 1961. A new and rapid colorimetric determination of acetylcholinesterase activity. *Biochemical Pharmacology,* 7 (2), 88-95.

Etim, N., Williams, M.E., Akpabio, U. and Offiong, E.E., 2014. Haematological parameters and factors affecting their values. *Agricultural Science,* 2 (1), 37-47.

Eyer, P., 2003. The role of oximes in the management of organophosphorus pesticide poisoning. *Toxicological Reviews,* 22 (3), 165-190.

Fabrizi, L., Gemma, S., Testai, E. and Vittozzi, L., 1999. Identification of the cytochrome P450 isoenzymes involved in the metabolism of diazinon in the rat liver. *Journal of Biochemical and Molecular Toxicology,* 13 (1), 53-61.

Flaskos, J., Harris, W., Sachana, M., Munoz, D., Tack, J. and Hargreaves, A., 2007. The effects of diazinon and cypermethrin on the differentiation of neuronal and glial cell lines. *Toxicology and Applied Pharmacology,* 219 (2-3), 172-180.

Flaskos, J., McLean, W.G. and Hargreaves, A.J., 1994. The toxicity of organophosphate compounds towards cultured PC12 cells. *Toxicology Letters,* 70 (1), 71-76.

Flaskos, J., Sachana, M., Pen, M., Harris, W.C. and Hargreaves, A.J., 2006. Effects of phenyl saligenin phosphate on phosphorylation of pig brain tubulin in vitro. *Environmental Toxicology and Pharmacology,* 22 (1), 70-74.

Folk, J.E., Park, M.H., Chung, S.I., Schrode, J., Lester, E.P. and Cooper, H.L., 1980. Polyamines as physiological substrates for transglutaminases. *The Journal of Biological Chemistry,* 255 (8), 3695-3700.

Forsprecher, J., Wang, Z., Nelea, V. and Kaartinen, M., 2009. Enhanced osteoblast adhesion on transglutaminase 2-crosslinked fibronectin. *Amino Acids,* 36 (4), 747.

Fowler, M.J., Flaskos, J., McLean, W.G. and Hargreaves, A.J., 2001. Effects of neuropathic and non-neuropathic isomers of tricresyl phosphate and their microsomal activation on the production of axon-like processes by differentiating mouse N2a neuroblastoma cells. *Journal of Neurochemistry,* 76 (3), 671-678.

Foxenberg, R.J., Ellison, C.A., Knaak, J.B., Ma, C. and Olson, J.R., 2011. Cytochrome P450-specific human PBPK/PD models for the organophosphorus pesticides: chlorpyrifos and parathion. *Toxicology,* 285 (1-2), 57-66.

Freshney, R.I., 2006. Basic principles of cell culture. *Culture of Cells for Tissue Engineering*, 11-14.

Fukuto, T.R., 1990. Mechanism of action of organophosphorus and carbamate insecticides. *Environmental Health Perspectives*, 87, 245-254.

Gallazzini, M., Ferraris, J.D., Kunin, M., Morris, R.G. and Burg, M.B., 2006. Neuropathy target esterase catalyzes osmoprotective renal synthesis of glycerophosphocholine in response to high NaCl. *Proceedings of the National Academy of Sciences of the United States of America,* 103 (41), 15260-15265.

Garcia, S.J., Seidler, F.J., Qiao, D. and Slotkin, T.A., 2002. Chlorpyrifos targets developing glia: effects on glial fibrillary acidic protein. *Developmental Brain Research,* 133 (2), 151-161.

Gargiulo, R.J., Mitchell, G.A., Hudson, P.M., Pochron, S.P., Huseby, R.M. and Smith, R.E., 1981. Analytical fluorogenic substrates for proteolytic enzymes. *United States Patent,* 4,275,153.

Gentry, P.A., and Wood, R.D., 2005. Thrombin generation: a positive or negative response to trauma in dogs? *Veterinary Journal (London, England: 1997),* 169 (1), 10-11.

Glynn, P., 2006. A mechanism for organophosphate-induced delayed neuropathy. *Toxicology Letters,* 162 (1), 94-97.

Golderman, V., Shavit-Stein, E., Tamarin, I., Rosman, Y., Shrot, S., Rosenberg, N., Maggio, N., Chapman, J. and Eisenkraft, A., 2016. The organophosphate paraoxon and its antidote obidoxime inhibit thrombin activity and affect coagulation in vitro. *PloS One,* 11 (9), e0163787.

Gomez, K., and Bolton-Maggs, P., 2008. Factor XI deficiency. *Haemophilia,* 14 (6), 1183-1189.

Gordon, S. and Taylor, P.R., 2005. Monocyte and macrophage heterogeneity. *Nature Reviews Immunology,* 5 (12), 953.

Grenard, P., Bates, M.K. and Aeschlimann, D., 2001. Evolution of transglutaminase genes: identification of a transglutaminase gene cluster on human chromosome 15q15. Structure of the gene encoding transglutaminase X and a novel gene family member, transglutaminase Z. *The Journal of Biological Chemistry,* 276 (35), 33066-33078.

Griffin, M., Casadio, R. and Bergamini, C.M., 2002. Transglutaminases: nature's biological glues. *The Biochemical Journal,* 368 (Pt 2), 377-396.

Grigoryan, H., Li, B., Xue, W., Grigoryan, M., Schopfer, L.M. and Lockridge, O., 2009. Mass spectral characterization of organophosphate-labeled lysine in peptides. *Analytical Biochemistry,* 394 (1), 92-100.

Grigoryan, H., Schopfer, L.M., Thompson, C.M., Terry, A.V., Masson, P. and Lockridge, O., 2008. Mass spectrometry identifies covalent binding of soman, sarin, chlorpyrifos oxon, diisopropyl fluorophosphate, and FP-biotin to tyrosines on tubulin: a potential mechanism of long term toxicity by organophosphorus agents. *Chemico-Biological Interactions,* 175 (1-3), 180-186.

Grube, A., Donaldson, D., Kiely, T. and Wu, L., 2011. Pesticides industry sales and usage. *US EPA, Washington, DC*.

Gupta, R.C., 2006. Classification and uses of organophosphates and carbamates. *In:* Classification and uses of organophosphates and carbamates. *Toxicology of Organophosphate & Carbamate Compounds.* Elsevier, 2006, pp. 5-24.

Guyton, K.Z., Loomis, D., Grosse, Y., El Ghissassi, F., Benbrahim-Tallaa, L., Guha, N., Scoccianti, C., Mattock, H., Straif, K. and International Agency for Research on Cancer Monograph Working Group, IARC, Lyon, France, 2015. Carcinogenicity of tetrachlorvinphos, parathion, malathion, diazinon, and glyphosate. *The Lancet.Oncology,* 16 (5), 490-491.

Hahn, T., Desoye, G., Lang, I. and Skofitsch, G., 1993. Location and activities of acetylcholinesterase and butyrylcholinesterase in the rat and human placenta. *Anatomy and Embryology,* 188 (5), 435-440.

Hansch, C., McKarns, S.C., Smith, C.J. and Doolittle, D.J., 2000. Comparative QSAR evidence for a free-radical mechanism of phenol-induced toxicity. *Chemico-Biological Interactions,* 127 (1), 61-72.

Hargreaves, A.J., 2012. Neurodegenerations induced by organophosphorous compounds. *Neurodegenerative Diseases.* Springer, 2012, pp. 189-204.

Hargreaves, A.J., Fowler, M.J., Sachana, M., Flaskos, J., Bountouri, M., Coutts, I.C., Glynn, P., Harris, W. and McLean, W.G., 2006. Inhibition of neurite outgrowth in differentiating

mouse N2a neuroblastoma cells by phenyl saligenin phosphate: effects on MAP kinase (ERK 1/2) activation, neurofilament heavy chain phosphorylation and neuropathy target esterase activity. *Biochemical Pharmacology,* 71 (8), 1240-1247.

Harper, A., 2005. A survey of health effects in aircrew exposed to airborne contaminants. *Journal of Occupational Health and Safety Australia and New Zealand,* 21 (5), 433.

Harris, W., Muñoz, D., Bonner, P. and Hargreaves, A., 2009. Effects of phenyl saligenin phosphate on cell viability and transglutaminase activity in N2a neuroblastoma and HepG2 hepatoma cell lines. *Toxicology in Vitro,* 23 (8), 1559-1563.

Hatjian, B., Mutch, E., Williams, F., Blain, P. and Edwards, J., 2000. Cytogenetic response without changes in peripheral cholinesterase enzymes following exposure to a sheep dip containing diazinon in vivo and in vitro. *Mutation Research/Genetic Toxicology and Environmental Mutagenesis,* 472 (1-2), 85-92.

Heger, C.D., and Collins, R.N., 2004. Platelet activation and "crossover appeal": Rab and Rho families united by common links to serotonin. *Molecular Interventions,* 4 (2), 79-81.

Heilmair, R., Eyer, F. and Eyer, P., 2008. Enzyme-based assay for quantification of chlorpyrifos oxon in human plasma. *Toxicology Letters,* 181 (1), 19-24.

Helm, C.E., Zisch, A. and Swartz, M.A., 2007. Engineered blood and lymphatic capillaries in 3-D VEGF-fibrin-collagen matrices with interstitial flow. *Biotechnology and Bioengineering,* 96 (1), 167-176.

Henriksson, P., Becker, S., Lynch, G. and McDonagh, J., 1985. Identification of intracellular factor XIII in human monocytes and macrophages. *The Journal of Clinical Investigation,* 76 (2), 528-534.

Henson, P.M., Gould, D. and Becker, E.L., 1976. Activation of stimulus-specific serine esterases (proteases) in the initiation of platelet secretion. I. Demonstration with organophosphorus inhibitors. *The Journal of Experimental Medicine,* 144 (6), 1657-1673.

Hethershaw, E.L., Cilia La Corte, A., Duval, C., Ali, M., Grant, P.J., Ariëns, R.A. and Philippou, H., 2014. The effect of blood coagulation factor XIII on fibrin clot structure and fibrinolysis. *Journal of Thrombosis and Haemostasis,* 12 (2), 197-205.

Hirahara, K., Shinbo, K., Takahashi, M. and Matsuishi, T., 1993. Suppressive effect of human blood coagulation factor XIII on the vascular permeability induced by anti-guinea pig endothelial cell antiserum in guinea pigs. *Thrombosis Research,* 71 (2), 139-148.

Hortin, G.L., Warshawsky, I. and Laude-Sharp, M., 2001. Macromolecular chromogenic substrates for measuring proteinase activity. *Clinical Chemistry,* 47 (2), 215-222.

Hou, S., Xue, L., Yang, W., Fang, L., Zheng, F. and Zhan, C., 2013. Substrate selectivity of high-activity mutants of human butyrylcholinesterase. *Organic & Biomolecular Chemistry,* 11 (43), 7477-7485.

Howden, R., 2006. *Characterisation of neural transglutaminases and their potential roles in organophosphate toxicity.* Nottingham Trent University (United Kingdom).

Hsieh, L., and Nugent, D., 2008. Factor XIII deficiency. *Haemophilia,* 14 (6), 1190-1200.

Huntington, J., 2005. Molecular recognition mechanisms of thrombin. *Journal of Thrombosis and Haemostasis,* 3 (8), 1861-1872.

Huntington, J.A., 2008. How Na activates thrombin–a review of the functional and structural data. *Biological Chemistry,* 389 (8), 1025-1035.

Iismaa, S.E., Mearns, B.M., Lorand, L. and Graham, R.M., 2009. Transglutaminases and disease: lessons from genetically engineered mouse models and inherited disorders. *Physiological Reviews,* 89 (3), 991-1023.

Inbal, A., and Dardik, R., 2006. Role of coagulation factor XIII (FXIII) in angiogenesis and tissue repair. *Pathophysiology of Haemostasis and Thrombosis,* 35 (1-2), 162-165.

Inbal, A., Lubetsky, A., Krapp, T., Caste, D., Shaish, A., Dickneitte, G., Modis, L., Muszbek, L. and Inbal, A., 2005. Impaired wound healing in factor XIII deficient mice. *Thrombosis and Haemostasis,* 94 (08), 432-437.

Jain, P.T., and Pento, J.T., 1991. A vehicle for the evaluation of hydrophobic compounds in cell culture. *Research Communications in Chemical Pathology and Pharmacology,* 74 (1), 105-116.

Jamalzadeh, L., Ghafoori, H., Sariri, R., Rabuti, H., Nasirzade, J., Hasani, H. and Aghamaali, M.R., 2016. Cytotoxic effects of some common organic solvents on MCF-7, RAW-264.7 and human umbilical vein endothelial cells. *Avicenna Journal of Medical Biochemistry,* 4 (1), 10-33453.

Jayo, A., Conde, I., Lastres, P., Jiménez-Yuste, V. and González-Manchón, C., 2009. Possible role for cellular FXIII in monocyte-derived dendritic cell motility. *European Journal of Cell Biology,* 88 (8), 423-431.

Jbilo, O., Bartels, C.F., Chatonnet, A., Toutant, J. and Lockridge, O., 1994. Tissue distribution of human acetylcholinesterase and butyrylcholinesterase messenger RNA. *Toxicon,* 32 (11), 1445-1457.

Jiang, W., Duysen, E.G., Hansen, H., Shlyakhtenko, L., Schopfer, L.M. and Lockridge, O., 2010. Mice treated with chlorpyrifos or chlorpyrifos oxon have organophosphorylated tubulin in the brain and disrupted microtubule structures, suggesting a role for tubulin in neurotoxicity associated with exposure to organophosphorus agents. *Toxicological Sciences,* 115 (1), 183-193.

Johnson, K., Hashimoto, S., Lotz, M., Pritzker, K. and Terkeltaub, R., 2001. Interleukin-1 induces pro-mineralizing activity of cartilage tissue transglutaminase and factor XIIIa. *The American Journal of Pathology,* 159 (1), 149-163.

Jońca, J., Żuk, M., Wasąg, B., Janaszak-Jasiecka, A., Lewandowski, K., Wielgomas, B., Waleron, K. and Jasiecki, J., 2015. New insights into butyrylcholinesterase activity assay: serum dilution factor as a crucial parameter. *PloS One,* 10 (10), e0139480.

Joo, S., 2012. Mechanisms of platelet activation and integrin αIIβ3. *Korean Circulation Journal,* 42 (5), 295-301.

Kappelmayer, J., Simon, Á., Katona, É., Szanto, A., Nagy, L., Kiss, A., Kiss, C. and Muszbek, L., 2005. Coagulation factor XIII-A. *Thrombosis and Haemostasis,* 94 (08), 454-459.

Karimi, M., Bereczky, Z., Cohan, N. and Muszbek, L., 2009. Factor XIII deficiency. *In: Seminars in thrombosis and hemostasis,* © Thieme Medical Publishers, pp. 426-438.

Karki, P., Ansari, J., Bhandary, S. and Koirala, S., 2004. Cardiac and electrocardiographical manifestations of acute organophosphate poisoning. *Singapore Medical Journal,* 45, 385-389.

Katona, É., Haramura, G., Kárpáti, L., Fachet, J. and Muszbek, L., 2000. A simple, quick one-step ELISA assay for the determination of complex plasma factor XIII (A2B2). *Thrombosis and Haemostasis,* 83 (02), 268-273.

Katsumaro, T., and Tohru, H., 1985. Diazinon concentrations and blood cholinesterase activities in rats exposed to diazinon. *Toxicology Letters,* 25 (1), 7-10.

Kaushik, R., Rosenfeld, C.A. and Sultatos, L., 2007. Concentration-dependent interactions of the organophosphates chlorpyrifos oxon and methyl paraoxon with human recombinant acetylcholinesterase. *Toxicology and Applied Pharmacology,* 221 (2), 243-250.

Kávai, M., Ádány, R., Pásti, G., Surányi, P., Szücs, G., Muszbek, L., Boján, F. and Szegedi, G., 1992. Marker profile, enzyme activity, and function of a human myelomonocytic leukemia cell line. *Cellular Immunology,* 139 (2), 531-540.

Ki, Y., Park, J.H., Lee, J.E., Shin, I.C. and Koh, H.C., 2013. JNK and p38 MAPK regulate oxidative stress and the inflammatory response in chlorpyrifos-induced apoptosis. *Toxicology Letters,* 218 (3), 235-245.

Klöck, C., and Khosla, C., 2012. Regulation of the activities of the mammalian transglutaminase family of enzymes. *Protein Science,* 21 (12), 1781-1791.

Komaromi, I., Bagoly, Z. and Muszbek, L., 2011. Factor XIII: novel structural and functional aspects. *Journal of Thrombosis and Haemostasis,* 9 (1), 9-20.

Köprücü, S.Ş., et al., 2006. Acute toxicity of organophosphorous pesticide diazinon and its effects on behavior and some hematological parameters of fingerling European catfish (Silurus glanis L.). *Pesticide Biochemistry and Physiology,* 86 (2), 99-105.

Korsgren, C., Lawler, J., Lambert, S., Speicher, D. and Cohen, C.M., 1990. Complete amino acid sequence and homologies of human erythrocyte membrane protein band

4.2. *Proceedings of the National Academy of Sciences of the United States of America,* 87 (2), 613-617.

Korte, W.C., Szadkowski, C., Gähler, A., Gabi, K., Kownacki, E., Eder, M., Degiacomi, P., Zoller, N., Devay, J. and Lange, J., 2009. Factor XIII substitution in surgical cancer patients at high risk for intraoperative bleeding. *Anesthesiology: The Journal of the American Society of Anesthesiologists,* 110 (2), 239-245.

Koseki-Kuno, S., Yamakawa, M., Dickneite, G. and Ichinose, A., 2003. Factor XIII A subunit-deficient mice developed severe uterine bleeding events and subsequent spontaneous miscarriages. *Blood,* 102 (13), 4410-4412.

Kulkarni, S., and Jackson, S.P., 2004. Platelet factor XIII and calpain negatively regulate integrin alphaIIbbeta3 adhesive function and thrombus growth. *The Journal of Biological Chemistry,* 279 (29), 30697-30706.

Kumar, S., 2015. Plasma Exosomes and Drug Metabolic Cytochrome P450 Enzymes. *J Drug Metab Toxicol,* 6 (10.4172), 2157-7609.1000.

Kumar, S., Diwan, S.K. and Dubey, S., 2014. Myocardial infarction in organophosphorus poisoning: Association or just chance? *Journal of Emergencies, Trauma, and Shock,* 7 (2), 131-132.

Larkin, D.J., and Tjeerdema, R.S., 2000. Fate and effects of diazinon. *Reviews of Environmental Contamination and Toxicology,* 166, 49-82.

Larsen, C.C., Sørensen, B., Nielsen, J.D. and Astrup, J., 2012. Reduced clot-stability during the first 6 hours after aneurysmal subarachnoid haemorrhage–a prospective case-control study. *Thrombosis Research,* 129 (5), e229-e232.

Lauer, P., Metzner, H.J., Zettlmeißl, G., Li, M., Smith, A.G., Lathe, R. and Dickneite, G., 2002. Targeted inactivation of the mouse locus encoding coagulation factor XIII-A: hemostatic abnormalities in mutant mice and characterization of the coagulation deficit. *Thrombosis and Haemostasis,* 88 (12), 967-974.

Li, B., Eyer, P., Eddleston, M., Jiang, W., Schopfer, L.M. and Lockridge, O., 2013. Protein tyrosine adduct in humans self-poisoned by chlorpyrifos. *Toxicology and Applied Pharmacology,* 269 (3), 215-225.

Li, B., Nachon, F., Froment, M., Verdier, L., Debouzy, J., Brasme, B., Gillon, E., Schopfer, L.M., Lockridge, O. and Masson, P., 2007c. Binding and hydrolysis of soman by human serum albumin. *Chemical Research in Toxicology,* 21 (2), 421-431.

Li, B., Ricordel, I., Schopfer, L.M., Baud, F., Mégarbane, B., Nachon, F., Masson, P. and Lockridge, O., 2010. Detection of adduct on tyrosine 411 of albumin in humans poisoned by dichlorvos. *Toxicological Sciences,* 116 (1), 23-31.

Li, B., Schopfer, L.M., Grigoryan, H., Thompson, C.M., Hinrichs, S.H., Masson, P. and Lockridge, O., 2008. Tyrosines of human and mouse transferrin covalently labeled by

organophosphorus agents: a new motif for binding to proteins that have no active site serine. *Toxicological Sciences,* 107 (1), 144-155.

Li, B., Schopfer, L.M., Hinrichs, S.H., Masson, P. and Lockridge, O., 2007b. Matrix-assisted laser desorption/ionization time-of-flight mass spectrometry assay for organophosphorus toxicants bound to human albumin at Tyr411. *Analytical Biochemistry,* 361 (2), 263-272.

Li, H., Schopfer, L.M., Nachon, F., Froment, M., Masson, P. and Lockridge, O., 2007a. Aging pathways for organophosphate-inhibited human butyrylcholinesterase, including novel pathways for isomalathion, resolved by mass spectrometry. *Toxicological Sciences,* 100 (1), 136-145.

Li, W., Costa, L.G., Richter, R.J., Hagen, T., Shih, D.M., Tward, A., Lusis, A.J. and Furlong, C.E., 2000. Catalytic efficiency determines the in-vivo efficacy of PON1 for detoxifying organophosphorus compounds. *Pharmacogenetics and Genomics,* 10 (9), 767-779.

Libretexts, 2020. *The Beer-Lambert Law*. Chemistry LibreTexts, viewed on 16 June 2020, <https://chem.libretexts.org/Bookshelves/Physical_and_Theoretical_Chemistry_Textbook_Maps/Supplemental_Modules_(Physical_and_Theoretical_Chemistry)/Spectroscopy/Electronic_Spectroscopy/Electronic_Spectroscopy_Basics/The_Beer-Lambert_Law > .

Licari, L.G., and Kovacic, J.P., 2009. Thrombin physiology and pathophysiology. *Journal of Veterinary Emergency and Critical Care,* 19 (1), 11-22.

Lin, C., and Ting, A.Y., 2006. Transglutaminase-catalyzed site-specific conjugation of small-molecule probes to proteins in vitro and on the surface of living cells. *Journal of the American Chemical Society,* 128 (14), 4542-4543.

Liu, H., Yi, M., Shi, X., Liang, P. and Gao, X., 2007. Substrate specificity of brain acetylcholinesterase and its sensitivity to carbamate insecticides in Carassius auratus. *Fish Physiology and Biochemistry,* 33 (1), 29-34.

Liu, J., Zhang, Y., Lin, D. and Xiao, R., 2009. Tanshinone IIA inhibits leukemia THP-1 cell growth by induction of apoptosis. *Oncology Reports,* 21 (4), 1075-1081.

Liyasova, M., Li, B., Schopfer, L.M., Nachon, F., Masson, P., Furlong, C.E. and Lockridge, O., 2011. Exposure to tri-o-cresyl phosphate detected in jet airplane passengers. *Toxicology and Applied Pharmacology*, 256 (3), 337-347.

Liyasova, M., Li, B., Schopfer, L.M., Nachon, F., Masson, P., Furlong, C.E. and Lockridge, O., 2011. Exposure to tri-o-cresyl phosphate detected in jet airplane passengers. *Toxicology and Applied Pharmacology*, 256 (3), 337-347.

Lockridge, O., 2013. Noncholinesterase protein targets of organophosphorus pesticides. *Advances in Molecular Toxicology.* Elsevier, 2013, pp. 179-205.

Lockridge, O., and Masson, P., 2000. Pesticides and susceptible populations: people with butyrylcholinesterase genetic variants may be at risk. *Neurotoxicology,* 21 (1-2), 113-126.

Lockridge, O., and Schopfer, L.M., 2010. Review of tyrosine and lysine as new motifs for organophosphate binding to proteins that have no active site serine. *Chemico-Biological Interactions,* 187 (1-3), 344-348.

Loewy, A.G., Dahlberg, A., Dunathan, K., Kriel, R. and Wolfinger, H.L., Jr, 1961. Fibrinase. II. Some physical properties. *The Journal of Biological Chemistry,* 236, 2634-2643.

López-Granero, C., Ruiz-Muñoz, A.M., Nieto-Escámez, F.A., Colomina, M.T., Aschner, M. and Sánchez-Santed, F., 2016. Chronic dietary chlorpyrifos causes long-term spatial memory impairment and thigmotaxic behavior. *Neurotoxicology,* 53, 85-92.

Lorand, L., and Graham, R.M., 2003. Transglutaminases: crosslinking enzymes with pleiotropic functions. *Nature Reviews Molecular Cell Biology,* 4 (2), 140.

Lotti, M., 2010. Clinical toxicology of anticholinesterase agents in humans. *Hayes' Handbook of Pesticide Toxicology.* Elsevier, 2010, pp. 1543-1589.

Lupu, F., Popescu, N.I. and Coggeshall, K.M., 2016. *Proteolytic Cascades.* Oxford: Academic Press.

Manini, P., Andreoli, R. and Niessen, W.M., 2004. Liquid chromatography–mass spectrometry in occupational toxicology: A novel approach to the study of biotransformation of industrial chemicals. *Journal of Chromatography A,* 1058 (1-2), 21-37.

Manna, P., and Jain, S.K., 2014. Effect of PIP3 on adhesion molecules and adhesion of THP-1 monocytes to HUVEC treated with high glucose. *Cellular Physiology and Biochemistry: International Journal of Experimental Cellular Physiology, Biochemistry, and Pharmacology,* 33 (4), 1197-1204.

Marsillach, J., Costa, L.G. and Furlong, C.E., 2013. Protein adducts as biomarkers of exposure to organophosphorus compounds. *Toxicology,* 307, 46-54.

Marsillach, J., Richter, R.J., Kim, J.H., Stevens, R.C., MacCoss, M.J., Tomazela, D., Suzuki, S.M., Schopfer, L.M., Lockridge, O. and Furlong, C.E., 2011. Biomarkers of organophosphorus (OP) exposures in humans. *Neurotoxicology,* 32 (5), 656-660.

Martin, A., De Vivo, G. and Gentile, V., 2011. Possible role of the transglutaminases in the pathogenesis of Alzheimer's disease and other neurodegenerative diseases. *International Journal of Alzheimer's Disease,* 2011, 865432.

Martins, I.M., Matos, M., Costa, R., Silva, F., Pascoal, A., Estevinho, L.M. and Choupina, A.B., 2014. Transglutaminases: recent achievements and new sources. *Applied Microbiology and Biotechnology,* 98 (16), 6957-6964.

Masson, P., and Lockridge, O., 2010. Butyrylcholinesterase for protection from organophosphorus poisons: catalytic complexities and hysteretic behavior. *Archives of Biochemistry and Biophysics,* 494 (2), 107-120.

Masson, P., Froment, M.T., Bartels, C.F. and Lockridge, O., 1997. Importance of aspartate-70 in organophosphate inhibition, oxime re-activation and aging of human butyrylcholinesterase. *The Biochemical Journal,* 325 (Pt 1) (Pt 1), 53-61.

Melching-Kollmuß, S., Dekant, W. and Kalberlah, F., 2010. Application of the "threshold of toxicological concern" to derive tolerable concentrations of "non-relevant metabolites" formed from plant protection products in ground and drinking water. *Regulatory Toxicology and Pharmacology,* 56 (2), 126-134.

Miao, Y., He, N. and Zhu, J., 2010. History and new developments of assays for cholinesterase activity and inhibition. *Chemical Reviews,* 110 (9), 5216-5234.

Michaelis, S., 2011. Contaminated aircraft cabin air. *J.Biol.Phys.Chem,* 11, 132-145.

Michałowicz, J., and Duda, W., 2007. Phenols--Sources and Toxicity. *Polish Journal of Environmental Studies,* 16 (3).

Modesto, K.A., and Martinez, C.B., 2010. Effects of Roundup Transorb on fish: hematology, antioxidant defenses and acetylcholinesterase activity. *Chemosphere,* 81 (6), 781-787.

Mora, P., Michel, X. and Narbonne, J.F., 1999. Cholinesterase activity as potential biomarker in two bivalves. *Environmental Toxicology and Pharmacology,* 7 (4), 253-260.

Moser, M., Li, Y., Vaupel, K., Kretzschmar, D., Kluge, R., Glynn, P. and Buettner, R., 2004. Placental failure and impaired vasculogenesis result in embryonic lethality for neuropathy target esterase-deficient mice. *Molecular and Cellular Biology,* 24 (4), 1667-1679.

Moser, M., Stempfl, T., Li, Y., Glynn, P., Büttner, R. and Kretzschmar, D., 2000. Cloning and expression of the murine sws/NTE gene. *Mechanisms of Development,* 90 (2), 279-282.

Mostafalou, S., and Abdollahi, M., 2013. Pesticides and human chronic diseases: evidences, mechanisms, and perspectives. *Toxicology and Applied Pharmacology,* 268 (2), 157-177.

Mouapi, K.N., Bell, J.D., Smith, K.A., Ariens, R.A., Philippou, H. and Maurer, M.C., 2016. Ranking reactive glutamines in the fibrinogen alphaC region that are targeted by blood coagulant factor XIII. *Blood,* 127 (18), 2241-2248.

Muñoz, D., Bonner, P. and Hargreaves, A., 2010. Effects of chlorpyrifos on transglutaminase activity in differentiating rat C6 glioma cells. *Toxicology in Vitro,* 24 (8), 2104-2107.

Muñoz-Quezada, M.T., Iglesias, V., Lucero, B., Steenland, K., Barr, D.B., Levy, K., Ryan, P.B., Alvarado, S. and Concha, C., 2012. Predictors of exposure to organophosphate pesticides in schoolchildren in the Province of Talca, Chile. *Environment International,* 47, 28-36.

Muszbek, L., Ádány, R., Kávai, M., Boda, Z. and Lopaciuk, S., 1988. Monocytes of patients congenitally deficient in plasma factor XIII lack factor XIII subunit A antigen and transglutaminase activity. *Thrombosis and Haemostasis,* 60 (02), 231-235.

Muszbek, L., Adany, R., Szegedi, G., Polgar, J. and Kavai, M., 1985. Factor XIII of blood coagulation in human monocytes. *Thrombosis Research,* 37 (3), 401-410.

Muszbek, L., Ariens, R.A. and Ichinose, A., 2007. Factor XIII: recomeded terms and abbreviations. *J Thromb Haemost,* 5, 181-183.

Muszbek, L., Bagoly, Z., Bereczky, Z. and Katona, E., 2008. The involvement of blood coagulation factor XIII in fibrinolysis and thrombosis. *Cardiovascular & Hematological Agents in Medicinal Chemistry (Formerly Current Medicinal Chemistry-Cardiovascular & Hematological Agents),* 6 (3), 190-205.

Muszbek, L., Bagoly, Z., Cairo, A. and Peyvandi, F., 2011. Novel aspects of factor XIII deficiency. *Current Opinion in Hematology,* 18 (5), 366-372.

Muszbek, L., Bereczky, Z., Bagoly, Z., Komáromi, I. and Katona, É., 2011. Factor XIII: a coagulation factor with multiple plasmatic and cellular functions. *Physiological Reviews,* 91 (3), 931-972.

Muszbek, L., Yee, V.C. and Hevessy, Z., 1999. Blood coagulation factor XIII: structure and function. *Thrombosis Research,* 94 (5), 271-305.

Mutch, E., Blain, P.G. and Williams, F.M., 1999. The role of metabolism in determining susceptibility to parathion toxicity in man. *Toxicology Letters,* 107 (1-3), 177-187.

Mutch, N., Robbie, L. and Booth, N., 2001. Human thrombi contain an abundance of active thrombin. *Thrombosis and Haemostasis,* 86 (10), 1028-1034.

Naderi, J., 2015. *Cellular Effects of Insulin in Human THP-1 Monocytes.* Biotechnology (MSc)., Norwegian University of Science and Technology-NTNU.

Naderi, M., Eshghi, P., Cohan, N., Miri-Moghaddam, E., Yaghmaee, M. and Karimi, M., 2012. Successful delivery in patients with FXIII deficiency receiving prophylaxis: report of 17 cases in Iran. *Haemophilia,* 18 (5), 773-776.

Naik, R.S., Liu, W. and Saxena, A., 2013. Development and validation of a simple assay for the determination of cholinesterase activity in whole blood of laboratory animals. *Journal of Applied Toxicology,* 33 (4), 290-300.

Namba, T., 1971. Cholinesterase inhibition by organophosphorus compounds and its clinical effects. *Bulletin of the World Health Organization,* 44 (1-3), 289-307.

National Toxicology Program, 1979. Bioassay of parathion forpossible carcinogencity. *Natl Cancer Inst Carcinog Tech Rep Ser,* 70, 1-123.

Nelea, V., Nakano, Y. and Kaartinen, M.T., 2008. Size distribution and molecular associations of plasma fibronectin and fibronectin crosslinked by transglutaminase 2. *The Protein Journal,* 27 (4), 223-233.

Nigg, H.N., and Knaak, J.B., 2000. Blood cholinesterases as human biomarkers of organophosphorus pesticide exposure. *Reviews of environmental contamination and toxicology.* Springer, 2000, pp. 29-111.

Nurminskaya, M., and Kaartinen, M.T., 2006. Transglutaminases in mineralized tissues. *Front Biosci,* 11 (2), 1591-1606.

Nurminskaya, M.V., and Belkin, A.M., 2012. Cellular functions of tissue transglutaminase. *International review of cell and molecular biology.* Elsevier, 2012, pp. 1-97.

Odii, B.O., and Coussons, P., 2014. Biological functionalities of transglutaminase 2 and the possibility of its compensation by other members of the transglutaminase family. *Thescientificworldjournal,* 2014, 714561.

Okechukwu, E.O., Auta, J. and Balogun, J., 2007. Effects of acute nominal doses of chlorpyrifos-ethyl on some haematological indices of African catfish Clarias gariepinus-Teugels. *J.Fish.Int,* 2, 190-194.

Page, B., PAGE, M. and NOEL, C., 1993. A new fluorometric assay for cytotoxicity measurements in-vitro. *International Journal of Oncology,* 3 (3), 473-476.

Pallister, C., and Watson, M., 1999. *Haematology.* Butterworth-Heinemann.

Patocka, J., Kuca, K. and Jun, D., 2004. Acetylcholinesterase and butyrylcholinesterase--important enzymes of human body. *Acta Medica (Hradec Kralove),* 47 (4), 215-228.

Peeples, E.S., Schopfer, L.M., Duysen, E.G., Spaulding, R., Voelker, T., Thompson, C.M. and Lockridge, O., 2004. Albumin, a new biomarker of organophosphorus toxicant exposure, identified by mass spectrometry. *Toxicological Sciences,* 83 (2), 303-312.

Peerschke, E.I., Zucker, M.B., Grant, R.A., Egan, J.J. and Johnson, M.M., 1980. Correlation between fibrinogen binding to human platelets and platelet aggregability. *Blood,* 55 (5), 841-847.

Peris-Sampedro, F., Basaure, P., Reverte, I., Cabré, M., Domingo, J.L. and Colomina, M.T., 2015. Chronic exposure to chlorpyrifos triggered body weight increase and memory impairment depending on human apoE polymorphisms in a targeted replacement mouse model. *Physiology & Behavior,* 144, 37-45.

Perrier, J., Durand, A., Giardina, T. and Puigserver, A., 2005. Catabolism of intracellular N-terminal acetylated proteins: involvement of acylpeptide hydrolase and acylase. *Biochimie,* 87 (8), 673-685.

Petroianu, G., Toomes, M., Maleck, W., Bergler, W. and Rüfer, R., 1997. In vitro paraoxon (E 600) exposure: no activating effect on human blood coagulation. *Toxicology,* 119 (2), 167-173.

Petroianu, G., Toomes, M., Maleck, W., Bergler, W. and Rüfer, R., 1999. Intravenous paraoxon (POX) exposure: coagulation studies in mini pigs. *Chemico-Biological Interactions,* 119, 489-495.

Poet, T.S., Wu, H., Kousba, A.A. and Timchalk, C., 2003. In vitro rat hepatic and intestinal metabolism of the organophosphate pesticides chlorpyrifos and diazinon. *Toxicological Sciences,* 72 (2), 193-200.

Pohanka, M., 2011. Cholinesterases, a target of pharmacology and toxicology. *Biomedical Papers of the Medical Faculty of Palacky University in Olomouc,* 155 (3).

Polgar, J., Hidasi, V. and Muszbek, L., 1990. Non-proteolytic activation of cellular protransglutaminase (placenta macrophage factor XIII). *The Biochemical Journal,* 267 (2), 557-560.

Pomeroy-Black, M., and Ehrich, M., 2012. Organophosphorus compound effects on neurotrophin receptors and intracellular signaling. *Toxicology in Vitro,* 26 (5), 759-765.

Pope, C.N., 1999. Organophosphorus pesticides: do they all have the same mechanism of toxicity? *Journal of Toxicology and Environmental Health Part B: Critical Reviews,* 2 (2), 161-181.

Qin, Y.Z., Zhong, X.H., Chen, G.X., Zhao, D.W., Yang, D.M. and Xiong, X.Y., 2011. Effects of organic solvents on proliferation of Hela cells line. *Zhong Yao Cai = Zhongyaocai = Journal of Chinese Medicinal Materials,* 34 (4), 563-566.

Qin, Z., 2012. The use of THP-1 cells as a model for mimicking the function and regulation of monocytes and macrophages in the vasculature. *Atherosclerosis,* 221 (1), 2-11.

Quatresooz, P., Paquet, P., Hermanns-Lê, T. and Piérard, G.E., 2008. Molecular mapping of factor XIIIa-enriched dendrocytes in the skin. *International Journal of Molecular Medicine,* 22 (4), 403-409.

Quistad, G.B., and Casida, J.E., 2000. Sensitivity of blood-clotting factors and digestive enzymes to inhibition by organophosphorus pesticides. *Journal of Biochemical and Molecular Toxicology,* 14 (1), 51-56.

Quistad, G.B., Klintenberg, R. and Casida, J.E., 2005. Blood acylpeptide hydrolase activity is a sensitive marker for exposure to some organophosphate toxicants. *Toxicological Sciences,* 86 (2), 291-299.

Rahman, M., and Siddiqui, M., 2006. Hematological and clinical chemistry changes induced by subchronic dosing of a novel phosphorothionate (RPR-V) in Wistar male and female rats. *Drug and Chemical Toxicology,* 29 (1), 95-110.

Rampersad, S.N., 2012. Multiple applications of Alamar Blue as an indicator of metabolic function and cellular health in cell viability bioassays. *Sensors,* 12 (9), 12347-12360.

Rathod, A.L., and Garg, R.K., 2017. Chlorpyrifos poisoning and its implications in human fatal cases: A forensic perspective with reference to Indian scenario. *Journal of Forensic and Legal Medicine,* 47, 29-34.

Ray, D.E., and Richards, P., 2001. The potential for toxic effects of chronic, low-dose exposure to organophosphates. *Toxicology Letters,* 120 (1-3), 343-351.

Reiner, E., 2001. Organophosphorus compounds and esterases: current research topics concerning the toxicity of and protection against organophosphates. *Arhiv Za Higijenu Rada i Toksikologiju,* 52 (3), 323-331.

Reinhart, W.H., 2003. Fibrinogen-marker or mediator of vascular disease? *Vascular Medicine,* 8 (3), 211-216.

Richards, P.G., Johnson, M.K. and Ray, D.E., 2000. Identification of acylpeptide hydrolase as a sensitive site for reaction with organophosphorus compounds and a potential target for cognitive enhancing drugs. *Molecular Pharmacology,* 58 (3), 577-583.

Richardson, V.R., Cordell, P., Standeven, K.F. and Carter, A.M., 2013. Substrates of Factor XIII-A: roles in thrombosis and wound healing. *Clinical Science (London, England: 1979),* 124 (3), 123-137.

Richter, R.J., Jarvik, G.P. and Furlong, C.E., 2009. Paraoxonase 1 (PON1) status and substrate hydrolysis. *Toxicology and Applied Pharmacology,* 235 (1), 1-9.

Robb, E.L., and Baker, M.B., 2019. Organophosphate Toxicity. *In:* Organophosphate Toxicity. *StatPearls.* Treasure Island (FL): StatPearls Publishing LLC, 2019.

Rozengart, E., and Basova, N., 2009. Substrate specificity of the cholinesterase of the pacific squid Todarodes pacificus. *In: Doklady Biochemistry and Biophysics*, Springer, pp. 134-138.

Sadler, J.E., 1998. *Biochemistry and Genetics of Von Willebrand Factor*.

Salyha, Y., 2010. Biological effects assessment of chlorpyrifos and some aspects of its neurotoxicity. *Visnyk of Lviv University.Biology Series*, 54, 3-14.

Sárváry, A., Szűcs, S., Balogh, I., Becsky, Á., Bárdos, H., Kávai, M., Seligsohn, U., Egbring, R., Lopaciuk, S. and Muszbek, L., 2004. Possible role of factor XIII subunit A in Fcγ and complement receptor-mediated phagocytosis. *Cellular Immunology,* 228 (2), 81-90.

Saxena, A., Redman, A.M., Jiang, X., Lockridge, O. and Doctor, B., 1999. Differences in active-site gorge dimensions of cholinesterases revealed by binding of inhibitors to human butyrylcholinesterase. *Chemico-Biological Interactions,* 119, 61-69.

Schmitt, F., Lagopoulos, L., Käuper, P., Rossi, N., Busso, N., Barge, J., Wagnières, G., Laue, C., Wandrey, C. and Juillerat-Jeanneret, L., 2010. Chitosan-based nanogels for selective delivery of photosensitizers to macrophages and improved retention in and therapy of articular joints. *Journal of Controlled Release,* 144 (2), 242-250.

Schopfer, L.M., Champion, M.M., Tamblyn, N., Thompson, C.M. and Lockridge, O., 2005. Characteristic mass spectral fragments of the organophosphorus agent FP-biotin and FP-biotinylated peptides from trypsin and bovine albumin (Tyr410). *Analytical Biochemistry,* 345 (1), 122-132.

Schopfer, L.M., Grigoryan, H., Li, B., Nachon, F., Masson, P. and Lockridge, O., 2010. Mass spectral characterization of organophosphate-labeled, tyrosine-containing peptides: characteristic mass fragments and a new binding motif for organophosphates. *Journal of Chromatography B,* 878 (17-18), 1297-1311.

Schröder, V., and Kohler, H., 2013. New developments in the area of factor XIII. *Journal of Thrombosis and Haemostasis,* 11 (2), 234-244.

Shah, M.D., and Iqbal, M., 2010. Diazinon-induced oxidative stress and renal dysfunction in rats. *Food and Chemical Toxicology,* 48 (12), 3345-3353.

Shi, D.Y., and Wang, S.J., 2017. Advances of Coagulation Factor XIII. *Chinese Medical Journal,* 130 (2), 219-223.

Sidiropoulou, E., Sachana, M., Flaskos, J., Harris, W., Hargreaves, A.J. and Woldehiwet, Z., 2009. Diazinon oxon affects the differentiation of mouse N2a neuroblastoma cells. *Archives of Toxicology,* 83 (4), 373-380.

Sigolaeva, L.V., Makower, A., Eremenko, A.V., Makhaeva, G.F., Malygin, V.V., Kurochkin, I.N. and Scheller, F.W., 2001. Bioelectrochemical analysis of neuropathy target esterase activity in blood. *Analytical Biochemistry,* 290 (1), 1-9.

Simon, Á., Bagoly, Z., Hevessy, Z., Csáthy, L., Katona, É., Vereb, G., Ujfalusi, A., Szerafin, L., Muszbek, L. and Kappelmayer, J., 2012. Expression of coagulation factor XIII subunit A in acute promyelocytic leukemia. *Cytometry Part B: Clinical Cytometry,* 82 (4), 209-216.

Sindrilaru, A., and Scharffetter-Kochanek, K., 2013. Disclosure of the culprits: Macrophages—Versatile regulators of wound healing. *Advances in Wound Care,* 2 (7), 357-368.

Singh, U.S., Pan, J., Kao, Y.L., Joshi, S., Young, K.L. and Baker, K.M., 2003. Tissue transglutaminase mediates activation of RhoA and MAP kinase pathways during retinoic acid-induced neuronal differentiation of SH-SY5Y cells. *The Journal of Biological Chemistry,* 278 (1), 391-399.

Škrinjarić-Špoljar, M., Simeon, V. and Reiner, E., 1973. Spontaneous reactivation and aging of dimethylphosphorylated acetylcholinesterase and cholinesterase. *Biochimica Et Biophysica Acta (BBA)-Enzymology,* 315 (2), 363-369.

Solbu, K., Thorud, S., Hersson, M., Øvrebø, S., Ellingsen, D., Lundanes, E. and Molander, P., 2007. Determination of airborne trialkyl and triaryl organophosphates originating from hydraulic fluids by gas chromatography–mass spectrometry: Development of methodology for combined aerosol and vapor sampling. *Journal of Chromatography A,* 1161 (1-2), 275-283.

Somanath, P.R., Ciocea, A. and Byzova, T.V., 2009. Integrin and growth factor receptor alliance in angiogenesis. *Cell Biochemistry and Biophysics,* 53 (2), 53-64.

Souri, M., Koseki-Kuno, S., Takeda, N., Degen, J.L. and Ichinose, A., 2008. Administration of factor XIII B subunit increased plasma factor XIII A subunit levels in factor XIII B subunit knock-out mice. *International Journal of Hematology,* 87 (1), 60-68.

Souri, M., Osaki, T. and Ichinose, A., 2015. The Non-catalytic B Subunit of Coagulation Factor XIII Accelerates Fibrin Cross-linking. *The Journal of Biological Chemistry,* 290 (19), 12027-12039.

Sporn, S.A., Eierman, D.F., Johnson, C.E., Morris, J., Martin, G., Ladner, M. and Haskill, S., 1990. Monocyte adherence results in selective induction of novel genes sharing homology with mediators of inflammation and tissue repair. *Journal of Immunology (Baltimore, Md.: 1950),* 144 (11), 4434-4441.

Spurlin, T.A., Bhadriraju, K., Chung, K., Tona, A. and Plant, A.L., 2009. The treatment of collagen fibrils by tissue transglutaminase to promote vascular smooth muscle cell contractile signaling. *Biomaterials,* 30 (29), 5486-5496.

Stephens, R., Spurgeon, A., Calvert, I.A., Beach, J., Levy, L.S., Harrington, J. and Berry, H., 1995. Neuropsychological effects of long-term exposure to organophosphates in sheep dip. *The Lancet,* 345 (8958), 1135-1139.

Stief, T., 2006. Thrombin generation by exposure of blood to endotoxin: a simple model to study disseminated intravascular coagulation. *Clinical and Applied thrombosis/hemostasis,* 12 (2), 137-161.

Straus, D.L., and Chambers, J.E., 1995. Inhibition of acetylcholinesterase and aliesterases of fingerling channel catfish by chlorpyrifos, parathion, and S, S, S-tributyl phosphorotrithioate (DEF). *Aquatic Toxicology,* 33 (3-4), 311-324.

Sun, F., Ding, J., Yu, H., Gao, R., Wang, H. and Pei, C., 2016. Identification of new binding sites of human transferrin incubated with organophosphorus agents via Q Exactive LC–MS/MS. *Journal of Chromatography B,* 1022, 256-264.

Sun, Y., et al., 2016. Wogonoside prevents colitis-associated colorectal carcinogenesis and colon cancer progression in inflammation-related microenvironment via inhibiting NF-kappaB activation through PI3K/Akt pathway. *Oncotarget,* 7 (23), 34300-34315.

Svoboda, M., Luskova, V., Drastichova, J. and Žlabek, V., 2001. The effect of diazinon on haematological indices of common carp (Cyprinus carpio L.). *Acta Veterinaria Brno,* 70 (4), 457-465.

Tacal, O., and Lockridge, O., 2010. Methamidophos, dichlorvos, O-methoate and diazinon pesticides used in Turkey make a covalent bond with butyrylcholinesterase detected by mass spectrometry. *Journal of Applied Toxicology,* 30 (5), 469-475.

Takahashi, H., Isobe, T., Horibe, S., Takagi, J., Yokosaki, Y., Sheppard, D. and Saito, Y., 2000. Tissue transglutaminase, coagulation factor XIII, and the pro-polypeptide of von

Willebrand factor are all ligands for the integrins alpha 9beta 1 and alpha 4beta 1. *The Journal of Biological Chemistry,* 275 (31), 23589-23595.

Tarhoni, M.H., Lister, T., Ray, D.E. and Carter, W.G., 2008. Albumin binding as a potential biomarker of exposure to moderately low levels of organophosphorus pesticides. *Biomarkers,* 13 (4), 343-363.

Ternström, L., Radulovic, V., Karlsson, M., Baghaei, F., Hyllner, M., Bylock, A., Hansson, K.M. and Jeppsson, A., 2010. Plasma activity of individual coagulation factors, hemodilution and blood loss after cardiac surgery: a prospective observational study. *Thrombosis Research,* 126 (2), e128-e133.

Terry Jr, A., Beck, W., Warner, S., Vandenhuerk, L. and Callahan, P.M., 2012. Chronic impairments in spatial learning and memory in rats previously exposed to chlorpyrfos or diisopropylfluorophosphate. *Neurotoxicology and Teratology,* 34 (1), 1-8.

Tham, L.G., Shukor, M.Y., Syed, M.A., Shamaan, N.A. and Othman, A.R., 2017. Partial purification of cholinesterase from Pangasius pangasius using affinity chromatography. *Journal of Environmental Microbiology and Toxicology,* 5 (2), 14-18.

Thompson, C.M., Prins, J.M. and George, K.M., 2010. Mass spectrometric analyses of organophosphate insecticide oxon protein adducts. *Environmental Health Perspectives,* 118 (1), 11-19.

Thompson, H.M., 1999. Esterases as markers of exposure to organophosphates and carbamates. *Ecotoxicology,* 8 (5), 369-384.

Tosetto, A., Castaman, G. and Rodeghiero, F., 1993. Acquired plasma factor XIII deficiencies. *Haematologica,* 78 (6 Suppl 2), 5-10.

Tracy, L.E., Minasian, R.A. and Caterson, E., 2016. Extracellular matrix and dermal fibroblast function in the healing wound. *Advances in Wound Care,* 5 (3), 119-136.

Tsuchiya, S., Yamabe, M., Yamaguchi, Y., Kobayashi, Y., Konno, T. and Tada, K., 1980. Establishment and characterization of a human acute monocytic leukemia cell line (THP-1). *International Journal of Cancer,* 26 (2), 171-176.

Ueki, S., Takagi, J. and Saito, Y., 1996. Dual functions of transglutaminase in novel cell adhesion. *Journal of Cell Science,* 109 (Pt 11) (Pt 11), 2727-2735.

Üner, N., Oruç, E.Ö., Sevgiler, Y., Şahin, N., Durmaz, H. and Usta, D., 2006. Effects of diazinon on acetylcholinesterase activity and lipid peroxidation in the brain of Oreochromis niloticus. *Environmental Toxicology and Pharmacology,* 21 (3), 241-245.

Ural, M.Ş., 2013. Chlorpyrifos-induced changes in oxidant/antioxidant status and haematological parameters of Cyprinus carpio carpio: ameliorative effect of lycopene. *Chemosphere,* 90 (7), 2059-2064.

van Tienhoven, M., Atkins, J., Li, Y. and Glynn, P., 2002. Human neuropathy target esterase catalyzes hydrolysis of membrane lipids. *The Journal of Biological Chemistry,* 277 (23), 20942-20948.

Versteeg, H.H., Heemskerk, J.W., Levi, M. and Reitsma, P.H., 2013. New fundamentals in hemostasis. *Physiological Reviews,* 93 (1), 327-358.

Walther, D.J., Peter, J., Winter, S., Höltje, M., Paulmann, N., Grohmann, M., Vowinckel, J., Alamo-Bethencourt, V., Wilhelm, C.S. and Ahnert-Hilger, G., 2003. Serotonylation of small GTPases is a signal transduction pathway that triggers platelet α-granule release. *Cell,* 115 (7), 851-862.

Walther, D.J., Stahlberg, S. and Vowinckel, J., 2011. Novel roles for biogenic monoamines: from monoamines in transglutaminase-mediated post-translational protein modification to monoaminylation deregulation diseases. *The FEBS Journal,* 278 (24), 4740-4755.

Wang, F., 2006. Culture of animal cells: a manual of basic technique. *In Vitro Cellular & Developmental Biology-Animal,* 42 (5), 169-169.

Weigel, P.H., Fuller, G.M. and LeBoeuf, R.D., 1986. A model for the role of hyaluronic acid and fibrin in the early events during the inflammatory response and wound healing. *Journal of Theoretical Biology,* 119 (2), 219-234.

Wetherell, J.R., and French, M.C., 1986. The hydrolysis of succinyldithiocholine and related thiocholine esters by human plasma and purified cholinesterase. *Biochemical Pharmacology,* 35 (6), 939-945.

Winder, C., and Balouet, J., 2000. Aerotoxic syndrome: adverse health effects following exposure to jet oil mist during commercial flights. *In: Proc. Intl Congress on Occupational Health,* pp. 196-199.

Wogram, J., Sturm, A., Segner, H. and Liess, M., 2001. Effects of parathion on acetylcholinesterase, butyrylcholinesterase, and carboxylesterase in three-spined stickleback (Gasterosteus aculeatus) following short-term exposure. *Environmental Toxicology and Chemistry,* 20 (7), 1528-1531.

Wu, J., Luan, T., Lan, C., Lo, T.W.H. and Chan, G.Y.S., 2007. Removal of residual pesticides on vegetable using ozonated water. *Food Control,* 18 (5), 466-472.

Yan, C., Jiao, L., Zhao, J., Yang, H. and Peng, S., 2012. Repeated exposures to chlorpyrifos lead to spatial memory retrieval impairment and motor activity alteration. *Neurotoxicology and Teratology,* 34 (4), 442-449.

Zamfir, L., Rotariu, L. and Bala, C., 2011. A novel, sensitive, reusable and low potential acetylcholinesterase biosensor for chlorpyrifos based on 1-butyl-3-methylimidazolium tetrafluoroborate/multiwalled carbon nanotubes gel. *Biosensors and Bioelectronics,* 26 (8), 3692-3695.

Zemskov, E.A., Janiak, A., Hang, J., Waghray, A. and Belkin, A.M., 2006. The role of tissue transglutaminase in cell-matrix interactions. *Frontiers in Bioscience: A Journal and Virtual Library,* 11, 1057-1076.

Appendix

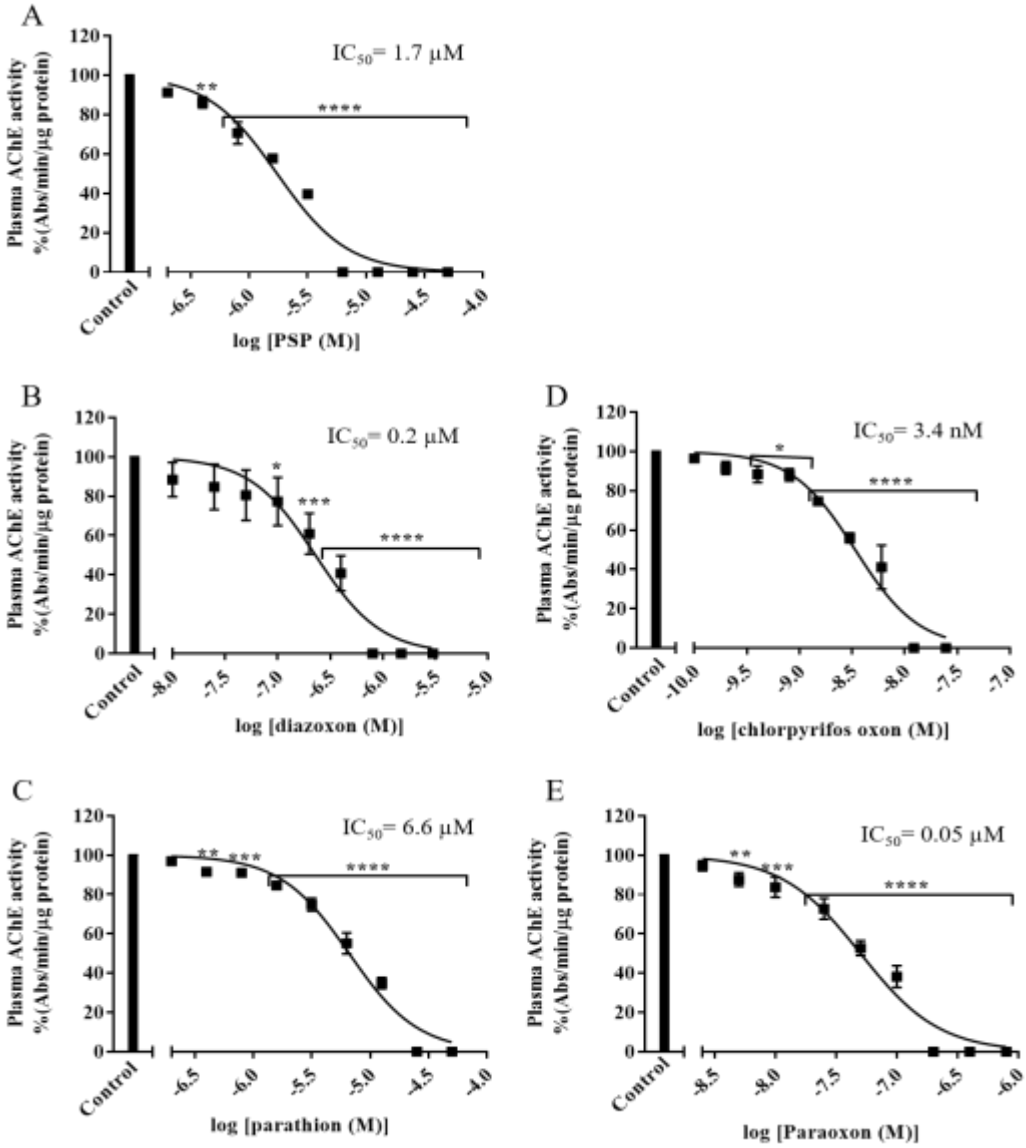

Figure 8- 1: OPs IC_{50} for plasma acetylcholinesterase activity.

Diluted human plasma samples (~1.5 mg/ml) were incubated 30 min on ice with a range of OPs concentrations as indicated in graphs prior to being subjected to the Ellman assay as described in materials and methods. A) PSP, B) diazoxon, C) parathion, D) chlorpyrifos oxon, E) paraoxon. Data points represent the mean ± SEM of butyrylcholinesterase specific activity from three independent experiments. *p<0.05, **p<0.01, ***p<0.001, ****p<0.0001 versus non OP-treated control (=100%).

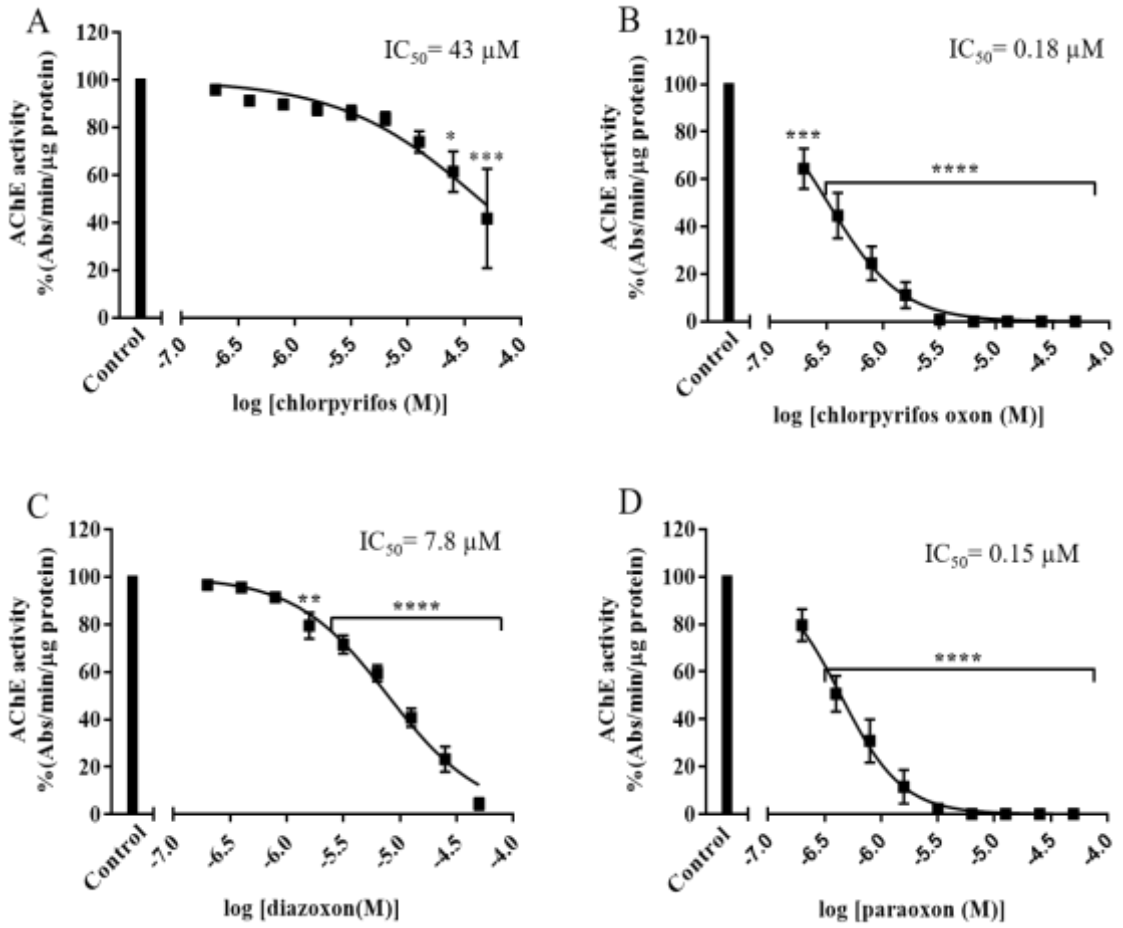

Figure 8- 2: OP IC_{50} for pure acetylcholinesterase activity.

Pure electric eel acetylcholinesterase (0.4 µg/ml) samples were incubated 30 min on ice with a range of OPs as indicated prior to being subjected to the Ellman assay as described in materials and methods. A) chlorpyrifos, B) chlorpyrifos oxon, C) diazoxon, D) paraoxon. Data points represent the mean ± SEM of acetylcholinesterase specific activity from three independent experiments. *p<0.05, **p<0.01, ***p<0.001, ****p<0.0001 versus non OP-treated control (=100%).

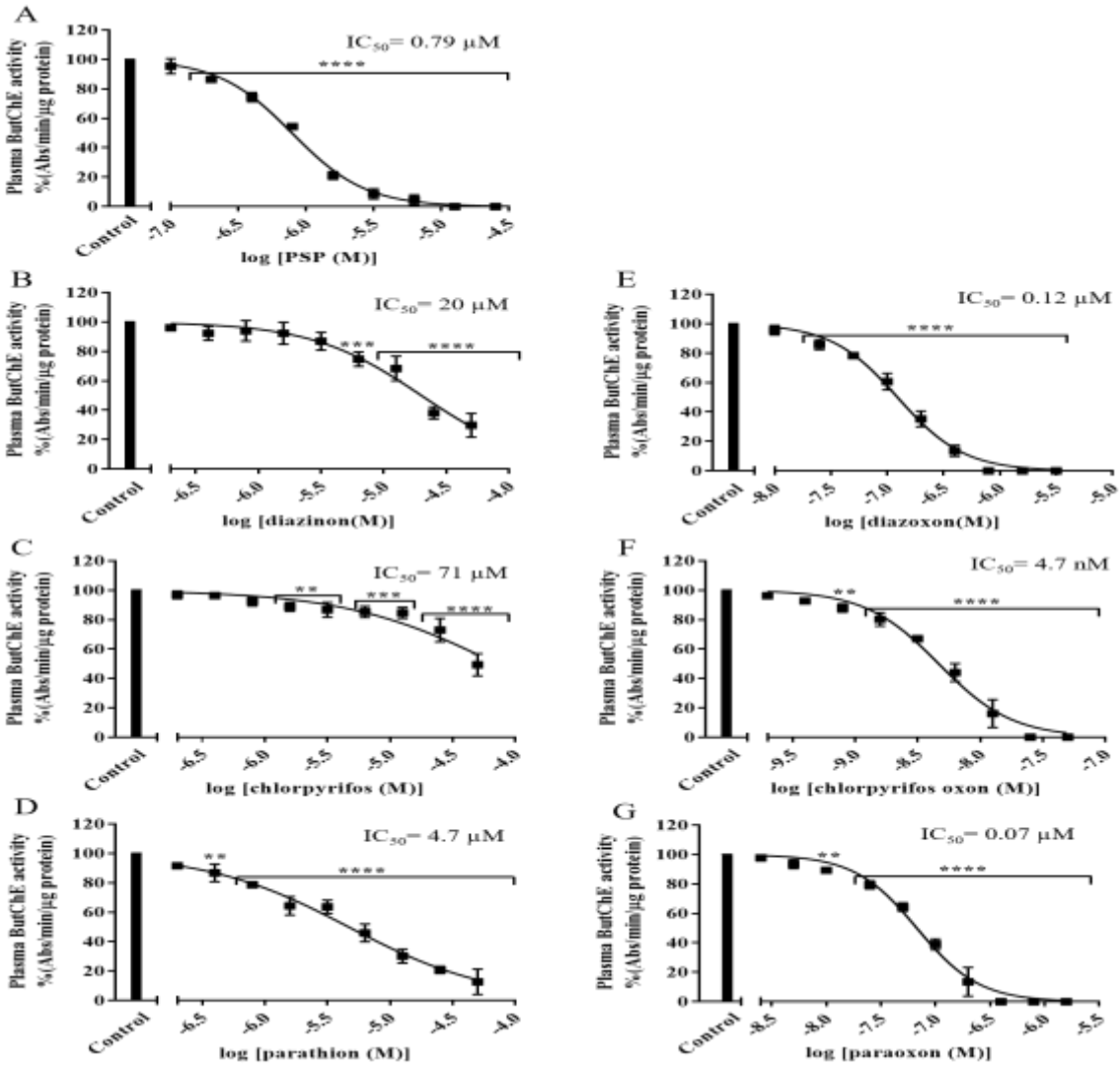

Figure 8- 3: OPs IC_{50} for plasma butyrylcholinesterase activity.

Diluted human plasma samples (~1.5 mg/ml) were incubated 30 min on ice with a range of OPs concentrations as indicated in graphs prior to being subjected to the Ellman assay as described in materials and methods. A) PSP, B) diazinon, C) chlorpyrifos, D) parathion. E) diazoxon, F) chlorpyrifos oxon and G) parathion. Data points represent the mean ± SEM of utyrylcholinesterase specific activity from three independent experiments. *p<0.05, **p<0.01, ***p<0.001, ****p<0.0001 versus non OP-treated control (=100%).

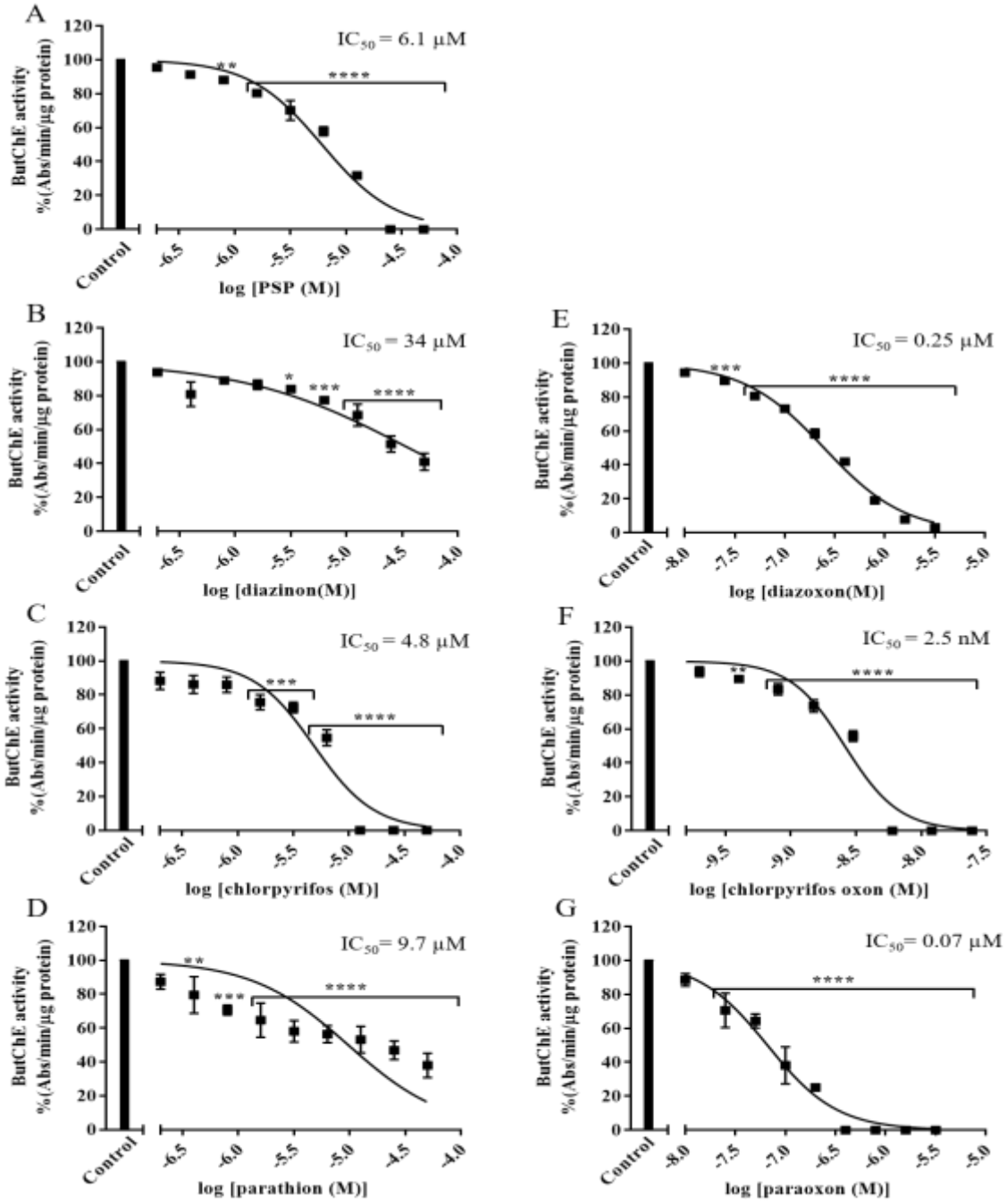

Figure 8- 4: OPs IC_{50} for pure butyrylcholinesterase activity.

Pure equine butyrylcholinesterase (0.4 µg/ml) samples were incubated 30 min on ice with a range of OPs as indicated prior to being subjected to the Ellman assay as described in materials and methods. A) PSP, B) diazinon, C) chlorpyrifos, D) parathion, E) diazoxon, F) chlorpyrifos oxon, G) paraoxon. Data points represent the mean ± SEM of butyrylcholinesterase specific activity from three independent experiments. *p<0.05, **p<0.01, ***p<0.001, ****p<0.0001 versus non OP-treated control (=100%).

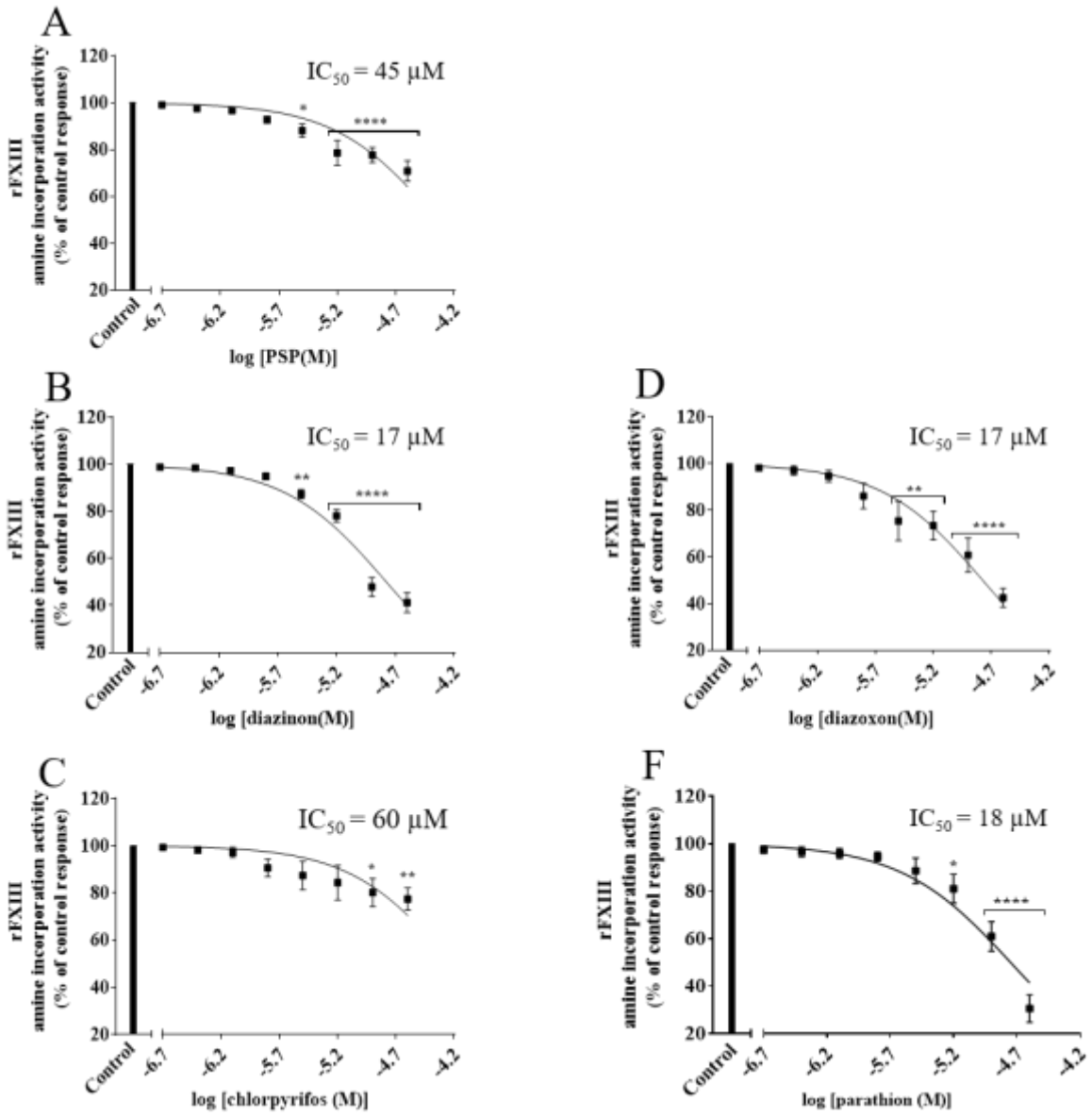

Figure 8- 5: OPs IC_{50} of pure rFXIII-mediated amine incorporation activity.

Human rFXIII (~0.02 ng/µl) was pre-incubated for 30 min on ice with the indicated concentrations of each OP in the biotin-cadaverine incorporation assay, as described in Materials and Methods. Plots shown are for: A) PSP, B) diazinon, C) chlorpyrifos, D) diazoxon, F) parathion. Data points represent the mean ± SEM of normalized pure rFXIII activity from three independent experiments. *p<0.05, **p<0.01, ***p<0.001, ****p< 0.0001 versus non OP-treated control (=100%).

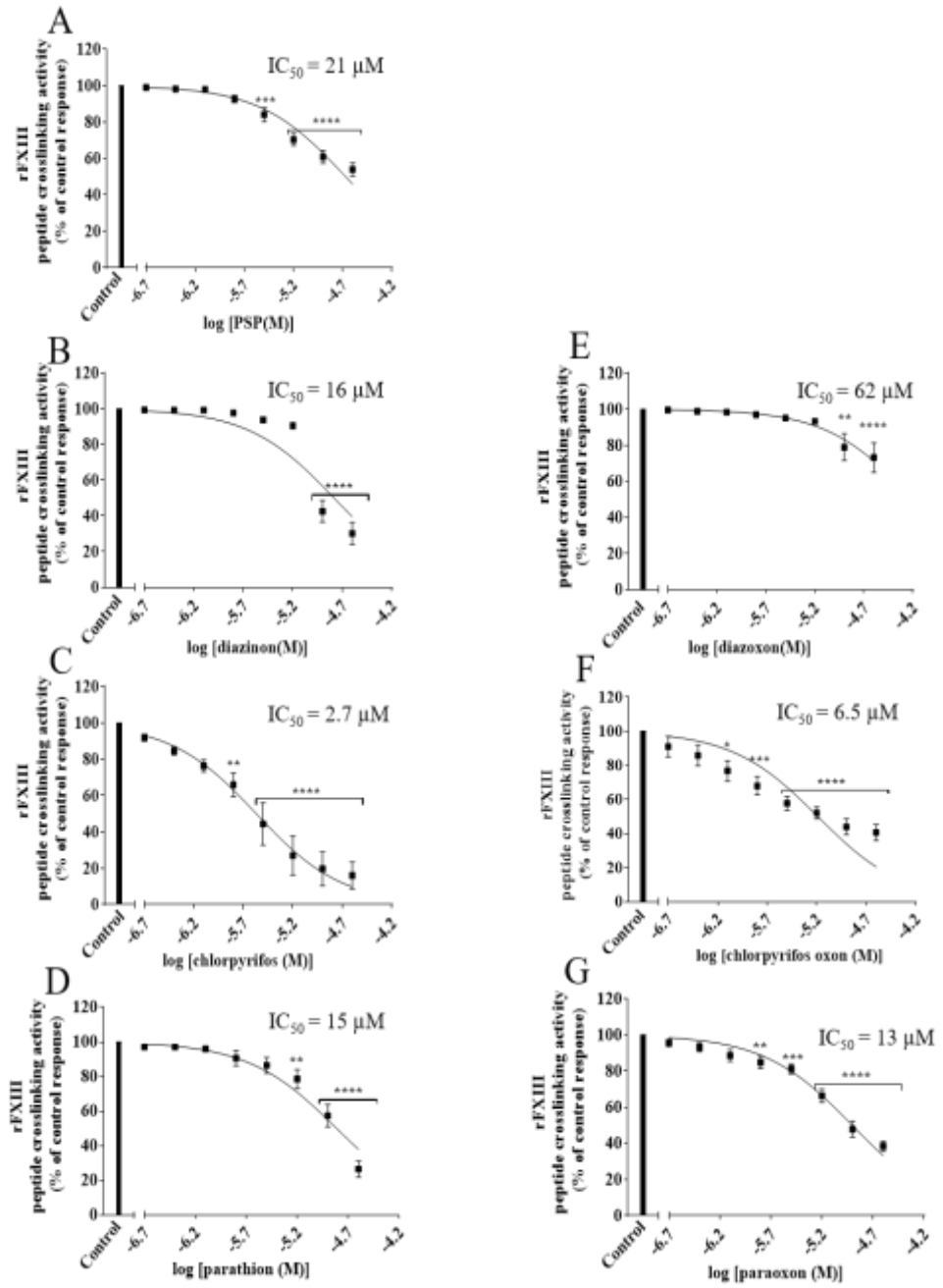

Figure 8- 6: OPs IC_{50} of pure rFXIII-mediated peptide crosslinking activity.

Human rFXIII (~0.005 ng/µl) was pre-incubated for 30 min on ice with the indicated concentrations of each OP in the biotin-labelled peptide F11KA crosslinking assay, as described in Materials and Methods. Plots shown are for: A) PSP, B) diazinon, C) chlorpyrifos, D) parathion, E) diazoxon, F) chlorpyrifos oxon and G) paraoxon. Data points represent the mean ± SEM of normalized pure rFXIII activity from three independent experiments. *p<0.05, **p<0.01, ***p<0.001, ****p<0.0001 versus non OP-treated control (=100%).

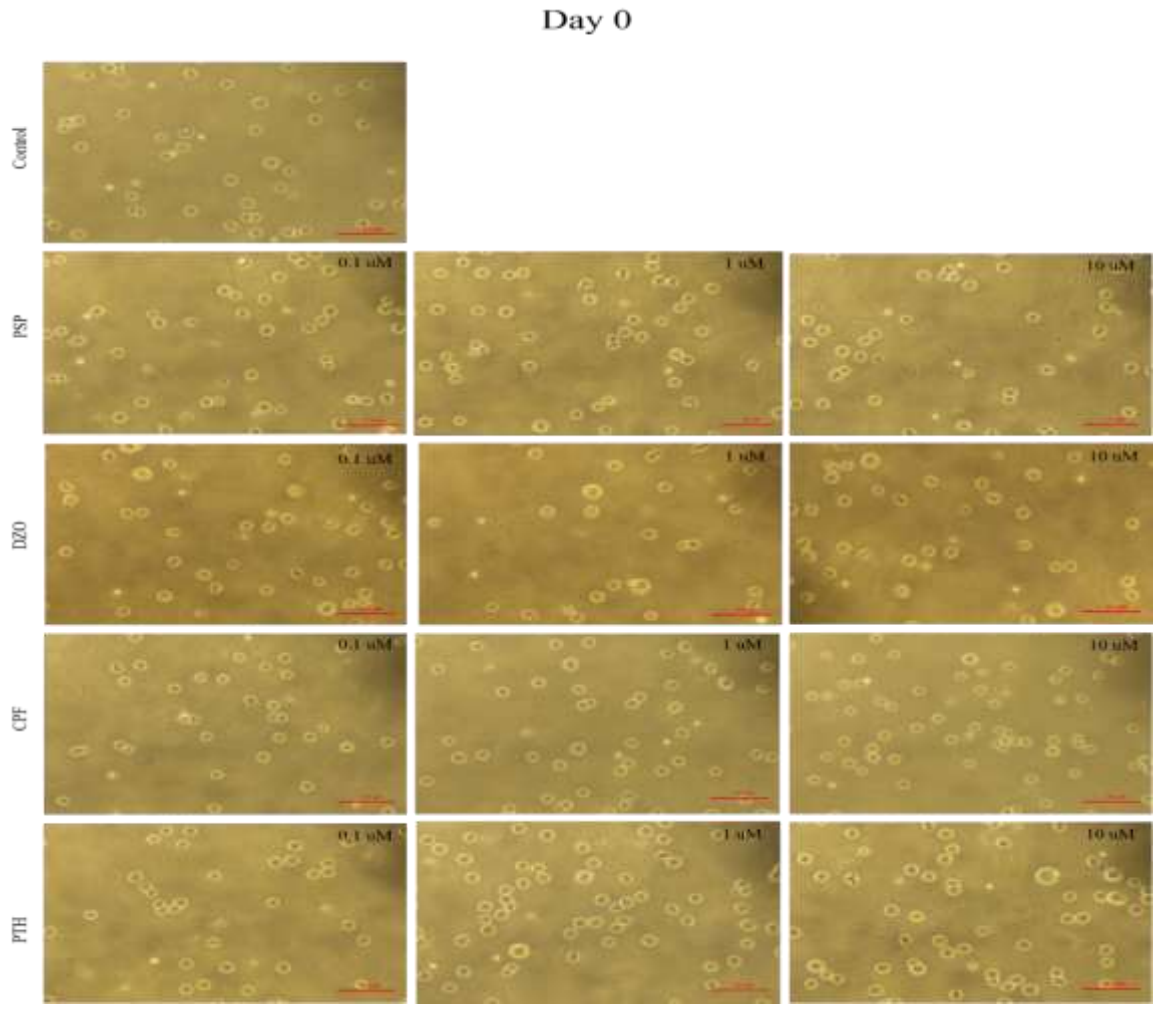

Figure 8- 7: Images of treated THP-1 cells with OPs day 0.

THP-1 cells were plated in equal density of 200,000 cells/ml per 75 flasks cultured in growth medium. The cells were treated with PSP, DZO, CPF, and PTH with three final concentration of each 0.1, 1, and 10 µM. Control sample was treated with 0.01 % (v/v) DMSO. Cells were monitored under the inverted light microscope at (10x) magnification. Scale bar 0.1 µm.

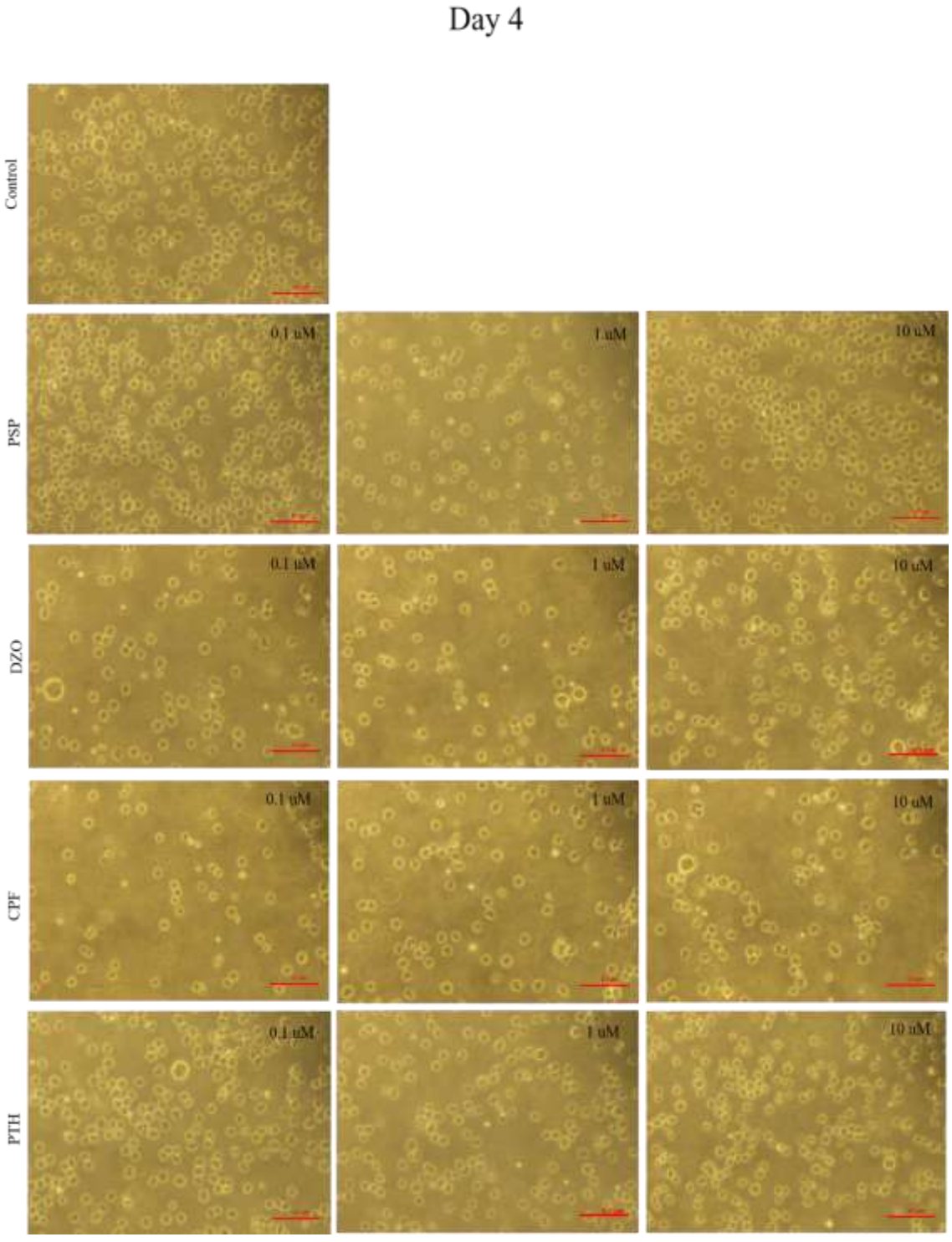

Figure 8- 8: Images of treated THP-1 cells with OPs day 4.

THP-1 cells were plated in equal density of 200,000 cells/ml per 75 flasks cultured in growth medium. The Cells were incubated for up to 4 days and treated with PSP, DZO, CPF, and PTH with three final concentration of each 0.1, 1, and 10 µM. Control sample was treated with 0.01 % (v/v) DMSO. Cells were monitored under the inverted light microscope at (10x) magnification. Scale bar 0.1 µm.